NASA/TM—2009-213642/REV1

Impact Testing on Reinforced Carbon-Carbon Flat Panels With BX–265 and PDL–1034 External Tank Foam for the Space Shuttle Return to Flight Program

Matthew E. Melis, Duane M. Revilock, and Michael J. Pereira
Glenn Research Center, Cleveland, Ohio

Karen H. Lyle
Langley Research Center, Hampton, Virginia

December 2009

NASA STI Program . . . in Profile

Since its founding, NASA has been dedicated to the advancement of aeronautics and space science. The NASA Scientific and Technical Information (STI) program plays a key part in helping NASA maintain this important role.

The NASA STI Program operates under the auspices of the Agency Chief Information Officer. It collects, organizes, provides for archiving, and disseminates NASA's STI. The NASA STI program provides access to the NASA Aeronautics and Space Database and its public interface, the NASA Technical Reports Server, thus providing one of the largest collections of aeronautical and space science STI in the world. Results are published in both non-NASA channels and by NASA in the NASA STI Report Series, which includes the following report types:

- TECHNICAL PUBLICATION. Reports of completed research or a major significant phase of research that present the results of NASA programs and include extensive data or theoretical analysis. Includes compilations of significant scientific and technical data and information deemed to be of continuing reference value. NASA counterpart of peer-reviewed formal professional papers but has less stringent limitations on manuscript length and extent of graphic presentations.

- TECHNICAL MEMORANDUM. Scientific and technical findings that are preliminary or of specialized interest, e.g., quick release reports, working papers, and bibliographies that contain minimal annotation. Does not contain extensive analysis.

- CONTRACTOR REPORT. Scientific and technical findings by NASA-sponsored contractors and grantees.

- CONFERENCE PUBLICATION. Collected papers from scientific and technical conferences, symposia, seminars, or other meetings sponsored or cosponsored by NASA.

- SPECIAL PUBLICATION. Scientific, technical, or historical information from NASA programs, projects, and missions, often concerned with subjects having substantial public interest.

- TECHNICAL TRANSLATION. English-language translations of foreign scientific and technical material pertinent to NASA's mission.

Specialized services also include creating custom thesauri, building customized databases, organizing and publishing research results.

For more information about the NASA STI program, see the following:

- Access the NASA STI program home page at *http://www.sti.nasa.gov*

- E-mail your question via the Internet to *help@sti.nasa.gov*

- Fax your question to the NASA STI Help Desk at 443–757–5803

- Telephone the NASA STI Help Desk at 443–757–5802

- Write to:
  NASA Center for AeroSpace Information (CASI)
  7115 Standard Drive
  Hanover, MD 21076–1320

NASA/TM—2009-213642/REV1

Impact Testing on Reinforced Carbon-Carbon Flat Panels With BX–265 and PDL–1034 External Tank Foam for the Space Shuttle Return to Flight Program

Matthew E. Melis, Duane M. Revilock, and Michael J. Pereira
Glenn Research Center, Cleveland, Ohio

Karen H. Lyle
Langley Research Center, Hampton, Virginia

National Aeronautics and
Space Administration

Glenn Research Center
Cleveland, Ohio 44135

December 2009

Level of Review: This material has been technically reviewed by technical management.

Available from

NASA Center for Aerospace Information
7115 Standard Drive
Hanover, MD 21076–1320

National Technical Information Service
5285 Port Royal Road
Springfield, VA 22161

Available electronically at http://gltrs.grc.nasa.gov

Impact Testing on Reinforced Carbon-Carbon Flat Panels With BX–265 and PDL–1034 External Tank Foam for the Space Shuttle Return to Flight Program

Matthew E. Melis, Duane M. Revilock, and Michael J. Pereira
National Aeronautics and Space Administration
Glenn Research Center
Cleveland, Ohio 44135

Karen H. Lyle
National Aeronautics and Space Administration
Langley Research Center
Hampton, Virginia 23681

Summary

Following the tragedy of the Orbiter *Columbia* (STS–107) on February 1, 2003, a major effort commenced to develop a better understanding of debris impacts and their effect on the space shuttle subsystems. An initiative to develop and validate physics-based computer models to predict damage from such impacts was a fundamental component of this effort. To develop the models it was necessary to physically characterize reinforced carbon-carbon (RCC) along with ice and foam debris materials, which could shed on ascent and impact the orbiter RCC leading edges. The validated models enabled the launch system community to use the impact analysis software LS–DYNA (Livermore Software Technology Corp.) to predict damage by potential and actual impact events on the orbiter leading edge and nose cap thermal protection systems.

Validation of the material models was done through a three-level approach: Level 1—fundamental tests to obtain independent static and dynamic constitutive model properties of materials of interest, Level 2—subcomponent impact tests to provide highly controlled impact test data for the correlation and validation of the models, and Level 3—full-scale orbiter leading-edge impact tests to establish the final level of confidence for the analysis methodology.

This report discusses the Level 2 test program conducted in the NASA Glenn Research Center (GRC) Ballistic Impact Laboratory with external tank foam impact tests on flat RCC panels, and presents the data observed. The Level 2 testing consisted of 54 impact tests in the NASA GRC Ballistic Impact Laboratory on 6- by 6-in. and 6- by 12-in. flat plates of RCC and evaluated two types of debris projectiles: BX–265 and PDL–1034 external tank foam. These impact tests helped determine the level of damage generated in the RCC flat plates by each projectile and validated the use of the foam and RCC models for use in LS–DYNA.

Introduction

On February 1, 2003, the Orbiter *Columbia* broke apart during reentry resulting in the loss of seven crewmembers. For the next several months an extensive investigation of the accident ensued, involving a nationwide team of experts spanning dozens of technical disciplines from NASA, industry, and academia.

The Columbia Accident Investigation Board (CAIB), a group of experts assembled to conduct an investigation independent of NASA, concluded in August 2003 that the cause of the loss of *Columbia* and its crew was a breach in the left-wing leading-edge reinforced carbon-carbon (RCC) thermal protection system initiated by the impact of thermal insulating foam that had separated from the orbiter's external fuel tank 81 seconds into that mission's launch. During reentry, this breach allowed superheated air to penetrate behind the leading edge and erode the aluminum structure of the left wing, which ultimately led to the breakup of the orbiter.

The CAIB report (ref. 1) made over two dozen recommendations to increase the overall safety of the shuttle for future launches. Prior to the *Columbia* accident, there were no sophisticated analysis tools in

existence to reliably quantify the debris impact damage threat to the shuttle system. As a consequence, CAIB recommendation R3.8–2 directed NASA to "Develop, validate, and maintain physics-based computer models to evaluate thermal protection system damage from debris impacts. These tools should provide realistic and timely estimates of any impact damage from possible debris from any source that may ultimately impact the orbiter. Establish impact damage thresholds that trigger responsive corrective action, such as on-orbit inspection and repair, when indicated." In response to R3.8–2, an Agency debris assessment team, often informally referred to as the DYNA team, consisting of members from Glenn Research Center (GRC), Langley Research Center (LaRC), Johnson Space Center (JSC), and Boeing, was assembled to develop such a tool using LS–DYNA (ref. 2). LS–DYNA is a commercial finite element code that utilizes an explicit formulation (as opposed to the more common implicit formulation) to predict a wide range of transient dynamic phenomena.

As a critical path element of NASA's Return to Flight Program for the STS–114 mission, the primary objectives set for the DYNA team were to develop analysis models for potential debris and RCC materials. RCC is used as the thermal protection system on the Orbiter leading edge and nose cap. To address these objectives, the team established a three-level approach: (1) fundamental tests to obtain independent static and dynamic constitutive model properties of materials of interest, (2) subcomponent impact tests to provide highly controlled impact test data for the correlation and validation of the models, and (3) full-scale impact tests to establish the final level of confidence for the analysis methodology. The debris materials under primary consideration were external tank thermal protection foams BX–265 and PDL, and ice, which also might shed off of the external tank.

All of the Level 2 impact testing for this program was conducted at the NASA GRC Ballistic Impact Laboratory in Cleveland, Ohio. The objective of this report is to provide details of the Level 2 impact test program and the experimental facilities used to conduct the tests, and present the observed data in an organized form (Appendixes A through F) for the Space Shuttle Program. Although there are a number of noted observations made about some of the data throughout, it is beyond the scope of this report to draw any technical conclusions about what is presented. For the Return to Flight program, both external tank foam and ice were tested on RCC. This report covers the foam impact testing program and the ice testing program is covered in reference 3. Although this report is largely comprehensive in outlining the details and procedures of the actual testing, a complete description can be obtained in the Orbiter RCC Flat Panel Impact Testing Plan (ref. 4).

Test Program

Program Objectives

Initially, the objective of the foam impact test program was to establish projectile velocities for each material of a fixed size and shape that initiates the threshold of visual damage on simply supported 6- by 6-in. and 6- by 12-in. flat RCC panels at impact angles of 90° and 45°. However as shuttle program requirements evolved, the focus changed to include establishing thresholds for damage detectable by nondestructive evaluation (NDE) with ultrasound and pulse thermography. In addition, RCC panel deformations were to be measured with a three-dimensional image correlation (digital photogrammetry) deformation measurement system throughout the entire spectrum of impact velocities for each test series. Observations made during each test were used to corroborate the validity of LS–DYNA deformation and damage RCC/projectile constitutive models to reliably predict actual or potential threats to the Space Shuttle Orbiter.

Test Series Description

The external tank foam impact testing was divided into six series: BX–265 foam on 6- by 6-in. at 90° and 45° impact angles, BX–265 foam on 6- by 12-in. at 90° and 45° impact angles, and PDL–1034 foam on 6- by 6-in. panels at 90° and 45° impact angles.

Each RCC flat panel was visually inspected before and after each impact test, in order to provide an indication of coating loss (spalling) due to the impact event. Another objective of this visual examination was to provide guidance for static and NDE testing. Posttest NDE inspection and digital photography were then performed on each panel.

Success Criteria

A NASA GRC Quality Assurance (QA) officer was present and provided quality assurance and configuration control for all tests. The QA officer verified all test plan requirement compliance and ensured that the resulting test data sheets were accurate and complete and that all success criteria were met for each test.

Each individual test was deemed successful provided that the projectile remained intact upon exit of the gun barrel and prior to impact on the RCC target panel and that interpretable high-speed digital video was acquired from the Vision Research Phantom (Vision Research, Inc.) cameras for velocity and deformation measurements. In addition, it was highly desirable that each of the following parameters were met:

- All projectile impact velocity parameters called for in this plan were kept within ±20 ft/s (as measured from digital high-speed video)
- Projectile impacted the expected target area within 0.25 in.
- Projectile rotational motion at impact was ≤5°, as determined by engineering review of video imagery after each shot
- Vacuum of 0.2±0.1 psi was maintained in test chamber for each test
- Load cell response data was not compromised by any extraneous vibratory loads independent of the projectile impact event

Test Facilities

All of the Level 2 RCC impact tests were conducted in the large vacuum gun (fig. 1) at the NASA GRC Ballistic Impact Laboratory in Cleveland, Ohio. The large vacuum gun is a single-stage compressed helium type with a 0.33 ft^3 pressure vessel. Barrels from 12 to 25 ft long, and inner diameters of 1.25 to 1.5 in., were fit to the chamber depending on the velocity and projectile requirements for each test.

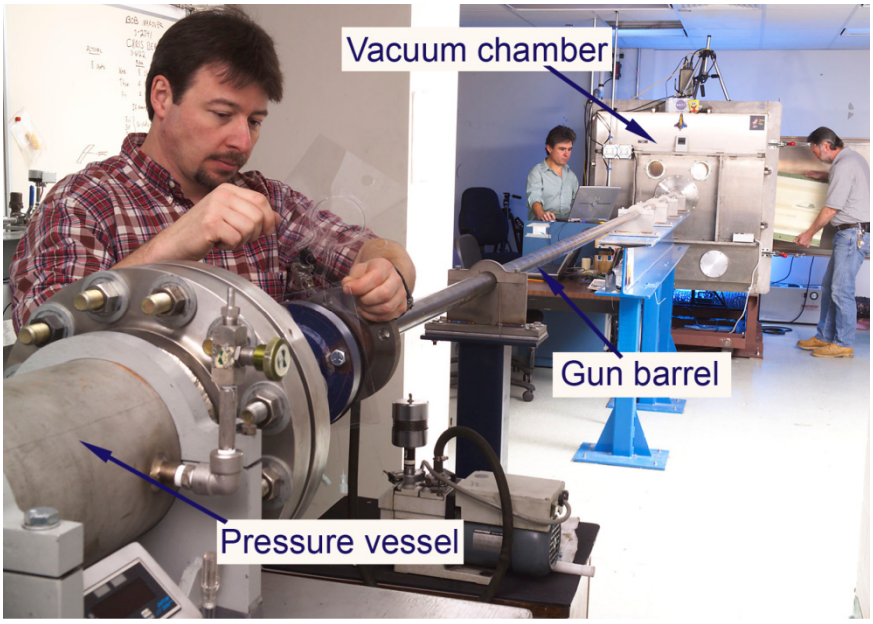

Figure 1.—Large vacuum gun with 2-in. barrel.

The large vacuum chamber has an inside dimension of 5 by 4 by 4 ft. It currently has provisions for 16 instrumentation feedthroughs (with ability to easily add additional ones). Viewing access ports on the front, side, top, and back allow for photo instrumentation with high-speed digital cameras. Four 120-V feedthroughs provide power for high-intensity lighting inside the chamber required for the high-speed digital imagery. The barrels for the large vacuum gun protrude into the vacuum chamber via a plate attachment that creates a circular opening with an o-ring seal to the chamber. Each barrel (each barrel has its own plate attachment) used with the vacuum chambers fit snugly against the o-ring to seal it with the chamber itself. This gun utilizes a Mylar (DuPont) burst disk system to release the helium propellant gas. The burst disk is in contact with an electronically heated nichrome wire, which melts the Mylar, releasing the propellant. Impact tests are conducted by simultaneously drawing a vacuum in the vacuum chamber and behind the projectile, to avoid pulling the projectile down the gun barrel prior to shooting.

Experimental Fixtures

Panel fixtures and mounts made from aluminum were fabricated for use in the large vacuum chamber to hold the RCC panels at 90° and 45° to the axis of the gun barrel. The construction was designed to be massive to minimize structural ringing due to the impacts, which could adversely affect load cell and deformation data. Figure 2 shows the panel fixture and mounts of the inside of the large vacuum chamber in its 45° configuration with the lighting system on and the high-speed cameras in place. The side of the panel fixture, shown in figures 3 and 4, is called out in the photograph.

Alignment of the test article with respect to the gun barrel shot line was accomplished through the use of a center-bore laser alignment tool inserted in the barrel such that the laser beam represented the centerpoint axis of the gun. The beam projected onto the test targets and was used to establish the correct fixture alignments and aim points for any given test conditions.

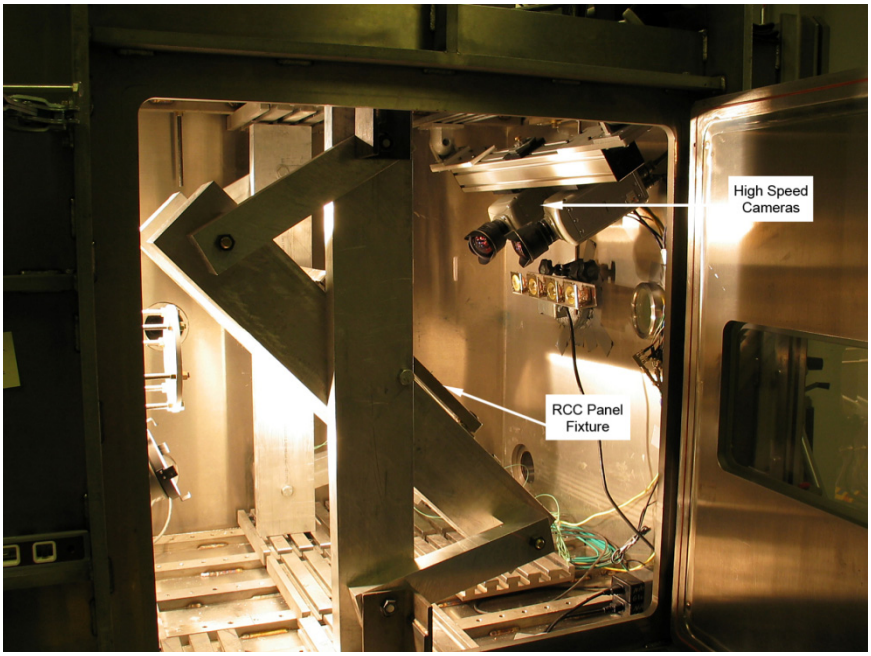

Figure 2.—RCC flat panel fixture assembly mounted in large vacuum chamber for 45° impact tests.

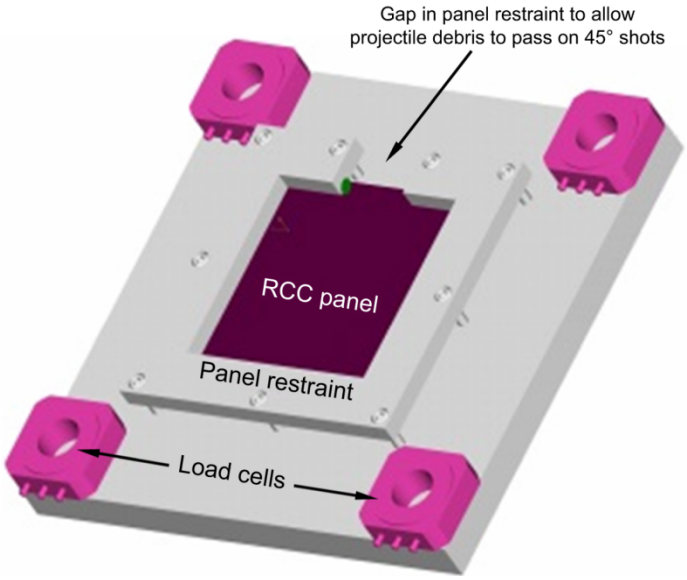

Figure 3.—Overview of reinforced carbon-carbon (RCC) flat panel holder fixture with load cells at corners.

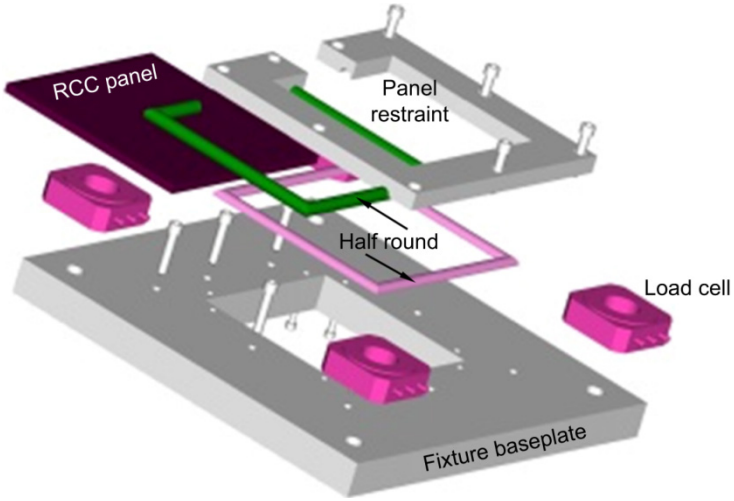

Figure 4.—Exploded view of reinforced carbon-carbon (RCC) flat panel holder fixture.

Two panel fixtures were fabricated to accommodate the 6- by 6-in. and 6- by 12-in. RCC panels. Figures 3 and 4 depict the 6- by 6-in. fixture with a panel in assembled and exploded views, respectively. Load cells, discussed in the next section, are shown at the corners of the fixture. The 6- by 6-in. panels were simply supported on all four edges in their mounts by being clamped in the frame between half-round aluminum bar stock around the complete perimeter of the panels and secured by 9 bolts torqued to 8 in.-lb using a calibrated torque wrench. This torque limit was established with a study to establish the safe clamping pressure without crushing the RCC material or coating. The 6- by 12-in. panels were only restrained (simply supported) on the 6-in. edges at the same torque limit. The frames were designed to contact the RCC panels just inside of each panel edge. Hence, the actual distance between the center lines of the half-round aluminum bar supports was 5 7/8 in.[2] for the 6- by 6-in. frame, and 11 7/8 in. for the 6- by 12-in. frame.

Instrumentation and Data Acquisition System

Load-time histories in three directions (one axial or normal and two shear to the panel face) were acquired from four piezoelectric three-axis load cells for each test using load cells mounted in the fixture used to hold the flat panels for testing. The fixture had a load cell mounted at each corner of the target panels shown in figures 3 and 4. Measurements taken from the load cells were averaged and filtered to obtain force time histories of each impact event.

The load cells were Kistler Model 9067 piezoelectric three-axis load washers (Kistler). They have a measurement range of ±10,000 lb in the normal axis and ±4500 lb in two shear directions. The load cell sensitivities are 17 picocoulomb/lb in the normal direction and 35 picocoulomb/lb in the shear direction. At the onset of the test program, the full usefulness of the load cell data had yet to be identified, and it was recorded for each test essentially because it was relatively straightforward to do so. However, because of the complex dynamic response of the overall large vacuum gun test structure, the load cell data did not accurately represent the impact loads on the RCC and ultimately used for validating the LS–DYNA models. Consequently, load cell data is not presented or discussed further in this report.

Accelerometers were attached at several locations on the test frame in the large vacuum gun in order to identify and resolve potential response anomalies from the impact tests as well as quantify the degree of movement that the test frame experienced. Fortunately, there were no anomalies that arose during the entire foam test series, and the test frame displacements were within an expected range.

The application of strain gages to the RCC panels was considered initially as the plan for this test program was being developed; however, it was determined that strain gage data on RCC could be misleading and of low quality. This was established through laboratory level tests, which indicated that strain gages produce erratic data largely due to the craze cracking of the silicon carbide (SiC) coating on the panels. The full-field three-dimensional deformation measurements taken with the ARAMIS system (discussed below) ultimately provided full-field strain data that was of high value to the validation effort.

Two data acquisition systems were utilized to record signals from the load cells and accelerometers during testing: The first was a Spectral Dynamics model VX2805D 8-channel, 16-bit, 5- Msample/s/ channel system with signal conditioning capabilities. The second was an IOtech WaveBook 516E, 16-bit, 1-Msample/s system with eight analog input channels, eight strain gage conditioning channels, and 8 ICP sensor channels. Dual-mode Kistler model 5010B charge amps were used to power the load cells.

High-Speed Cameras

High-speed digital Phantom cameras were used to document each impact test. For the majority of the program, both Phantom 5 and Phantom 7 cameras from Vision Research (ref. 5) were used and for a select number of tests, Photron (ref. 6) FASTCAMS were used. The cameras measured projectile velocity and captured the damage and deformation dynamics resulting in each test in addition to being utilized with the three-dimensional displacement measurement system. Typically, five high-speed cameras would document one of these impact tests.

Various resolutions and frame rates were used depending on the requirements for each test as there is a direct tradeoff between frame rates and image resolution with the Phantom cameras. Higher frame rates result in lower resolution images. Typically frame rates of around 29000 frames per second or more were used during these tests at resolutions of 256 by 256 or 256 by 128 pixels. It was a test goal to have exposure times of 2-20 (driven by light and viewing angle) μs to try to limit motion blur to 2 pixels.

The Phantom cameras record a continuous 1- to 2-s loop on an internal memory chip until stopped and do not require a trigger system to start recording. They are triggered manually to stop data acquisition at the sound of the gun blast, thus capturing the impact event in its entirety. Once the cameras were triggered, all of the recorded information was downloaded to laptop computers. All high-speed video captured in this test program has been archived by the Shuttle Program at Johnson Space Center and is easily accessible for viewing to the interested reader (contacts: Justin Kerr or Jim Hyde).

Optical Full-Field Three-Dimensional Displacement Image Correlation Measurement System

Deformation and computed strains of the back side (opposite of the impact side) of the RCC panels were obtained using the ARAMIS system built by GOM mbH (ref. 7) acquired from Trilion Optical Test Systems (refs. 8 to 10). ARAMIS is a three-dimensional image correlation photogrammetry system that captures full field displacement measurements under static, quasistatic, and ballistic impact loading.

The system works off image pairs taken simultaneously with two Phantom 7 cameras set up on a fixed beam, which viewed the back of the RCC panels undergoing impact. The image pairs were typically taken at 37.17 increments (~27 000 frames/s) with the exception of those taken in appendix D, which were 69.44 increments (~14 400 frames/s). The camera pair was set up outside the large vacuum chamber for the 90° impact tests and inside the chamber for the 45° tests. Inside mounting was necessary for the 45° tests to optimize the view of the panel backs. The outside mount configuration is shown in figure 5.

In order for the ARAMIS system to make its measurements, a painted speckle or spot pattern must be applied to the field area of interest. The backside of each panel was painted before the impact testing was performed. Testing was performed on small samples of RCC that were painted for use with the ARAMIS system. A scanning electron microscope was used to confirm that the paint did not excessively wick into the RCC panels and potentially change the RCC material performance and NDE techniques or flash thermography, and ultrasound tests revealed no adverse interference or artifacts due to the speckled paint pattern on the backside of the panels. The speckled pattern can be seen on the post-impact photographs in the appendices of this report. As the test program proceeded, an optimum paint pattern was adapted going from a “spatter” pattern to a pattern spray painted through a uniform stencil. This accounts for the two types of patterns seen in the photographs. The paint patterns were created by applying paint to the back of each test panel in two layers. The first layer is white paint that has a high reflectivity rating followed by black spray paint applied in a random speckle pattern or through the stencil. The inset in the lower right-hand corner of figure 5 shows the uniform paint pattern on the back of an RCC panel.

Figure 5.—ARAMIS Three-Dimensional Deformation/Strain Measurement System shown with static camera assembly setup at large vacuum gun viewing ports. Inset in lower right corner depicts paint pattern on back of the reinforced carbon-carbon panel.

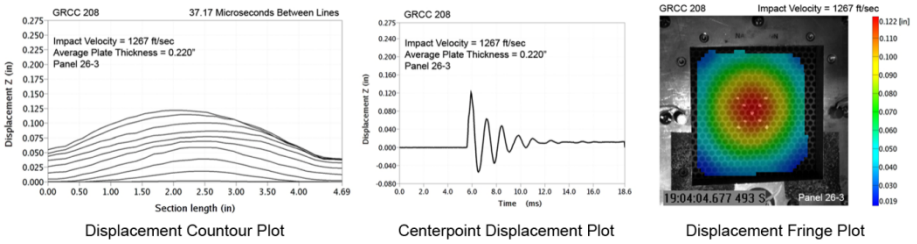

Displacement Countour Plot | Centerpoint Displacement Plot | Displacement Fringe Plot

Figure 6.—Example output plots from the ARAMIS displacement measurement system.

Using photogrammetric principals, the three-dimensional coordinates of the surface of the specimen can be calculated precisely from observing the paint pattern from two known points of view. On the basis of the three-dimensional coordinates, the three-dimensional displacements, the strains, and shape of the specimen were calculated with a high degree of accuracy and resolution. The results can be rapidly post-processed after each test and visualized in similar fashion to finite element results. Three types of ARAMIS output are presented in the appendices of this report: Displacement cross sections at various times on a panel, center point displacements as a function of time, and full-field color displacement fringe plot at maximum displacement of each panel. An example of these plots is shown in figure 6.

Velocity Measurement

Posttest evaluation of the high-speed Phantom camera video established impact velocities for each test as well as provided verification of projectile integrity and orientation in flight.

To set up for obtaining projectile velocities, a camera was mounted orthogonal to the path of the projectile and a calibration bar was seated in the end gun barrel and projected into the test chamber along the centerline axis of the barrel. The calibration bar had precisely machined markings 0.5 in. apart on a section the same diameter as the foam projectiles to be shot. Given this device with known markings in the same plane of the projectile's motion, the relationship between physical distance in the plane of the projectile's trajectory and camera screen pixels was determined. The impact velocity of a projectile in a given test was then calculated from the following equation:

$$V_p = \mathrm{SF} \times \mathrm{PIX} \times \frac{\mathrm{FR}}{\mathrm{NF}}$$

where V_p is the velocity of the projectile, SF is the scaling factor in units of length per pixel, PIX is the number of pixels a mark on the projectile travels in a given number of frames (NF), and FR is the frame rate.

Pretest and Posttest RCC Panel Observations

Material Pedigrees

RCC Panel Pedigree and Fabrication

The RCC material used in this test program was obtained from Lockheed Martin Missiles & Fire Control in Dallas, Texas, through the Shuttle Program Office. Typically the material was provided in 12- by 12-in. panels and cut to 6- by 6-in. or 6- by 12-in. sizes at Southern Research Institute (SRI) in Birmingham, Alabama. The cut plan for the panels is discussed in appendix C of reference 4. In addition, it should be noted that due to material loss during the cutting process, the panels were delivered to GRC nominally at 5.9 by 5.9 in. and 5.9 by 11.9 in. but are referred to in whole numbers for easier referencing. SRI supported a significant number of engineering efforts relating to the RCC material studies. Much of this work was complementary and of great use to the LS–DYNA RCC constitutive model development.

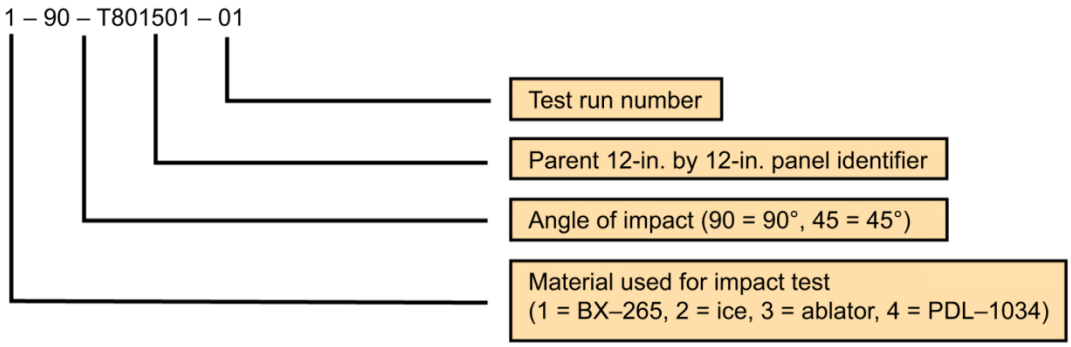

Figure 7.—Test numbering scheme for reinforced carbon-carbon flat panel impact tests.

Final reports from two of these studies may be of noteworthy interest to those reading this report: "Silicon Carbide Thickness Measurements of Various RCC Panels and Plates" (ref. 11), which provides further detail on the panels tested in this report, and "Correlation of RCC Substrate Properties" (ref. 12), which sheds some additional light on the weighted contributions of substrate RCC properties to the overall properties of coated RCC panels. In addition, it should be noted that significant work also was performed to obtain static and dynamic mechanical properties of the RCC material and is presented in references 13 and 14.

In the early stages of this test program, little RCC was available for testing and a number of panels were "found" to be in storage at Lockheed, which were made available for these impact tests. These panels lacked traceability documents typically associated with any RCC fabricated by Lockheed but were considered acceptable for this program. Test results on some of the found panels were demonstrated to be suspect and are noted appropriately in the appendices. Found RCC material was only used in the test series in appendices A and B (Lots 2 and 3, set 6). For the remaining panels in the test program, Lockheed newly manufactured additional 12- by 12-in. panels, which had full traceability documentation.

RCC material pedigrees to be used in this test program were identified through shipping documents that accompanied the deliveries to GRC. Reference to relevant shipping documents was recorded by the quality officer for each test to ensure traceability.

For the purpose of identifying test panels, each flat panel was labeled with the unique identifier relating to the 12- by 12-in. parent panel and then assigned an additional number identifying the order in which it was cut from the parent panel. The application of this numbering scheme can be seen in the tables at the beginning of each appendix under the first column labeled "Test No." Expanding upon this, a test number identifier was assigned to each test which incorporated the assigned panel numbers. It included the test number (counted sequentially), the angle of impact, and the projectile material. An example of the flat panel/test identification is given in figure 7. This example identifies the first impact test in the RCC impact testing was performed on subpanel 1 cut from parent T8015 and shot with BX–265 at a 90° impact angle. It should be noted that the NASA GRC Ballistic Impact Laboratory maintained its own test numbering scheme along with the aforementioned one. Test numbers were assigned sequentially after the prefix GRCC. It is presented in the appendices for clarity and completeness as the numbering used for the data archives follows this format.

Foam Pedigree and Fabrication

For foam impact testing, two materials were used: BX–265 and PDL–1034. All projectiles were fabricated foam sprayed and fabricated at NASA Michoud Assembly Facility (MAF) per STP–1540 (Lockheed standard for the spraying of BX–265) and STP–1532 (Lockheed standard for the spraying of PDL–1034). Projectiles were rough cut from the 2-ft by 2-ft by 4-in.-thick base panels in the "Parallel to Rise" direction per figure 8. Rough-cut blocks were then mounted into a lathe and turned down to a final

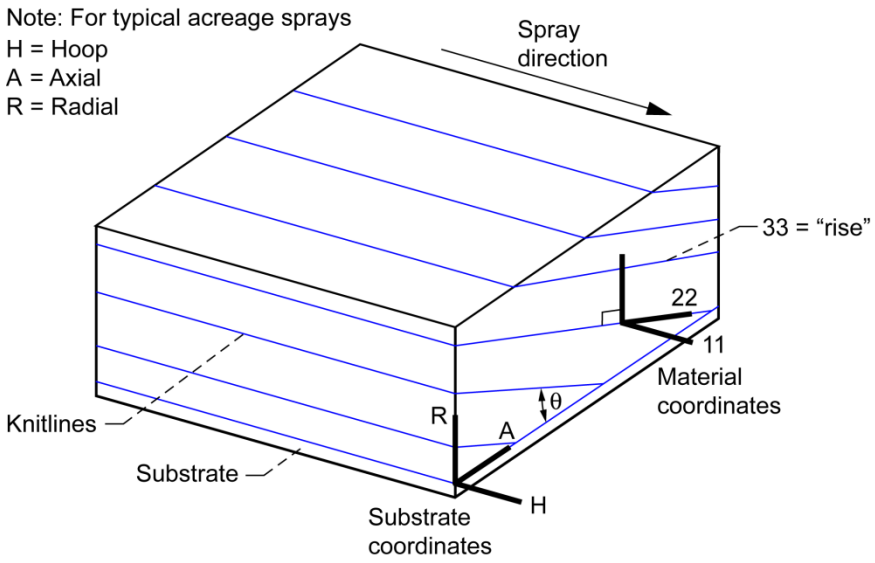

Figure 8.—External tank foam cut direction nomenclature.

diameter of 1.25 in. (+0, –0.015 in.) for 90° tests and 1.50 in. (+0, –0.015 in.) for 45° tests and cut to a final length of 3.00±0.01 in. Further machining of the length as necessary was performed to produce projectiles with consistent weight (±0.001 lb).

Digital Photography

Digital photographs were taken of the front, back, and all four edges of each RCC panels both prior to and after impact testing to document any changes in the panel condition after testing. All of the posttest images are presented in this report for each panel. Both pretest and posttest images have been archived in digital form by the Shuttle Program and are easily accessible to the interested reader (contacts: Justin Kerr or Jim Hyde). In addition, these photographs have been all assigned NASA GRC C-numbers (seen in the lower right-hand corner of the appendices images) and will remain in the GRC archives, accessible through the NASA GRC Imaging Technology Center.

Nondestructive Evaluation

Nondestructive evaluation (NDE) was performed on each RCC panel before and after testing to baseline the specimens and to evaluate the damage due to impact. The NDE not only characterized any damage due to the impact testing, but the findings from each panel's evaluation fed back into defining the parameters of the panel testing to follow. All NDE outlined in this report was performed by the NDE group at NASA GRC. Two NDE methods will be utilized for this program: pulse, or flash, thermography and through-transmission ultrasound.

Pulsed, or flash, thermography involves the heating of a specimen with a short duration pulse of energy and monitoring the transient thermal response of the surface of the specimen with an infrared camera. The thermal energy on the surface conducts into the cooler interior of the sample. In turn, there is a reduction of the surface temperature over time. This surface cooling will occur in a uniform manner as long as the material properties are consistent throughout the specimen. Subsurface defects that possess different material properties (e.g., thermal conductivity, density, or heat capacity) will affect the flow of heat in that particular region. This resistance in the conductive path causes a different cooling rate at the surface directly above the defect, when compared to the surrounding, defect-free material. The change in the subsurface conduction is seen as a nonuniform surface temperature profile as a function of time. Since

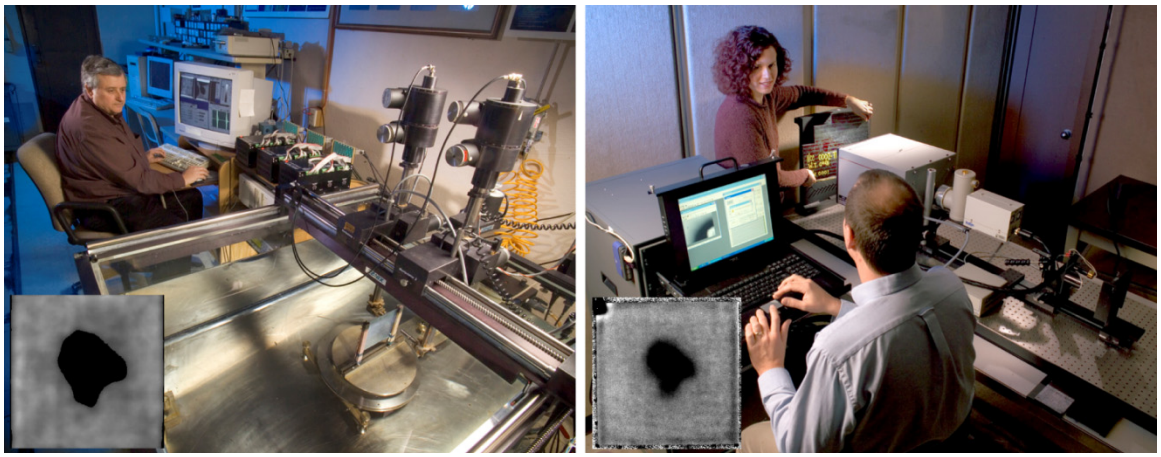

Figure 9.—Nondestructive evaluation facilities at NASA Glenn: through transmission ultrasonic immersion tank with reinforced carbon-carbon panel undergoing scanning (left) and thermal imaging setup to perform pulse thermography (right). Insets in the left corners of each photo depict sample output from each technique.

the method depends on the interaction of the defect with the advancing thermal front, defects that are located at greater depths will show up later. Due to lateral diffusion, deeper defects will tend to have less contrast than near-surface flaws. Therefore, the critical flaw size capability of a thermographic inspection system is a function of the defect size, depth, and the material properties of the component being tested. Analysis of thermographic data involves examination of images based on the temperature-time data or derivatives calculated from the original data sets. Anomalous areas can then be identified based on deviations in the cooling behavior. Figure 9 (right) shows the thermal imaging setup used to conduct pulse thermography with an example output image.

Through-transmission ultrasonic inspection utilizes two transducers, placed on opposite sides of a material for interrogation. One transducer sends an ultrasonic pulse through the material where it is received by the second. In scanning mode, the transducer pair is moved across the area of interest, and an image based on the amplitude of the received waveform is generated. Defects and other significant variations will result in the additional attenuation and scattering of the ultrasonic signal as it passes through the material, thus reducing the signal amplitude. Flaws are located in the image based on this decrease in signal amplitude. Minimum flaw resolution is a function of the wavelength of the ultrasonic signal flaw orientation. Resolution, in general, increases with increasing frequency. Figure 9 (left) shows the immersion ultrasonic tank and relevant hardware to perform the through-transmission ultrasonic inspection with a sample image.

Through-transmission ultrasound evaluation will require that the RCC panels be immersed in water during the scan process. Each RCC panel was weighed before each scan and then vacuum dried until the after-scan weight is that of the initial weight to ensure that all water absorbed from the immersion was removed from the panel. The vacuum drying process was accomplished referencing Southern Research standard specification for drying RCC panels. This specification used 180 °F heat while pulling a vacuum of approximately 10^{-3} torr. The weight of the flat panel was monitored until stabilization occurs.

Testing Summaries

Below are brief summaries of the external tank foam impact test program as organized into impact angle and foam type. Comprehensive data sets reside in each of the six appendices in the back of this report.

BX–265 on 6- by 6-in. Reinforced Carbon-Carbon (RCC) Panels at 90° Impact Angle (Appendix A)

Thirteen shots were conducted in this test series with impact velocities ranging from 1388 to 2109 ft/s. The RCC material shot in this test series was "found" material.

Panel A–146 is considered to be an anomalous panel in this test series. For reasons not fully quantified, this panel was prone to severe damage and lower impact velocities than other panels and was considered defective. Test results from Panel A–146 were consequently not considered valid but are presented in this report for completeness.

BX–265 on 6- by 6-in. Reinforced Carbon-Carbon (RCC) Panels at 45° Impact Angle (Appendix B)

Thirteen shots were conducted in this test series with impact velocities ranging from 1244 to 2440 ft/s. The RCC material shot in this test series was "found" material.

Panels from parent R1–47 is considered suspect panels in this test series. For reasons not fully quantified, tests with these panels yielded inconsistent results as compared to other panels in the test series. Test results from the R1–47 panels were consequently not considered as valid but are presented in this report for completeness.

BX–265 on 6- by 12-in. Reinforced Carbon-Carbon (RCC) Panels at 90° Impact Angle (Appendix C)

Seven shots were conducted in this test series with impact velocities ranging from 1054 to 1849 ft/s. The RCC material for this test series was tested in the as-manufactured condition.

Tests GRCC 169 and GRCC 170 were shot on the same panel, 54–1. GRCC 169, the foam projectile, came out damaged, crooked, and slow. An impromptu experiment was then conducted to determine if damage does accumulate. The second shot, GRCC 170 produced NDE detectable damage, despite its low velocity. Time constraints in the test lab did not allow for ultrasound or thermography to be performed between tests. Although not definitive in nature, this experiment did draw interest to the concept that damage might accumulate in the RCC material as a consequence of sequential hits that singularly would not damage the RCC.

All of the 6- by 12-in. panel tests were only simply supported on two ends. As a consequence, the wave propagation in these panels were dramatically different and less controlled and damped than in the 6- by 6-in. panels resulting in additional modes of vibration in the panels being significant which can be identified in the ARAMIS data presented in the appendix.

BX–265 on 6- by 12-in. Reinforced Carbon-Carbon (RCC) Panels at 45° Impact Angle (Appendix D)

Five shots were conducted in this test series with impact velocities ranging from 1381 to 2000 ft/s. The RCC material for this test series was tested in the as-manufactured condition.

All of the 6- by 12-in. panel tests were only simply supported on two ends. As a consequence, the wave propagation in these panels were dramatically different and less controlled and damped than in the 6- by 6-in. panels resulting in additional modes of vibration in the panels being significant which can be identified in the ARAMIS data presented in the appendix.

PDL–1034 on 6- by 6-in. Reinforced Carbon-Carbon (RCC) Panels at 90° Impact Angle (Appendix E)

Eight shots were conducted in this test series with impact velocities ranging from 960 to 1825 ft/s. The RCC material for this test series was tested in the as-manufactured condition.

PDL–1034 on 6- by 6-in. Reinforced Carbon-Carbon (RCC) Panels at 45° Impact Angle (Appendix F)

Eight shots were conducted in this test series with impact velocities ranging from 1122 to 2105 ft/s. The RCC material for this test series was tested in the as-manufactured condition.

Concluding Remarks

The Level 2 reinforced carbon-carbon (RCC) flat panel impact test program at the NASA Glenn Research Center Ballistic Impact Laboratory was successfully completed on time supporting NASA's Return to Flight with the STS–114 mission. The data in the appendices of this report present the results from 54 external tank foam impact tests (38 with BX–265 and 16 with PDL–1034), which were used to demonstrate the validity of BX–265, PDL, and RCC models developed and implemented in the LS–DYNA impact analysis program. As a point of interest, the final validation step of the LS–DYNA models was through correlation with observations from follow-on full-scale orbiter wing leading edge and nose cap impact tests performed at Southwest Research Institute (SwRI).

In preparation for the STS–114 launch, virtually hundreds of analyses with LS–DYNA were performed to establish certified impact damage thresholds for RCC thermal protection systems on the orbiter helping to recertify the shuttle system for flight. For the interested reader, references 15 through 25 provide additional details on much of the analysis development process with LS–DYNA, and references 26 through 29 highlight the efforts preformed to evaluate ice impacts on RCC. Reference 3 is the companion report to this one which provides all of the post-impact test data on the RCC panels from that program.

Appendices

Data from the external tank foam impact tests are presented in the following six appendices (A through F) as follows:

Appendix A—BX–265 on 6- by 6-in. Reinforced Carbon-Carbon (RCC) Flat Panels at 90° Impact Angle
Appendix B—BX–265 on 6- by 6-in. Reinforced Carbon-Carbon (RCC) Panels at 45° Impact Angle
Appendix C—BX–265 on 6- by 12-in. Reinforced Carbon-Carbon (RCC) Panels at 90° Impact Angle
Appendix D—BX–265 on 6- by 12-in. Reinforced Carbon-Carbon (RCC) Panels at 45° Impact Angle
Appendix E—PDL–1034 on 6- by 6-in. Reinforced Carbon-Carbon (RCC) Panels at 90° Impact Angle
Appendix F—PDL–1034 on 6- by 6-in. Reinforced Carbon-Carbon (RCC) Panels at 45° Impact Angle

In each appendix, the data are organized in the following fashion:

1. A table summarizing the appendix test series.
2. Baseline and posttest imagery from ultrasound and thermography nondestructive evaluations arranged in order of ascending impact velocities. (It should be noted that in the thermography imagery, black spots appear in the upper left or right corners of the panels. This is an artifact of the fixturing to hold the panels during evaluation.)
3. Displacement contours output from ARAMIS showing the displacements along a cross-sectional line on the back of the panels at uniform increments of time as the panels were impacted. Note the sectional line for the 6- by 12-in. panels were taken along the long edge of the panels.
4. Displacement trace plots output from ARAMIS of the panel centerpoints as a function of time.
5. ARAMIS full-field color fringe plots taken from the point of maximum displacement of the panel resulting from the impact. (Note that in some of these plots, coating loss on the backside of the panels obscured ARAMIS from measuring accurate displacements. In these cases, the plots shown were selected just before or after failure of the panels. Knowing maximum displacement for a panel subject to failure is less meaningful for analysis correlation since the structure of the panel is compromised.)
6. High-resolution digital photography of each panel show front, back, and edge composite views as well as isometric views of both front and back of each panel.

Appendix A.—Test Data

BX–265 External Tank Foam Impact Testing at 90° Angle on 6- by 6-in. Reinforced Carbon-Carbon (RCC) Flat Panels

Notable Observations From the Appendix A Test Series

1. The RCC material used in this test series was “found” material.
2. For the first several impact tests in this test series, no digital photographs were taken of the panels from angles other than 90°. Only front, back, and side images were taken. Shortly into the program, it was determined that photos taken from an angle other than 90° would help to further visually distinguish damage on the panels. As a consequence, several of the tests in Appendix A will not have these images included.
3. Panel A–146 is considered to be an anomalous panel in this test series. For reasons not fully quantified, this panel was prone to severe damage and lower impact velocities than other panels and was considered defective. Test results from panel A–146 were consequently not considered valid but are presented in this report for completeness.
4. Lot 2 in the following test series table refers to remnant RCC material from the original qualification of ENKA (American Enka Corp.) fabric.
5. Lot 3, set 6 in the following test series table was used by Lockheed to indicate any piece of RCC that they had that could support the Return to Flight Program. They were at the RCC–3 Bimatrix condition, and resumed processing for silicon carbide (SiC) conversion coating, TEOS (tetra-ethyl-ortho-silicate), and type A.

Appendix A Test Series

BX-265 90 Degree Impact Test Parameters on 6" x 6" Reinforced Carbon-Carbon Panels

Test No.	Glenn Test Reference Number	Impact Velocity (ft/sec)	Panel ID Number	Lot Number	Average Panel Thickness (inches)	Visual Damage Observations	Mass of panel before test (grams)	Mass of panel after test (grams)	Projectile Weight (grams)	Projectile Length (inches)	Projectile Diameter (inches)	Test Date	Projectile ID Number
1-90-T801502-02	GRCC017	1388	T8015-2	2	0.244	No significant indications found	216.24	215.91	2.060	2.877	1.243	6/3/04	Foam: BX 265 8-17 JR 1881
1-90-T801503-03	GRCC019	1717	T8015-3	2	0.245	Small Backside indication located	217.37	no record	1.990	2.808	1.241	6/3/04	Foam: BX 265 8-10 JR 1881
1-90-A14604-08	GRCC025	1741	A146-4	2	0.214	Backside crack and coating loss	187.53	187.26	2.060	2.880	1.245	6/8/24	Foam: BX 265 JR 1885
1-90-A14603-07	GRCC023	1845	A146-3	2	0.214	Backside crack and coating loss	188.38	187.78	2.010	2.770	1.242	6/7/04	Foam: BX 265 8-01 JR 1881
1-90-T801504-04	GRCC020	1907	T8015-4	2	0.247	No significant indications found	216.43	216.16	1.960	2.730	1.240	6/4/04	Foam: BX 265 8-08 JR 1881
1-90-A15018-27	GRCC060	1952	A150-18	3, set 6	0.215	Front crack, backside coating loss	198.62	198.40	2.060	3.000	1.250	8/13/04	Foam: BX 265, JR1855 P4 287A
1-90-A15019-28	GRCC061	1978	A150-19	3, set 6	0.213	Front/back coating loss, through crack	199.18	198.88	2.090	3.010	1.248	8/13/04	Foam: BX 265, JR1855 P4 275B
1-90-A15017-26	GRCC059	2000	A150-17	3, set 6	0.213	Front/back coating loss, through crack	199.84	199.49	2.060	3.000	1.250	8/12/04	Foam: BX 265, JR1855 P4 270B
1-90-A14602-06	GRCC022	2002	A146-2	2	0.217	Front/back coating loss	185.50	183.98	1.990	2.750	1.240	6/7/04	Foam: BX 265 8-18 JR 1881
1-90-A14601-05	GRCC021	2015	A146-1	2	0.213	Backside coating loss, through crack	186.33	184.81	2.040	2.860	1.243	6/4/04	Foam: BX 265 8-20 JR 1881
1-90-T801501-01	GRCC015	2054	T8015-1	2	0.244	Front/back coating loss	216.94	215.88	2.210	3.070	1.252	6/3/04	Foam: BX 265 8-12 JR 1881
1-90-P20L23-24	GRCC057	2077	P20L-23	3, set 6	0.250	No significant indications found	227.88	227.73	1.960	3.000	1.244	8/12/04	Foam: BX 265, JR1855 P4 260B
1-90-P20L24-25	GRCC058	2109	P20L-24	3, set 6	0.250	No significant indications found	230.39	230.18	2.050	3.005	1.246	8/12/04	Foam: BX 265, JR1855 P4 276B

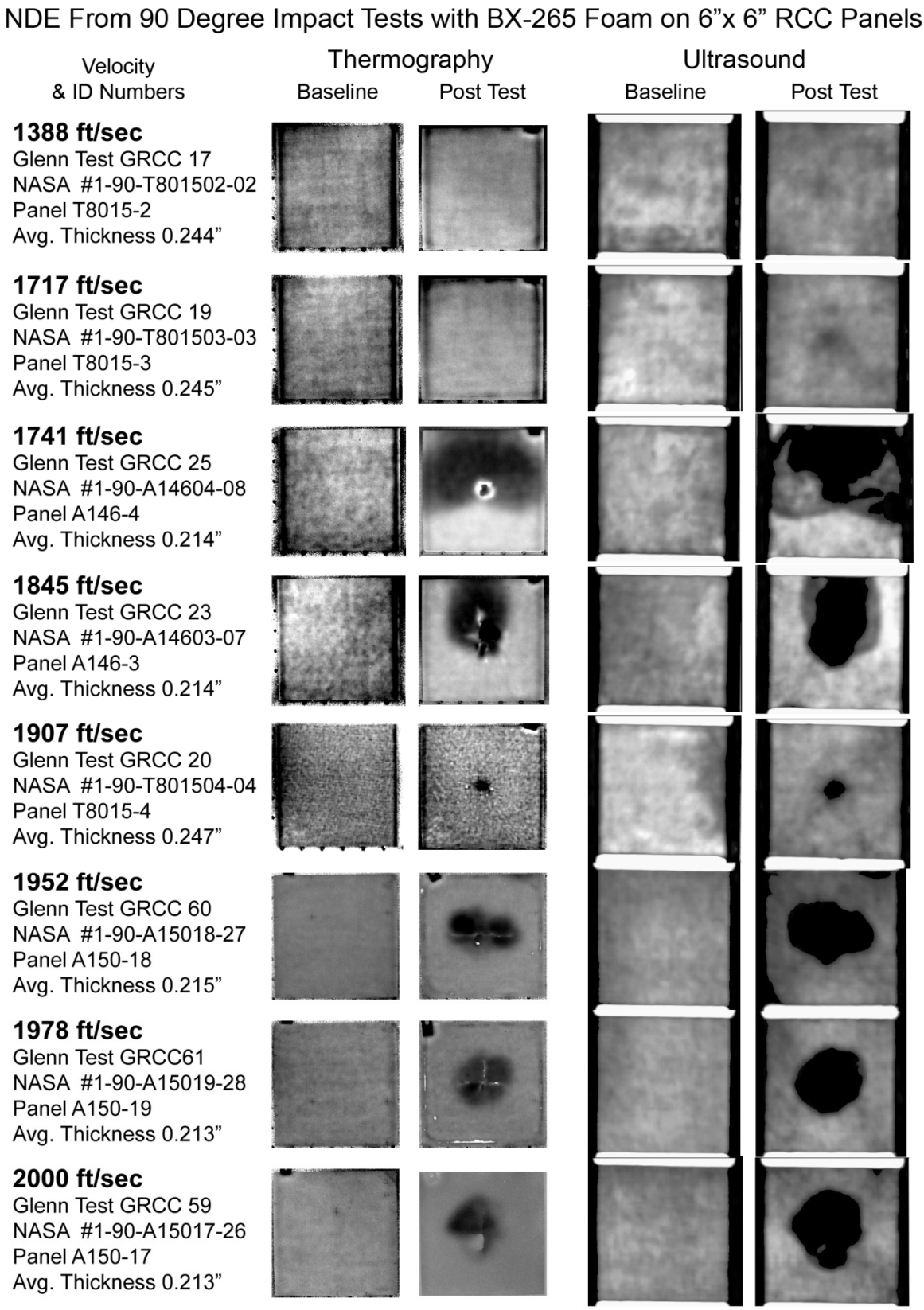

Figure A1–1.—Pulse thermography and ultrasound post impact pretest and posttest images of reinforced carbon-carbon 6- by 6-in. flat panels impacted with BX–265 foam cylinders (nominally 1.25 in. in diameter by 3 in.) at a 90° angle.

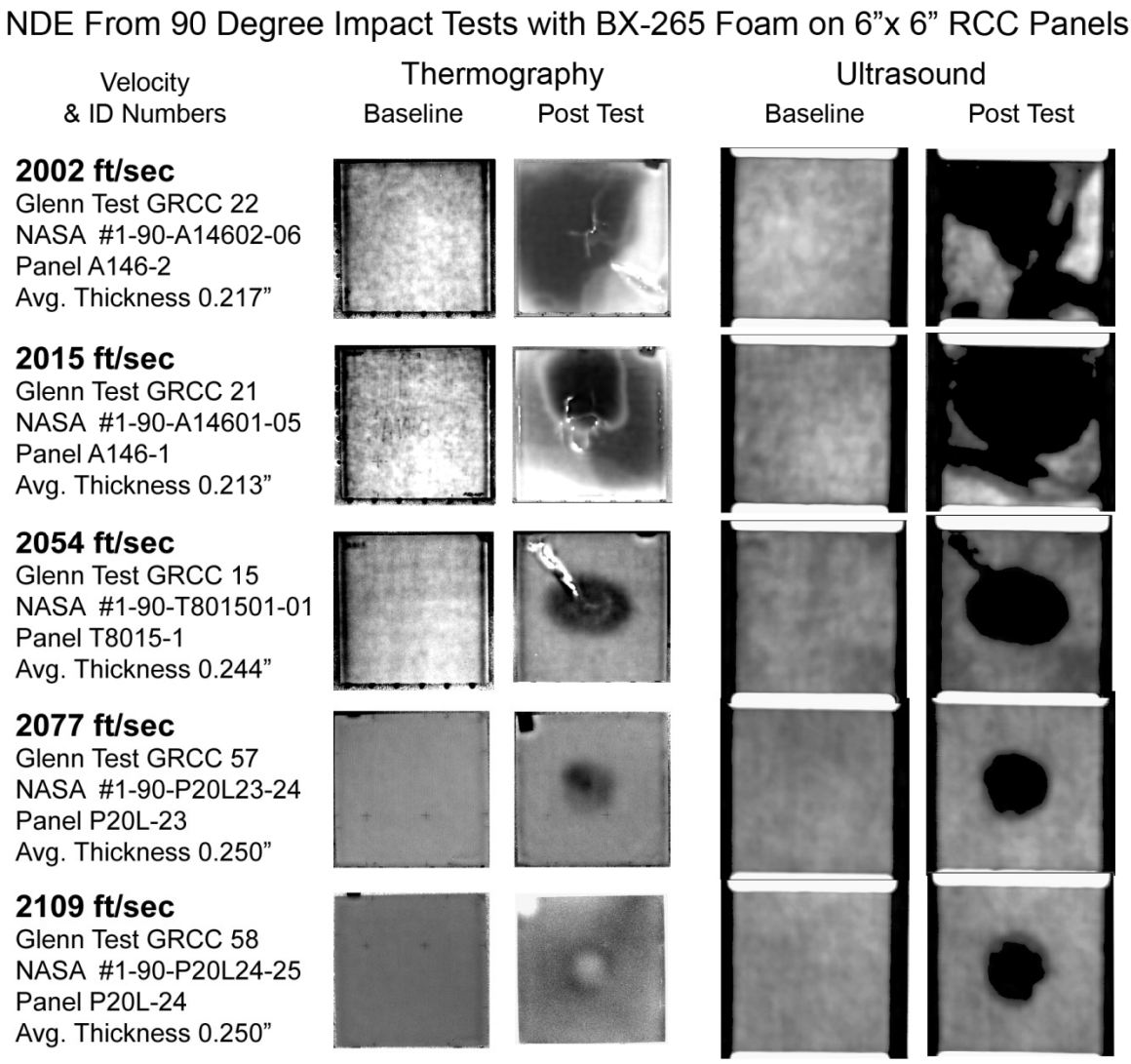

Figure A1—2.—Pulse thermography and ultrasound post impact pretest and posttest images of reinforced carbon-carbon 6- by 6-in. flat panels impacted with BX–265 foam cylinders (nominally 1.25 in. in diameter by 3 in.) at a 90° angle.

Aramis Displacement Contours from 90 Degree Impact Tests with BX-265 Foam on 6”x 6” RCC Panels

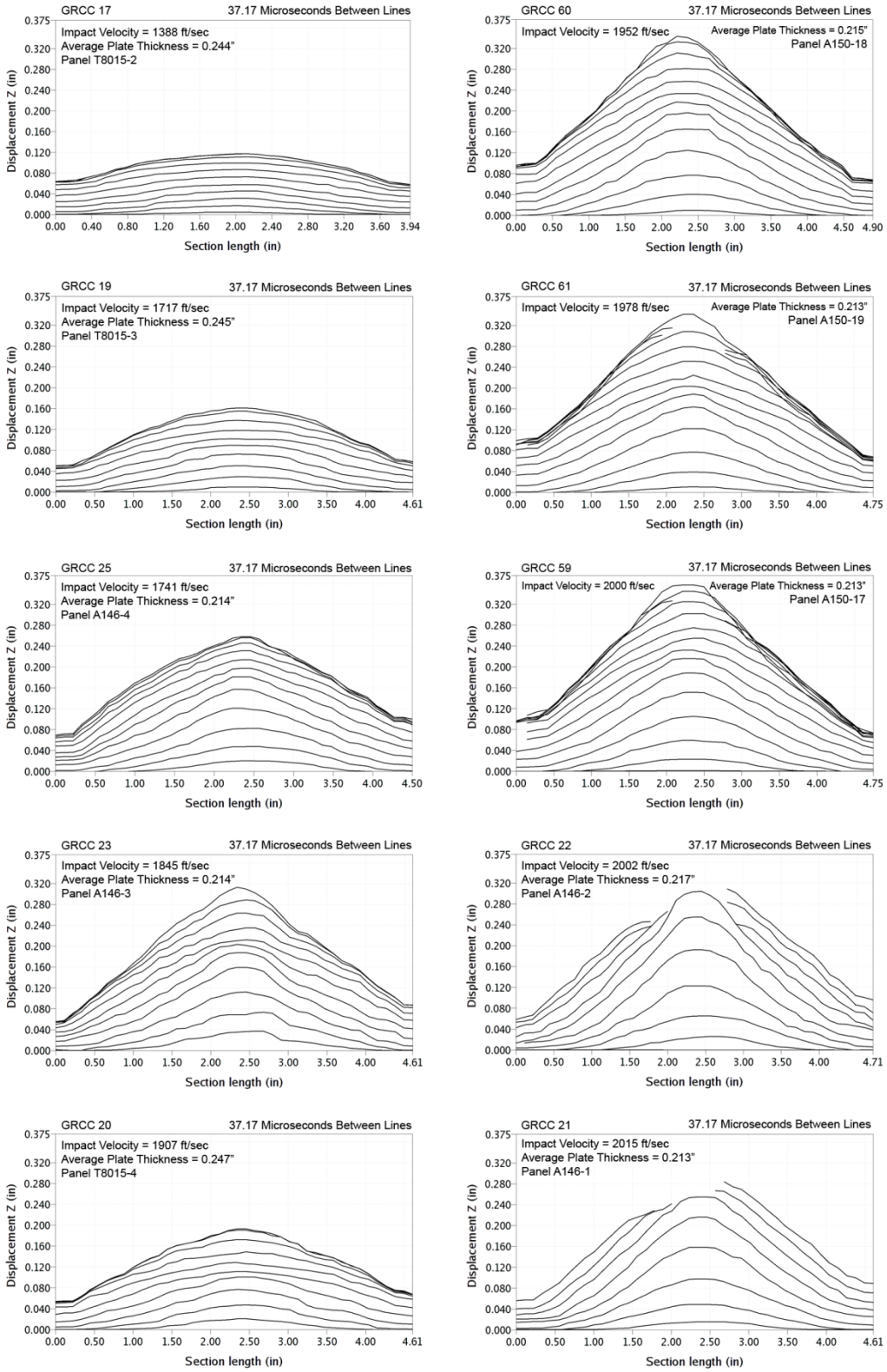

Figure A2–1.—ARAMIS out-of-plane deformation contours across centerline of 6- by 6-in. reinforced carbon-carbon flat panels measured at 37-μs increments undergoing impact with BX–265 foam cylinders (nominally 1.25 in. in diameter by 3 in.) at a 90° angle.

Aramis Displacement Contours from 90 Degree Impact Tests with BX-265 Foam on 6”x 6” RCC Panels

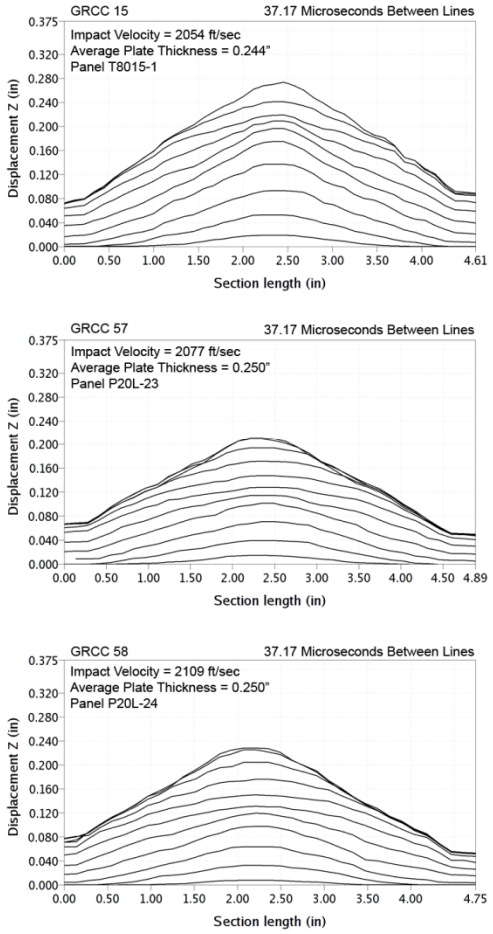

Figure A2–2.—ARAMIS out-of-plane deformation contours across centerline of 6- by 6-in. reinforced carbon-carbon flat panels plotted at 37-μs increments undergoing impact with BX–265 foam cylinders (nominally 1.25 in. in diameter by 3 in.) at a 90° angle.

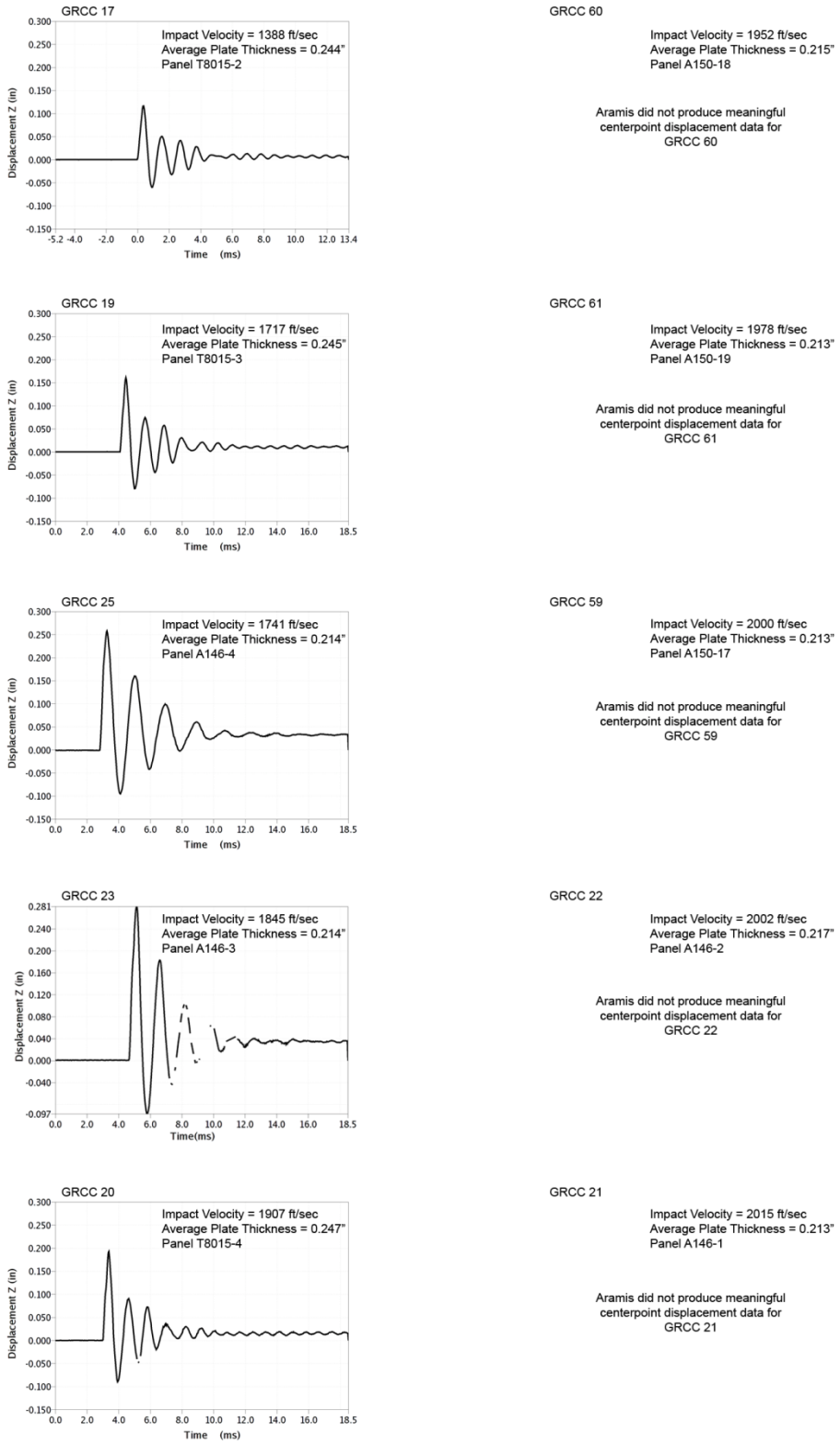

Figure A3–1.—ARAMIS centerpoint out-of-plane deformation vs. time of 6- by 6-in. reinforced carbon-carbon flat panels impacted with BX–265 foam cylinders (nominally 1.25 in. in diameter by 3 in.) at a 90° angle.

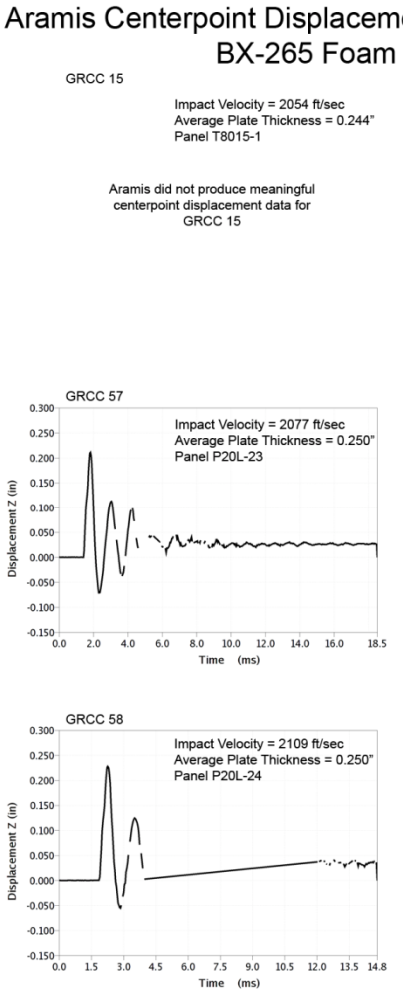

Figure A3–2.—ARAMIS centerpoint out-of-plane deformation versus time of 6- by 6-in. reinforced carbon-carbon flat panels impacted with BX–265 foam cylinders (nominally 1.25 in. in diameter by 3 in.) at a 90° angle.

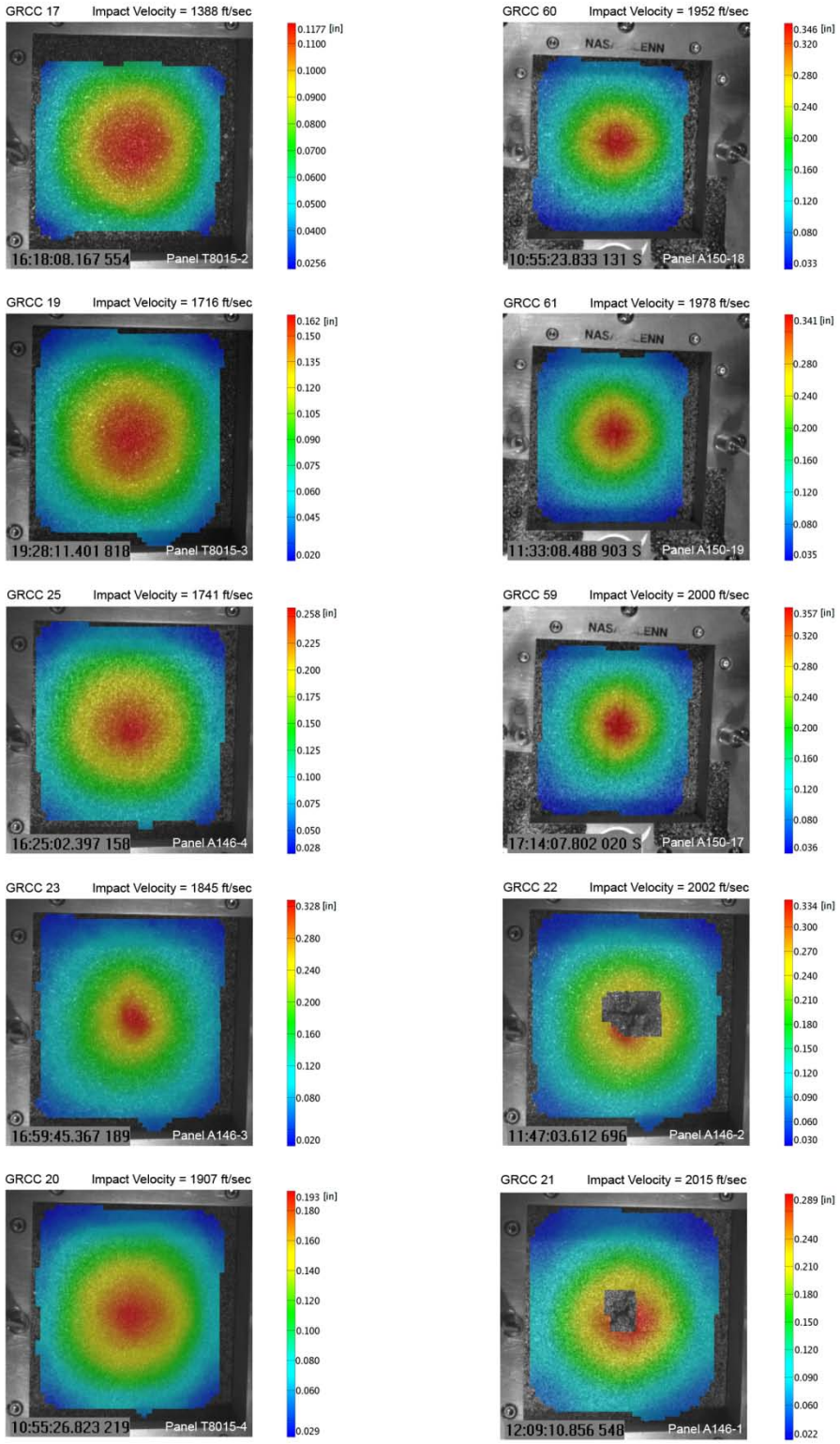

Figure A4–1.—ARAMIS color fringe plots depicting maximum deformation prior to material failure of 6- by 6-in. reinforced carbon-carbon flat panels as they undergo impact with BX–265 foam cylinders (nominally 1.25 in. in diameter by 3 in.) at a 90° angle.

Aramis Maximum Displacement Fringe Plots from 90 Degree Impact Tests
with BX-265 Foam on 6” x 6” RCC Panels

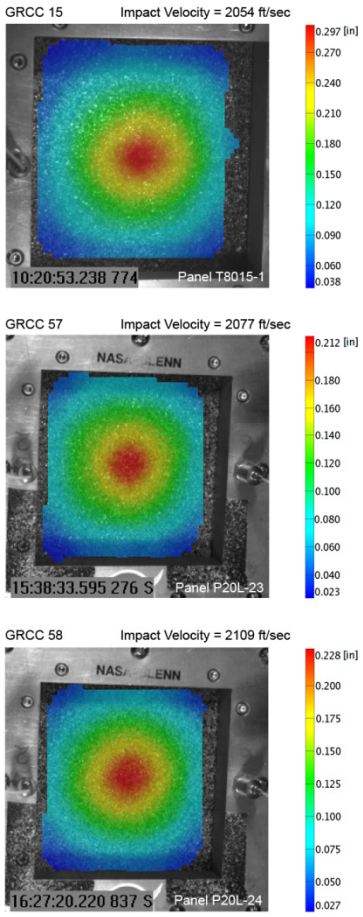

Figure A4–2.—ARAMIS color fringe plots depicting maximum deformation prior to material failure of 6- by 6-in. reinforced carbon-carbon flat panels as they undergo impact with BX–265 foam cylinders (nominally 1.25 in. in diameter by 3 in.) at a 90° angle.

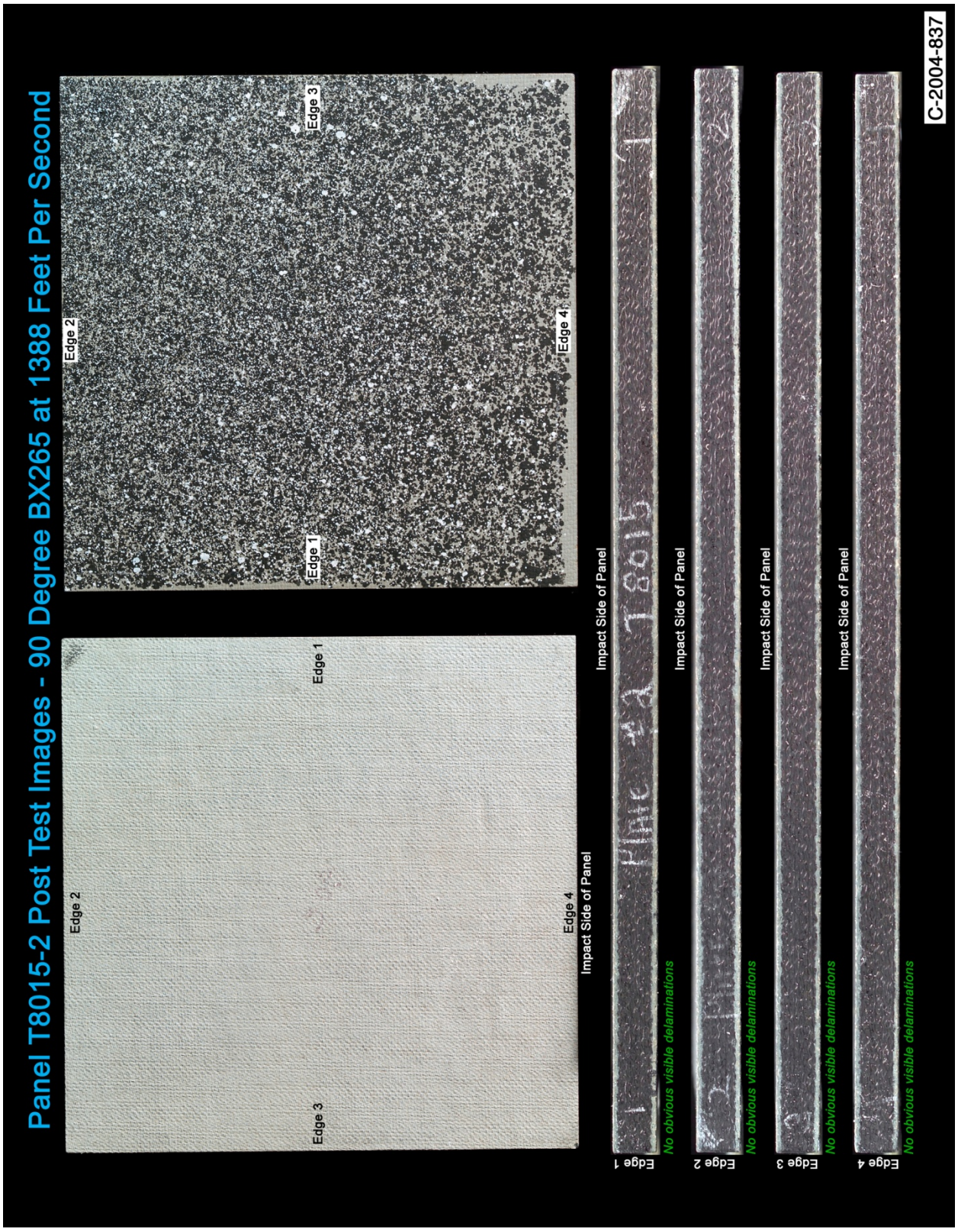

Figure A5–1.—Digital photography of edges and faces of panel T8015–2 at 1388 ft/s with a BX–265 foam cylinder (nominally 1.25 in. in diameter by 3 in.) at a 90° impact angle. Test GRCC 17.

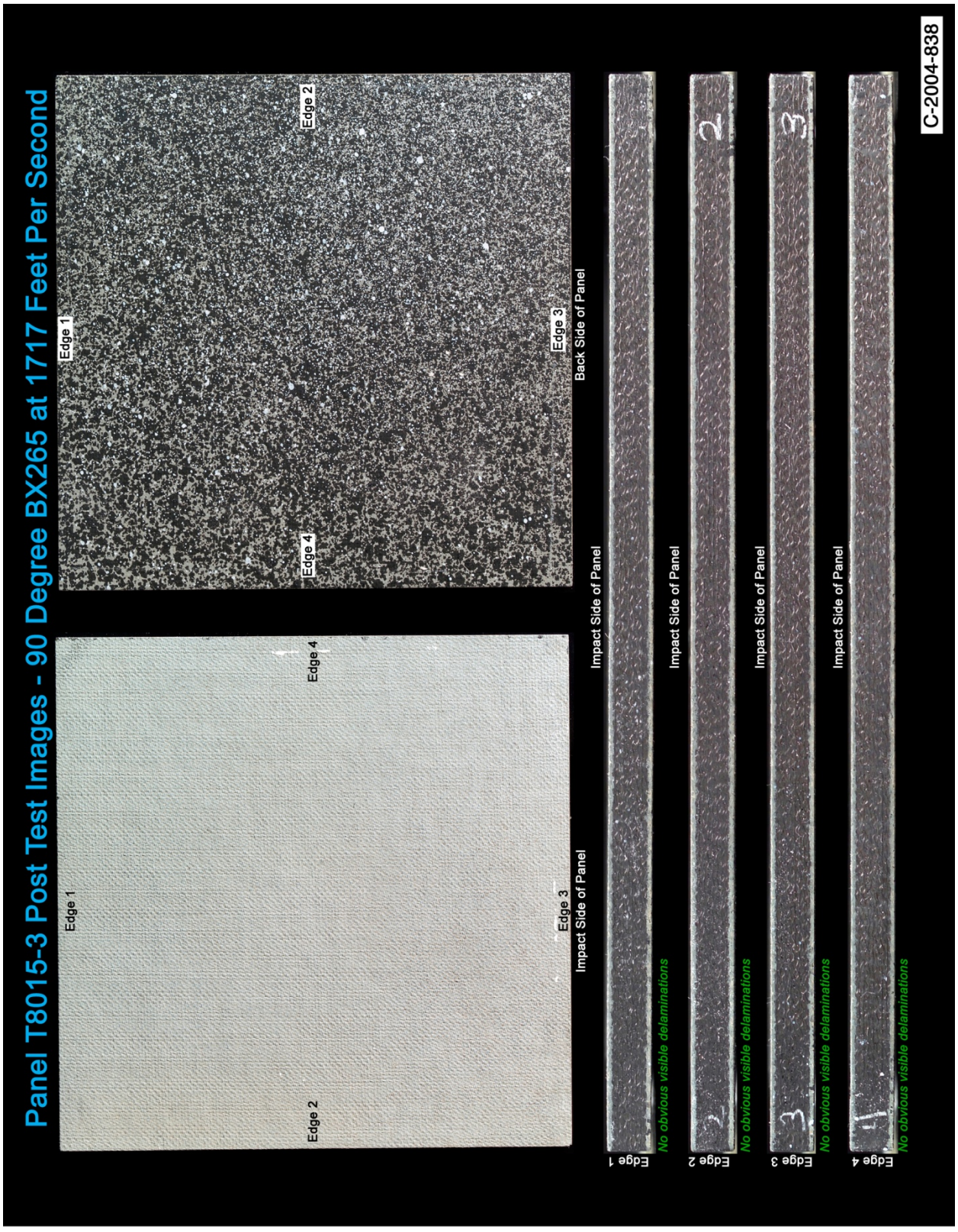

Figure A6–1.—Digital photography of edges and faces of panel T8015–3 at 1717 ft/s with a BX–265 foam cylinder (nominally 1.25 in. in diameter by 3 in.) at a 90° impact angle. Test GRCC 19.

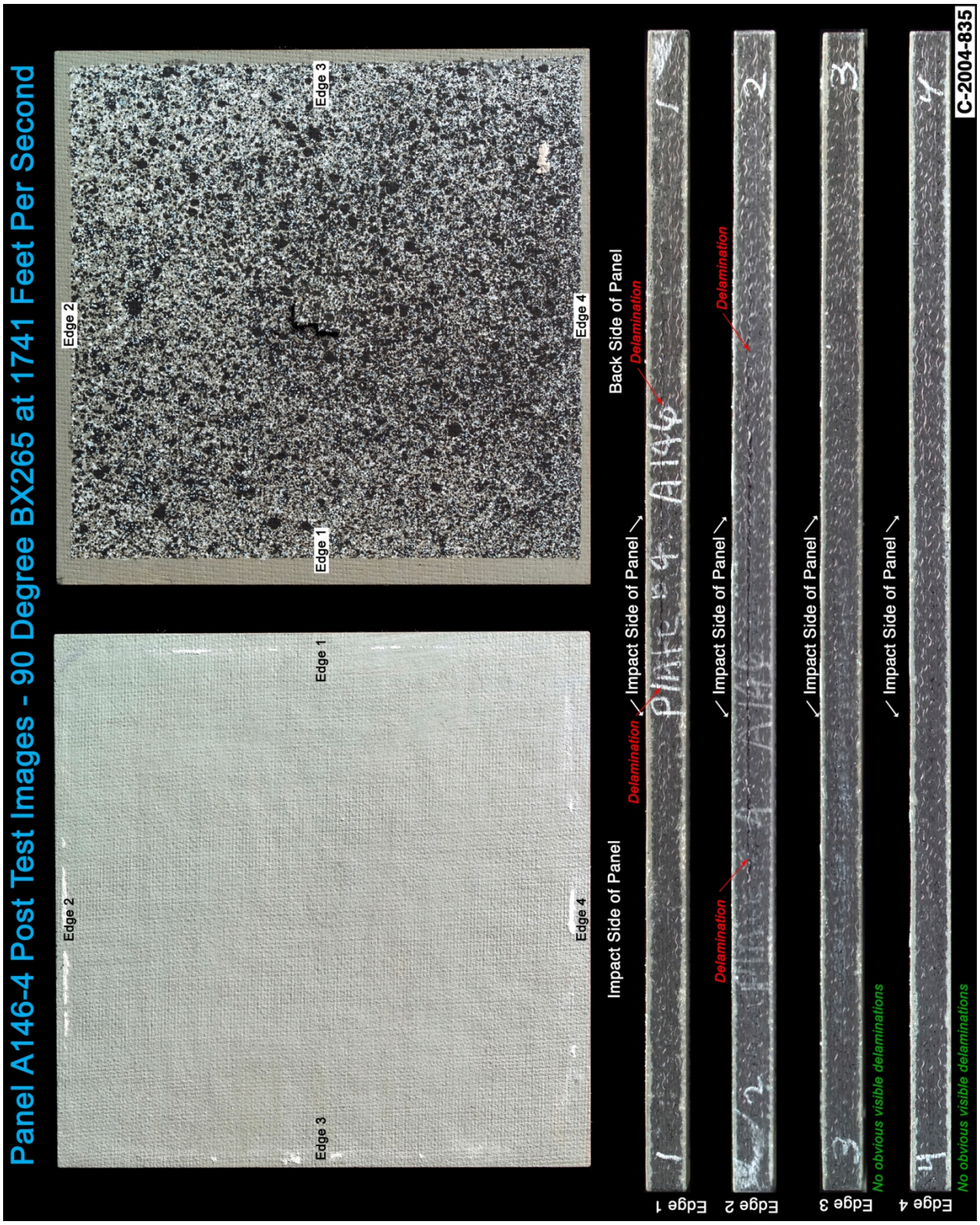

Figure A7–1.—Digital photography of edges and faces of panel A146–4 at 1741 ft/s with a BX–265 foam cylinder (nominally 1.25 in. in diameter by 3 in.) at a 90° impact angle. Test GRCC 25.

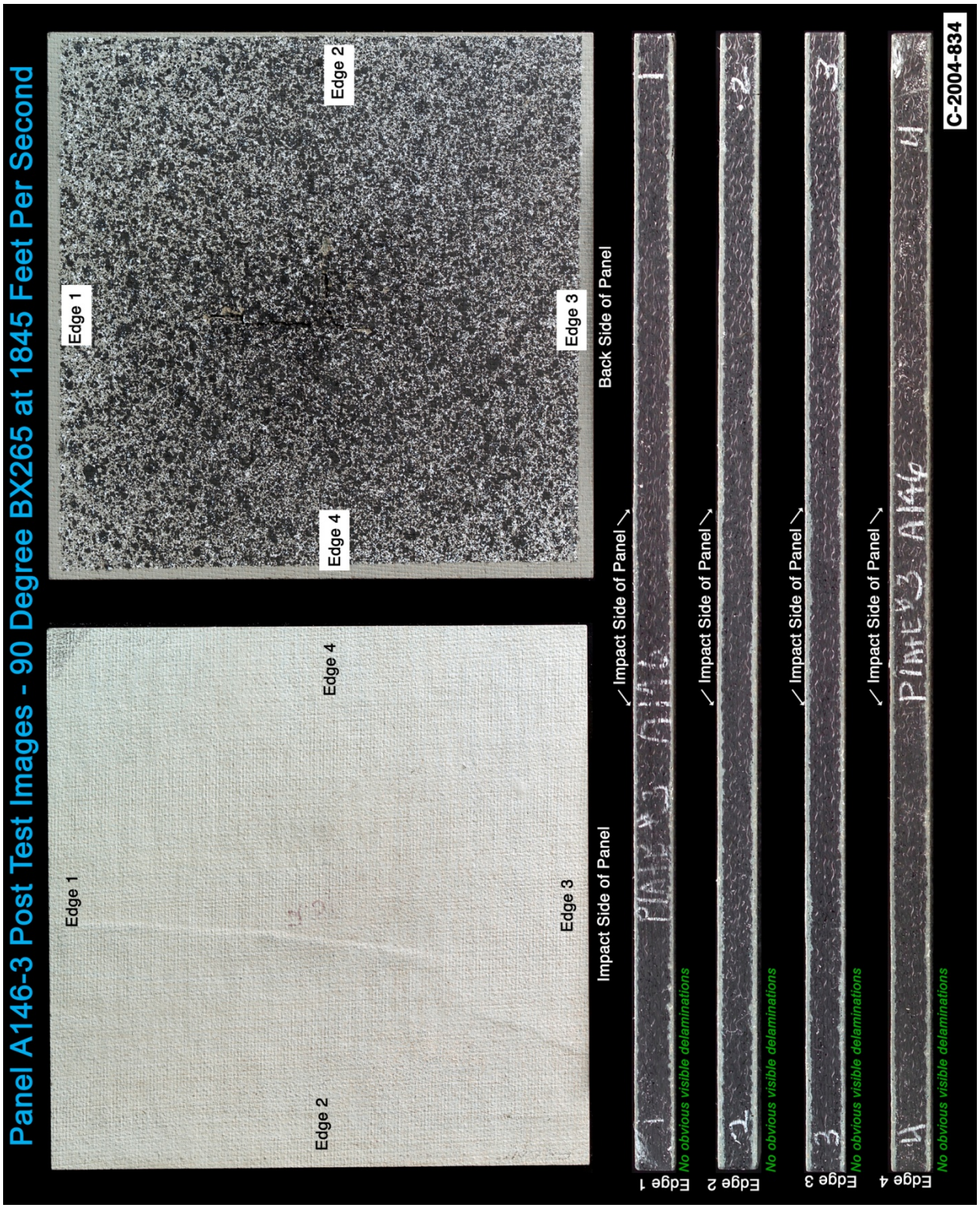

Figure A8–1.—Digital photography of edges and faces of panel A146–3 at 1845 ft/s with a BX–265 foam cylinder (nominally 1.25 in. in diameter by 3 in.) at a 90° impact angle. Test GRCC 23.

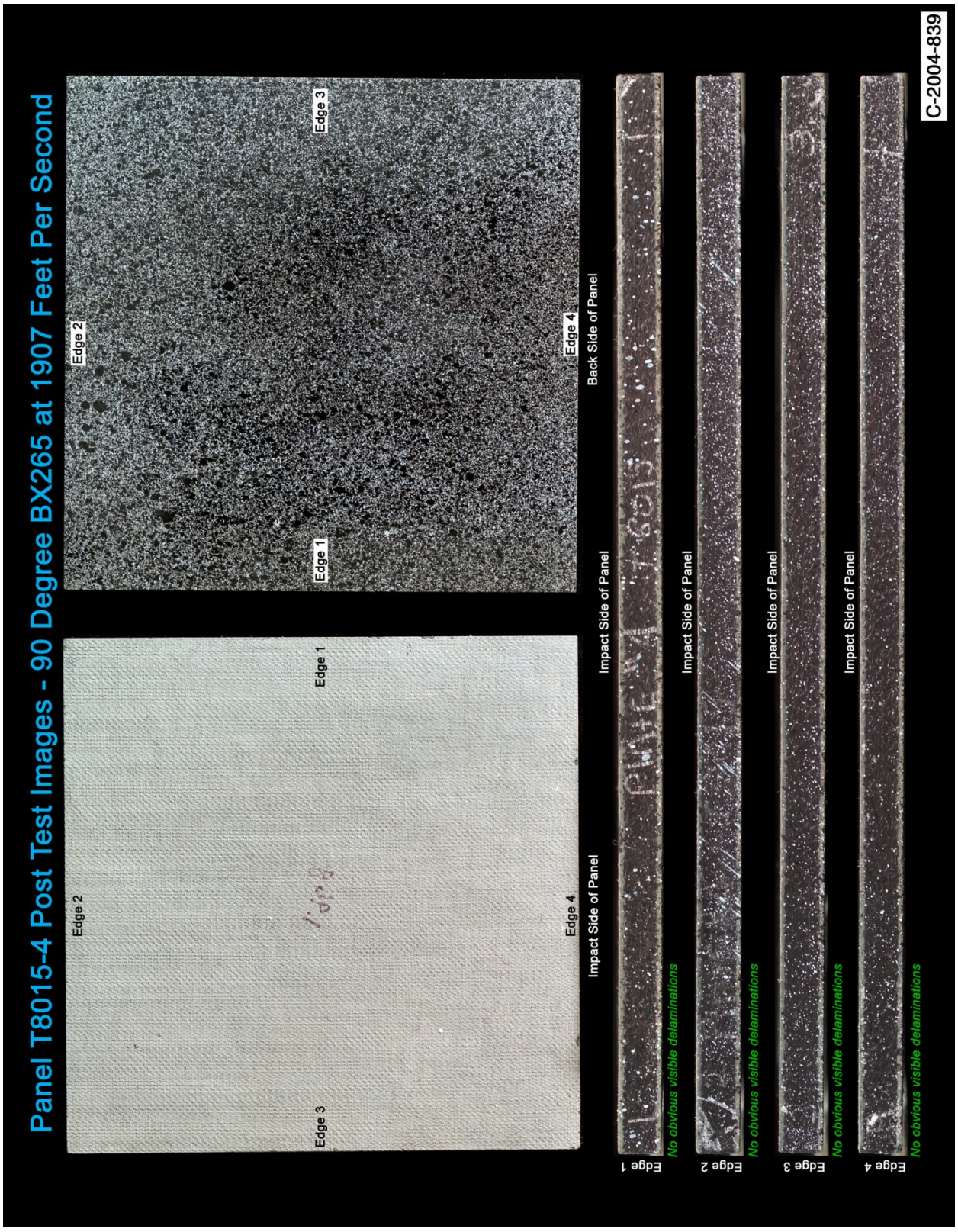

Figure A9–1.—Digital photography of edges and faces of panel T8015–4 at 1907 ft/s with a BX–265 foam cylinder (nominally 1.25 in. in diameter by 3 in.) at a 90° impact angle. Test GRCC 20.

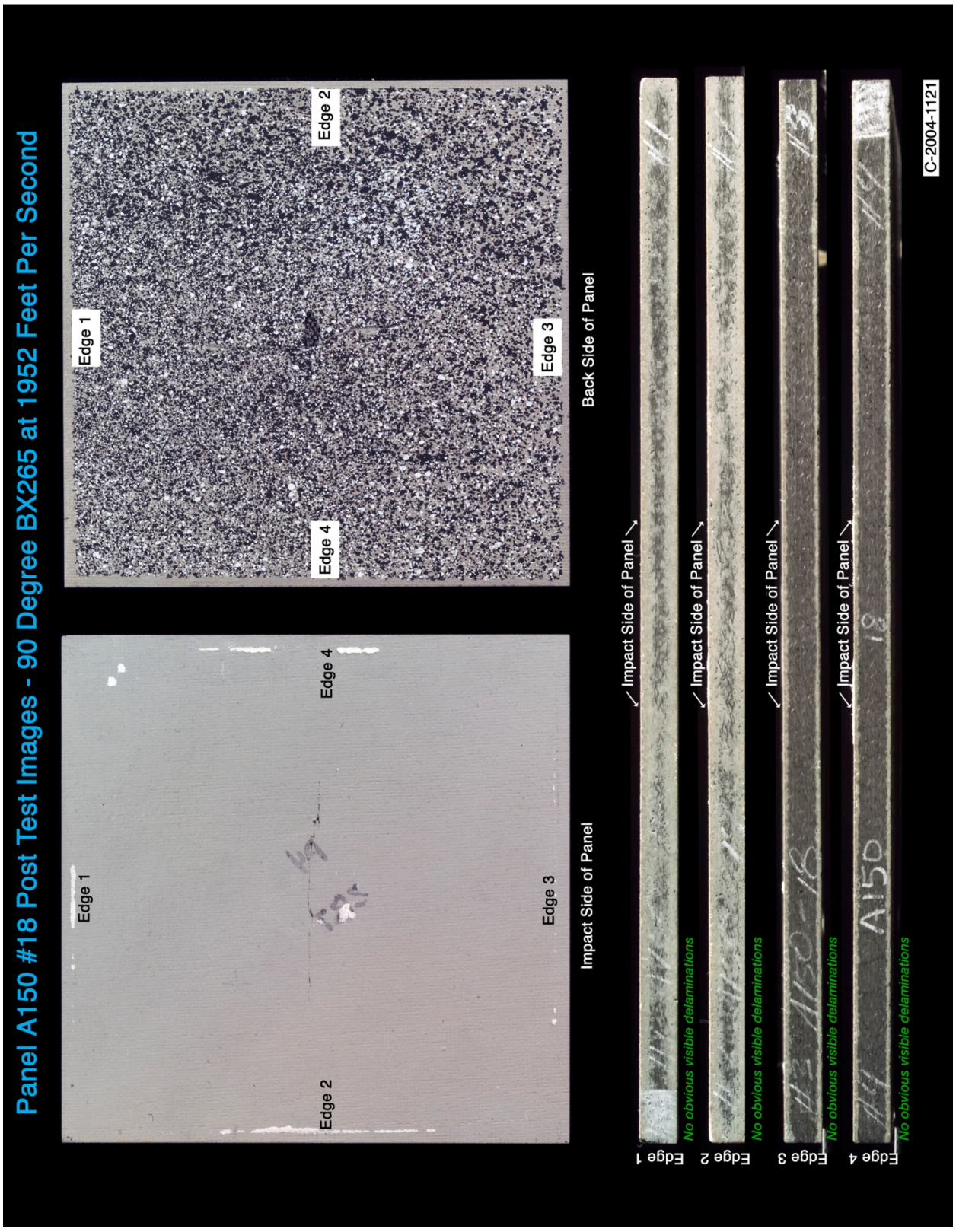

Figure A10–1.—Digital photography of edges and faces of panel A150–18 at 1952 ft/s with a BX–265 foam cylinder (nominally 1.25 in. in diameter by 3 in.) at a 90° impact angle. Test GRCC 60.

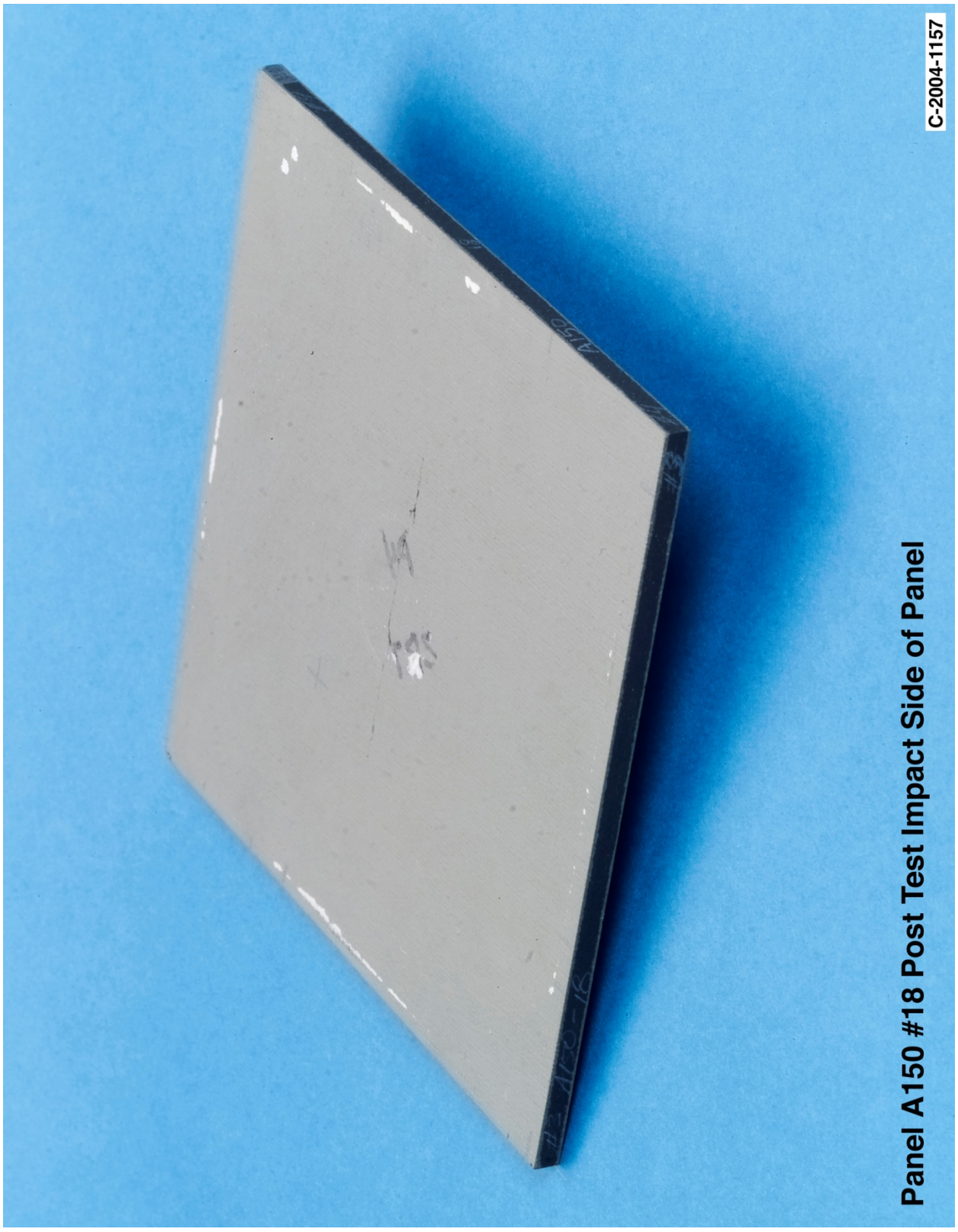

Figure A10–2.—Digital photography front (impact side) face of panel A150–18 at 1952 ft/s with a BX–265 foam cylinder (nominally 1.25 in. in diameter by 3 in.) at a 90° impact angle. Test GRCC 60.

Figure A10–3.—Digital photography of back face of panel A150–18 at 1952 ft/s with a BX–265 foam (nominally 1.25 in. in diameter by 3 in.) at a 90° impact angle. Test GRCC 60.

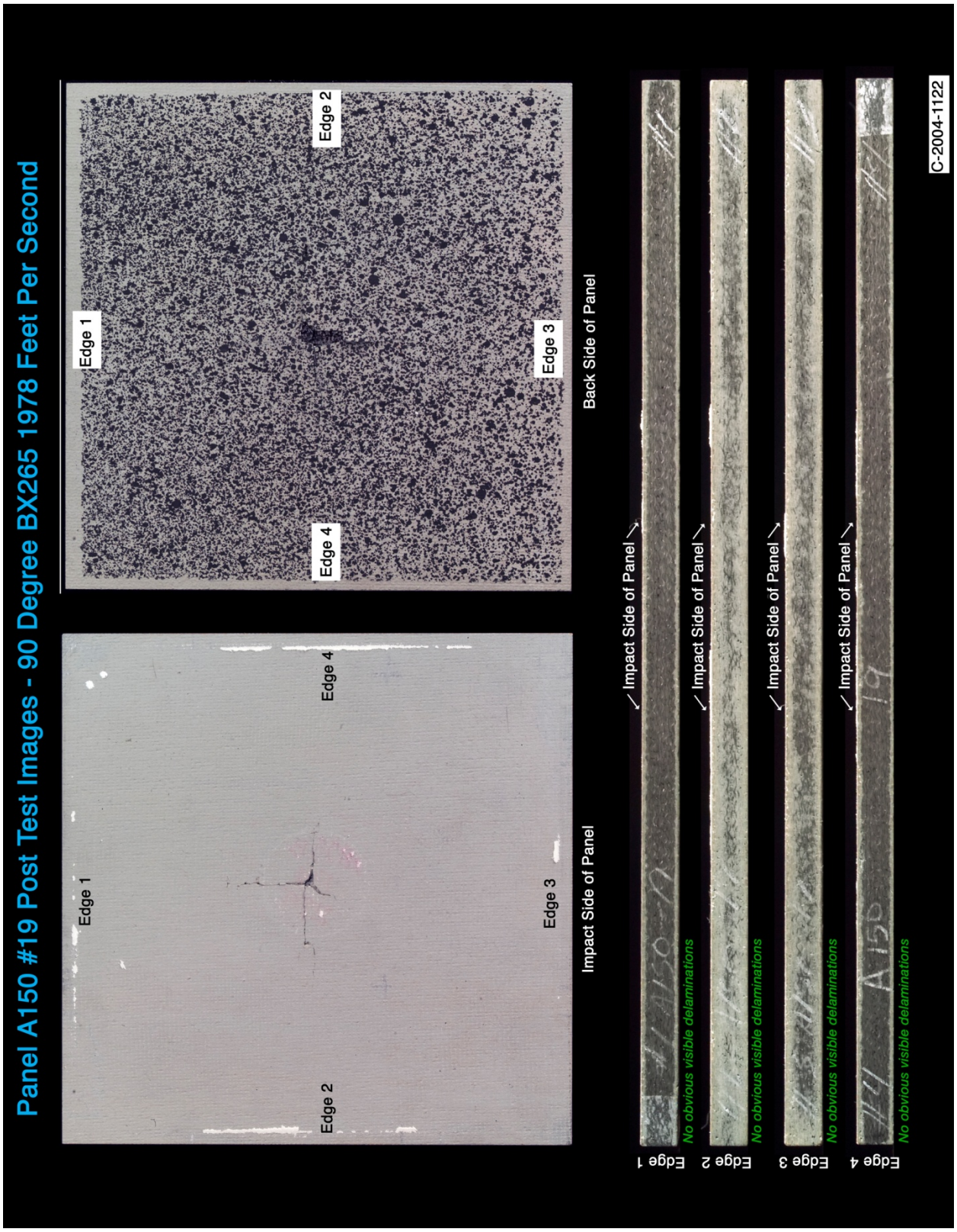

Figure A11–1.—Digital photography of edges and faces of panel A150–19 at 1978 ft/s with a BX–265 foam cylinder (nominally 1.25 in. in diameter by 3 in.) at a 90° impact angle. Test GRCC 61.

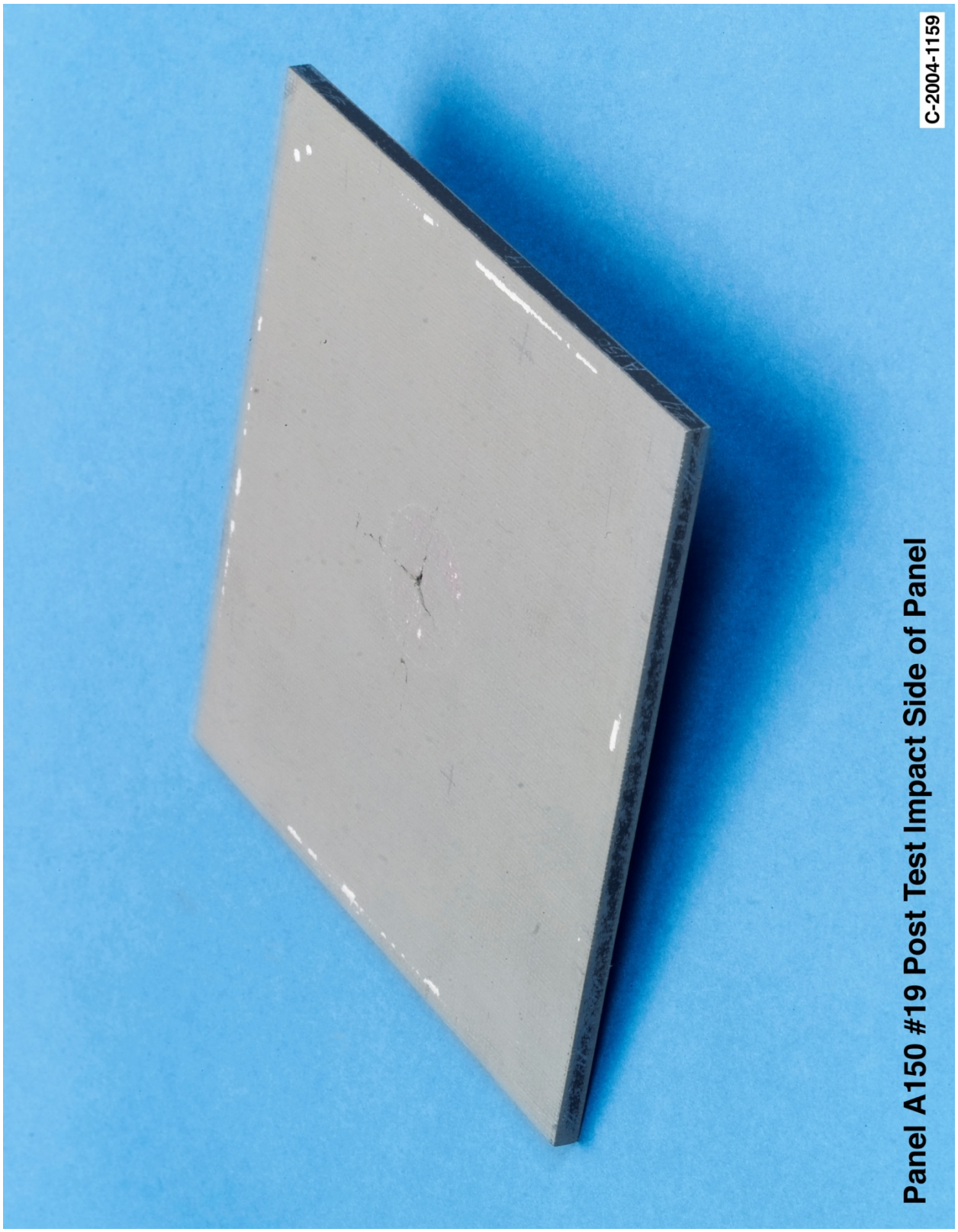

Figure A11–2.—Digital photography front (impact side) face of panel A150–19 at 1978 ft/s with a BX–265 foam cylinder (nominally 1.25 in. in diameter by 3 in.) at a 90° impact angle. Test GRCC 61.

Figure A11–3.—Digital photography of back face of panel A150–19 at 1978 ft/s with a BX–265 foam cylinder (nominally 1.25 in. in diameter by 3 in.) at a 90° impact angle. Test GRCC 61.

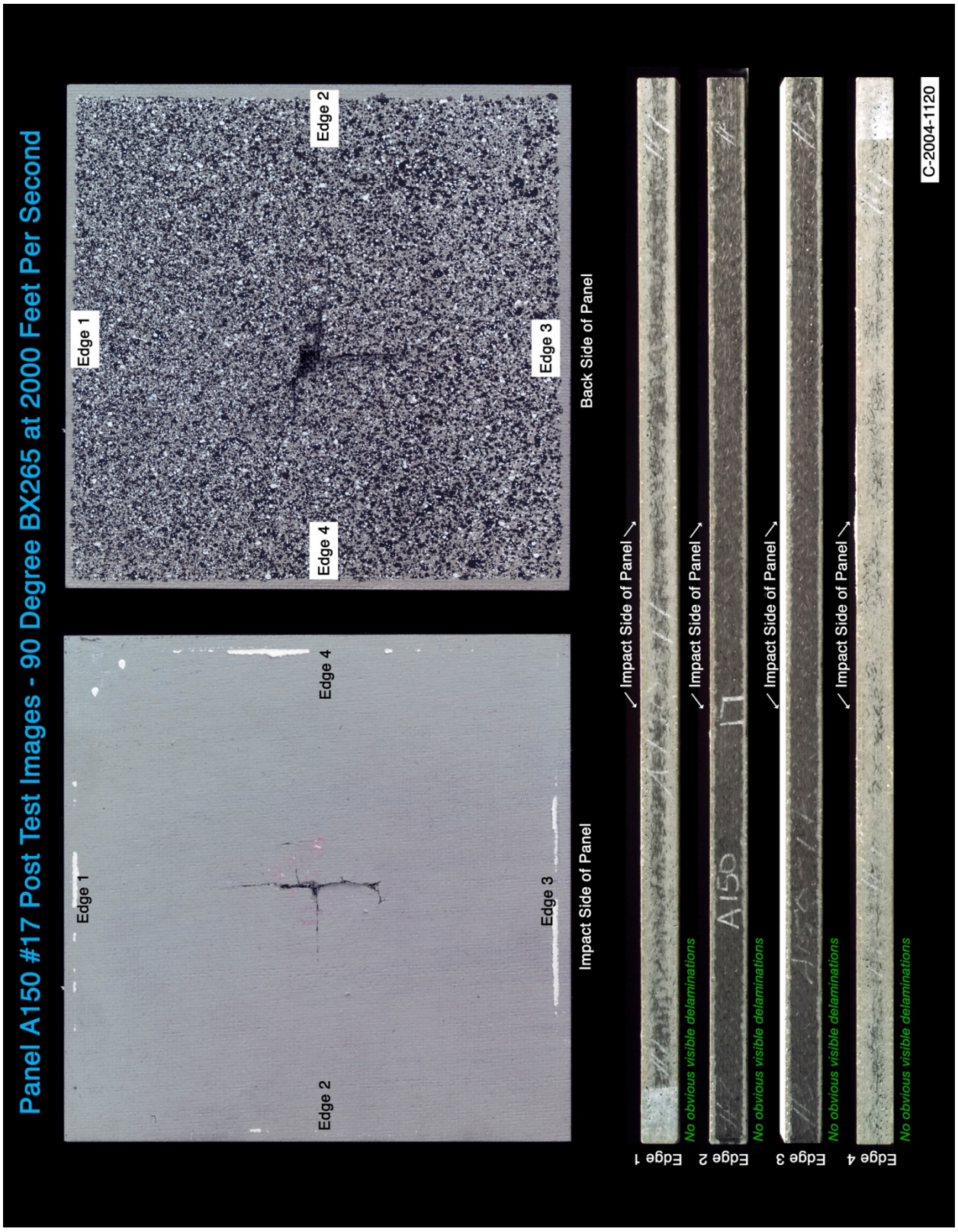

Figure A12–1.—Digital photography of edges and faces of panel A150–17 at 2000 ft/s with a BX–265 foam cylinder (nominally 1.25 in. in diameter by 3 in.) at a 90° impact angle. Test GRCC 59.

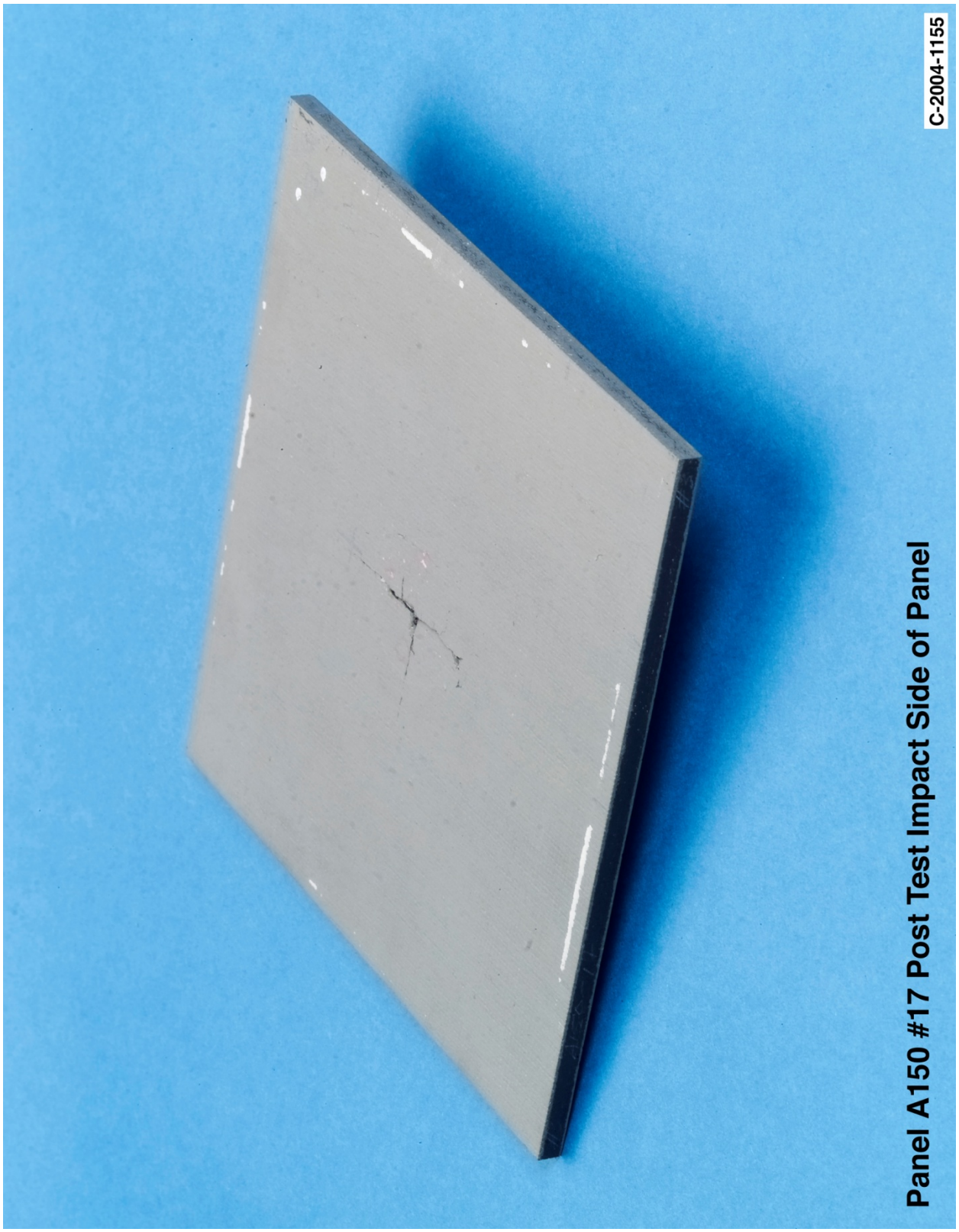

Figure A12–2.—Digital photography front (impact side) face of panel A150–17 at 2000 ft/s with a BX–265 foam cylinder (nominally 1.25 in. in diameter by 3 in.) at a 90° impact angle. Test GRCC 59.

Figure A12–3.—Digital photography of back face of panel A150–17 at 2000 ft/s with a BX–265 foam cylinder (nominally 1.25 in. in diameter by 3 in.) at a 90° impact angle. Test GRCC 59.

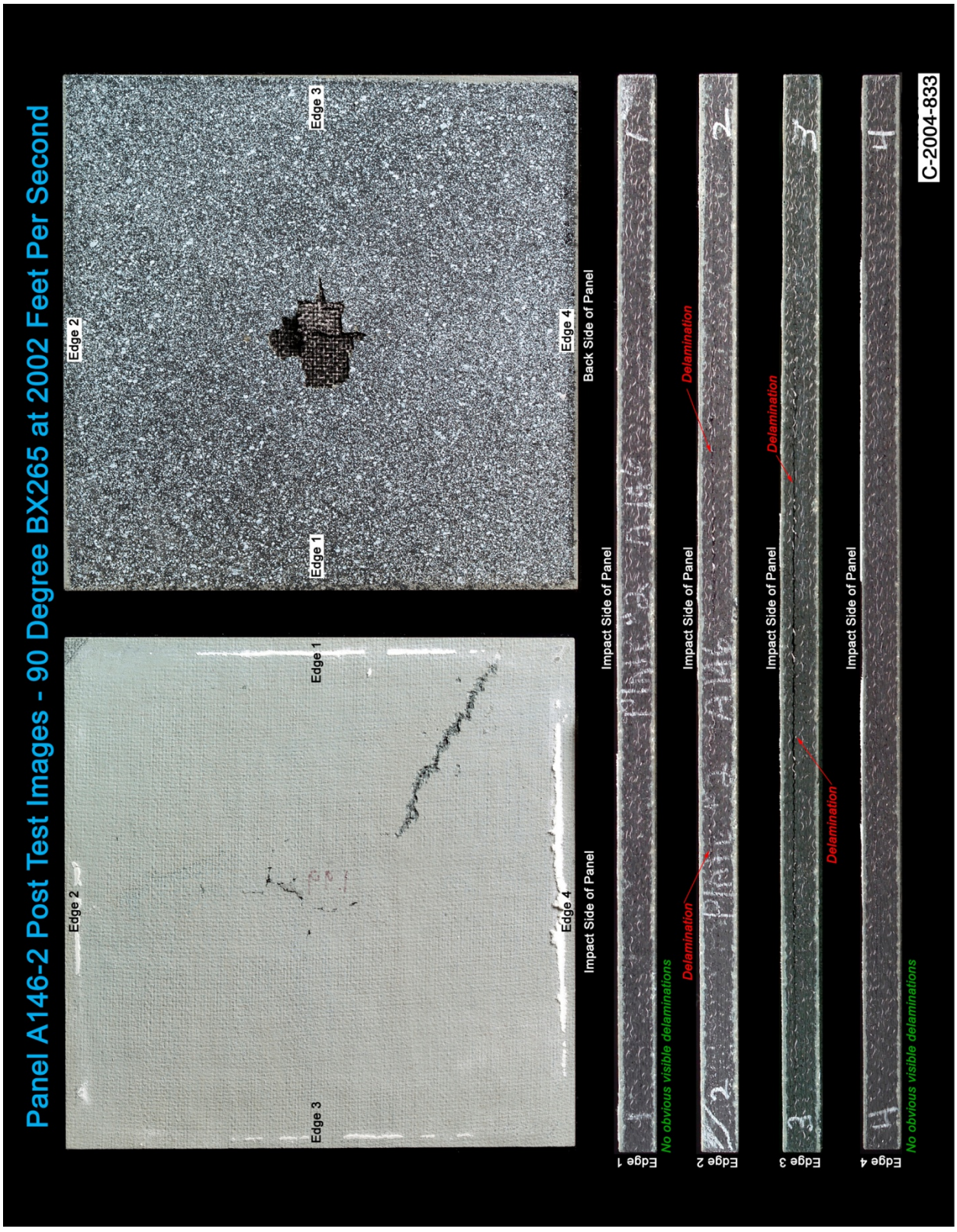

Figure A13–1.—Digital photography of edges and faces of panel A146–2 at 2002 ft/s with a BX–265 foam cylinder (nominally 1.25 in. in diameter by 3 in.) at a 90° impact angle. Test GRCC 22.

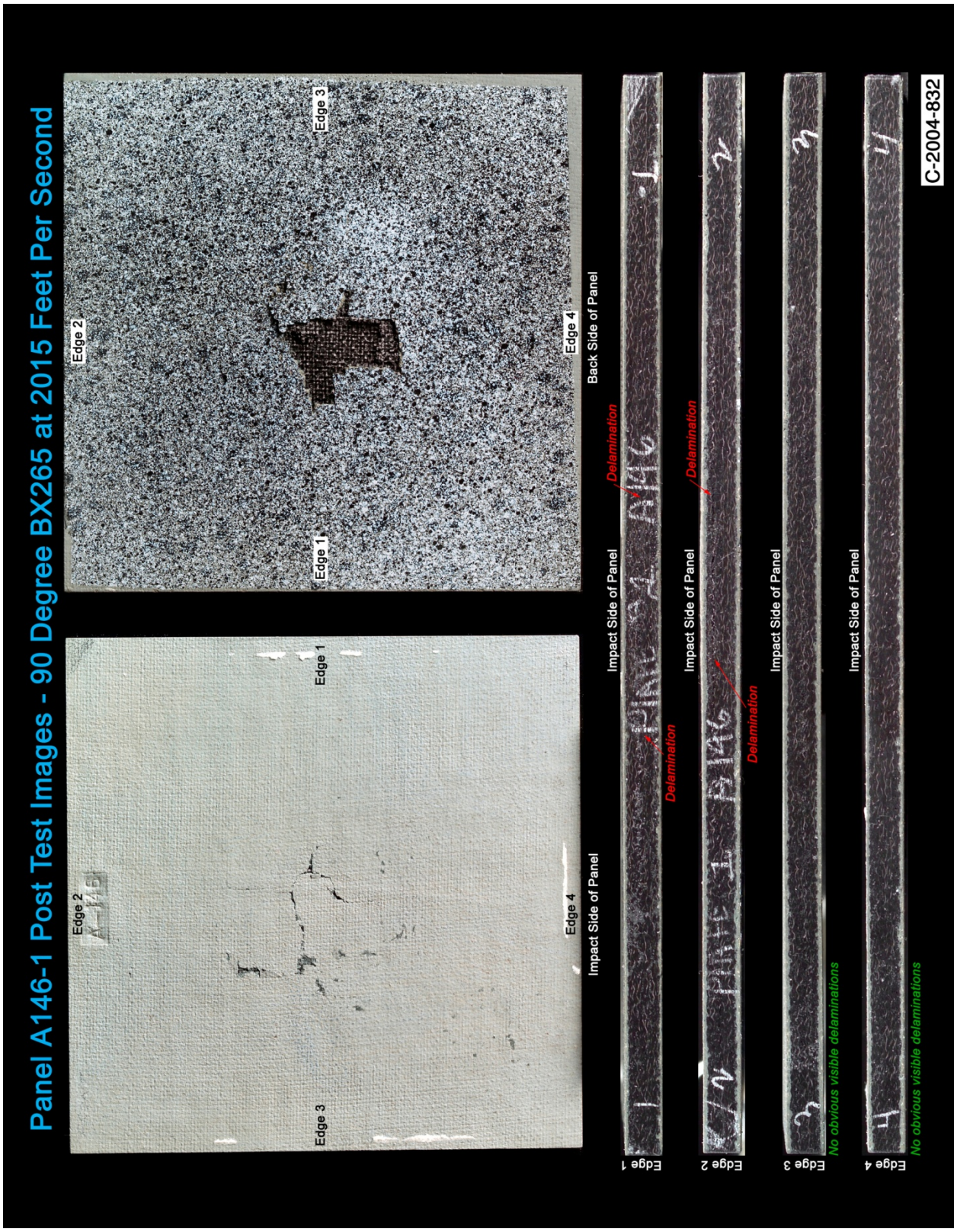

Figure A14–1.—Digital photography of edges and faces of panel A146–1 at 2015 ft/s with a BX–265 foam cylinder (nominally 1.25 in. in diameter by 3 in.) at a 90° impact angle. Test GRCC 21.

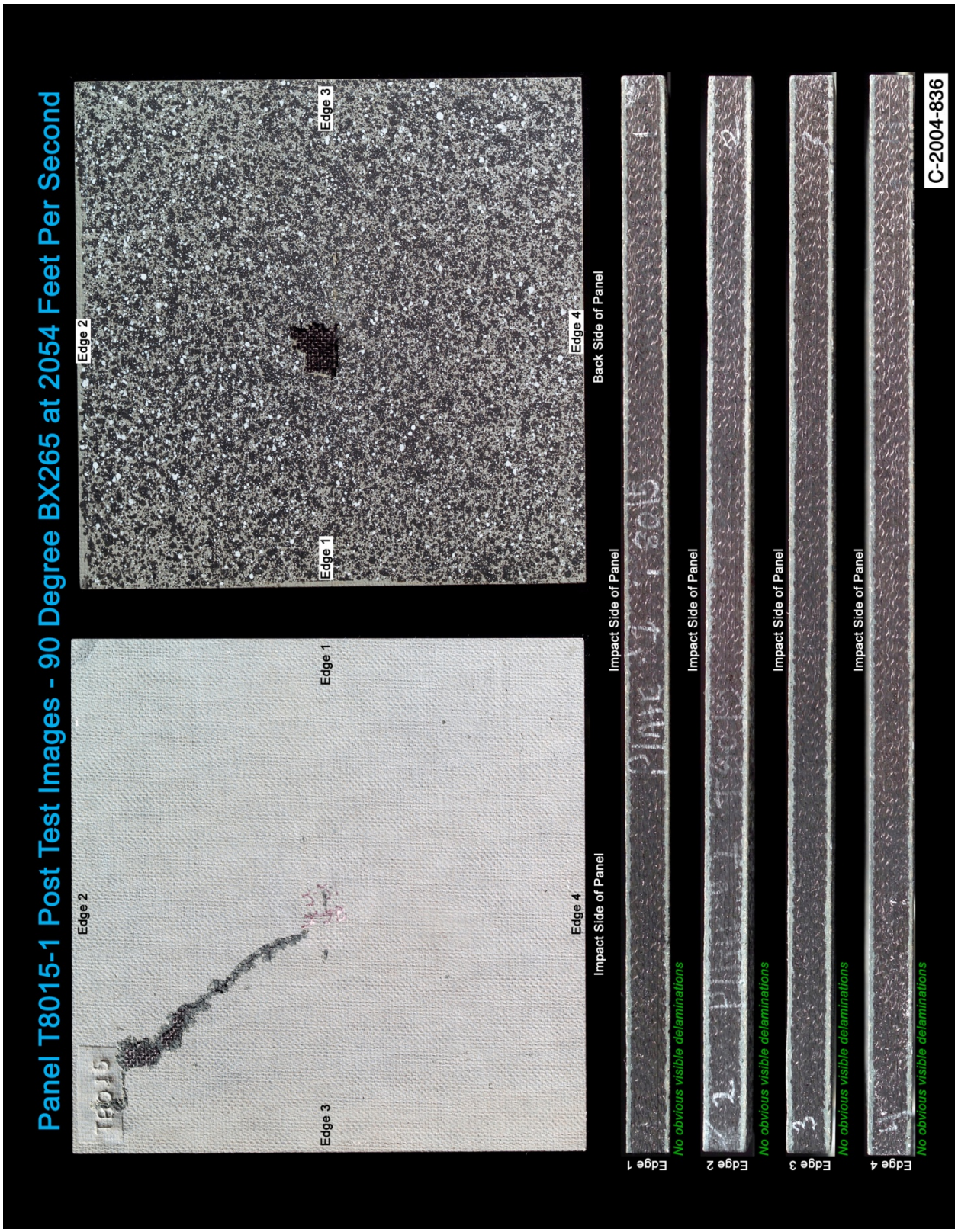

Figure A15–1.—Digital photography of edges and faces of panel T8015–1 at 2054 ft/s with a BX–265 foam cylinder (nominally 1.25 in. in diameter by 3 in.) at a 90° impact angle. Test GRCC 15.

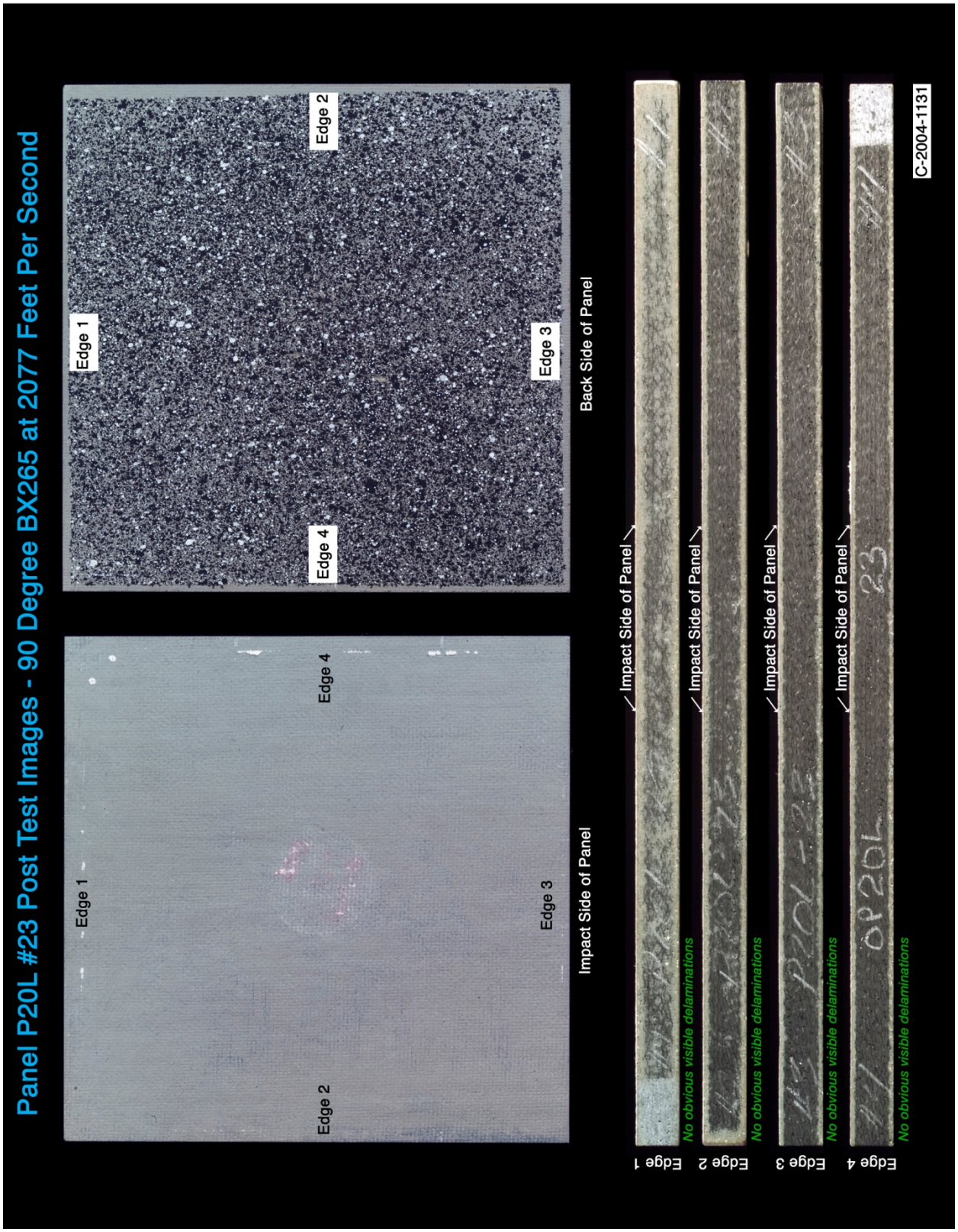

Figure A16–1.—Digital photography of edges and faces of panel P20L–23 at 2077 ft/s with a BX–265 foam cylinder (nominally 1.25 in. in diameter by 3 in.) at a 90° impact angle. Test GRCC 57.

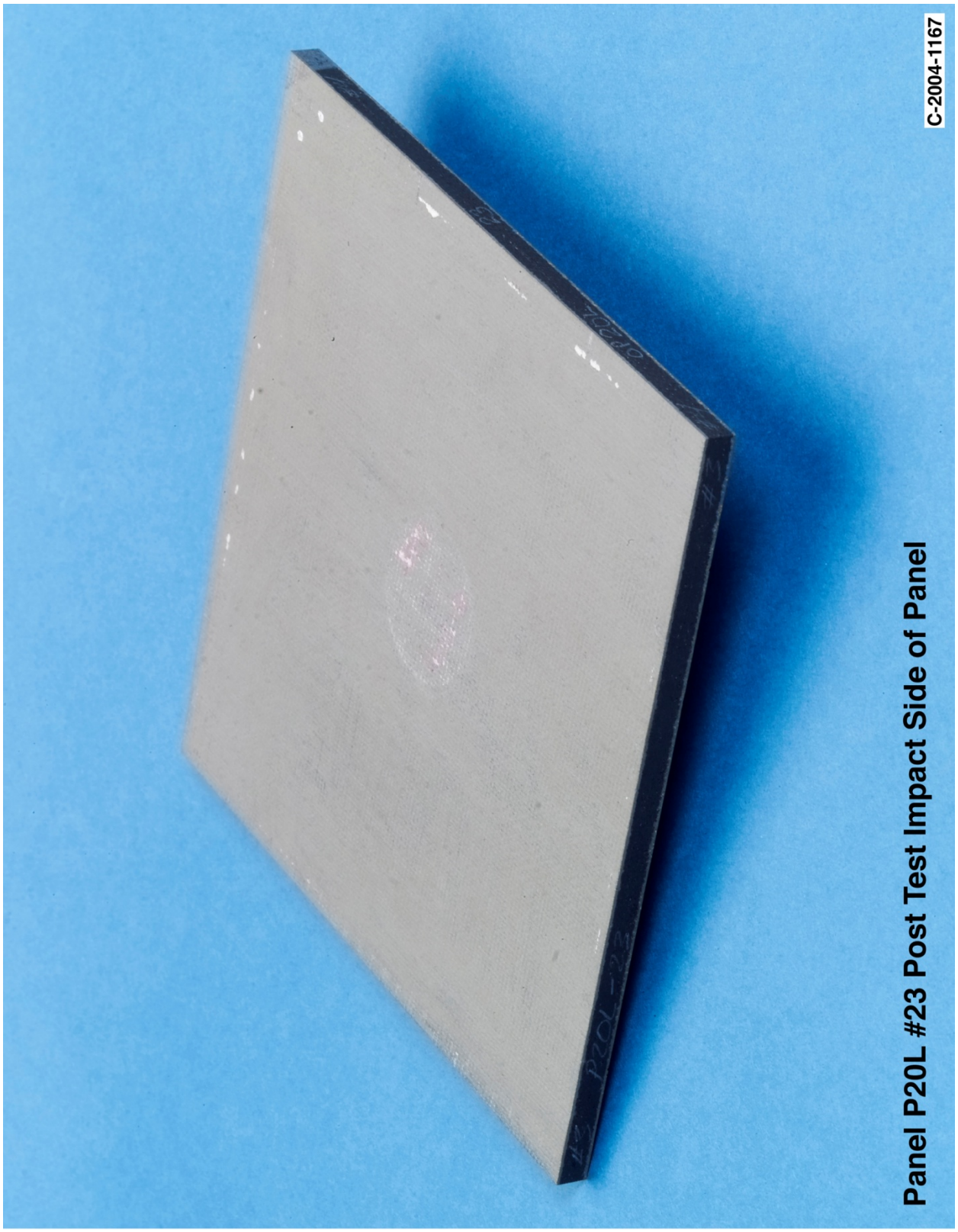

Figure A16–2.—Digital photography front (impact side) face of panel P20L–23 at 2077 ft/s with a BX–265 foam cylinder (nominally 1.25 in. in diameter by 3 in.) at a 90° impact angle. Test GRCC 57.

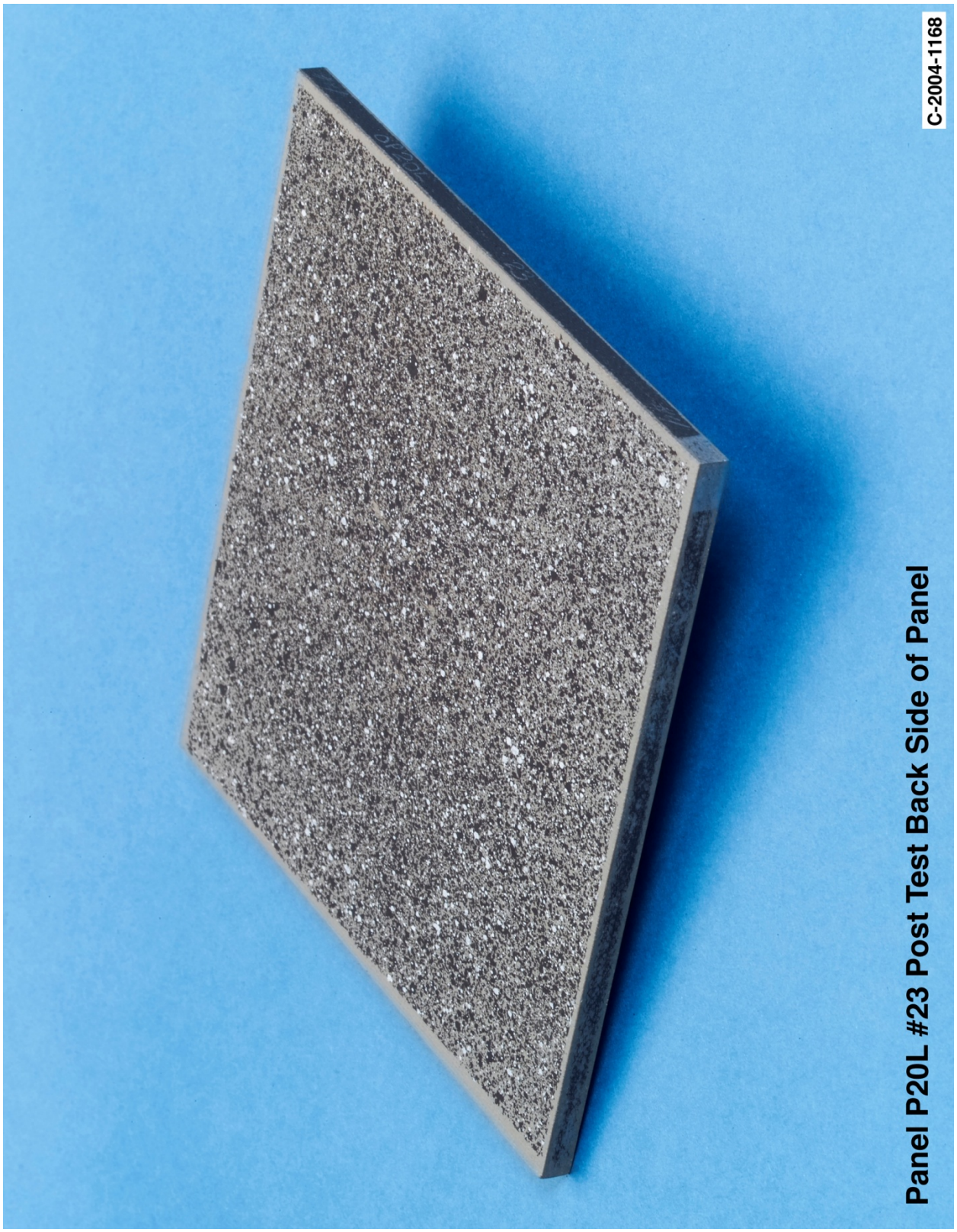

Figure A16–3.—Digital photography of back face of panel P20L–23 at 2077 ft/s with a BX–265 foam cylinder (nominally 1.25 in. in diameter by 3 in.) at a 90° impact angle. Test GRCC 57.

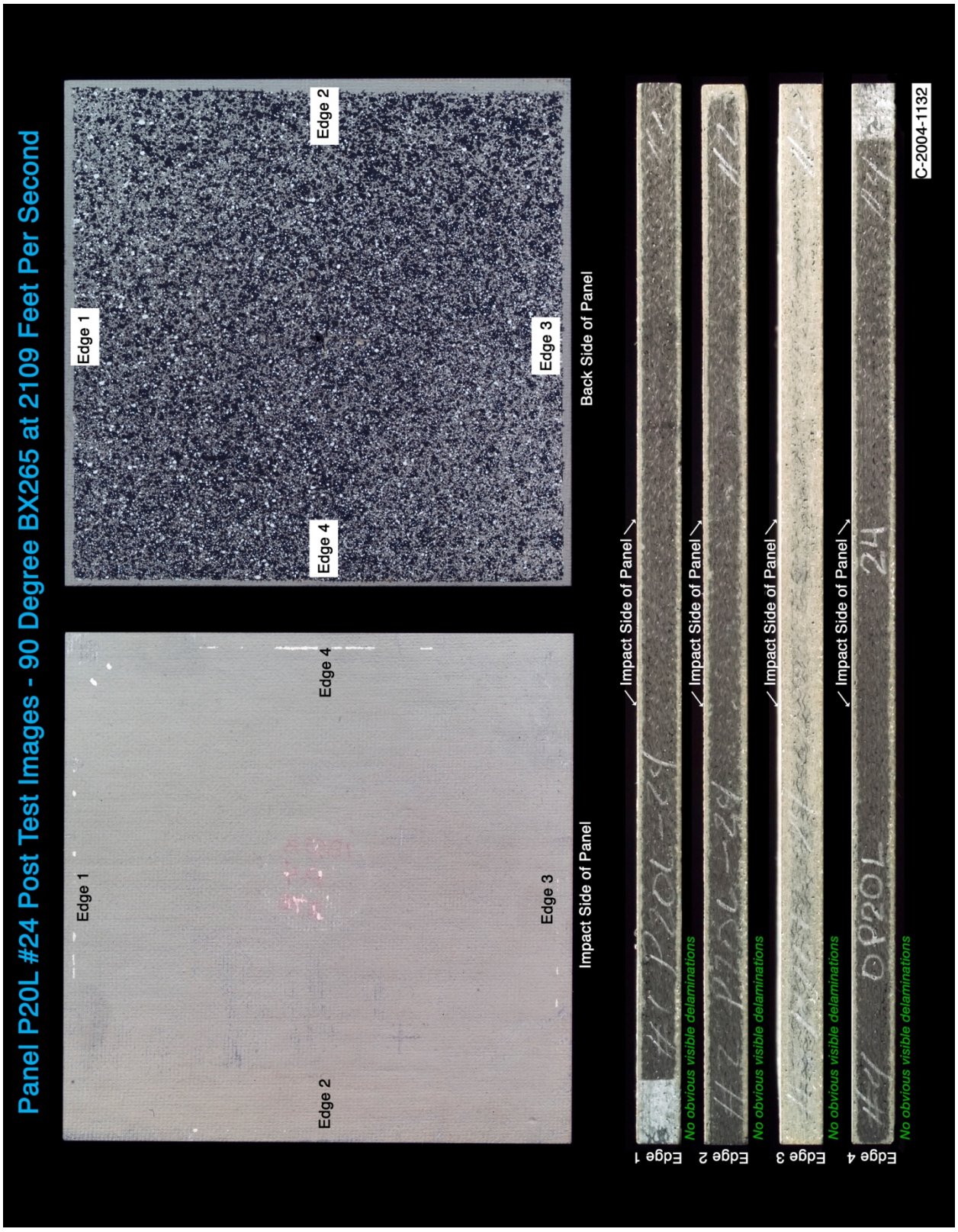

Figure A17–1.—Digital photography of edges and faces of panel P20L–24 at 2109 ft/s with a BX–265 foam cylinder (nominally 1.25 in. in diameter by 3 in.) at a 90° impact angle. Test GRCC 58.

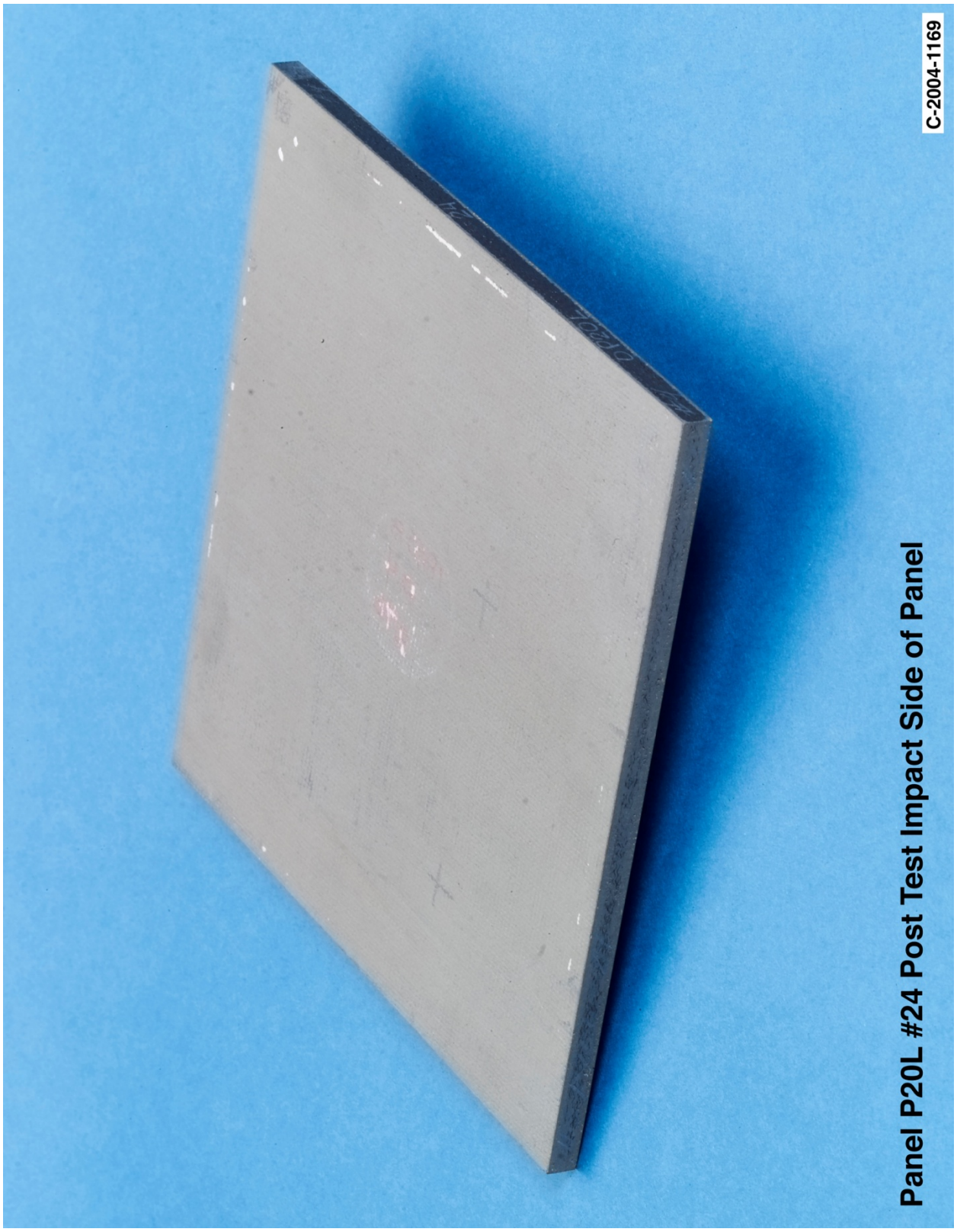

Figure A17–2.—Digital photography front (impact side) face of panel P20L–24 at 2109 ft/s with a long BX–265 foam cylinder (nominally 1.25 in. in diameter by 3 in.) at a 90° impact angle. Test GRCC 58.

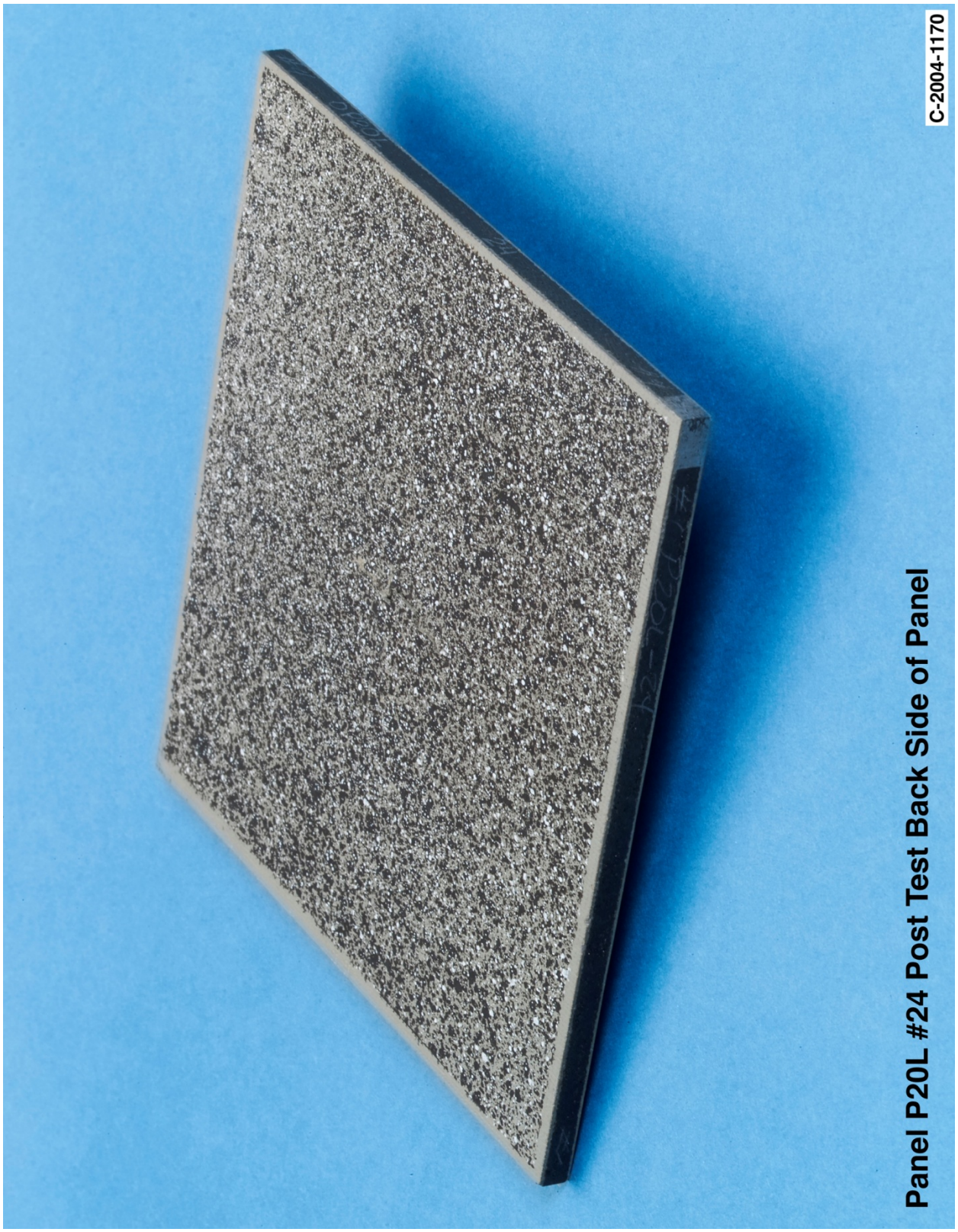

Figure A17–3.—Digital photography of back face of panel P20L–24 at 2109 ft/s with a BX–265 foam cylinder (nominally 1.25 in. in diameter by 3 in.) at a 90° impact angle. Test GRCC 58.

Appendix B.—Test Data

BX–265 External Tank Foam Impact Testing at a 45° Angle on 6- by 6-in. Reinforced Carbon-Carbon (RCC) Flat Panels

Notable Observations From the Appendix B Test Series

1. The reinforced carbon-carbon material used in this test series was “found” material.
2. Panels from parent R1–47 are considered suspect panels in this test series. For reasons not fully quantified, tests with these panels yielded inconsistent results as compared to other panels in the test series. Test results from the R1–47 panels were consequently not considered as valid but are presented in this report for completeness.
3. Lot 2 in the following test series table refers to remnant reinforced carbon-carbon material from the original qualification of ENKA (American Enka Corp.) fabric.
4. Lot 3, set 6 in the following test series table was used by Lockheed to indicate any piece of reinforced carbon-carbon that they had that could support the Return to Flight Program. They were at the reinforced carbon-carbon–3 Bimatrix condition, and resumed processing for silicon carbide (SiC) conversion coating, TEOS (tetra-ethyl-ortho-silicate, and type A.

Appendix B Test Series

BX-265 45 Degree Impact Test Parameters on 6" x 6" Reinforced Carbon-Carbon Panels

Test No.	Glenn Test Reference Number	Impact Velocity (ft/sec)	Panel ID Number	Lot Number	Average Panel Thickness (inches)	Visual Damage Observations	Mass of panel before test (grams)	Mass of panel after test (grams)	Projectile Weight (g)	Projectile Length (in)	Projectile Diameter (in)	Test Date	Projectile ID Number
1-45-R14716-12	GRCC040	100	R1-47-16	2	0.231	No damage, low speed misfire	202.25	202.19	3.050	2.714	1.474	8/2/04	Foam: BX 265, JR1855 P4 219A
1-45-R14715-11	GRCC031	550	R1-47-15	2	0.233	No damage, low speed misfire	201.69	201.55	2.800	3.048	1.490	7/22/04	Foam: BX 265, JR1871 16-34
1-45-R28509-13	GRCC041	1244	R285-9	2	0.244	No significant indications	220.51	220.34	3.020	2.549	1.497	8/2/04	Foam: BX 265, JR1855 P4 219B
1-45-R14714-10	GRCC030	1471	R1-47-14	2	0.232	small backside coating loss	201.34	201.25	2.970	3.030	1.495	7/22/04	Foam: BX 265 8-11
1-45-R28510-14	GRCC043	1837	R285-10	2	0.246	No significant indications	216.98	216.67	3.070	3.035	1.499	8/2/04	Foam: BX 265, JR1855 P4 290B
1-45-R28421-20	GRCC052	1910	R284-21	3, Set 6	0.242	No significant indications	222.39	222.28	3.030	3.000	1.497	8/9/04	Foam: BX 265, JR1855 P4 242B
1-45-A11226-23	GRCC055	1935	A112-26	3, Set 6	0.245	No significant indications	225.04	224.95	2.990	2.989	1.499	8/10/04	Foam: BX 265, JR1855 P4 277B
1-45-A11225-22	GRCC054	1940	A112-25	3, Set 6	0.243	No significant indications	223.50	223.44	3.040	2.992	1.497	8/9/04	Foam: BX 265, JR1855 P4 253B
1-45-R14715-18	GRCC049	1947	R1-47-15	2	0.233	No significant indications	201.56	201.45	3.010	3.003	1.497	8/4/04	Foam: BX 265, JR1855 P4 249B
1-45-R14716-17	GRCC048	1987	R1-47-16	2	0.231	Backside coating loss	201.98	183.18	3.020	3.001	1.496	8/4/04	Foam: BX 265, JR1855 P4 277A
1-45-R28422-21	GRCC053	2035	R284-22	3, Set 6	0.242	No significant indications	222.85	222.82	3.000	3.010	1.497	8/9/04	Foam: BX 265, JR1855 P4 242A
1-45-R28420-19	GRCC051	2230	R284-20	3, Set 6	0.240	small backside coating loss	224.08	223.83	3.010	2.996	1.496	8/9/04	Foam: BX 265, JR1855 P4 255B
1-45-R28512-16	GRCC046	2241	R285-12	2	0.243	Front/back coating loss	216.86	215.88	3.000	2.950	1.495	8/3/04	Foam: BX 265, JR1855 P4 221A
1-45-R14713-09	GRCC029	2371	R1-47-13	2	0.235	Through crack, large back coating loss	201.44	182.30	3.060	3.025	1.494	7/22/04	Foam: BX 265 8-10
1-45-R28511-15	GRCC045	2440	R285-11	2	0.243	Front/back coating loss	220.98	219.47	3.000	3.013	1.499	8/3/04	Foam: BX 265, JR1855 P4 221B

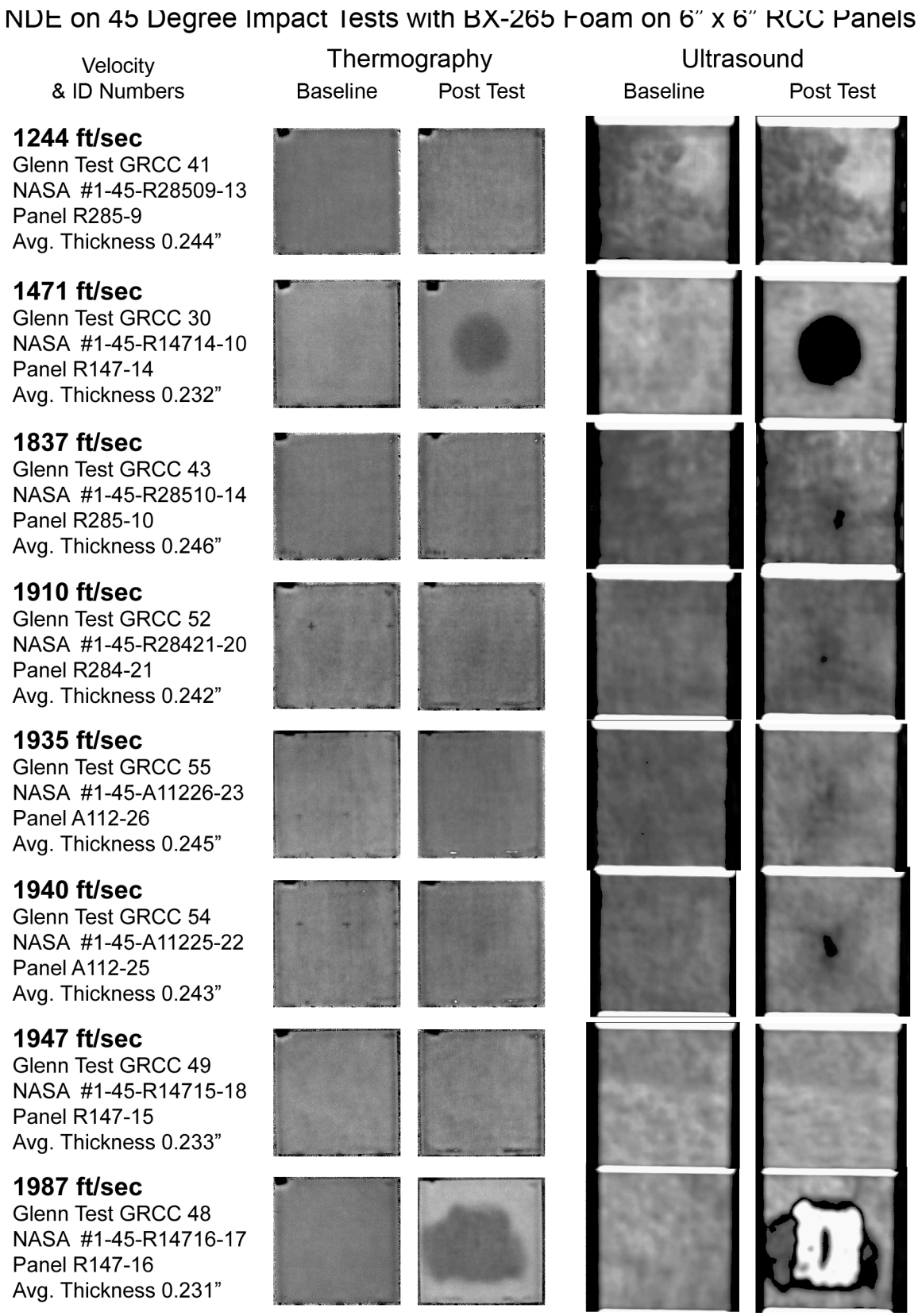

Figure B1–1.—Pulse thermography and ultrasound post impact pretest and posttest images of reinforced carbon-carbon 6- by 6-in. flat panels impacted with BX–265 foam cylinders (nominally 1.25 in. in diameter by 3 in.) at a 45° angle.

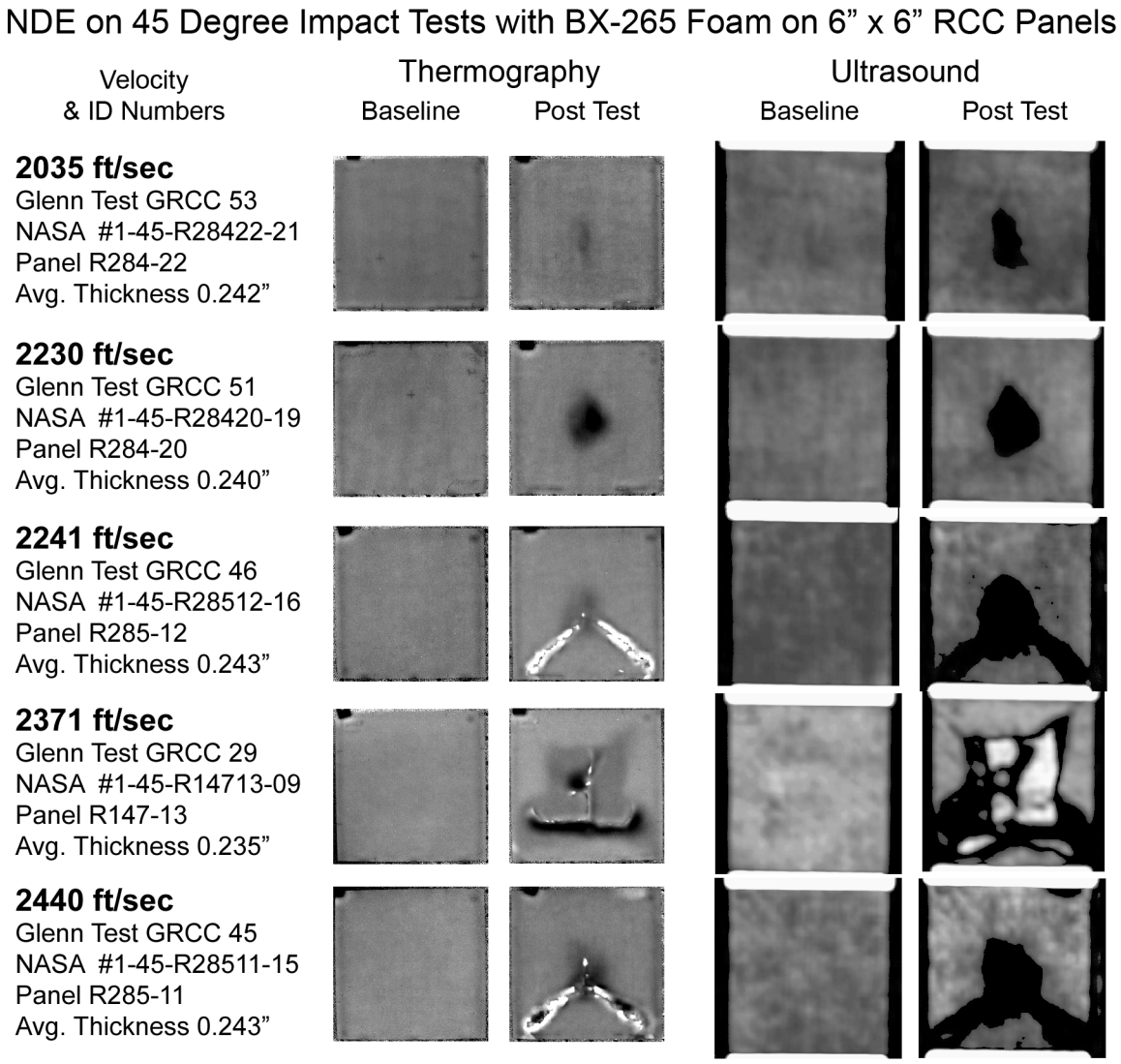

Figure B1–2.—Pulse thermography and ultrasound post impact pretest and posttest images of reinforced carbon-carbon 6- by 6-in. flat panels impacted with BX–265 foam cylinders (nominally 1.25 in. in diameter by 3 in.) at a 45° angle.

Aramis Displacement Contours from 45 Degree Impact Tests with BX-265 Foam on 6” x 6” RCC Panels

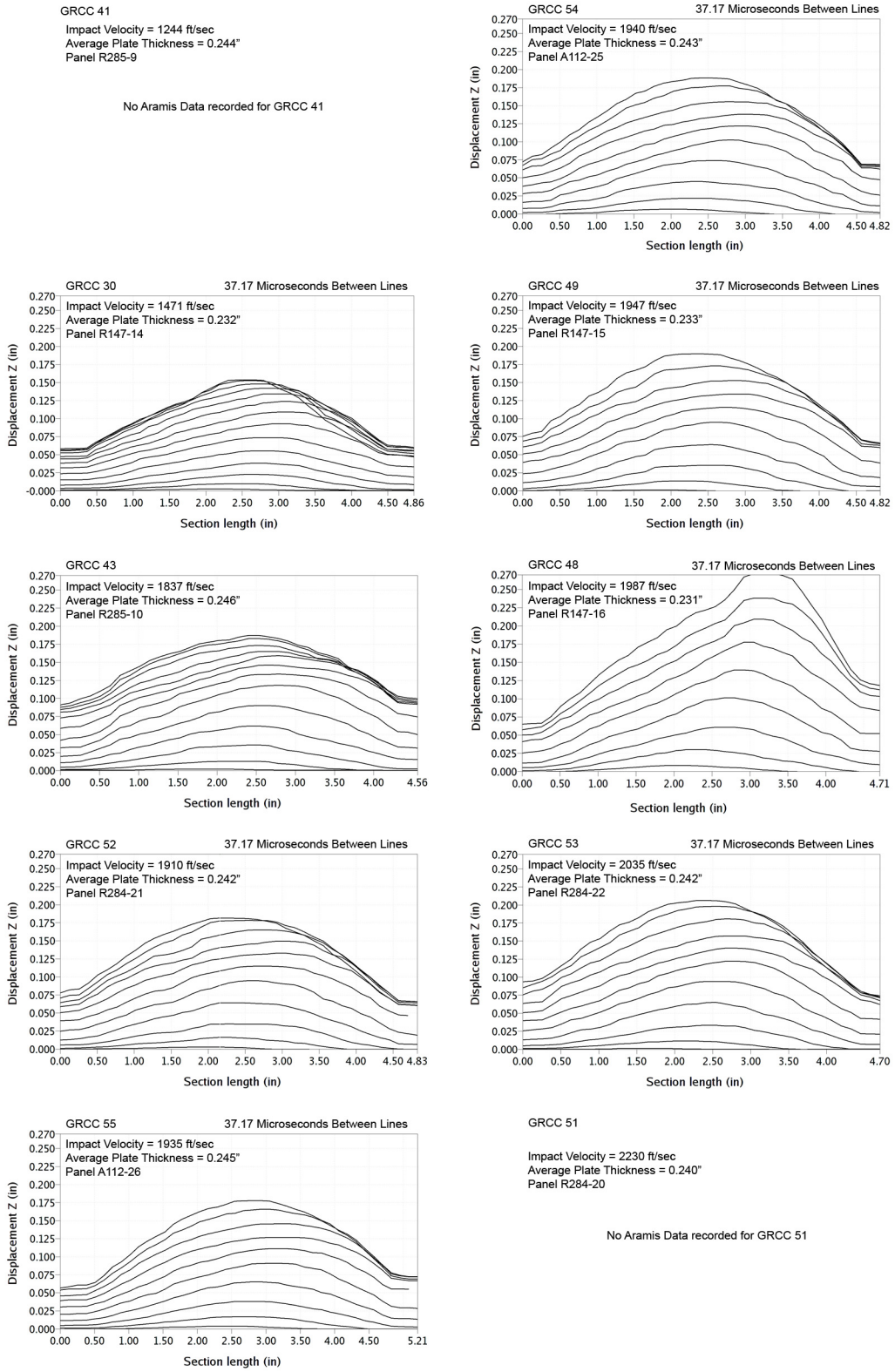

Figure B2–1.—ARAMIS out-of-plane deformation contours across centerline of 6- by 6-in. reinforced carbon-carbon flat panels measured at 37-μs increments undergoing impact with BX–265 foam cylinders (nominally 1.25 in. in diameter by 3 in.) at a 45° angle.

Aramis Displacement Contours from 45 Degree Impact Tests with BX-265 Foam on 6” x 6” RCC Panels

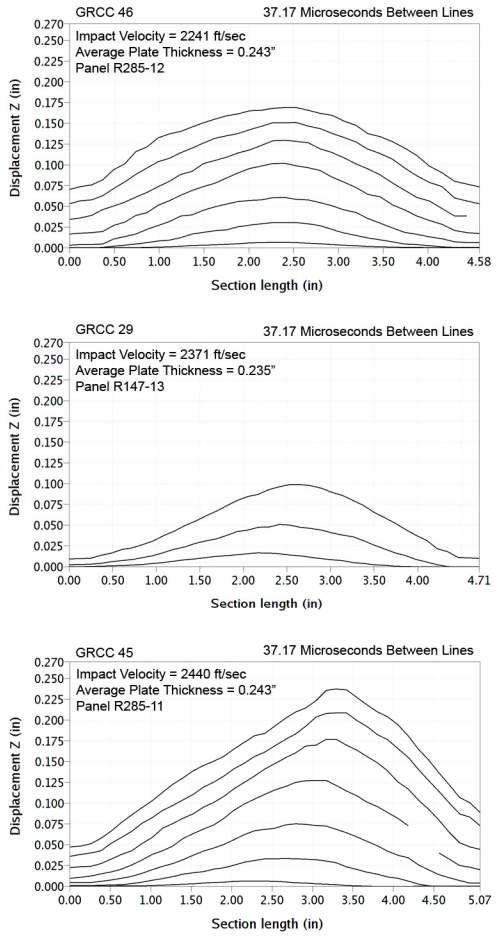

Figure B2–2.—ARAMIS out-of -plane deformation contours across centerline of 6- by 6-in. reinforced carbon-carbon flat panels plotted at 37- μs increments undergoing impact with BX–265 foam cylinders (nominally 1.25 in. in diameter by 3 in.) at a 45° angle.

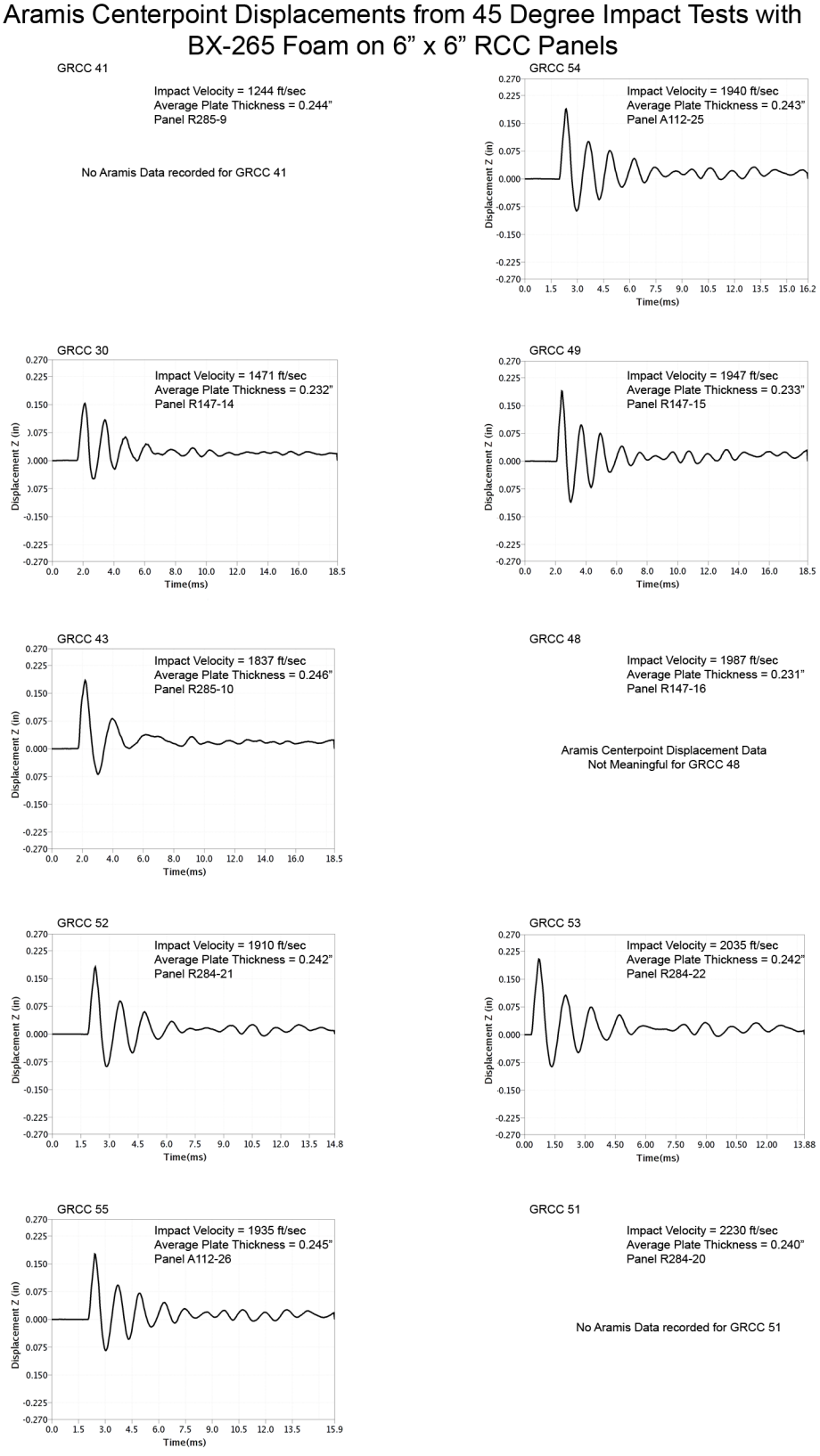

Figure B3–1.—ARAMIS centerpoint out-of-plane deformation vs. time of 6- by 6-in. reinforced carbon-carbon flat panels impacted with BX–265 foam cylinders (nominally 1.25 in. in diameter by 3 in.) at a 45° angle.

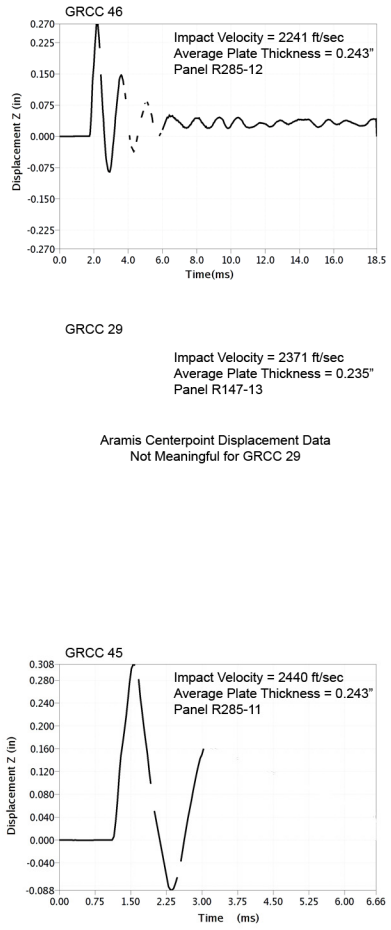

Figure B3–2.—ARAMIS centerpoint out-of-plane deformation vs. time of 6- by 6-in. reinforced carbon-carbon flat panels impacted with BX–265 foam cylinders (nominally 1.25 in. in diameter by 3 in.) at a 45° angle.

Aramis Maximum Displacement Fringe Plots from 45 Degree Impact Tests with BX-265 Foam on 6” x 6” RCC Panels

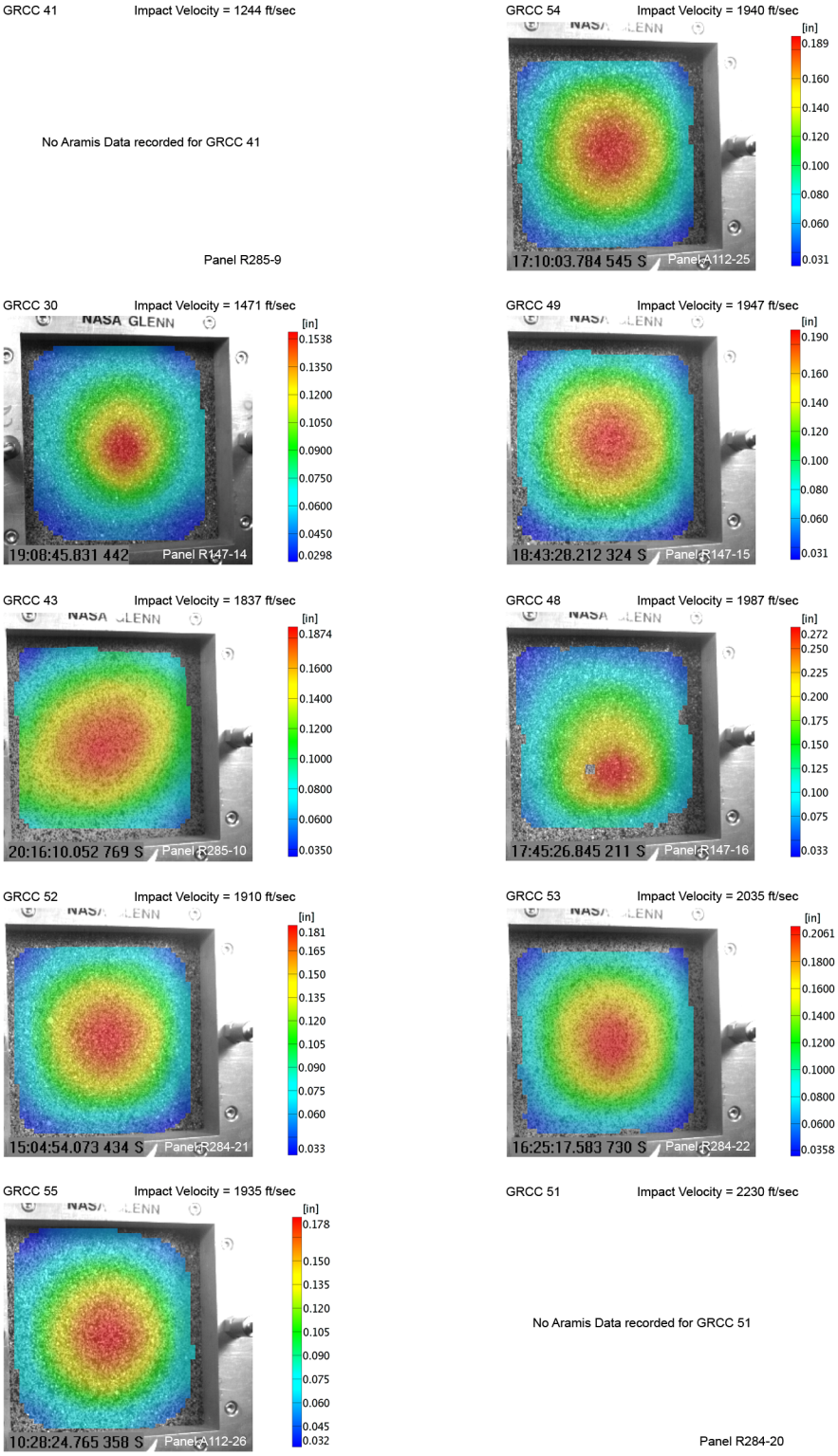

Figure B4–1.—ARAMIS color fringe plots depicting maximum deformation prior to material failure of 6- by 6-in. reinforced carbon-carbon flat panels as they undergo impact with BX–265 foam cylinders (nominally 1.25 in. in diameter by 3 in.) at a 45° angle.

Aramis Maximum Displacement Fringe Plots from 45 Degree Impact Tests with BX-265 Foam on 6” x 6” RCC Panels

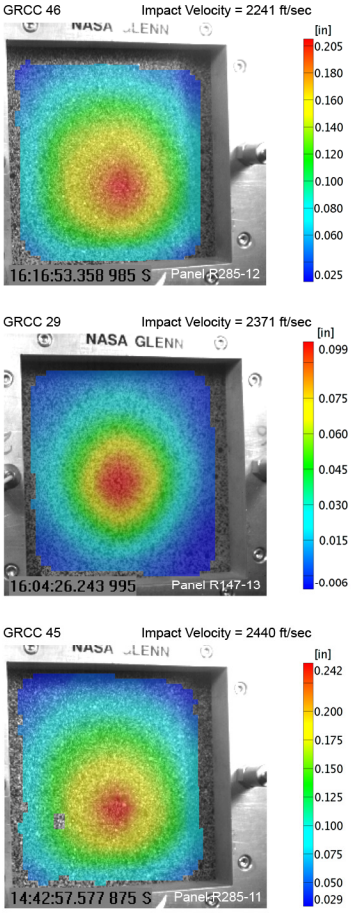

Figure B4–2.—ARAMIS color fringe plots depicting maximum deformation prior to material failure of 6- by 6-in. reinforced carbon-carbon flat panels as they undergo impact with BX–265 foam cylinders (nominally 1.25 in. in diameter by 3 in.) at a 45° angle.

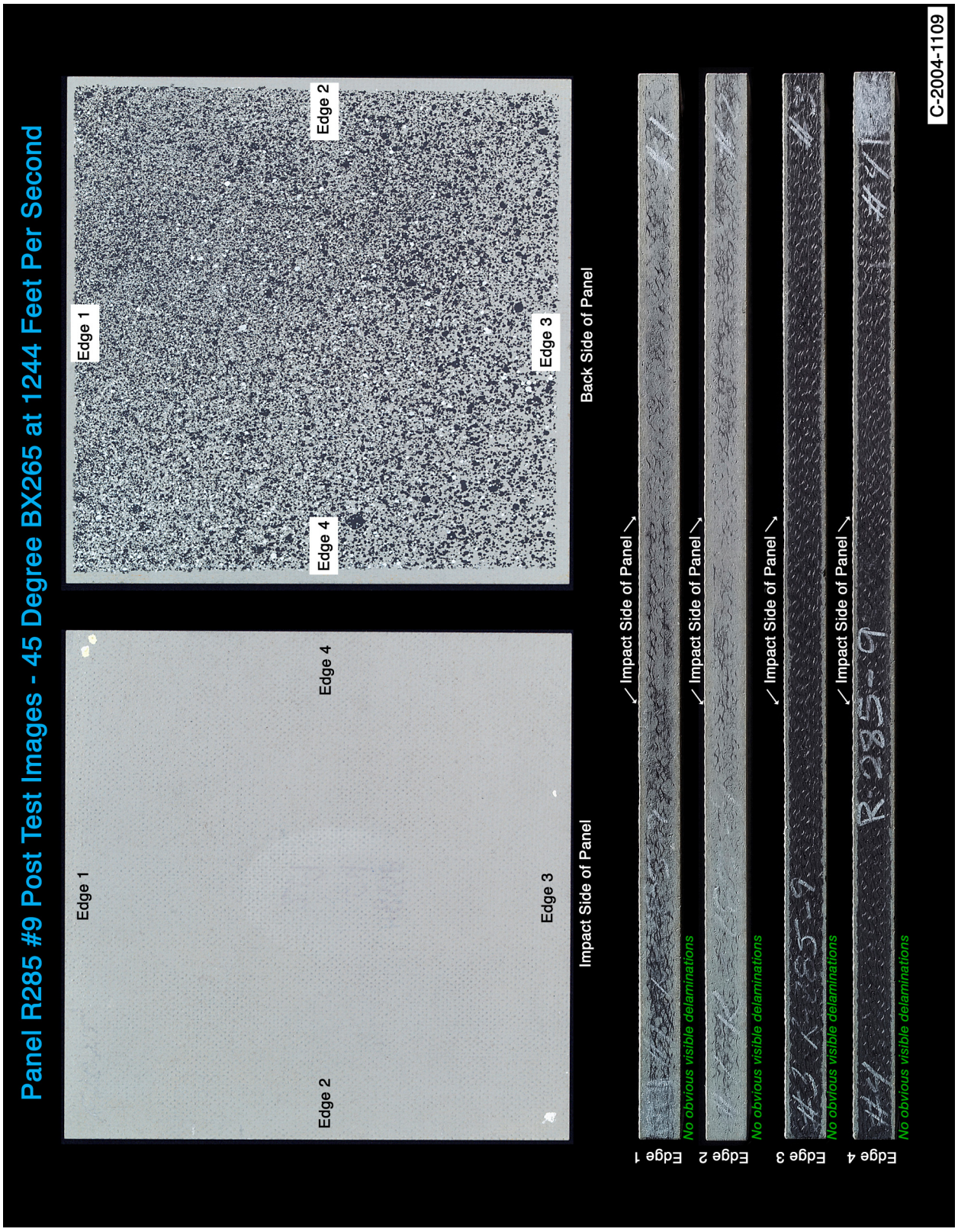

Figure B5–1.—Digital photography of edges and faces of panel R285–9 at 1244 ft/s with a BX–265 foam cylinder (nominally 1.25 in. in diameter by 3 in.) at a 45° impact angle. Test GRCC 41.

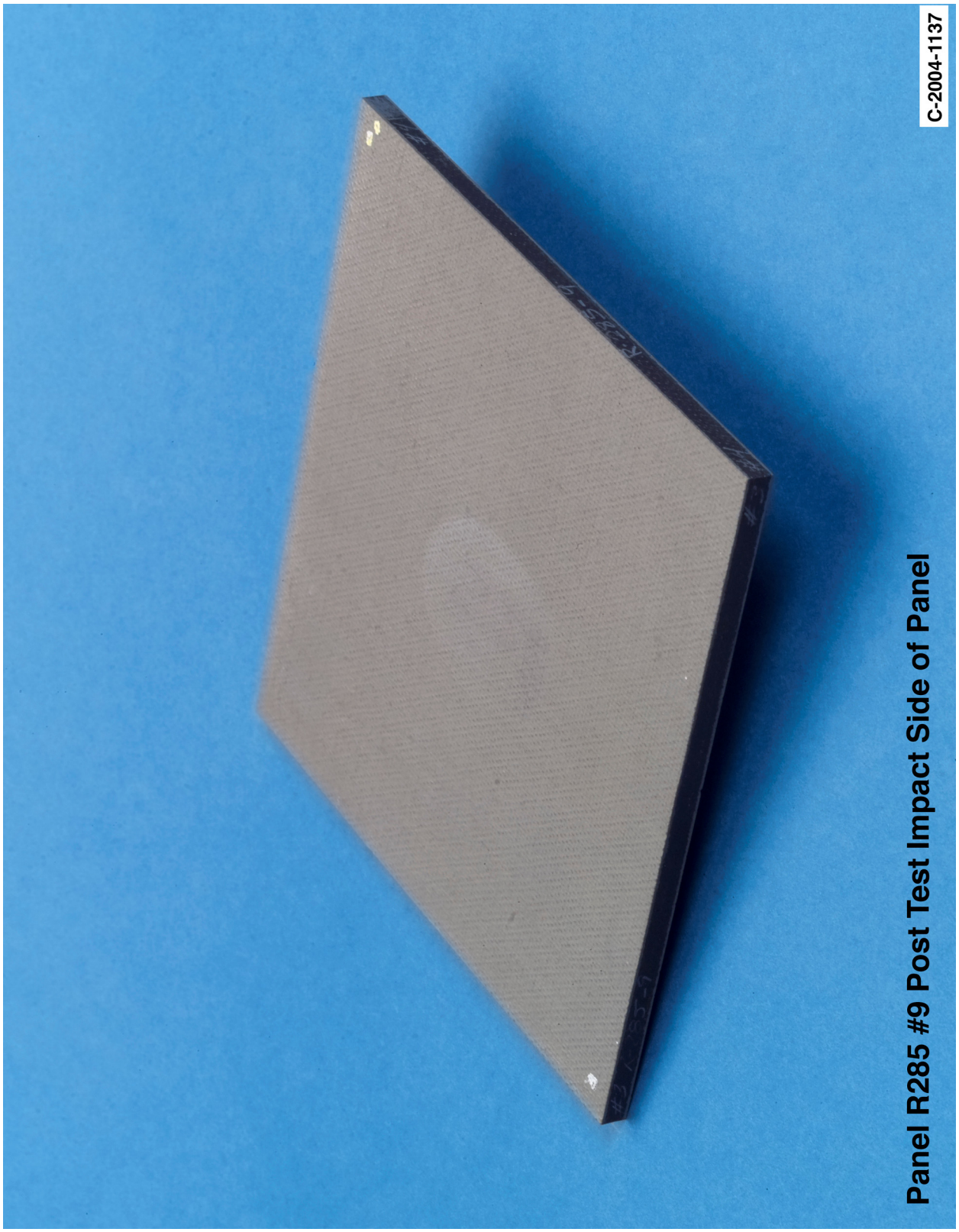

Figure B5–2.—Digital photography front (impact side) face of panel R285–9 at 1244 ft/s with a BX–265 foam cylinder (nominally 1.25 in. in diameter by 3 in.) at a 45° impact angle. Test GRCC 41.

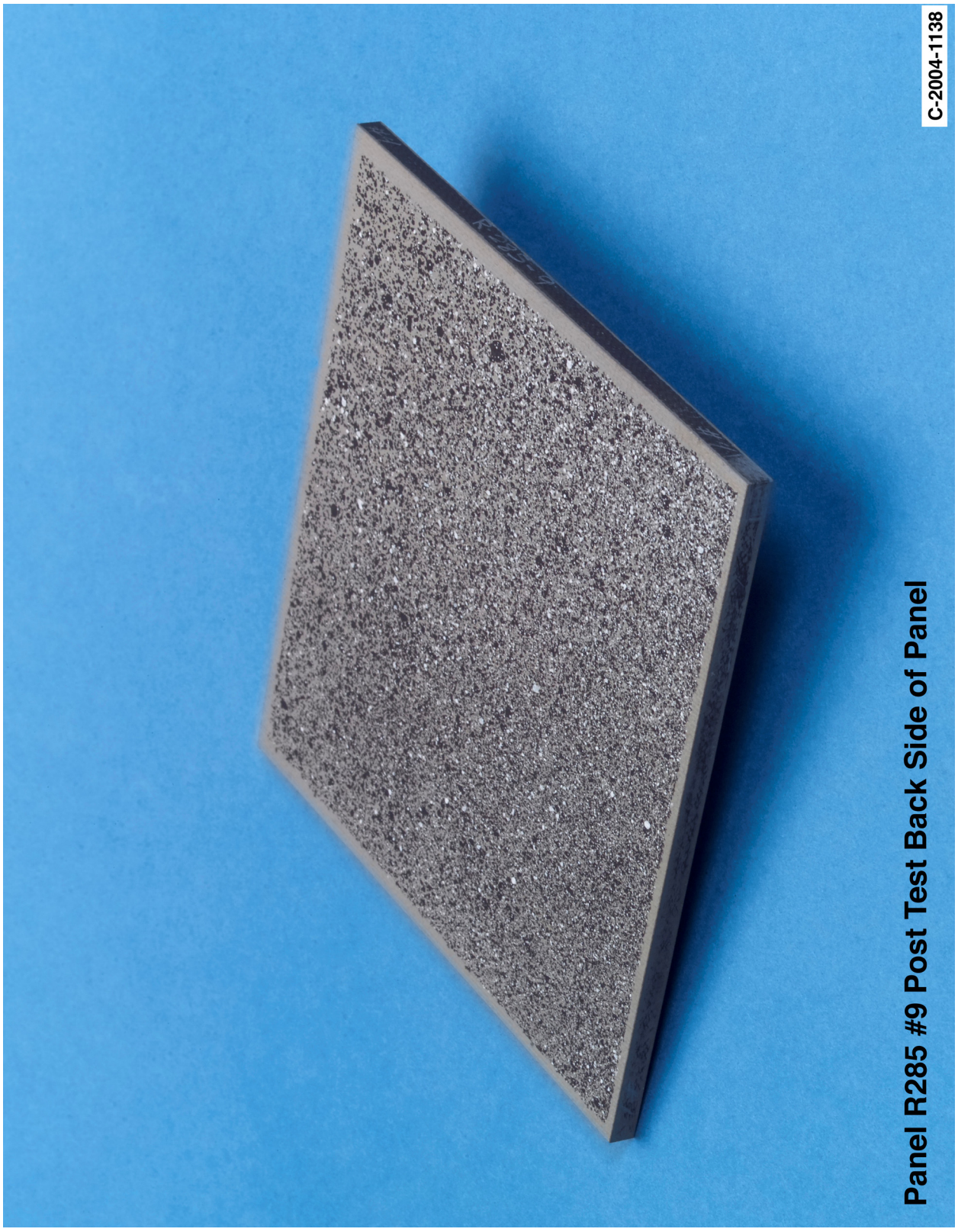

Figure B5–3.—Digital photography of back face of panel R285–9 at 1244 ft/s with a BX–265 foam cylinder (nominally 1.25 in. in diameter by 3 in.) at a 45° impact angle. Test GRCC 41.

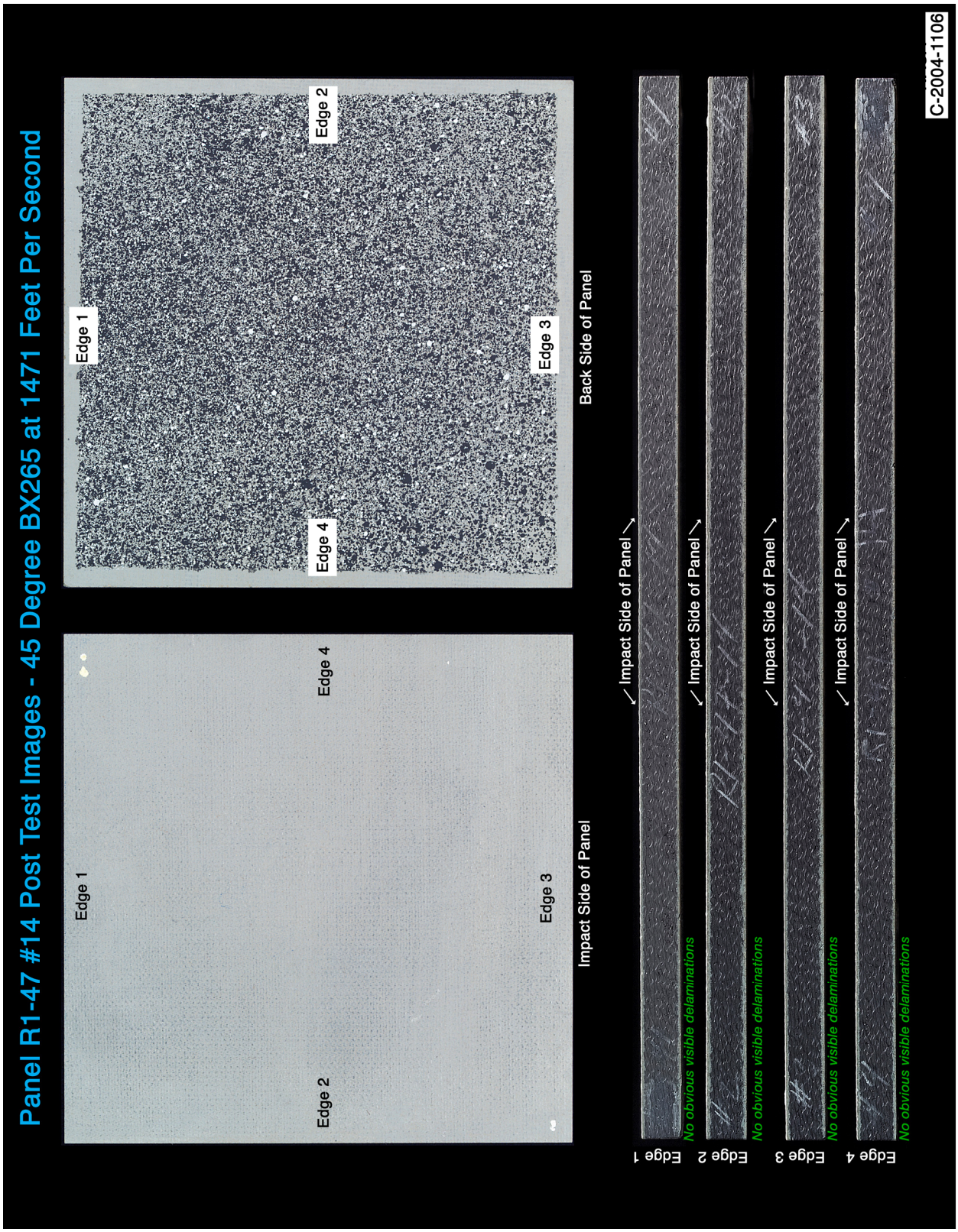

Figure B6–1.—Digital photography of edges and faces of panel R147–14 at 1471 ft/s with a BX–265 foam cylinder (nominally 1.25 in. in diameter by 3 in.) at a 45° impact angle. Test GRCC 30.

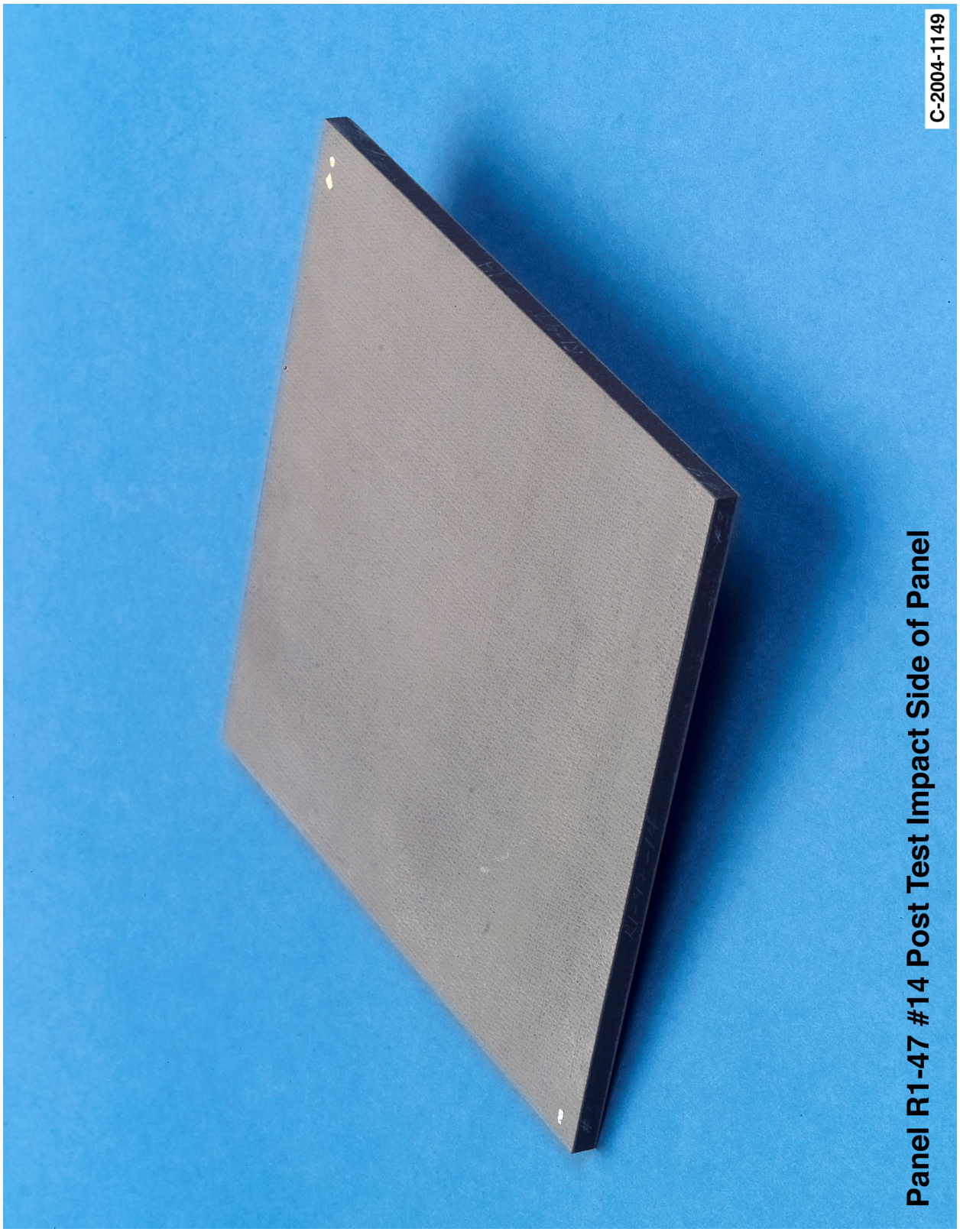

Figure B6–2.—Digital photography front (impact side) face of panel R147–14 at 1471 ft/s with a BX–265 foam cylinder (nominally 1.25 in. in diameter by 3 in.) at a 45° impact angle. Test GRCC 30.

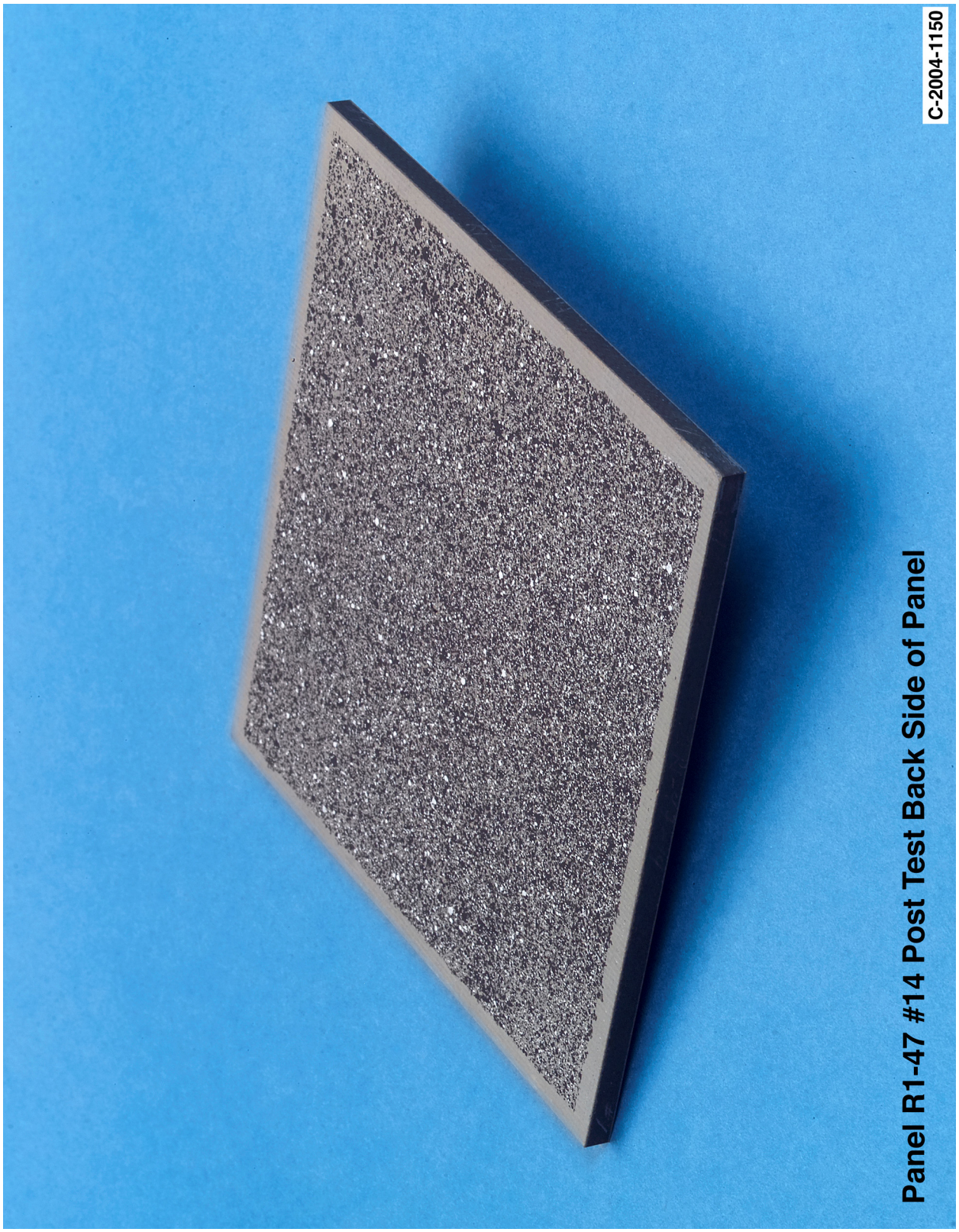

Figure B6–3.—Digital photography of back face of panel R147–14 at 1471 ft/s with a BX–265 foam cylinder (nominally 1.25 in. in diameter by 3 in.) at a 45° impact angle. Test GRCC 30.

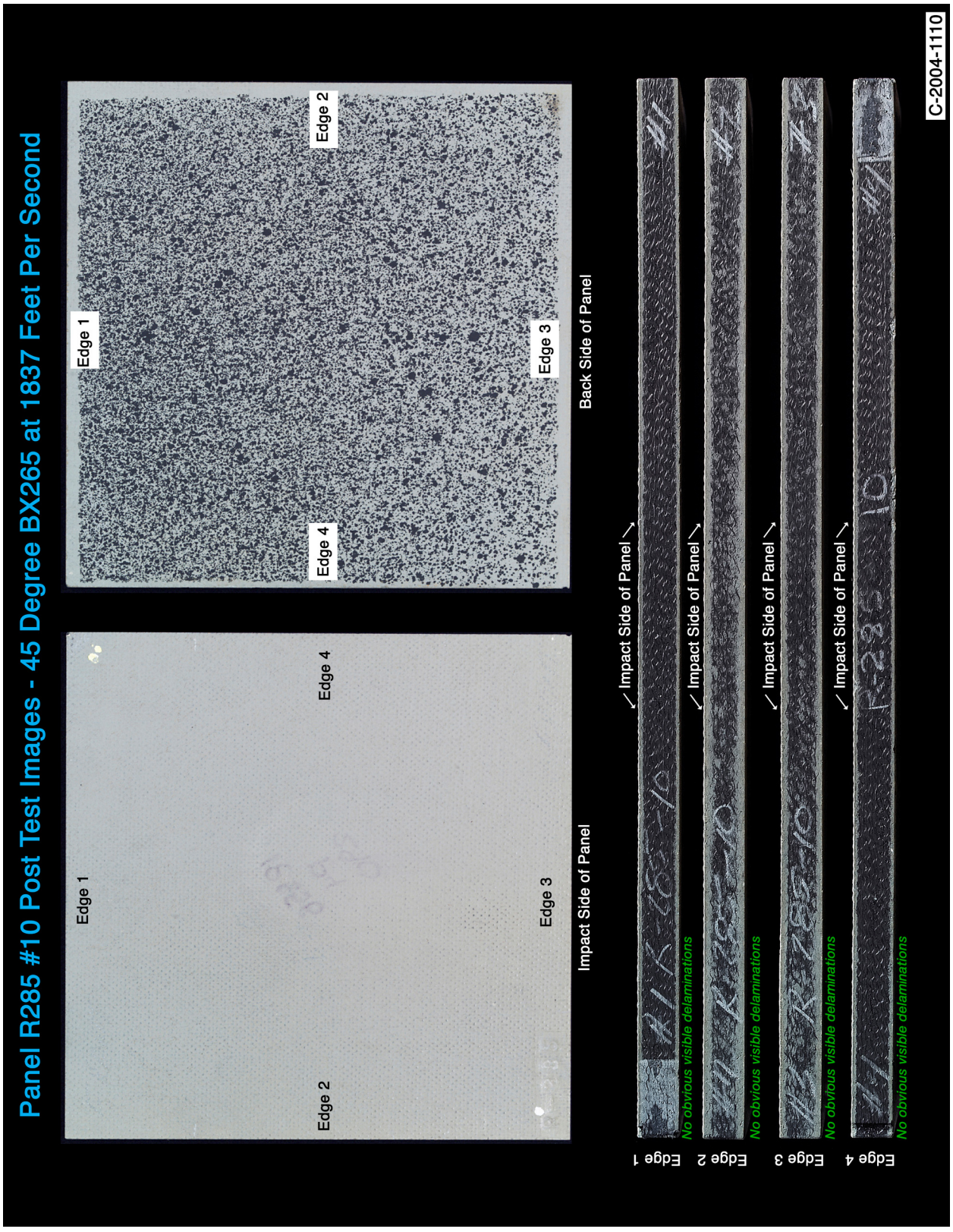

Figure B7–1.—Digital photography of edges and faces of panel R285–10 at 1837 ft/s with a BX–265 foam cylinder (nominally 1.25 in. in diameter by 3 in.) at a 45° impact angle. Test GRCC 43.

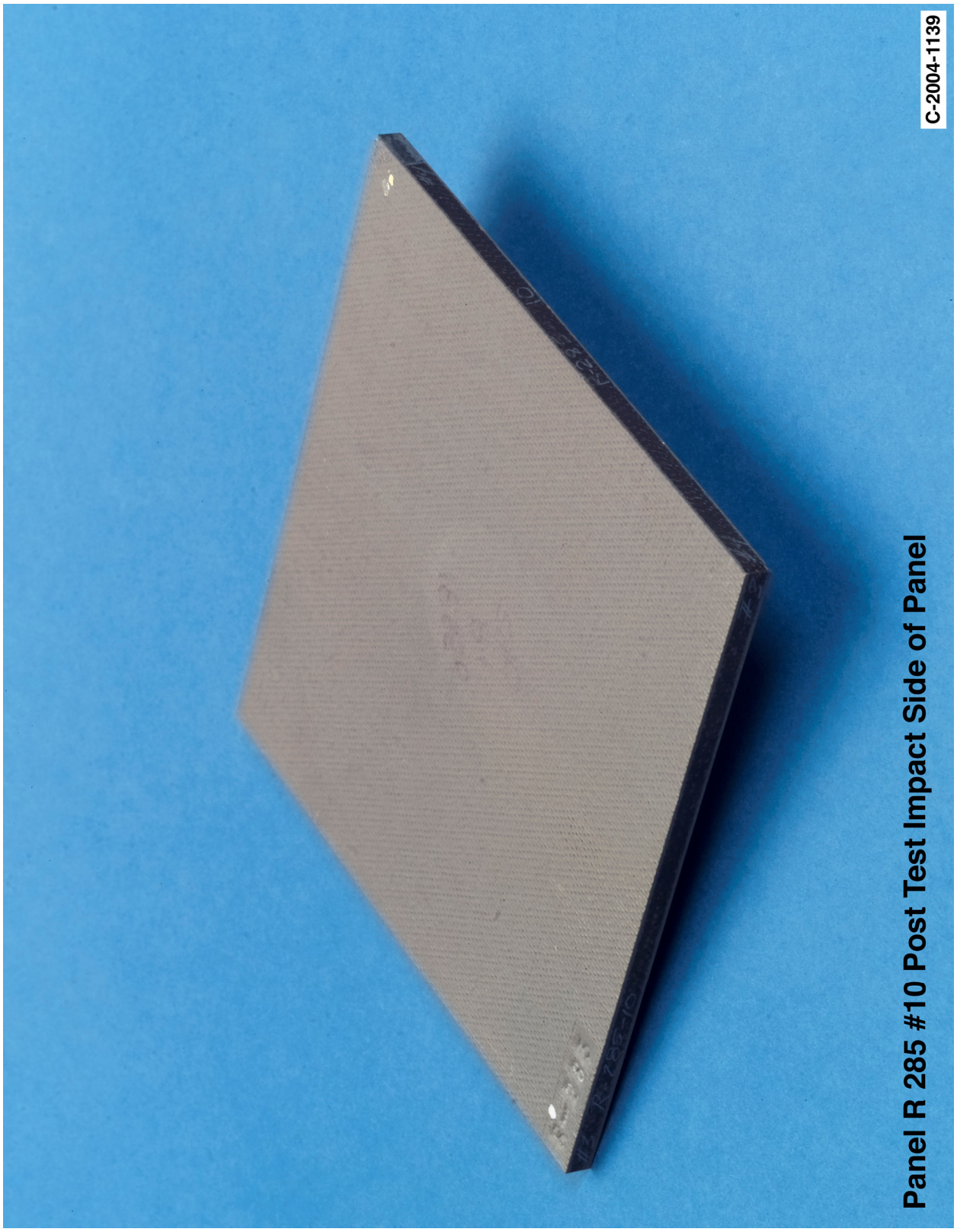

Figure B7–2.—Digital photography front (impact side) face of panel R285–10 at 1837 ft/s with a BX–265 foam cylinder (nominally 1.25 in. in diameter by 3 in.) at a 45° impact angle. Test GRCC 43.

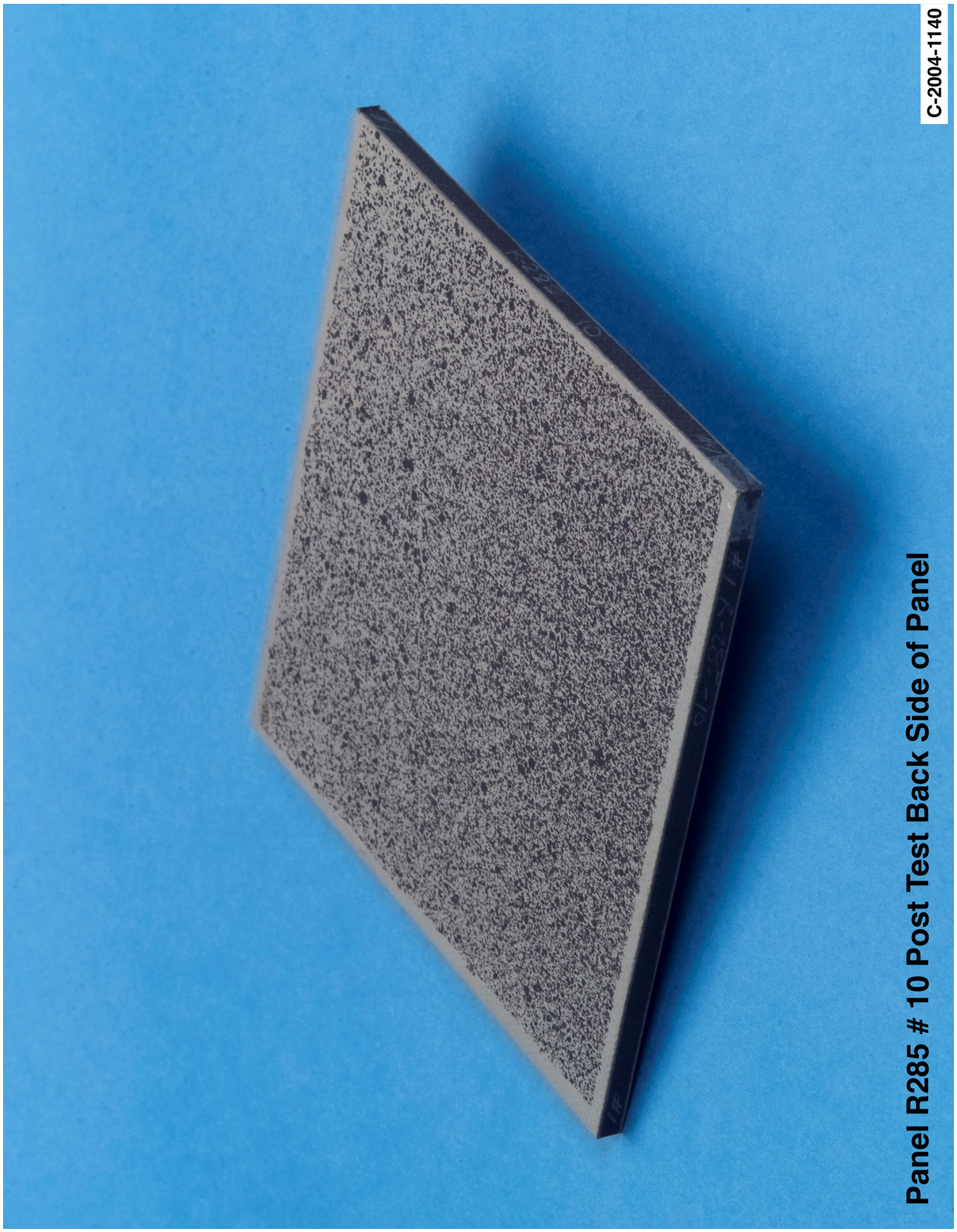

Figure B7–3.—Digital photography of back face of panel R285–10 at 1837 ft/s with a BX–265 foam cylinder (nominally 1.25 in. in diameter by 3 in.) at a 45° impact angle. Test GRCC 43.

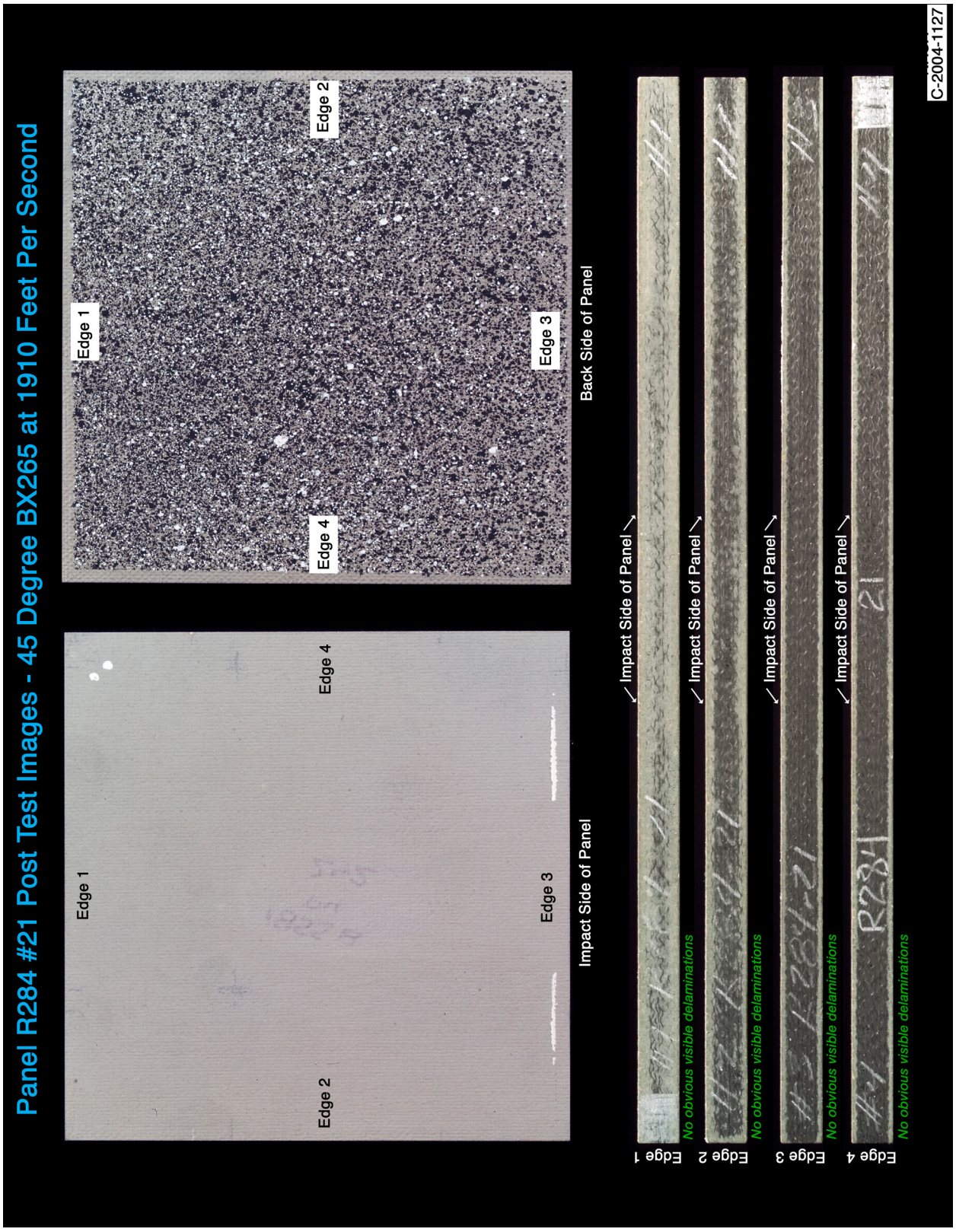

Figure B8–1.—Digital photography of edges and faces of panel R284–21 at 1910 ft/s with a BX–265 foam cylinder (nominally 1.25 in. in diameter by 3 in.) at a 45° impact angle. Test GRCC 52.

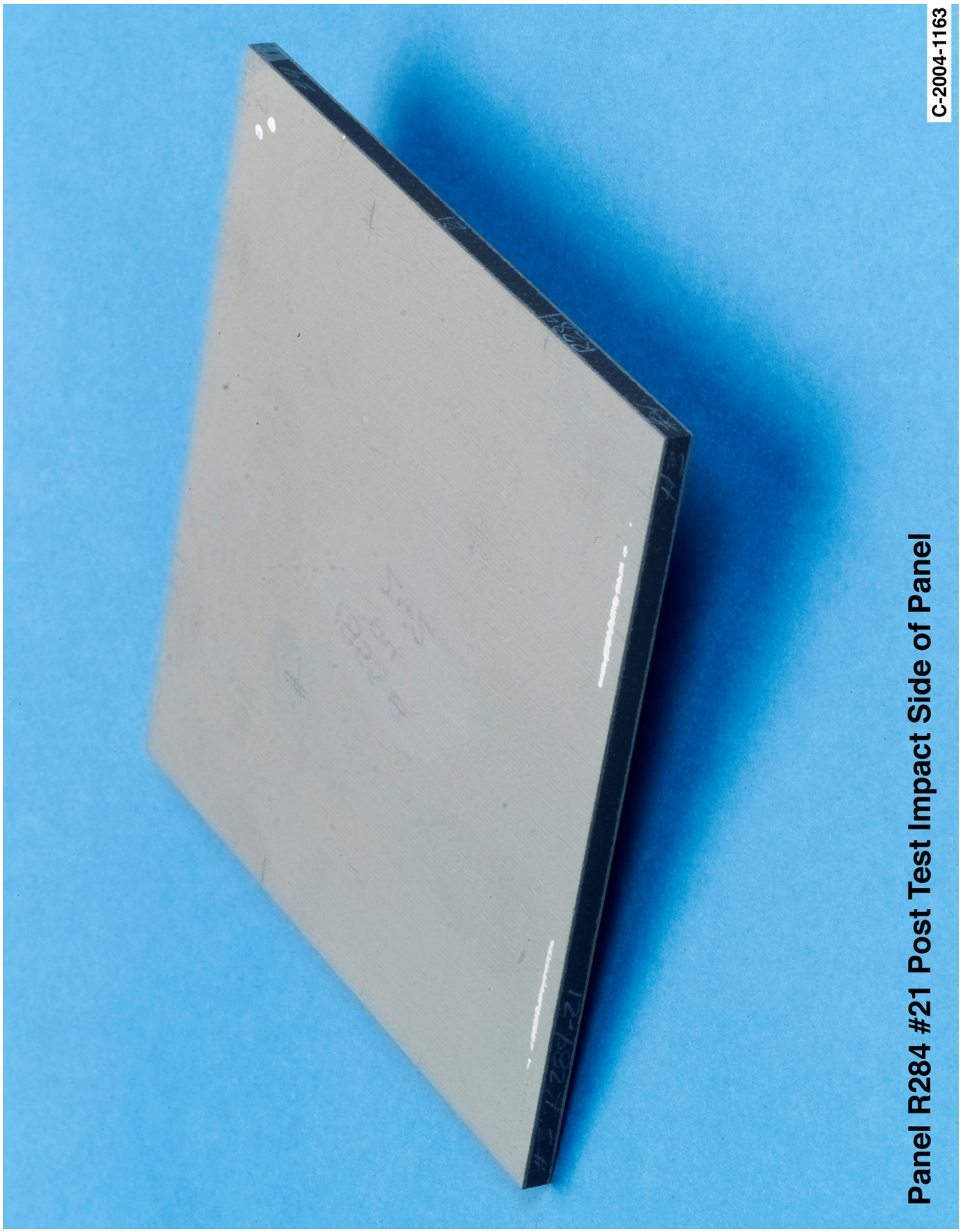

Figure B8–2.—Digital photography front (impact side) face of panel R284–21 at 1910 ft/s with a BX–265 foam cylinder (nominally 1.25 in. in diameter by 3 in.) at a 45° impact angle. Test GRCC 52.

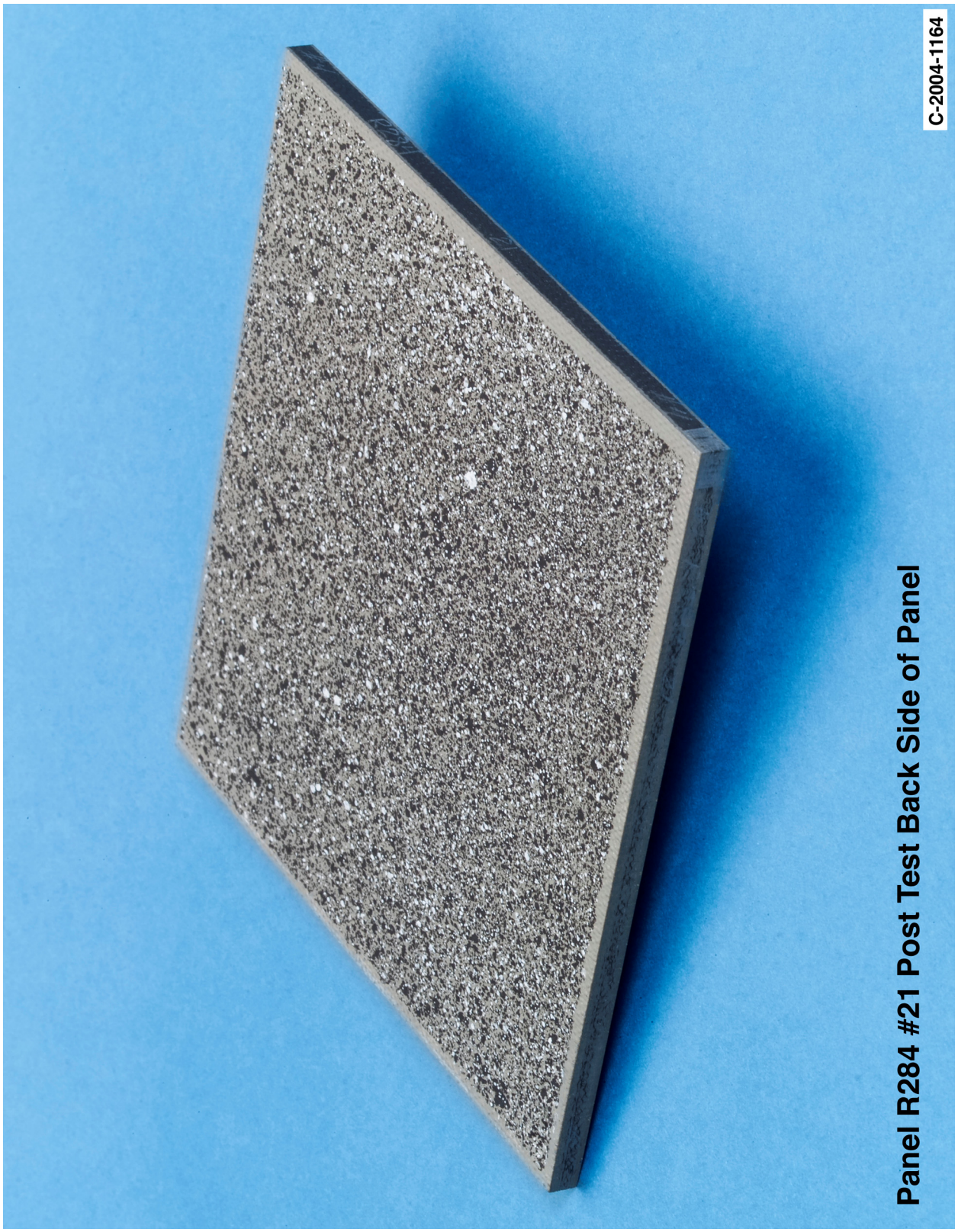

Figure B8–3.—Digital photography of back face of panel R284–21 at 1910 ft/s with a BX–265 foam cylinder (nominally 1.25 in. in diameter by 3 in.) at a 45° impact angle. Test GRCC 52.

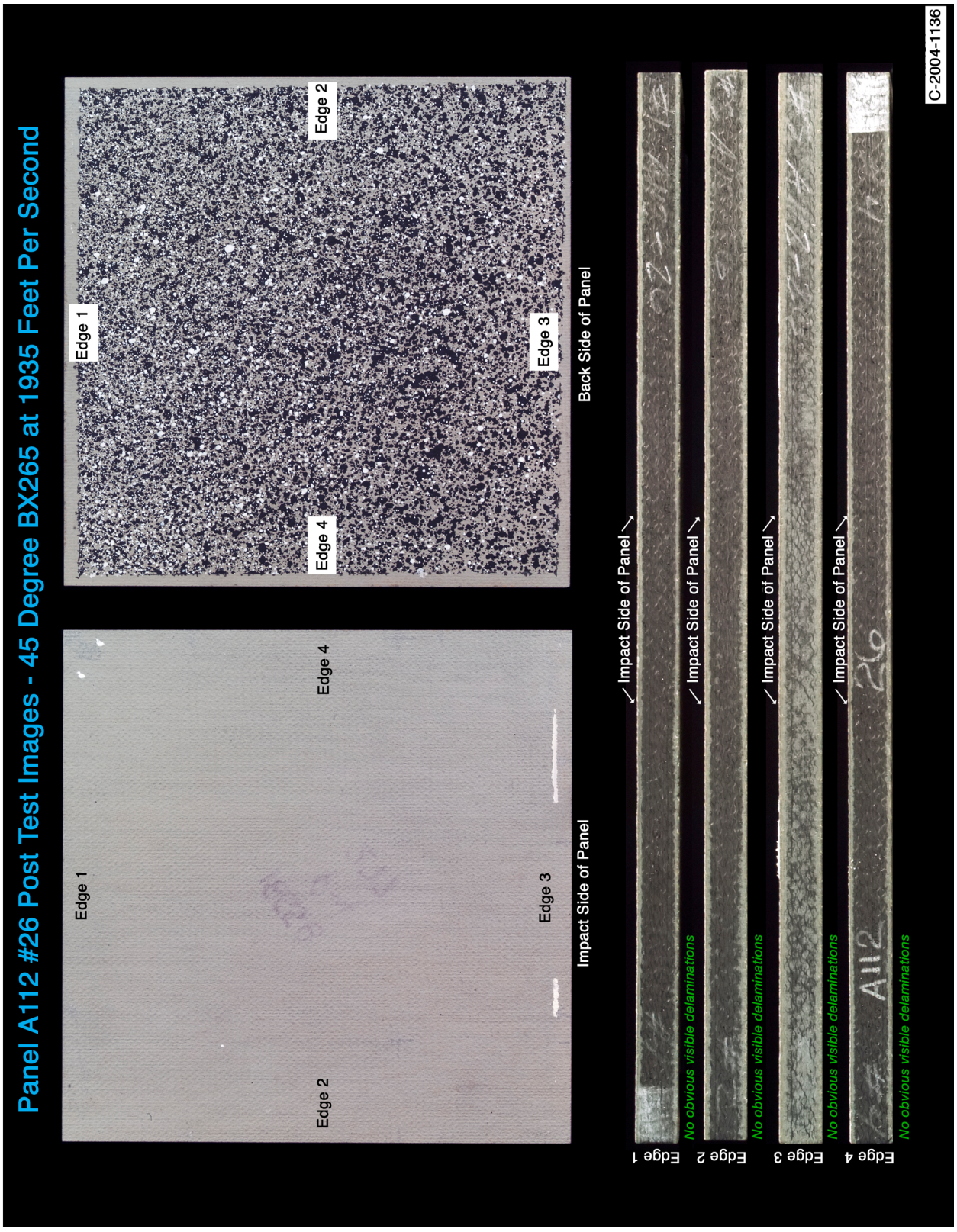

Figure B9–1.—Digital photography of edges and faces of panel A112–26 at 1935 ft/s with a BX–265 foam cylinder (nominally 1.25 in. in diameter by 3 in.) at a 45° impact angle. Test GRCC 55.

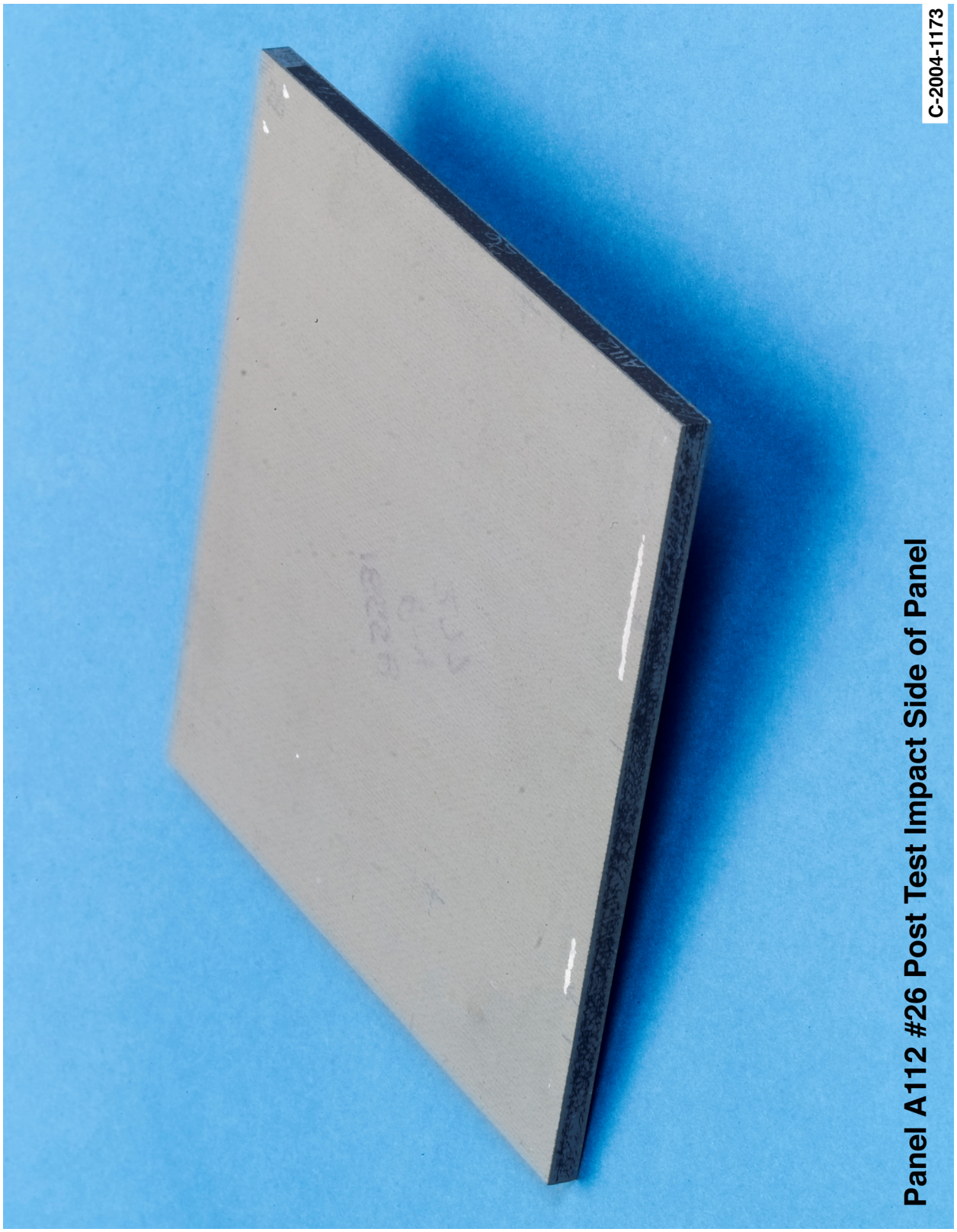

Figure B9–2.—Digital photography front (impact side) face of panel A112–26 at 1935 ft/s with a BX–265 foam cylinder (nominally 1.25 in. in diameter by 3 in.) at a 45° impact angle. Test GRCC 55.

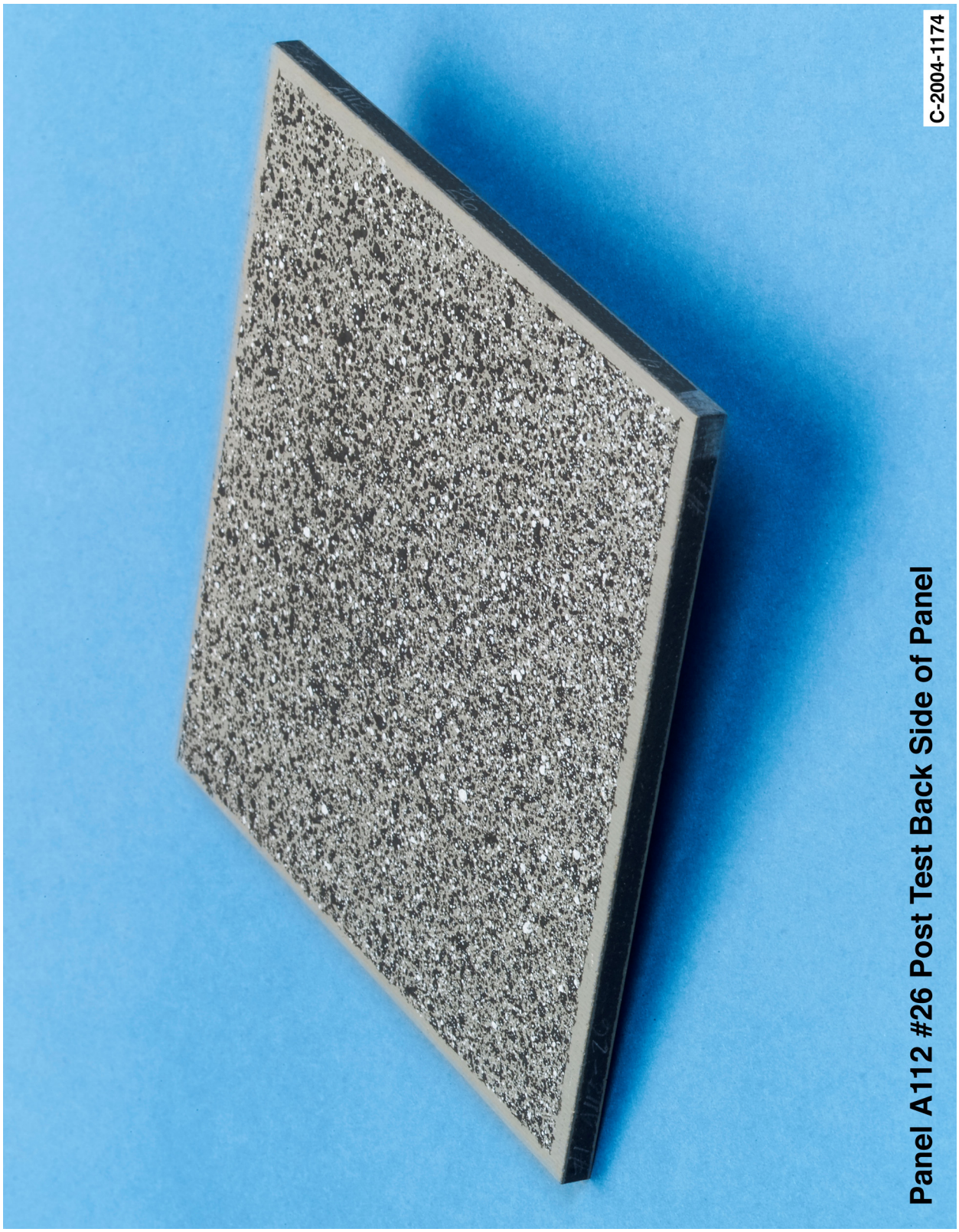

Figure B9–3.—Digital photography of back face of panel A112–26 at 1935 ft/s with a BX–265 foam cylinder (nominally 1.25 in. in diameter by 3 in.) at a 45° impact angle. Test GRCC 55.

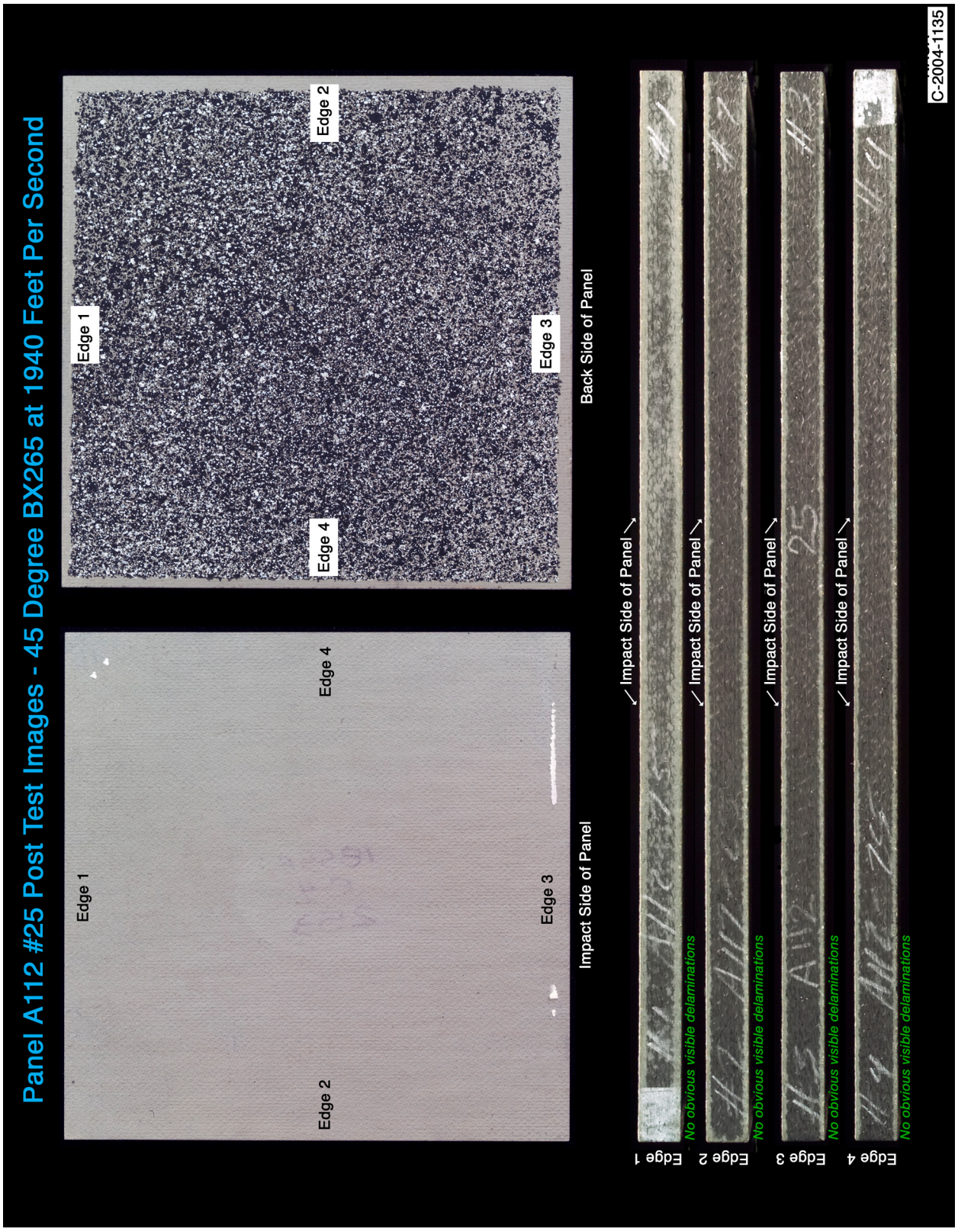

Figure B10–1.—Digital photography of edges and faces of panel A112–25 at 1940 ft/s with a BX–265 foam cylinder (nominally 1.25 in. in diameter by 3 in.) at a 45° impact angle. Test GRCC 54.

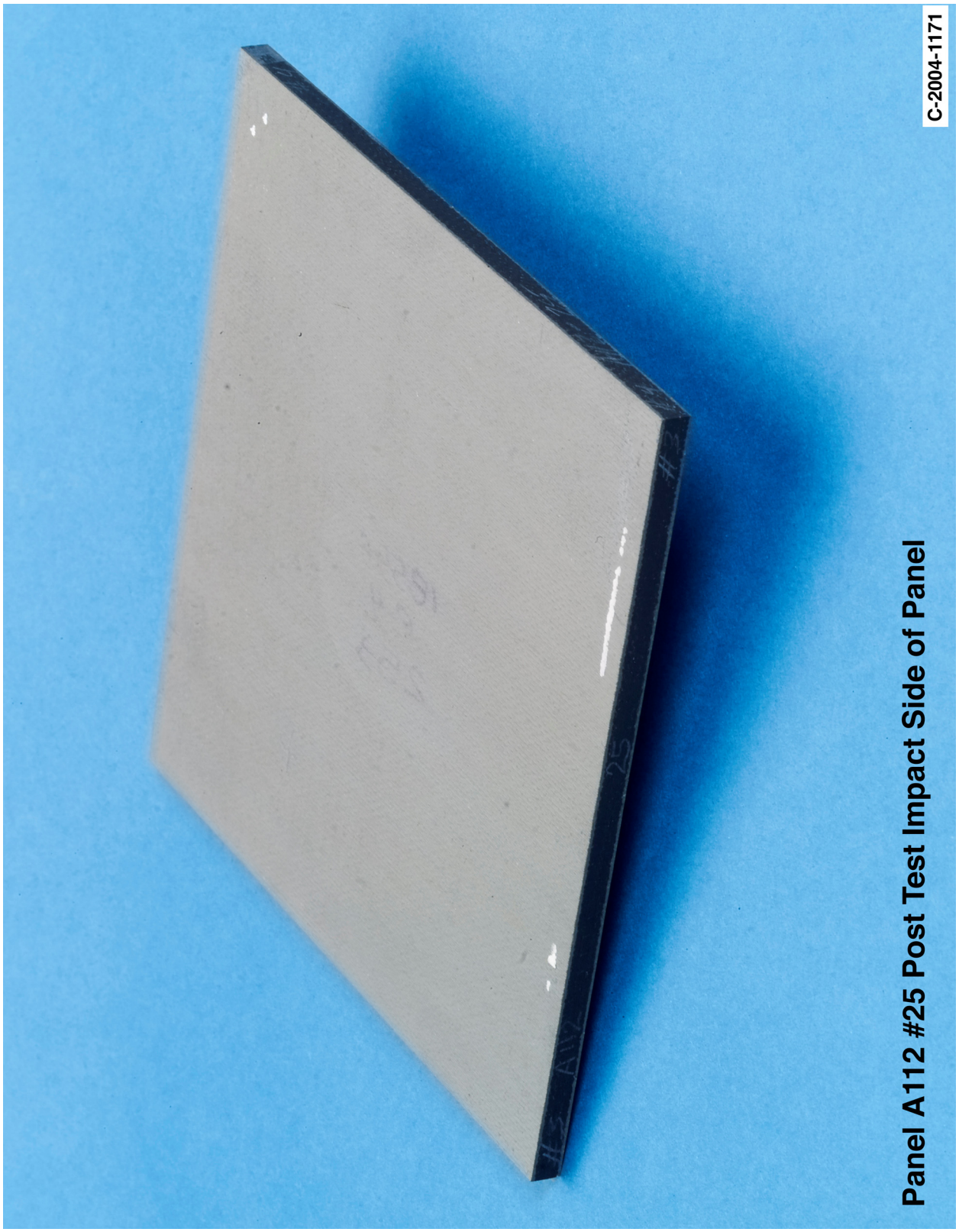

Figure B10–2.—Digital photography front (impact side) face of panel A112–25 at 1940 ft/s with a BX–265 foam cylinder (nominally 1.25 in. in diameter by 3 in.) at a 45° impact angle. Test GRCC 54.

Figure B10–3.—Digital photography of back face of panel A112–25 at 1940 ft/s with a BX–265 foam cylinder (nominally 1.25 in. in diameter by 3 in.) at a 45° impact angle. Test GRCC 54.

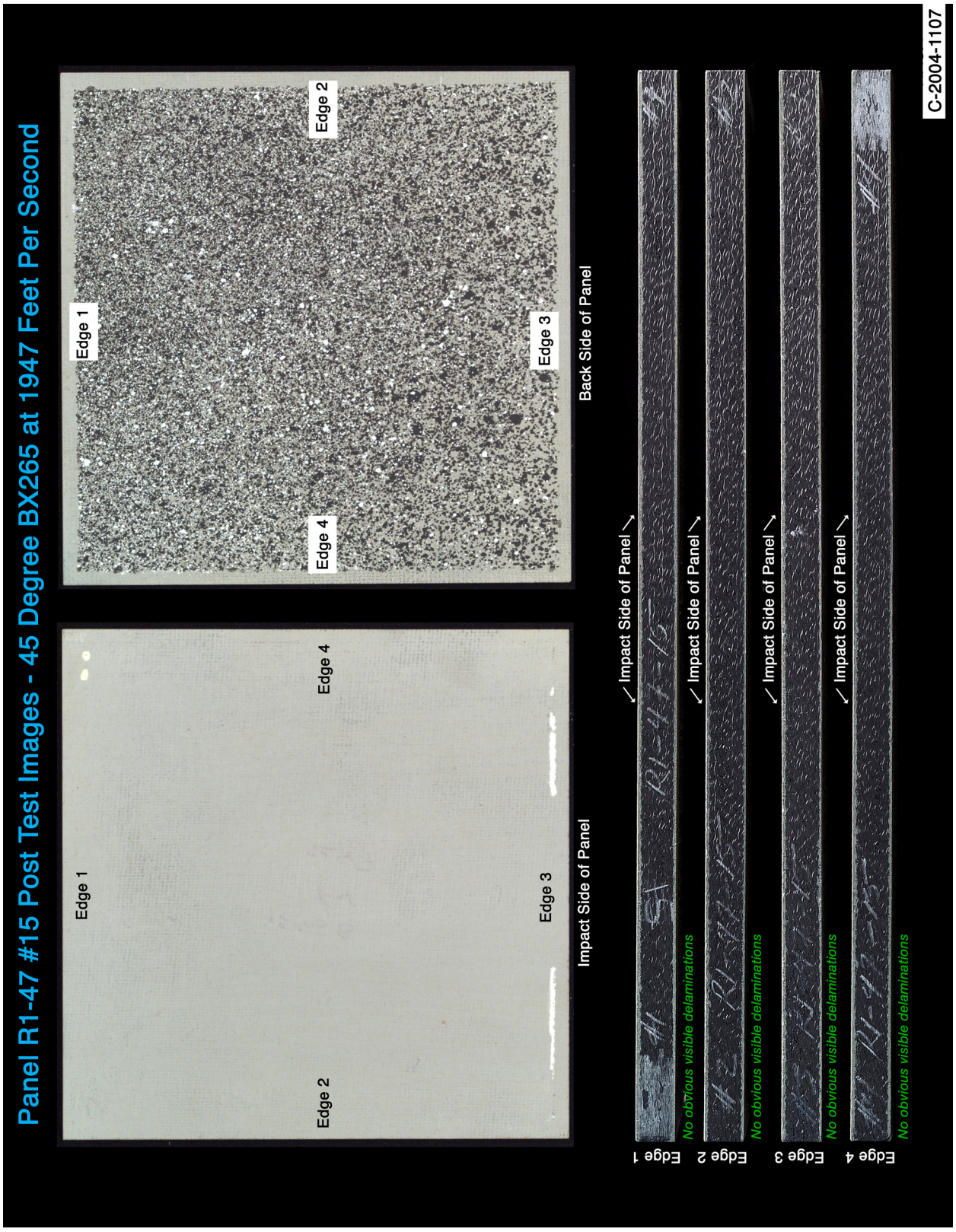

Figure B11–1.—Digital photography of edges and faces of panel R147–15 at 1947 ft/s with a BX–265 foam cylinder (nominally 1.25 in. in diameter by 3 in.) at a 45° impact angle. Test GRCC 49.

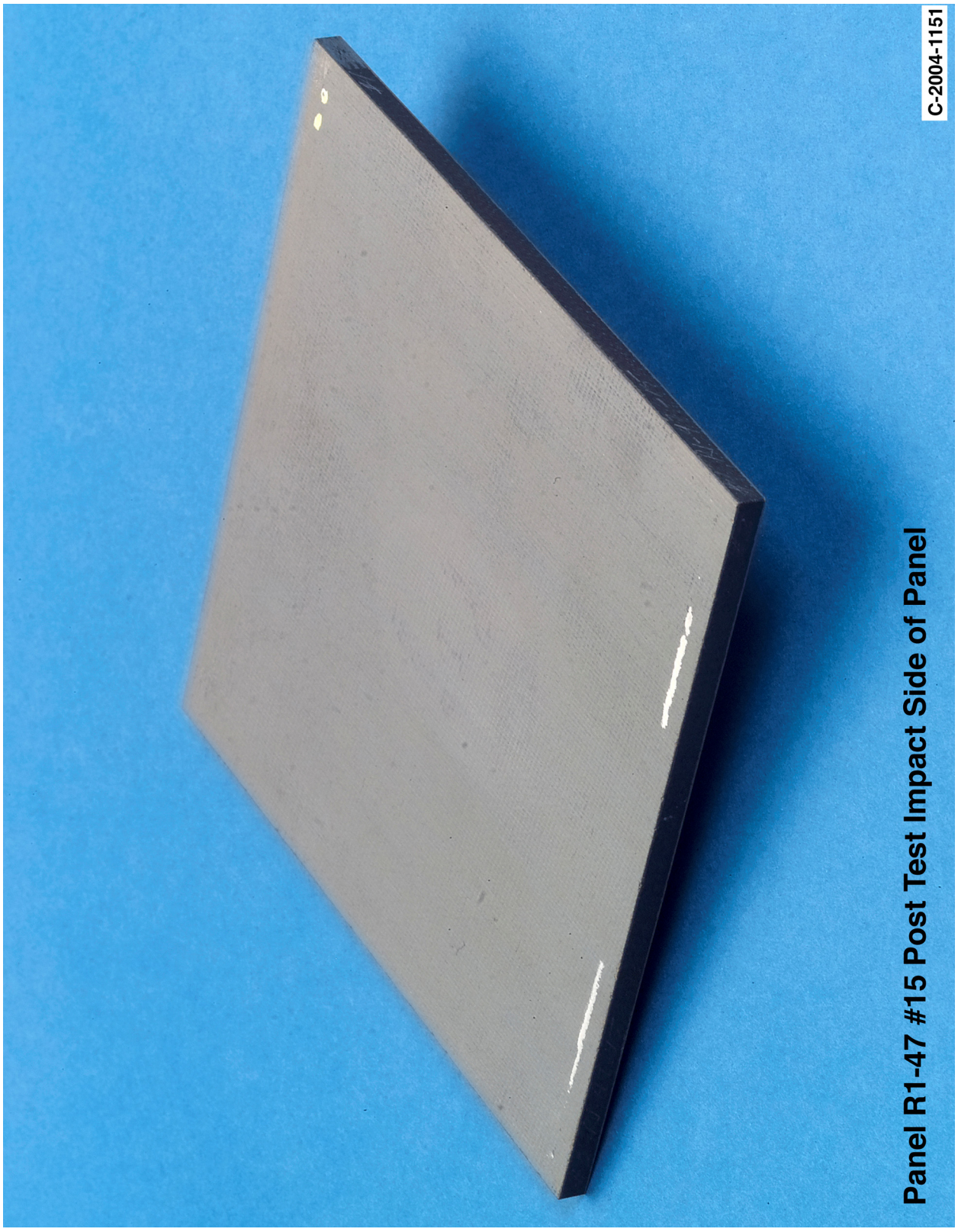

Figure B11–2.—Digital photography front (impact side) face of panel R147–15 at 1947 ft/s with a BX–265 foam cylinder (nominally 1.25 in. in diameter by 3 in.) at a 45° impact angle. Test GRCC 49.

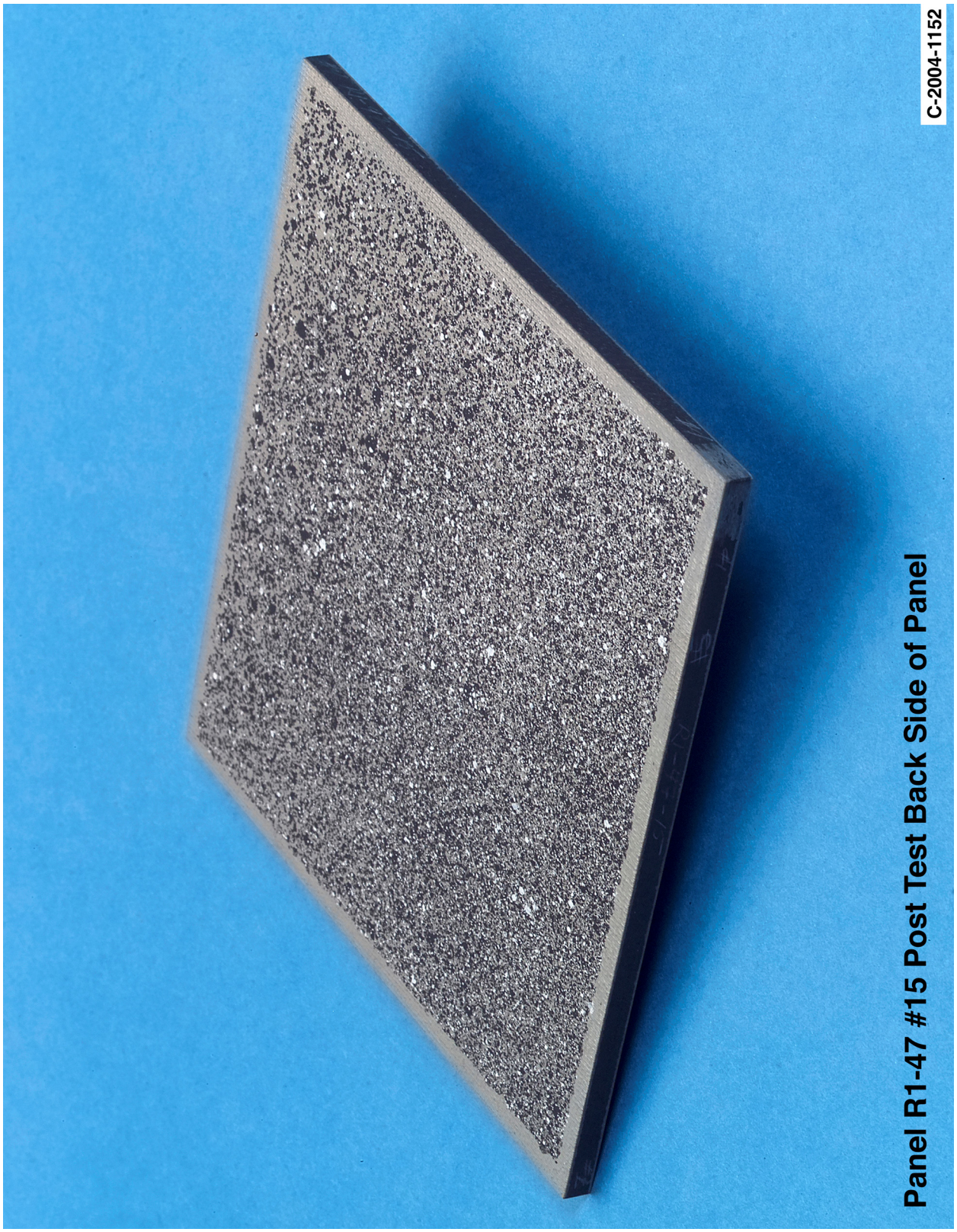

Figure B11–3.—Digital photography of back face of panel R147–15 at 1947 ft/s with a BX–265 foam cylinder (nominally 1.25 in. in diameter by 3 in.) at a 45° impact angle. Test GRCC 49.

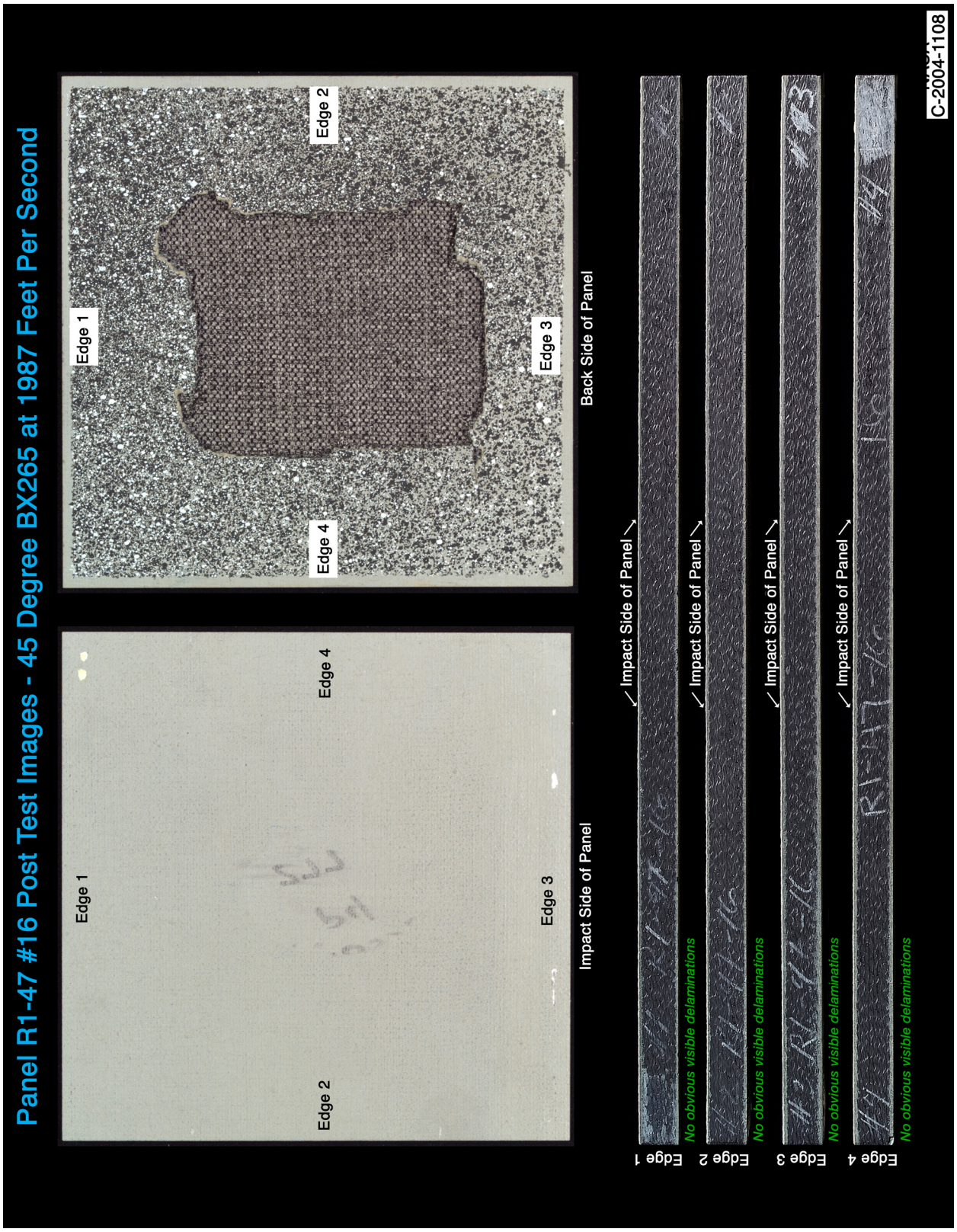

Figure B12–1.—Digital photography of edges and faces of panel R147–16 at 1987 ft/s with a BX–265 foam cylinder (nominally 1.25 in. in diameter by 3 in.) at a 45° impact angle. Test GRCC 48.

Figure B12–2.—Digital photography front (impact side) face of panel R147–16 at 1987 ft/s with a BX–265 foam cylinder (nominally 1.25 in. in diameter by 3 in.) at a 45° impact angle. Test GRCC 48.

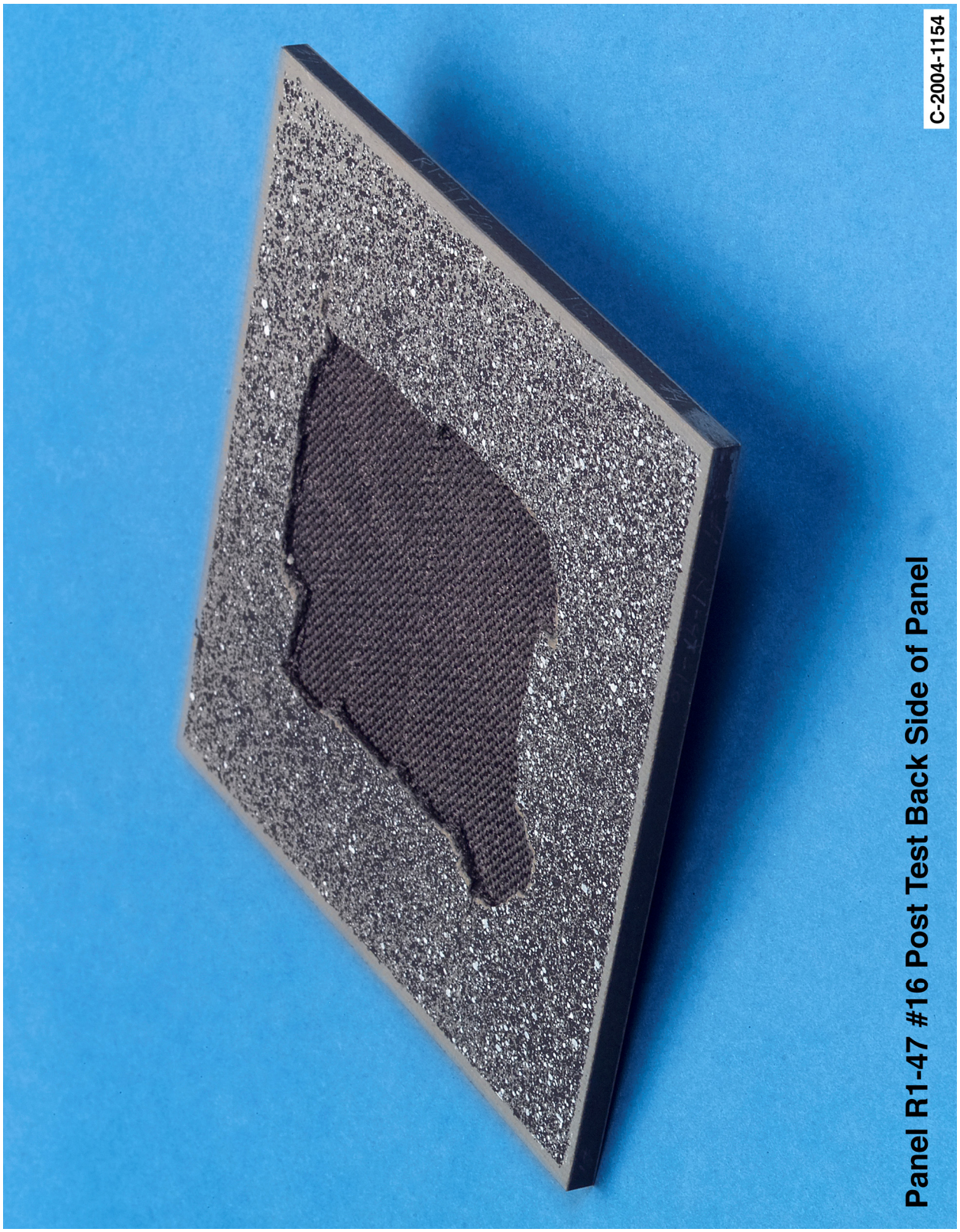

Figure B12–3.—Digital photography of back face of panel R147–16 at 1987 ft/s with a BX–265 foam cylinder (nominally 1.25 in. in diameter by 3 in.) at a 45° impact angle. Test GRCC 48.

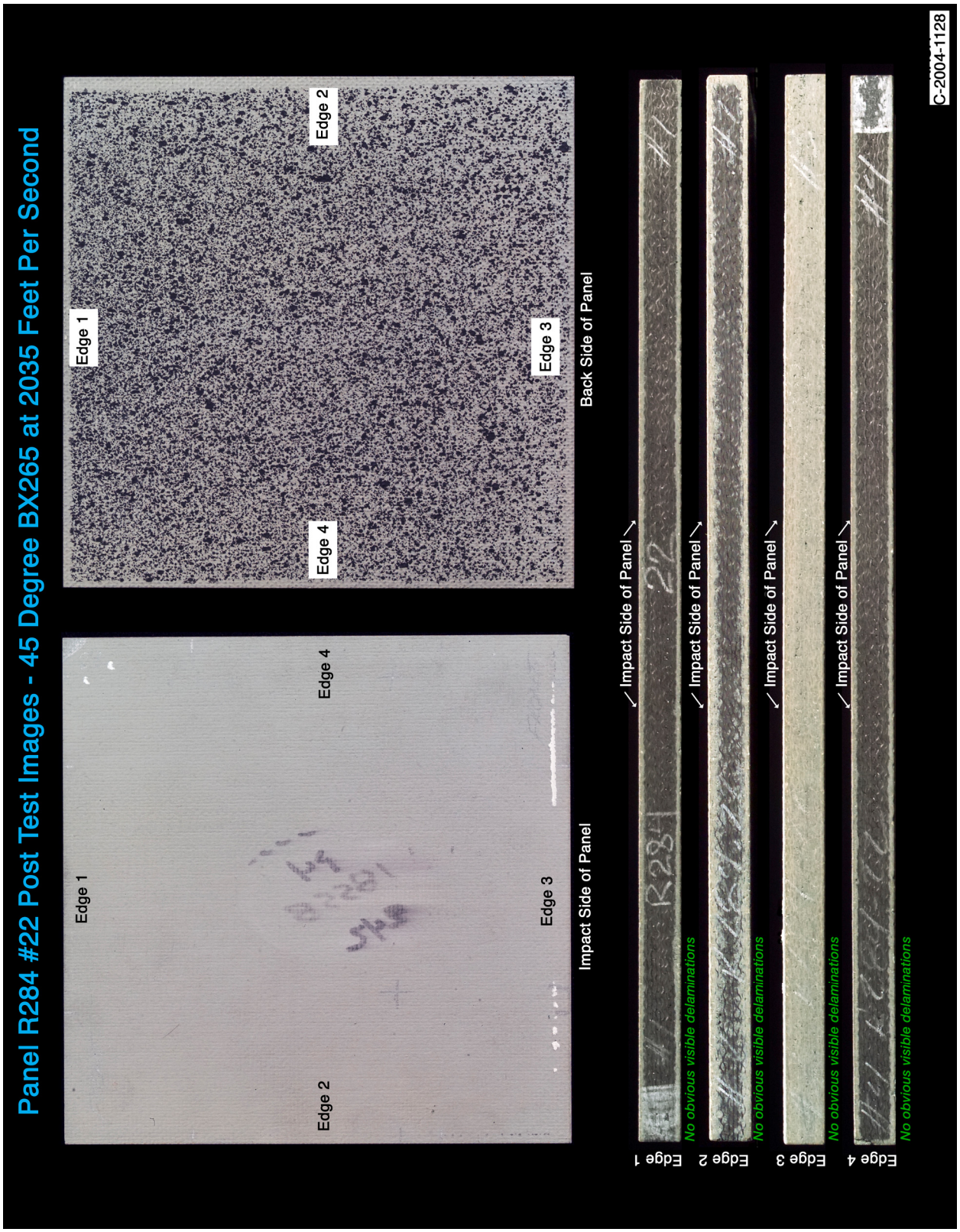

Figure B13–1.—Digital photography of edges and faces of panel R284–22 at 2035 ft/s with a BX–265 foam cylinder (nominally 1.25 in. in diameter by 3 in.) at a 45° impact angle. Test GRCC 53.

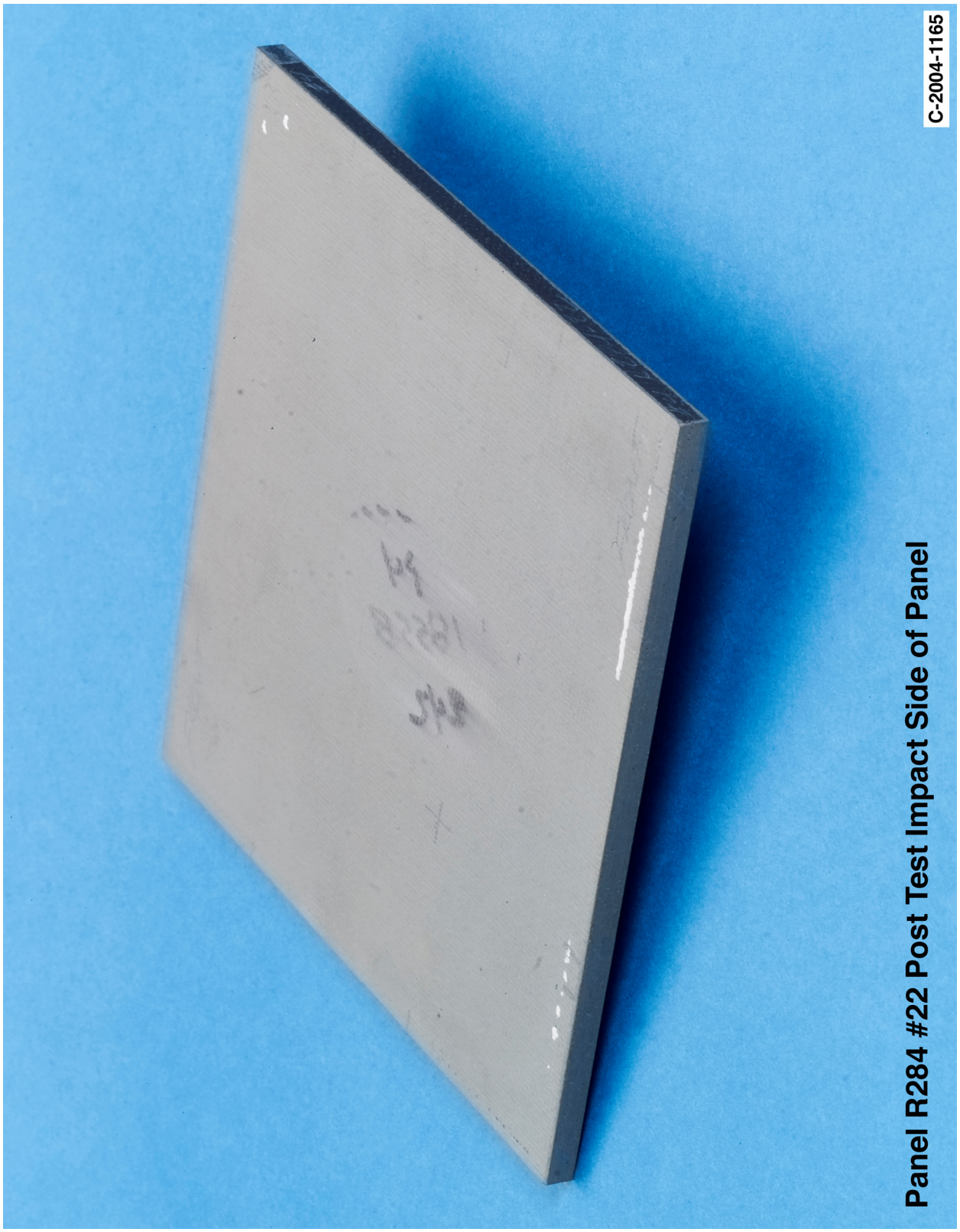

Figure B13–2.—Digital photography front (impact side) face of panel R284–22 at 2035 ft/s with a BX–265 foam cylinder (nominally 1.25 in. in diameter by 3 in.) at a 45° impact angle. Test GRCC 53.

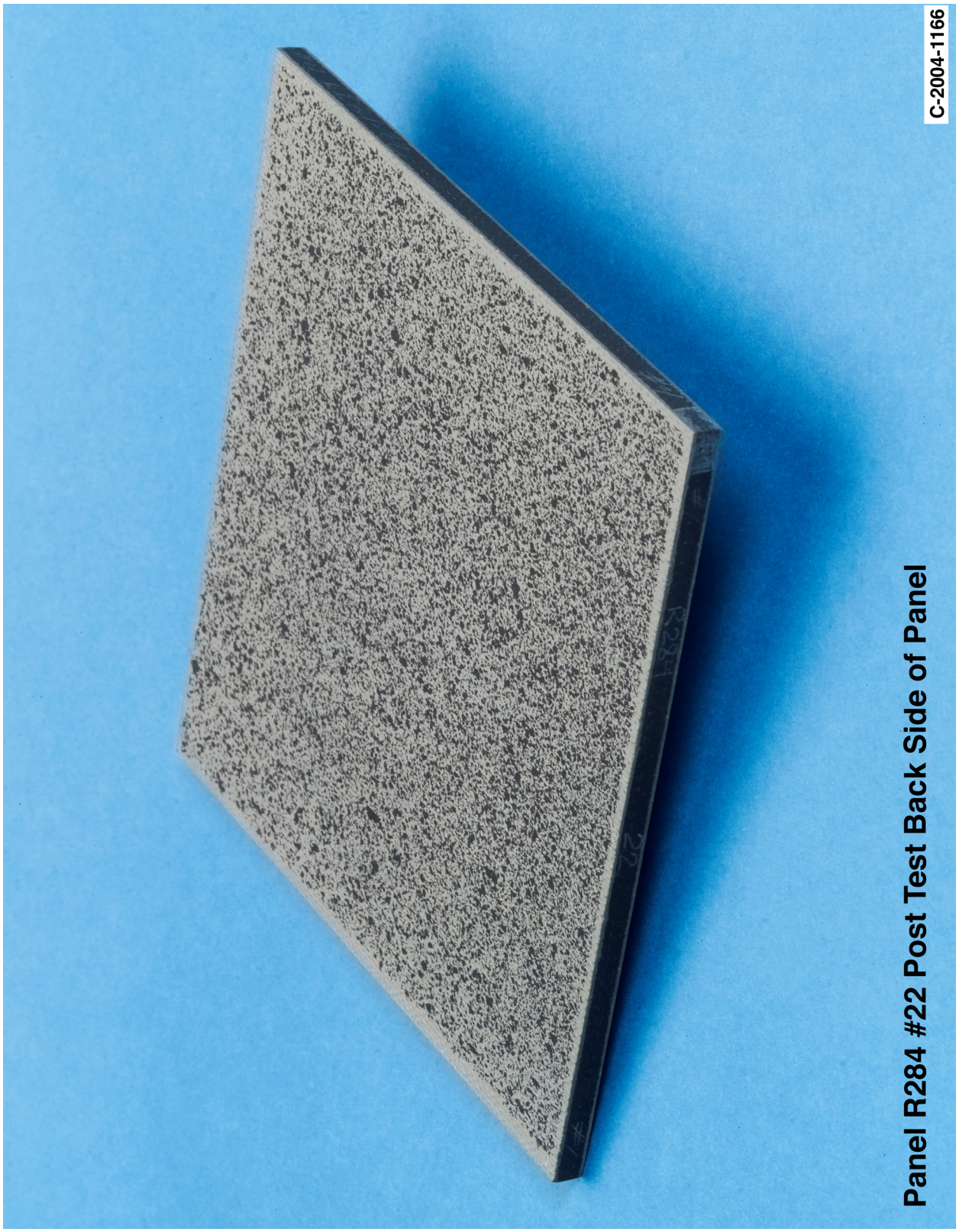

Figure B13–3.—Digital photography of back face of panel R284–22 at 2035 ft/s with a BX–265 foam cylinder (nominally 1.25 in. in diameter by 3 in.) at a 45° impact angle. Test GRCC 53.

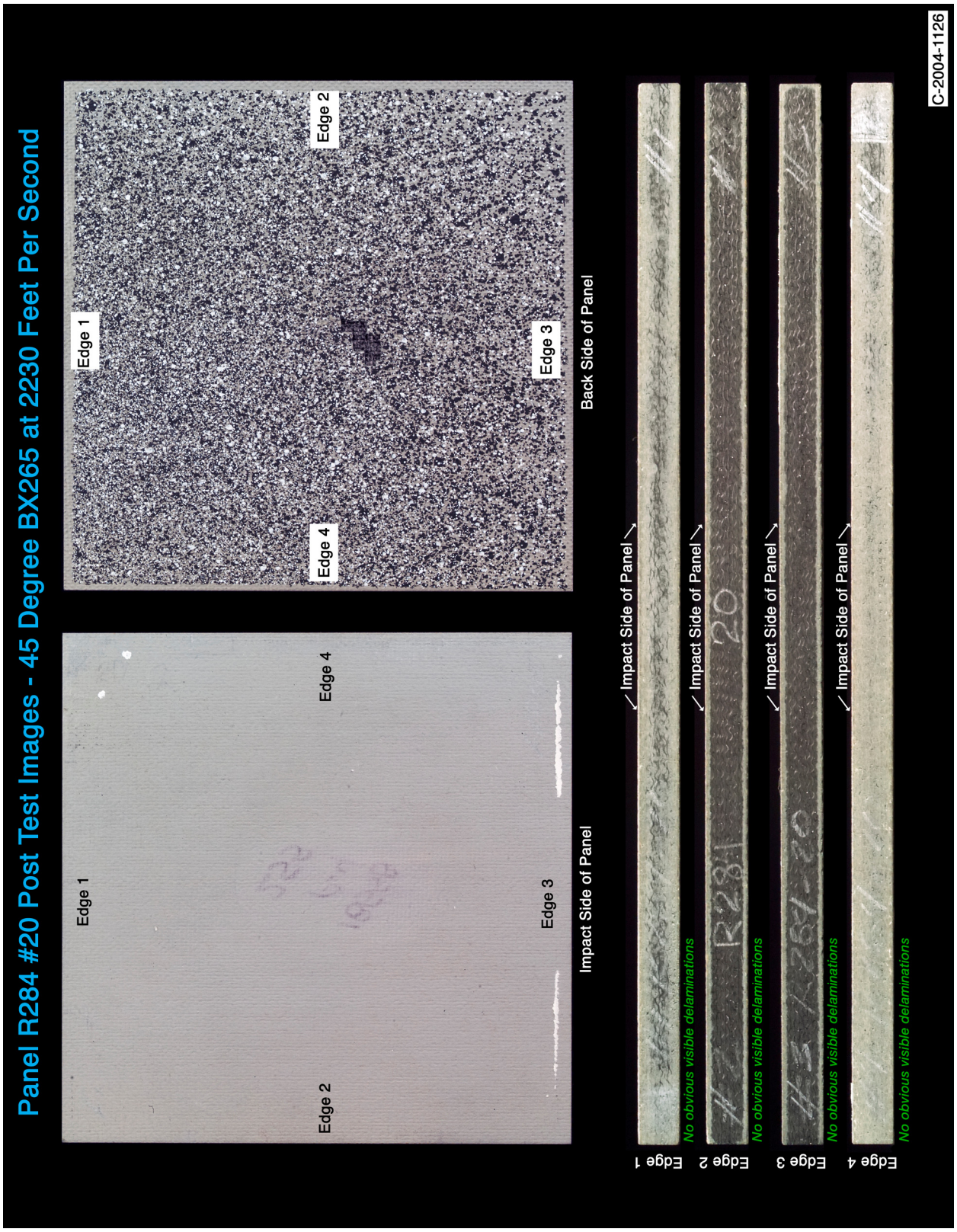

Figure B14–1.—Digital photography of edges and faces of panel R284–20 at 2230 ft/s with a BX–265 foam cylinder (nominally 1.25 in. in diameter by 3 in.) at a 45° impact. Test GRCC 51.

Figure B14–2.—Digital photography front (impact side) face of panel R284–20 at 2230 ft/s with a BX–265 foam cylinder (nominally 1.25 in. in diameter by 3 in.) at a 45° impact angle. Test GRCC 51.

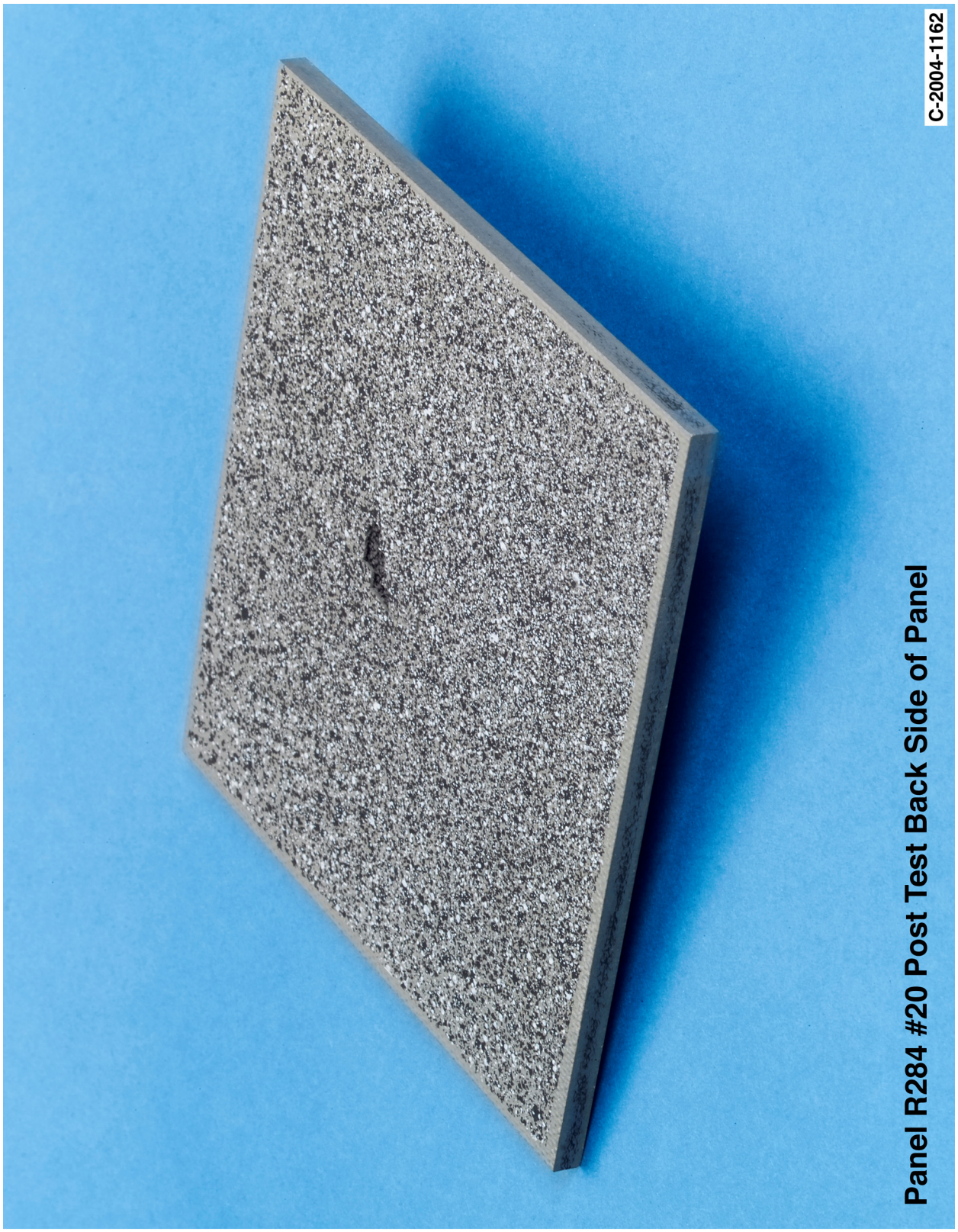

Figure B14–3.—Digital photography of back face of panel R284–20 at 2230 ft/s with a BX–265 foam cylinder (nominally 1.25 in. in diameter by 3 in.) at a 45° impact angle. Test GRCC 51.

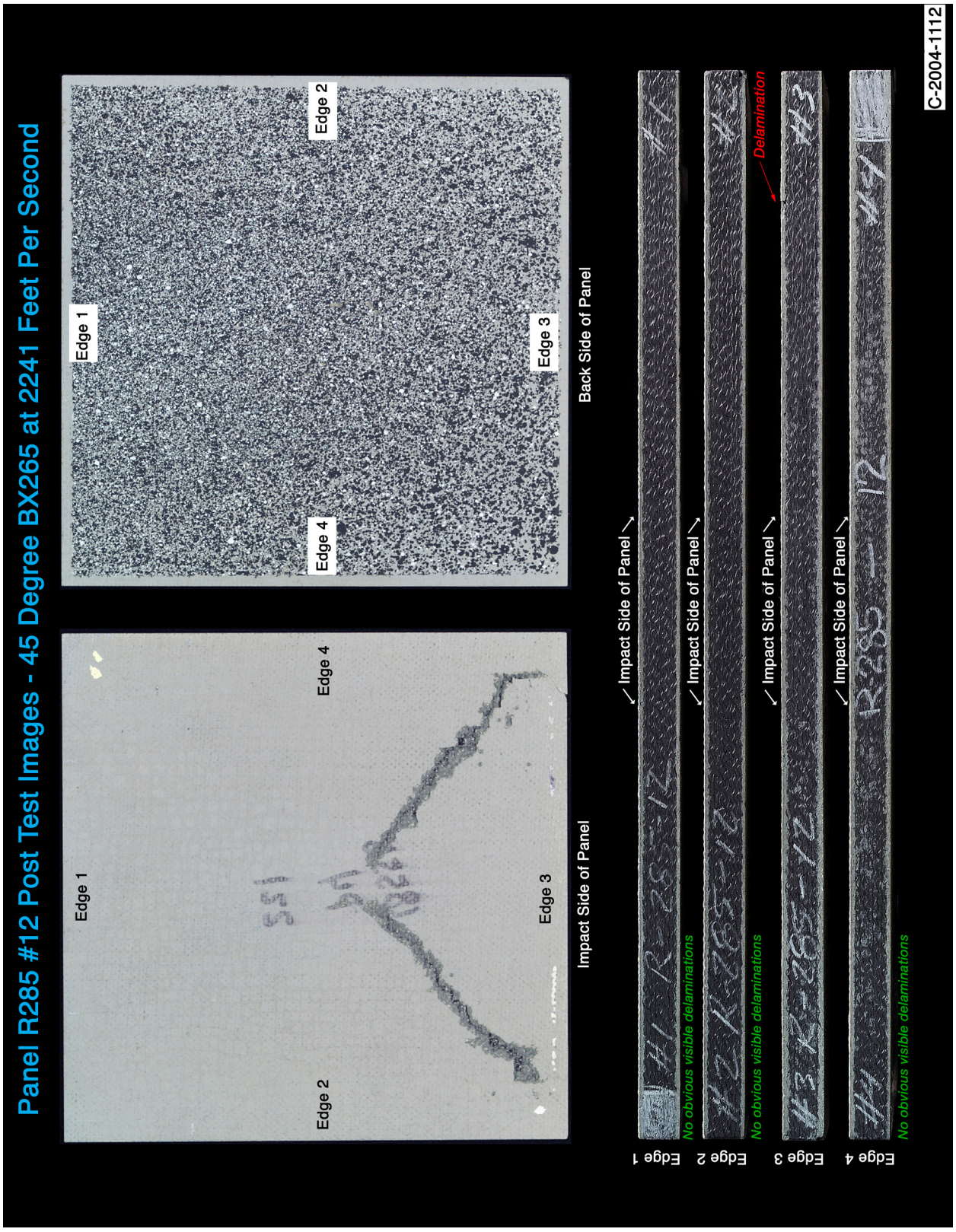

Figure B15–1.—Digital photography of edges and faces of panel R285–12 at 2241 ft/s with a BX–265 foam cylinder (nominally 1.25 in. in diameter by 3 in.) at a 45° impact angle. Test GRCC 46.

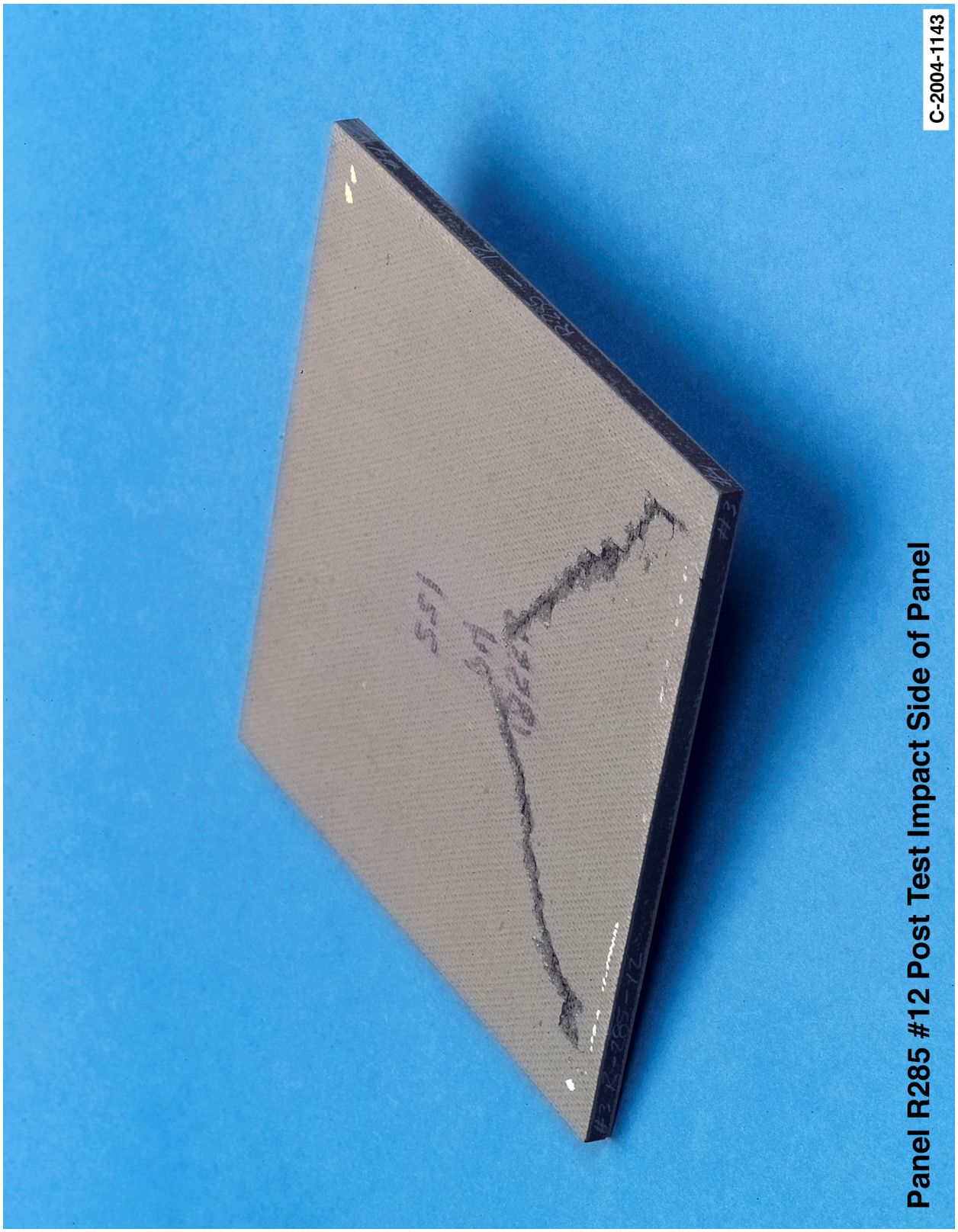

Figure B15–2.—Digital photography front (impact side) face of panel R285–12 at 2241 ft/s with a BX–265 foam cylinder (nominally 1.25 in. in diameter by 3 in.) at a 45° impact angle. Test GRCC 46.

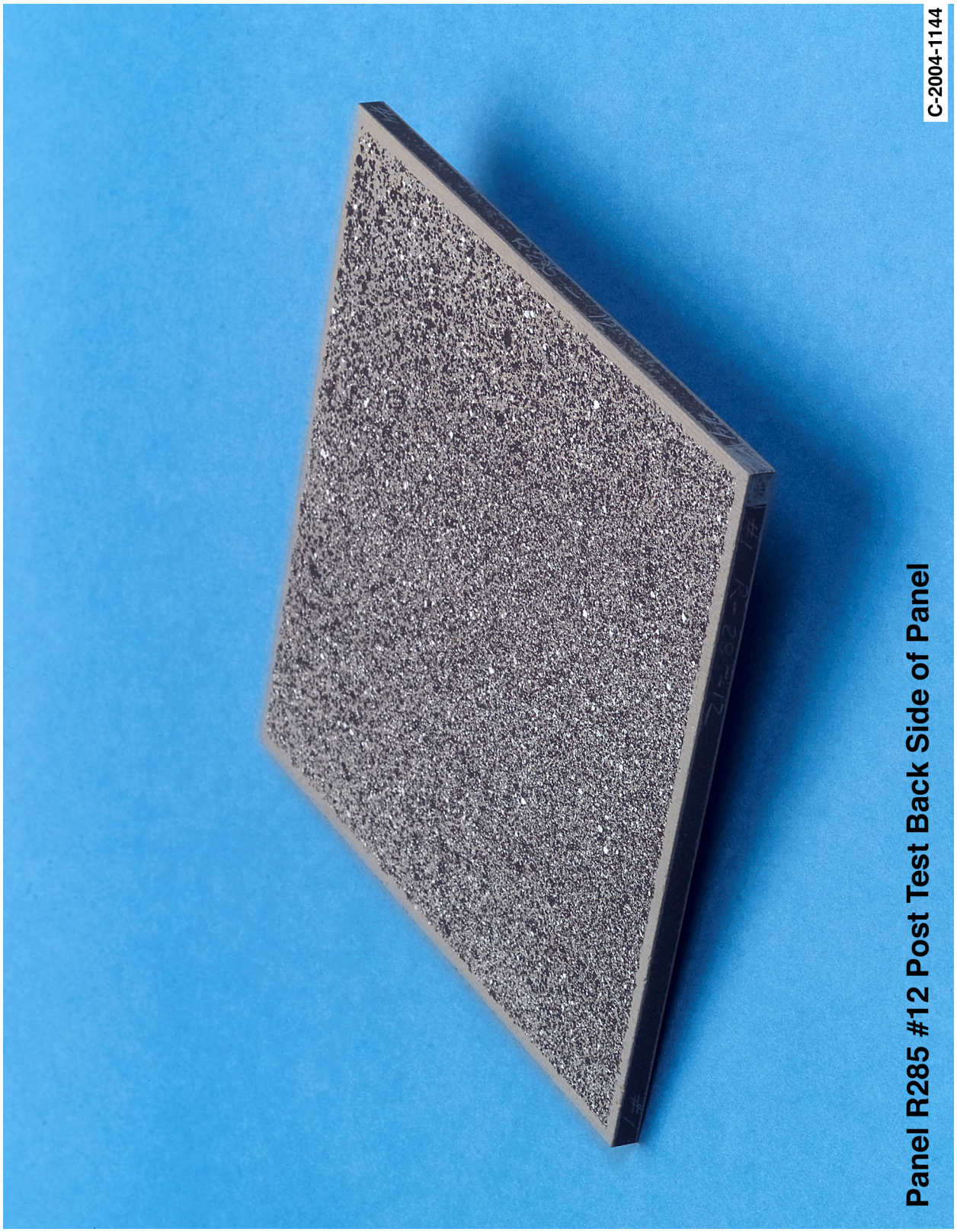

Figure B15–3.—Digital photography of back face of panel R285–12 at 2241 ft/s with a BX–265 foam cylinder (nominally 1.25 in. in diameter by 3 in.) at a 45° impact angle. Test GRCC 46.

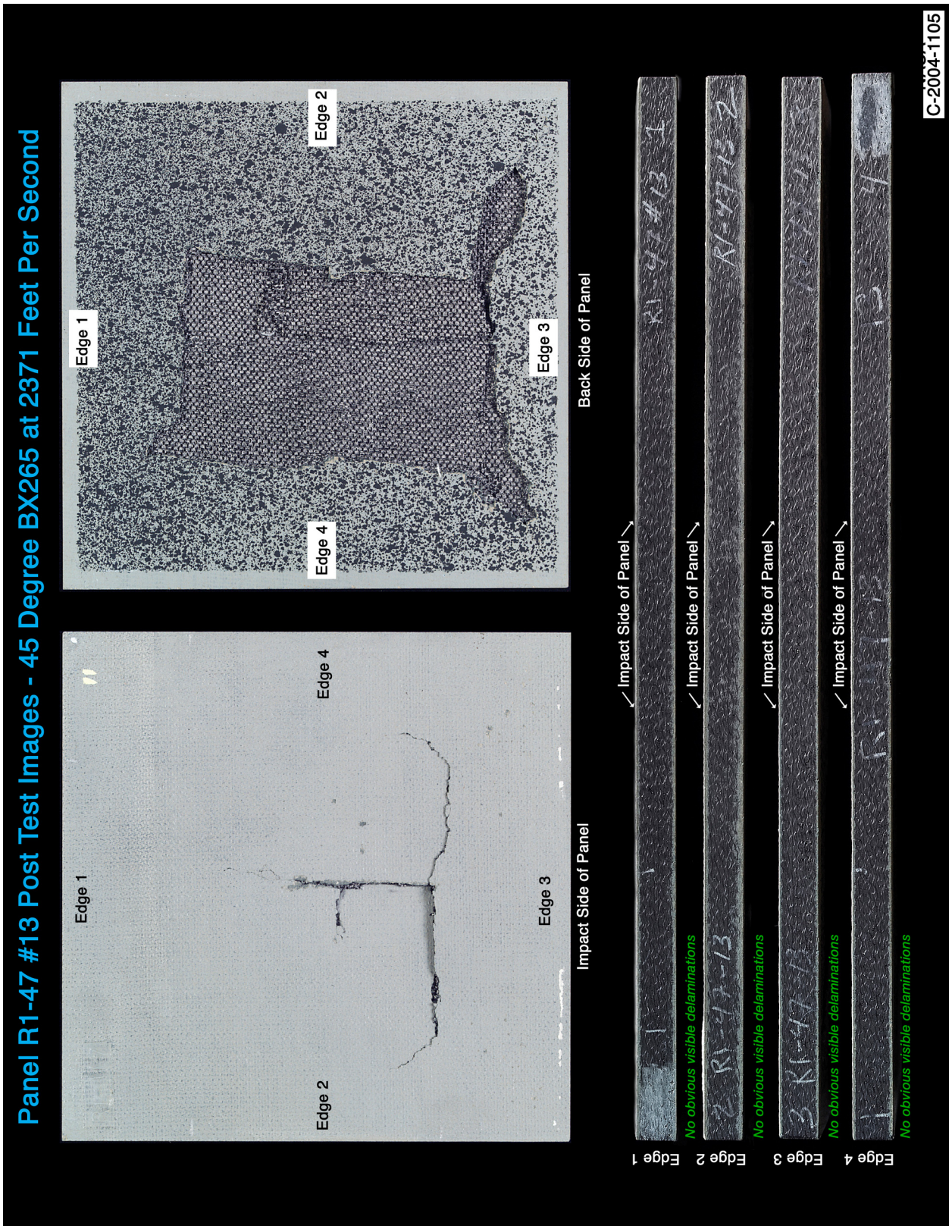

Figure B16–1.—Digital photography of edges and faces of panel R147–13 at 2371 ft/s with a BX–265 foam cylinder (nominally 1.25 in. in diameter by 3 in.) at a 45° impact angle. Test GRCC 29.

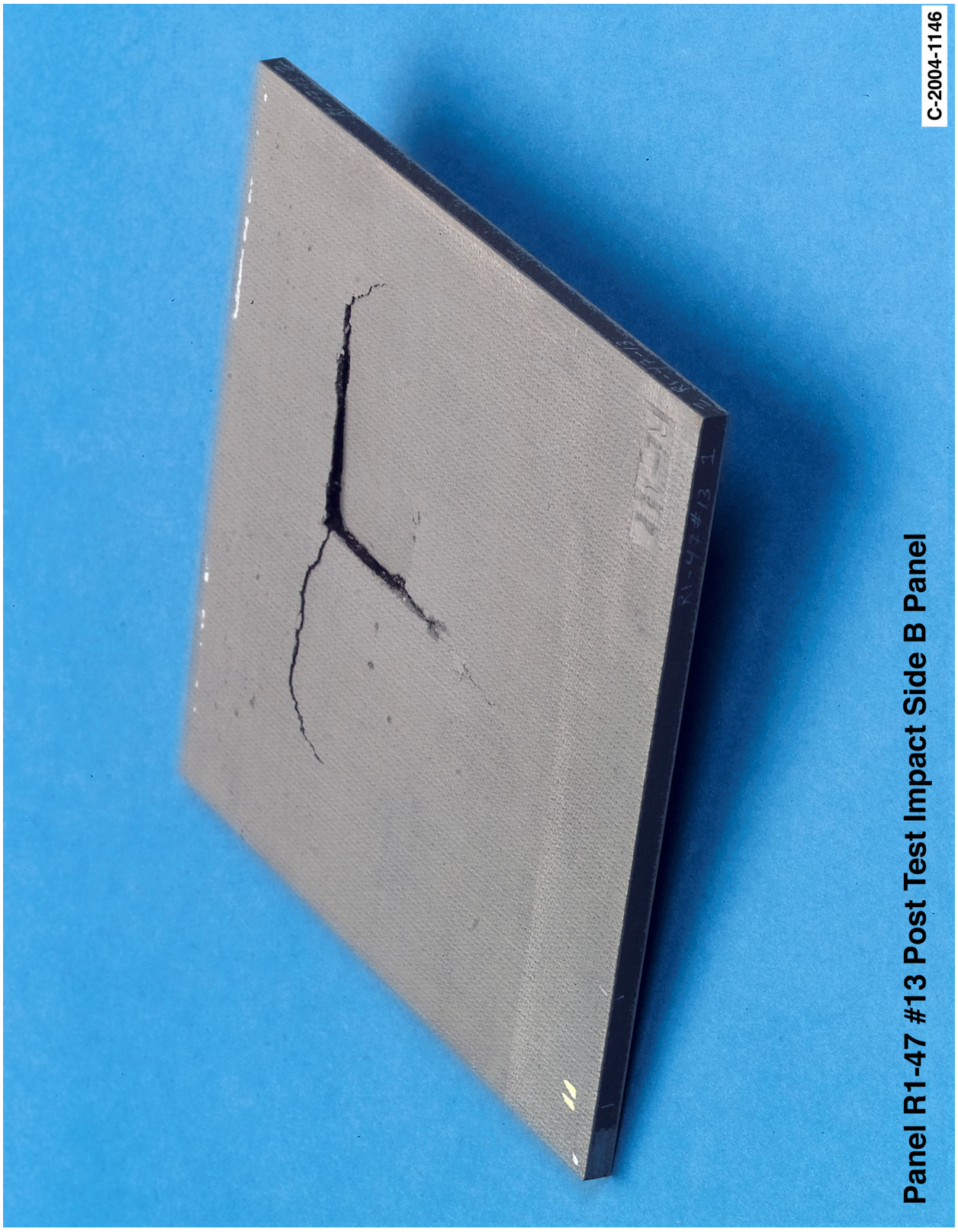

Figure B16–2.—Digital photography front (impact side) face of panel R147–13 at 2371 ft/s with a BX–265 foam cylinder (nominally 1.25 in. in diameter by 3 in.) at a 45° impact angle. Test GRCC 29.

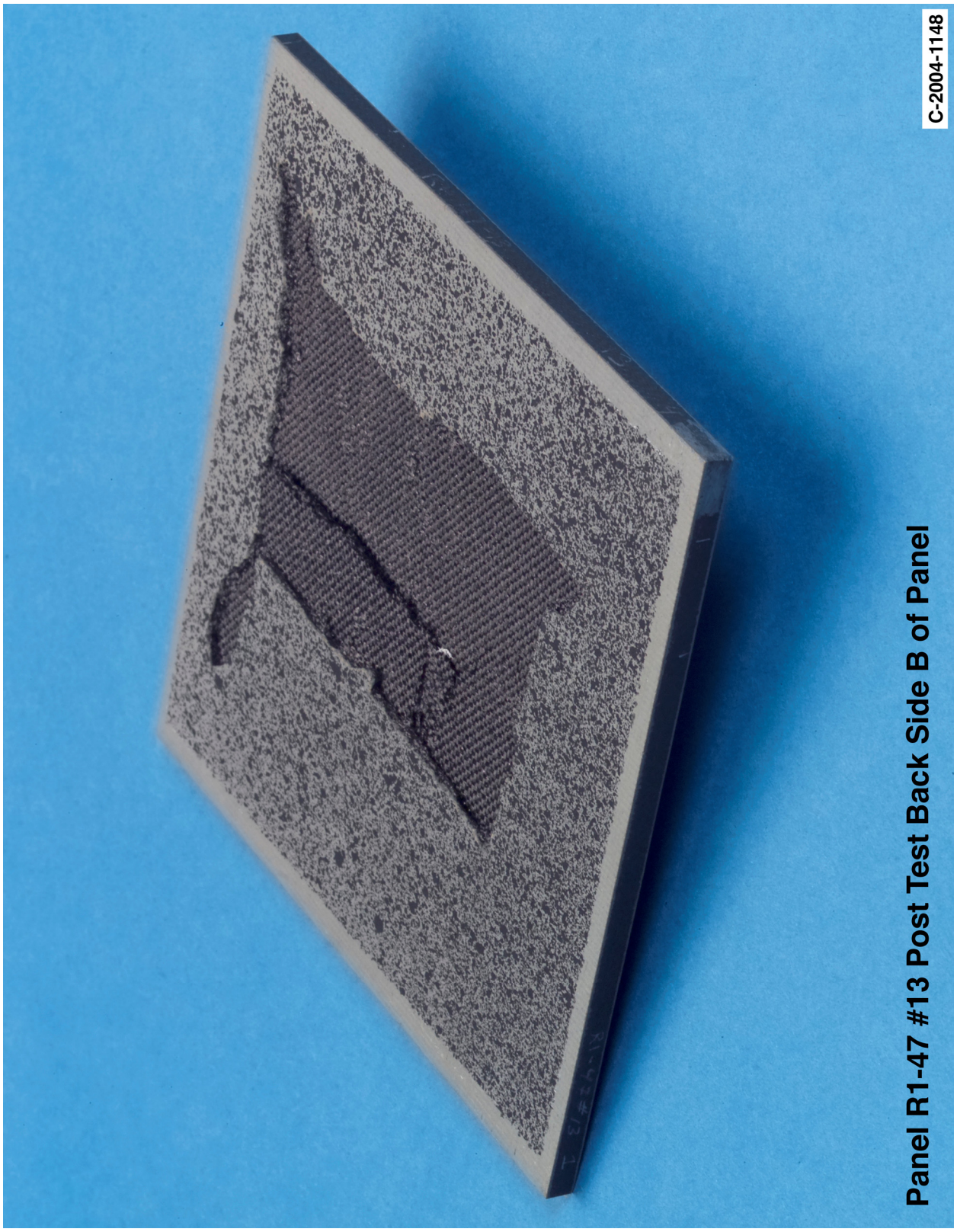

Figure B16–3.—Digital photography of back face of panel R147–13 at 2371 ft/s with a BX–265 foam cylinder (nominally 1.25 in. in diameter by 3 in.) at a 45° impact angle. Test GRCC 29.

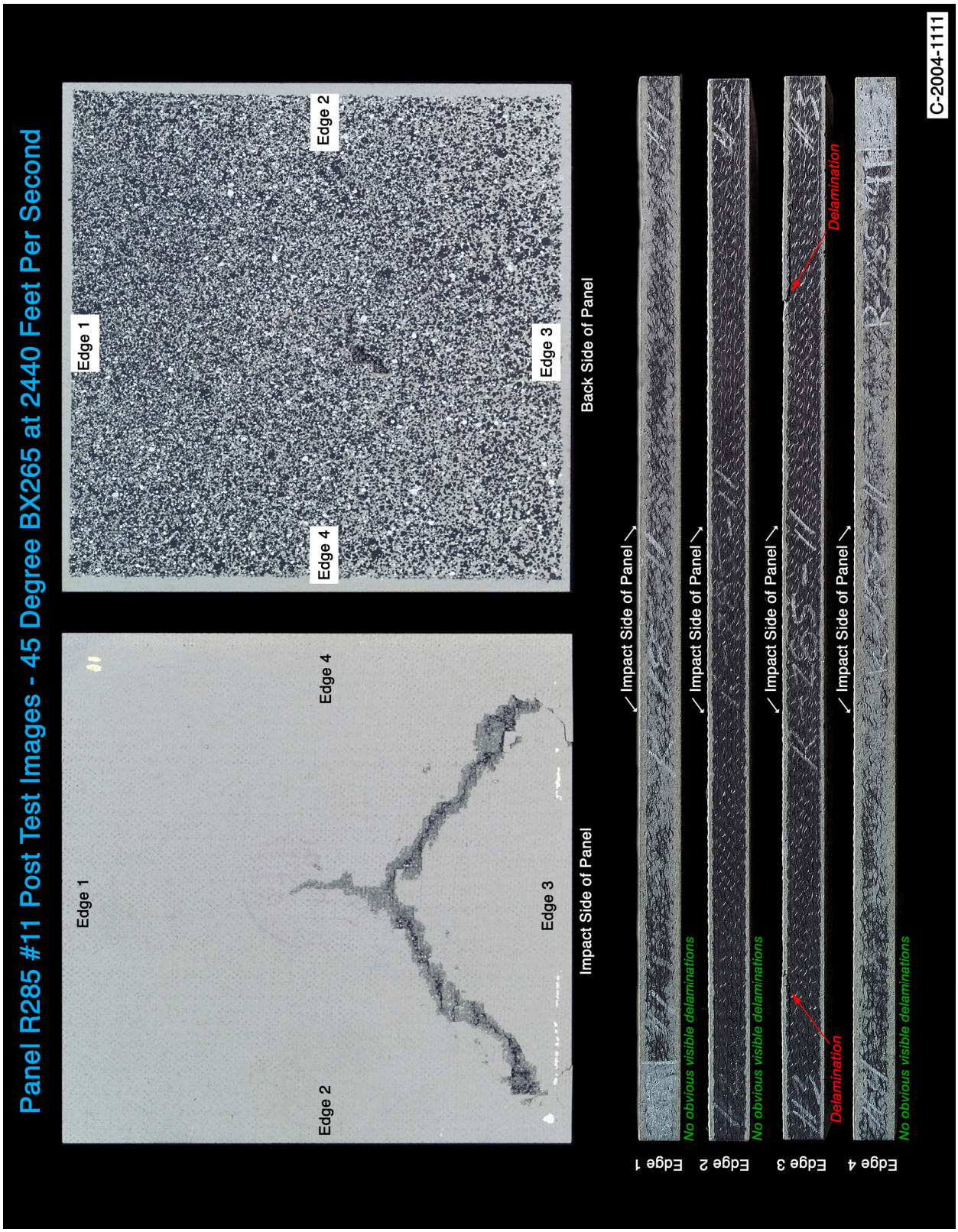

Figure B17–1.—Digital photography of edges and faces of panel R285–11 at 2440 ft/s with a BX–265 foam cylinder (nominally 1.25 in. in diameter by 3 in.) at a 45° impact angle. Test GRCC 45.

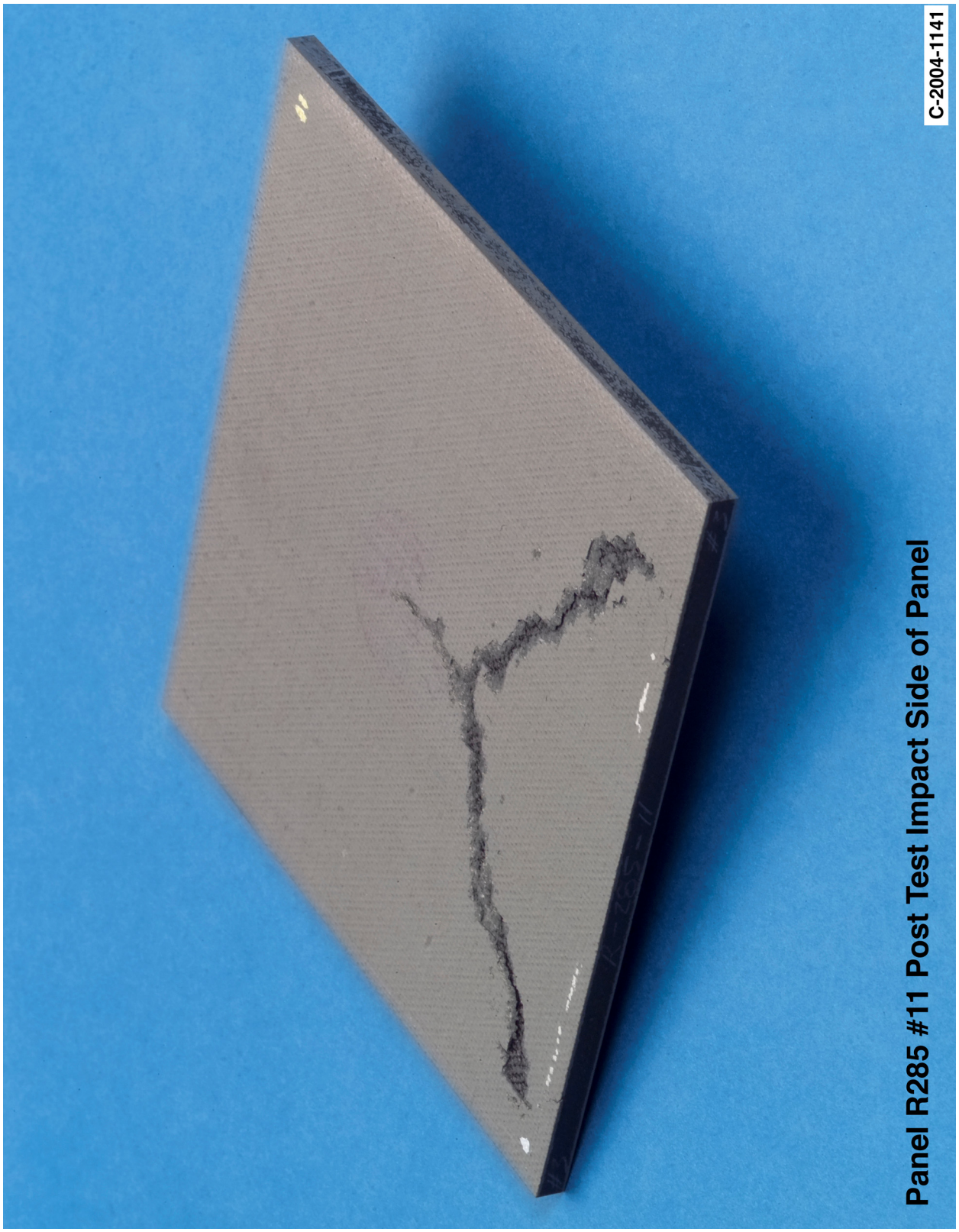

Figure B17–2.—Digital photography front (impact side) face of panel R285–11 at 2440 ft/s with a BX–265 foam cylinder (nominally 1.25 in. in diameter by 3 in.) at a 45° impact angle. Test GRCC 45.

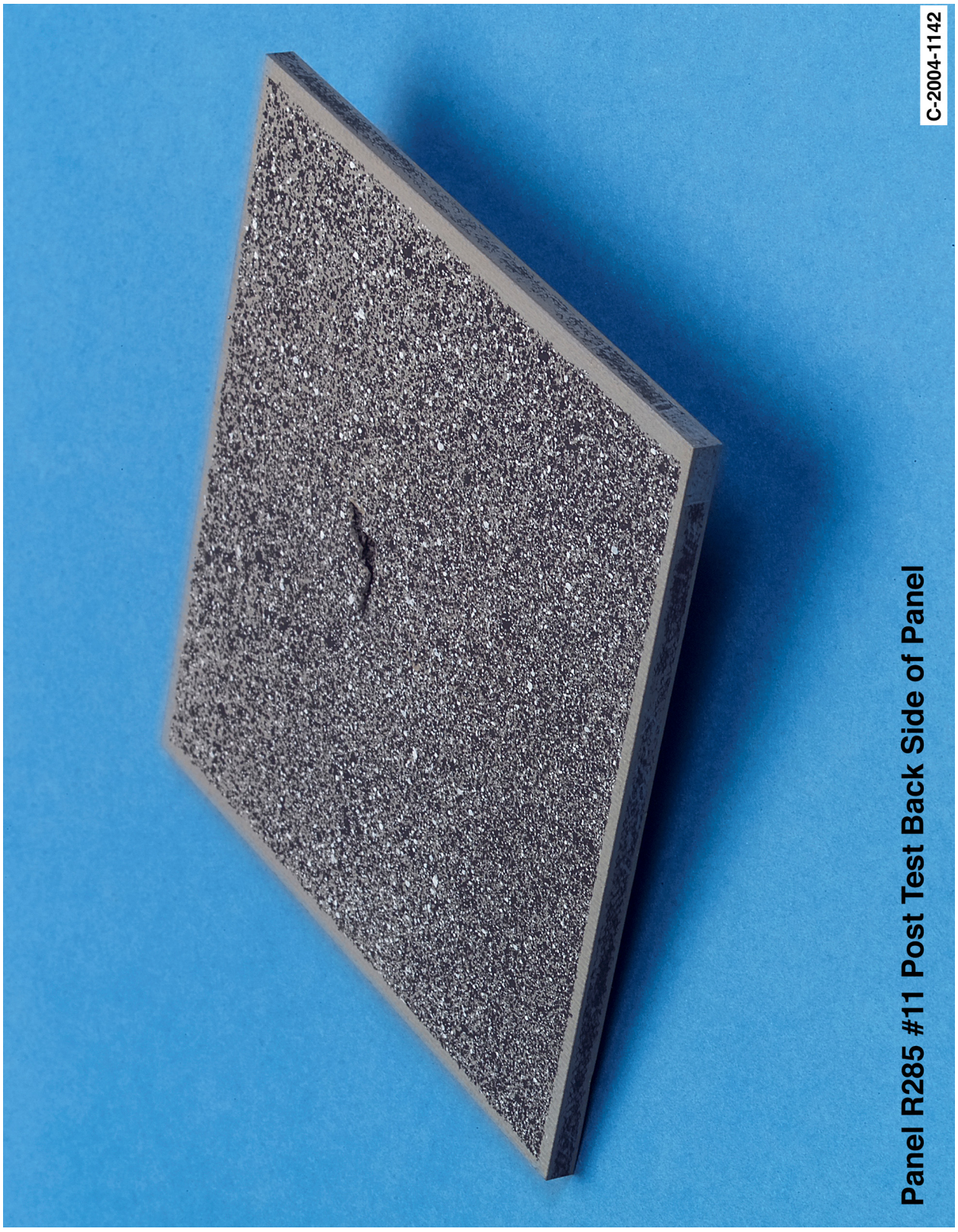

Figure B17–3.—Digital photography of back face of panel R285–11 at 2440 ft/s with a BX–265 foam cylinder (nominally 1.25 in. in diameter by 3 in.) at a 45° impact angle. Test GRCC 45.

Appendix C.—Test Data

BX–265 External Tank Foam Impact Testing at 90° Angle on 6- by 12-in. Reinforced Carbon-Carbon (RCC) Flat Panels

Notable Observations From the Appendix C Test Series

1. The RCC material used in this test series was tested in the as-manufactured condition.
2. Tests GRCC 169 and 170 were shot on the same panel, 54–1. GRCC 169 the foam projectile came out damaged, crooked, and slow. An impromptu experiment was then conducted to determine if damage does accumulate. The second shot, GRCC 170, produced NDE detectable damage, despite its low velocity. Time constraints in the test lab did not allow for ultrasound or thermography to be performed between tests.
3. The 6- by 12-in. panel tests were only simply supported on two ends. As a consequence, the wave propagation in these panels was dramatically different and less controlled and damped than in the 6- by 6-in. panels resulting in additional modes of vibration in the panels being significant. This behavior can be seen in both the C2–1 and C3–1 figures. In C2–1, this is noted by the irregular deformation contours plot as a function of time. In C3–1 the secondary modes of vibration are seen in the first loading cycle and dampen out in the second cycle.
4. Lot 3, (37–57) in the following test series table refers to Lockheed Set 3A, processing Batch 37–57, made specifically for the Return to Flight Program.

Appendix C Test Series

BX-265 90 Degree Impact Test Parameters on 6" x 12" Reinforced Carbon-Carbon Panels													
Test No.	Glenn Test Reference Number	Impact Velocity (ft/sec)	Panel ID Number	Lot Number	Average Panel Thickness (inches)	Visual Damage Observations	Mass of panel before test (grams)	Mass of panel after test (grams)	Projectile Weight (g)	Projectile Length (in)	Projectile Diameter (in)	Test Date	Projectile ID Number
1-90-541-12	GRCC169	1054	54-1	3,(37-57)	0.223	No significant indications	405.03	409.77	3.00	3.035	1.4955	1/25/05	Foam: BX 265, 1930-7-21-4
1-90-541-13	GRCC170	1194	54-1	3,(37-57)	0.223	Multiple hit - no significant indications	409.77	409.89	2.96	3.03	1.4915	1/25/05	Foam: BX 265, 1930-7-21-3
1-90-411-06	GRCC161	1262	41-1	3,(37-57)	0.222	No significant indications	413.92	413.80	2.92	2.994	1.495	1/24/05	Foam: BX 265, 1930-6-2-1
1-90-502-11	GRCC168	1264	50-2	3,(37-57)	0.220	No significant indications	398.70	398.63	2.98	2.99	1.494	1/25/05	Foam: BX 265, 1930-6-20-8
1-90-482-09	GRCC165	1461	48-2	3,(37-57)	0.222	No significant indications	411.75	411.65	2.95	3.0165	1.486	1/25/05	Foam: BX 265, 1930-6-2-4
1-90-412-07	GRCC163	1538	41-2	3,(37-57)	0.220	Coating chips lost on backside	408.34	408.25	2.95	3.035	1.494	1/24/05	Foam: BX 265, 1930-6-2-1
1-90-501-10	GRCC167	1849	50-1	3,(37-57)	0.223	Through crack, backside coating loss	402.96	402.76	2.97	3.009	1.4885	1/25/05	Foam: BX 265, 1930-6-20-7

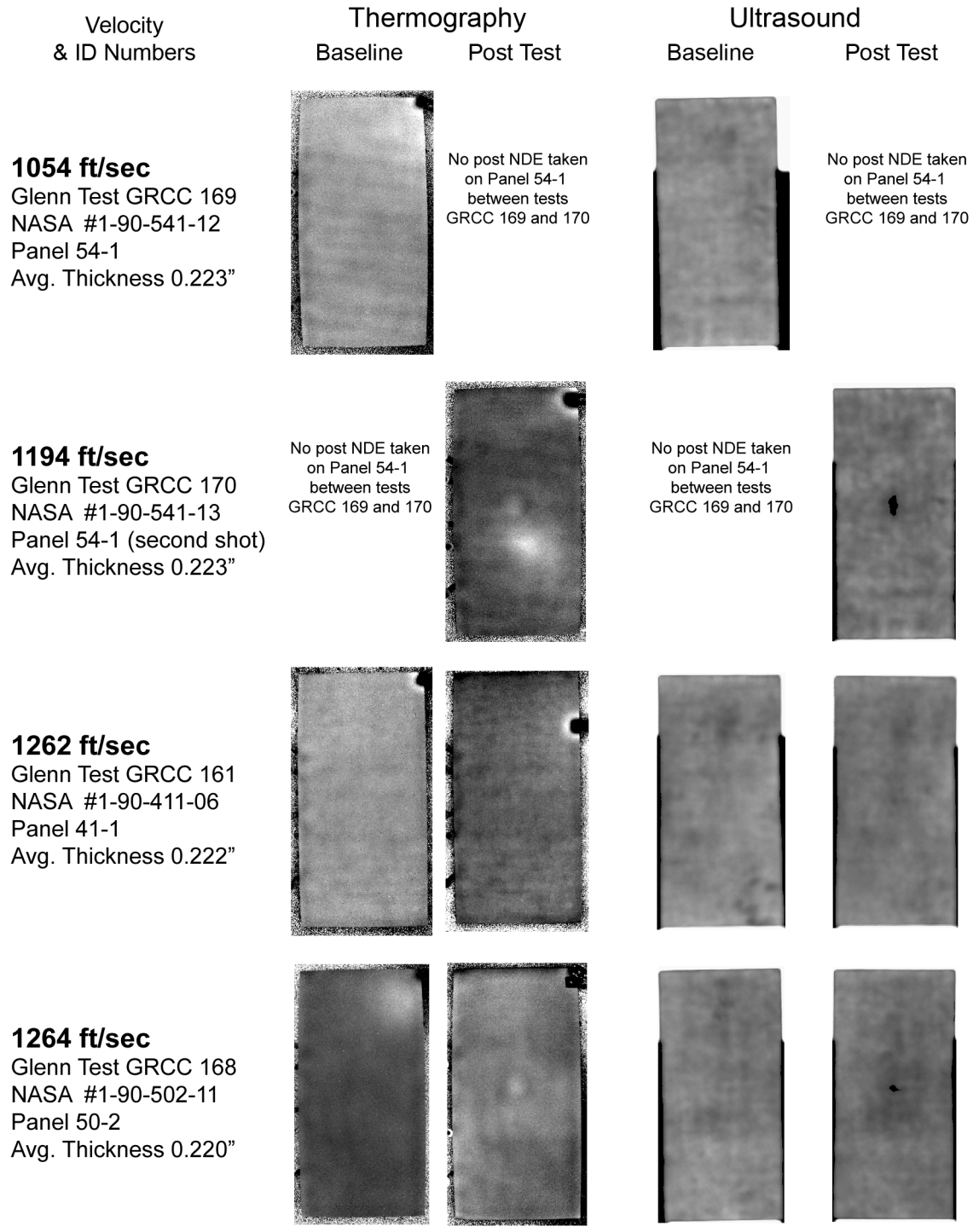

Figure C1–1.—Pulse thermography and ultrasound post impact pretest and posttest images of reinforced carbon-carbon 6- by 12-in. flat panels impacted with BX–265 foam cylinders (nominally 1.5 in. in diameter by 3 in.) at a 90° angle.

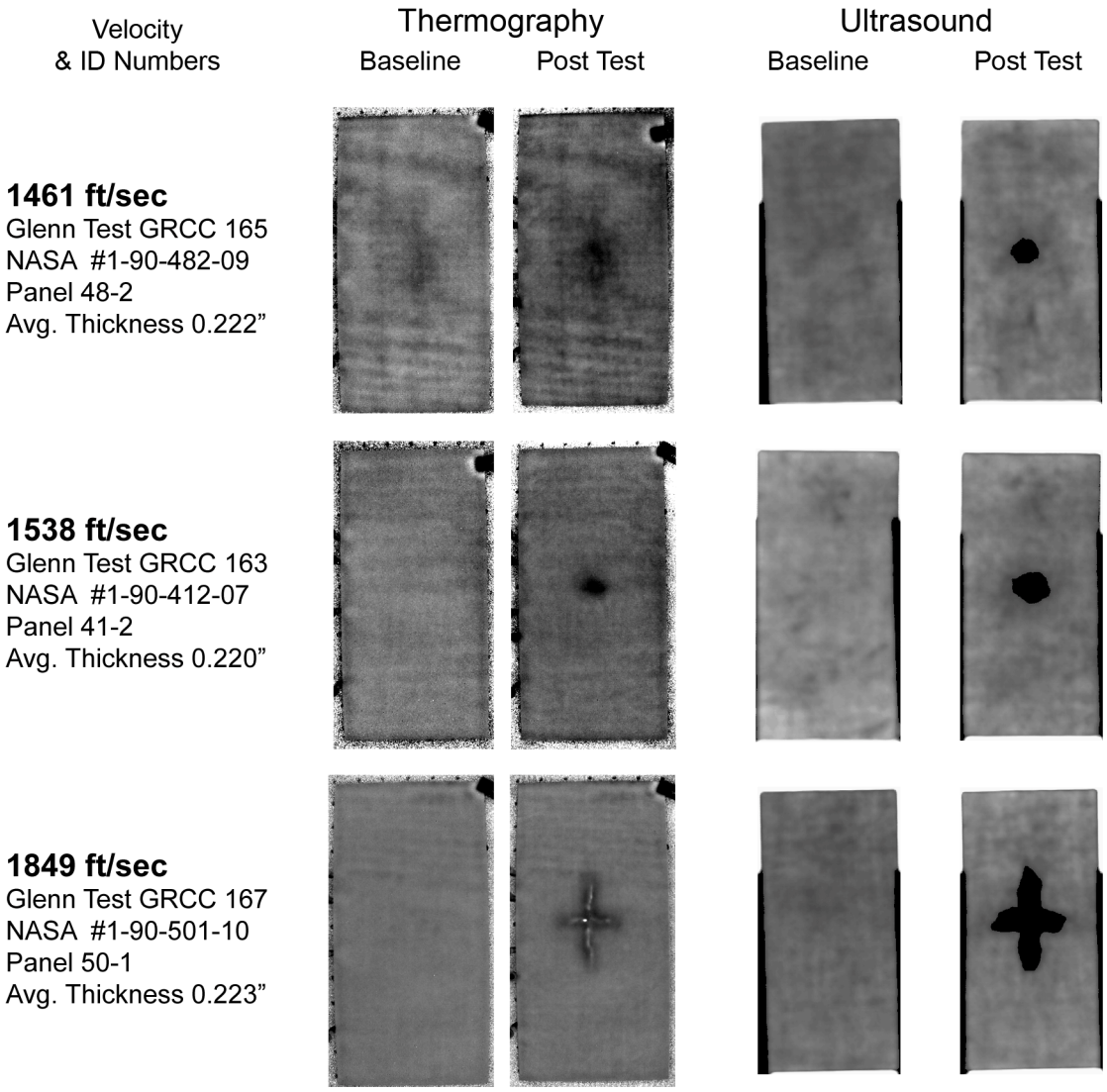

Figure C1–2.—Pulse thermography and ultrasound post impact pretest and posttest images of reinforced carbon-carbon 6- by 12-in. flat panels impacted with BX–265 foam cylinders (nominally 1.5 in. in diameter by 3 in.) at a 90° angle.

Aramis Displacement Contours from 90 Degree Impact Tests with BX-265 on 6” x 12” RCC Panels

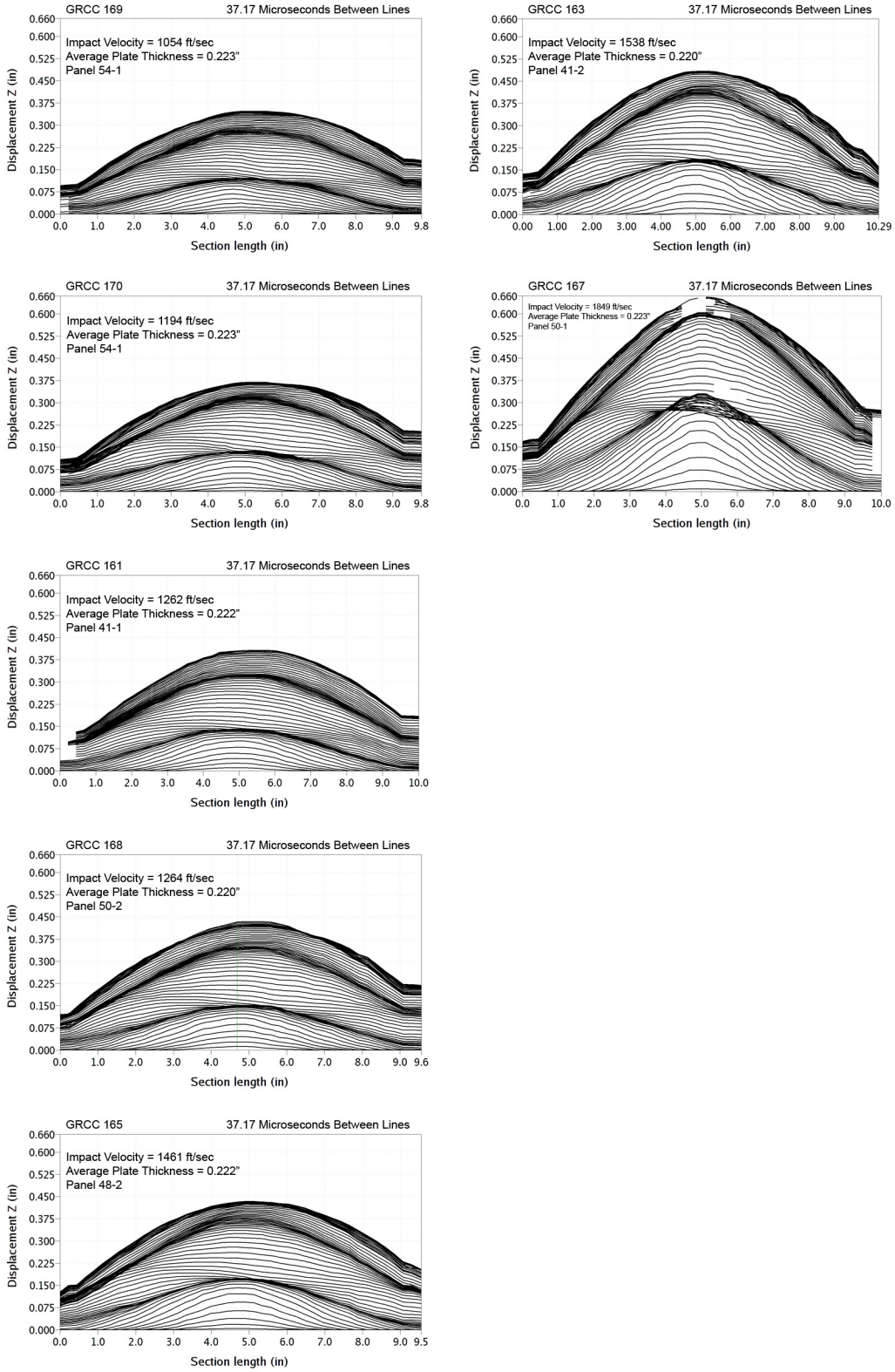

Figure C2–1.—ARAMIS out-of-plane deformation contours across centerline of 6- by 12-in. reinforced carbon-carbon flat panels measured at 37-μs increments undergoing impact with BX–265 foam cylinders (nominally 1.5 in. in diameter by 3 in.) at a 90° angle.

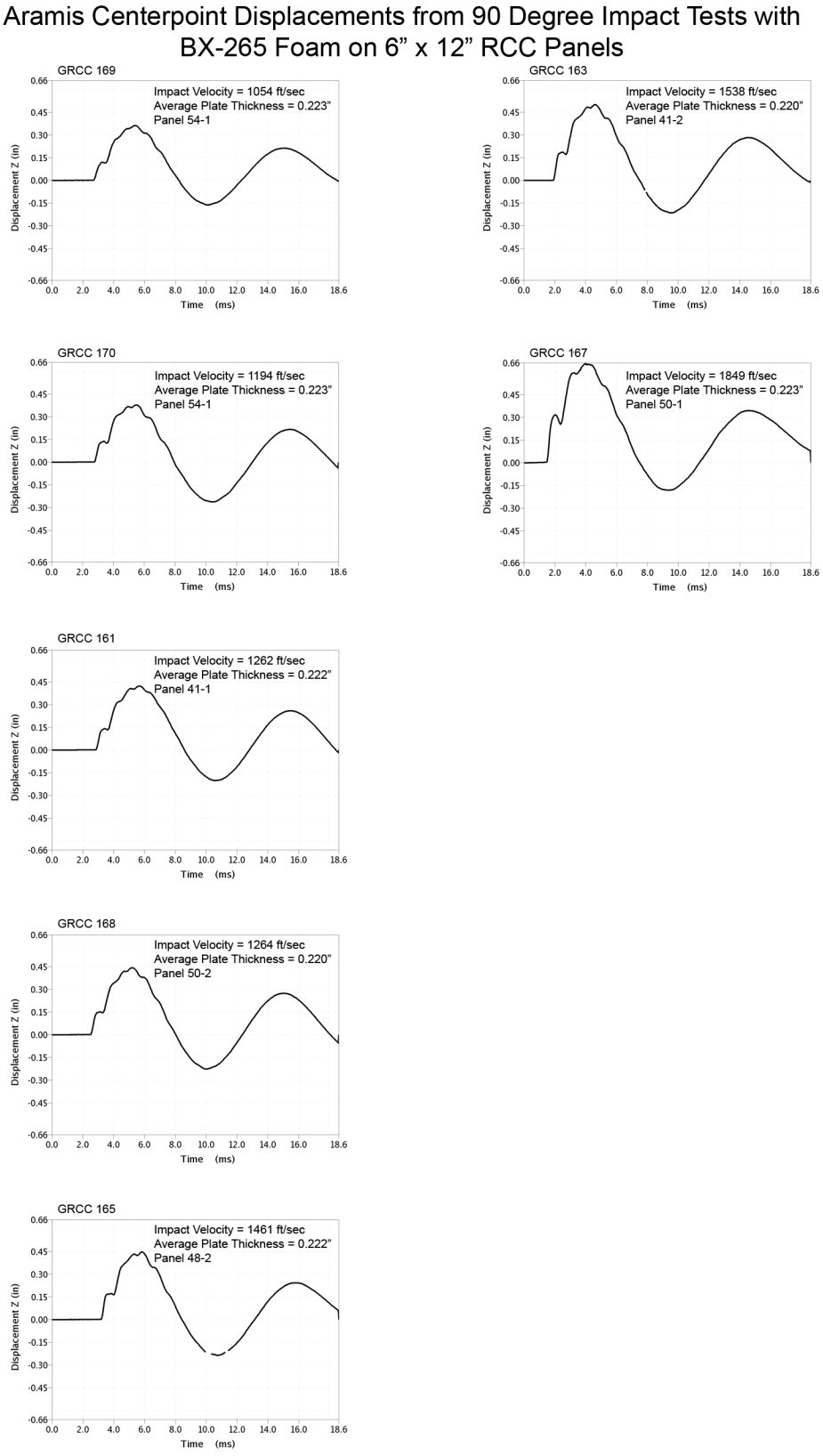

Figure C3–1.—ARAMIS centerpoint out-of-plane deformation vs. time of 6- by 12-in. reinforced carbon-carbon flat panels impacted with BX–265 foam cylinders (nominally 1.5 in. in diameter by 3 in.) at a 90° angle.

Aramis Maximum Displacement Fringe Plots from 90 Degree Impact Tests withBX-265 Foam on 6” x 12” RCC Panels

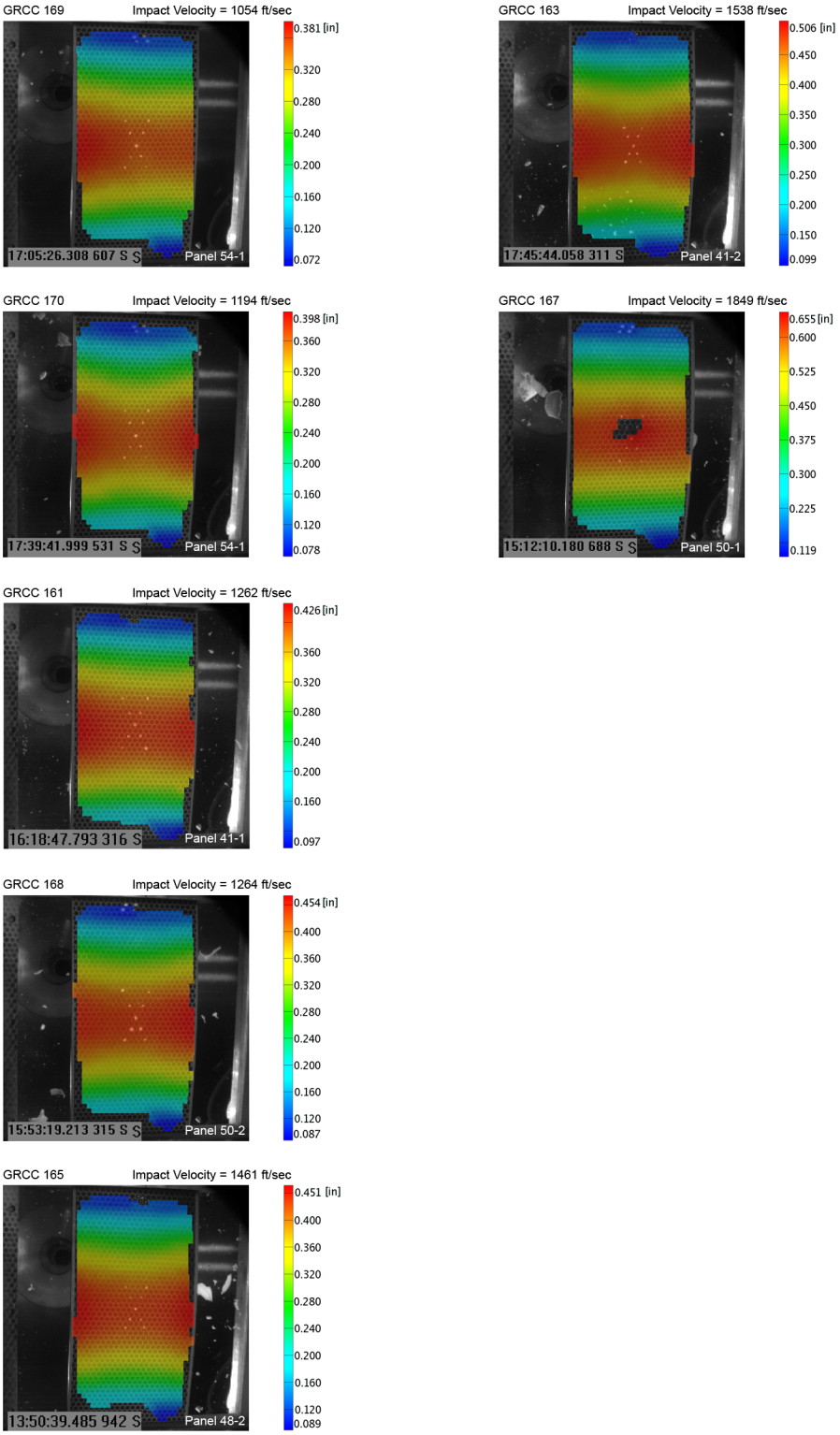

Figure C4–1.—ARAMIS color fringe plots depicting maximum deformation prior to material failure of 6- by 12-in. reinforced carbon-carbon flat panels as they undergo impact with BX–265 foam cylinders (nominally 1.5 in. in diameter by 3 in.) at a 90° angle.

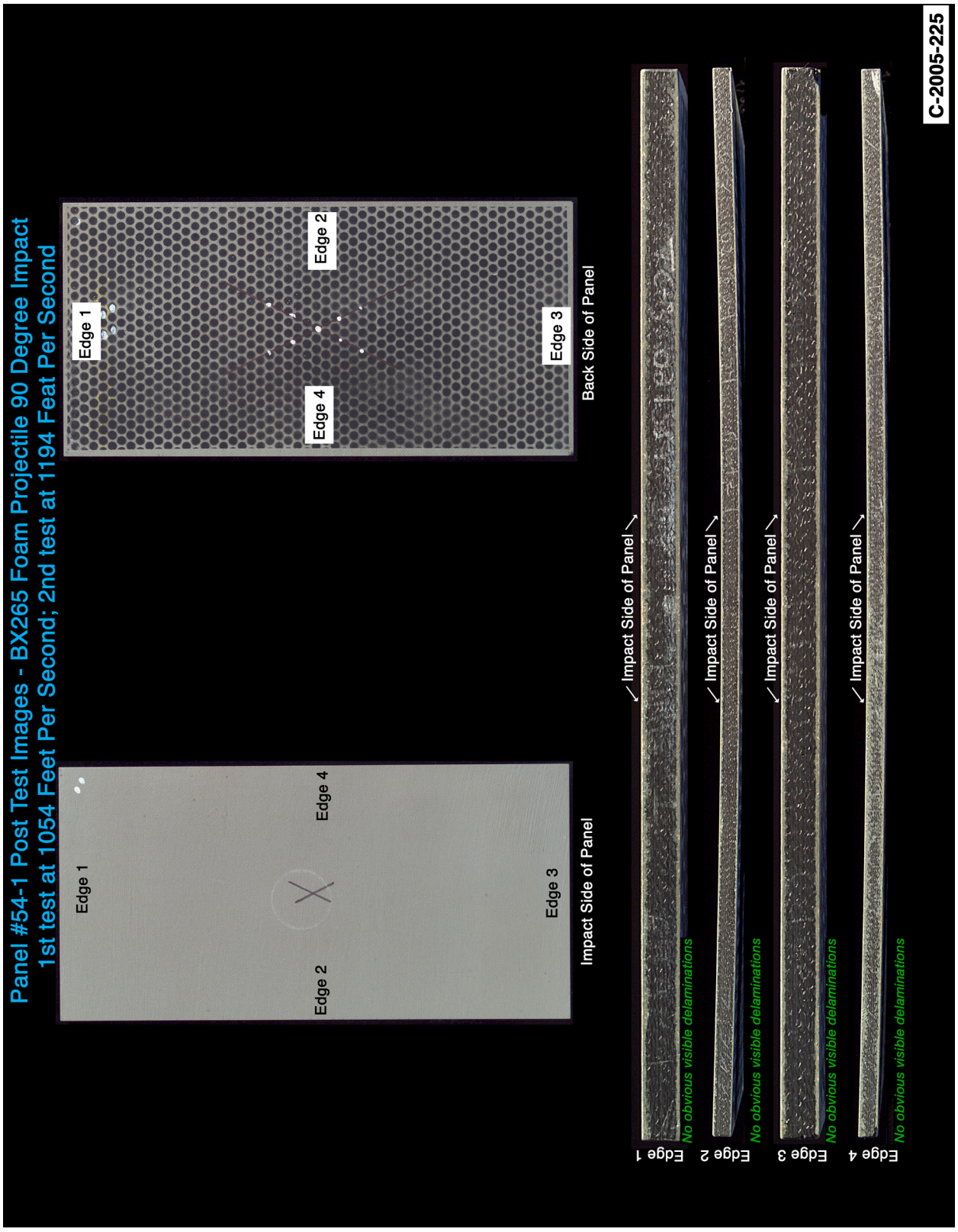

Figure C5–1.—Digital photography of edges and faces of panel 54–1 at 1194 ft/s with a BX–265 foam cylinder (nominally 1.5 in. in diameter by 3 in.) at a 90° impact angle. Test GRCC 170.

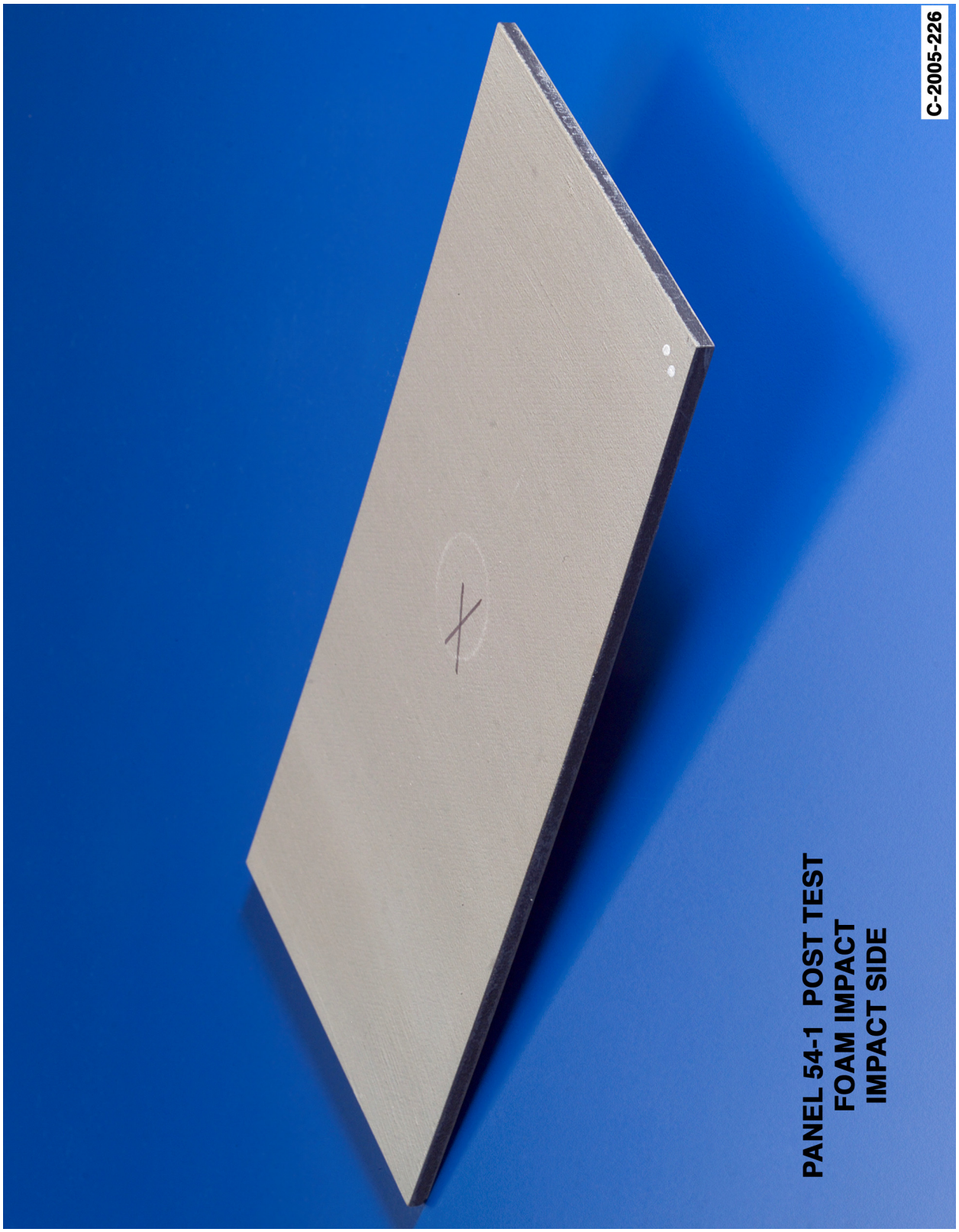

Figure C5–2.—Digital photography front (impact side) face of panel 54–1 at 1194 ft/s with a BX–265 foam cylinder (nominally 1.5 in. in diameter by 3 in.) at a 90° impact angle. Test GRCC 170.

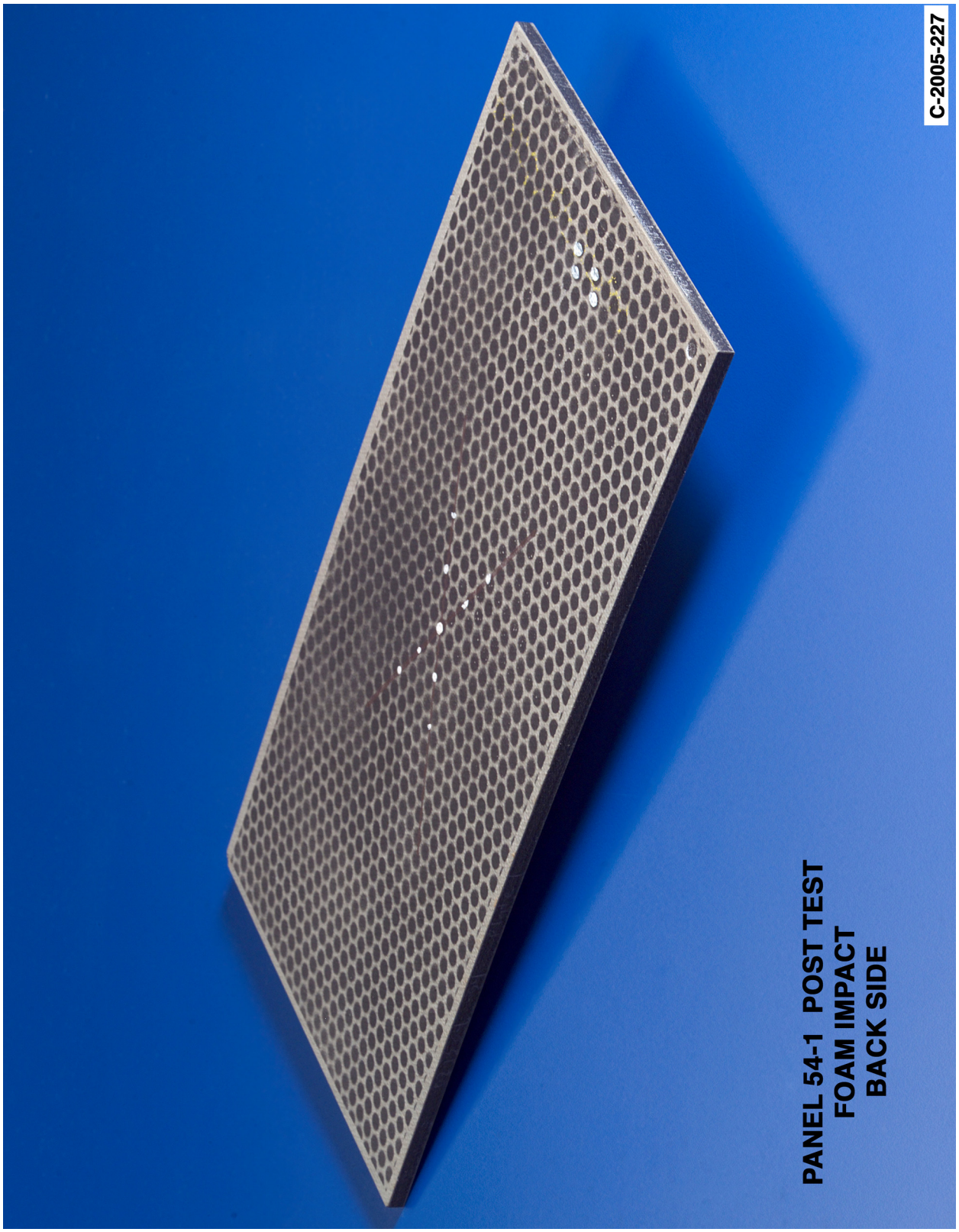

Figure C5–3.—Digital photography of back face of panel 54–1 at 1194 ft/s with a BX–265 foam cylinder (nominally 1.5 in. in diameter by 3 in.) at a 90° impact angle. Test GRCC 170.

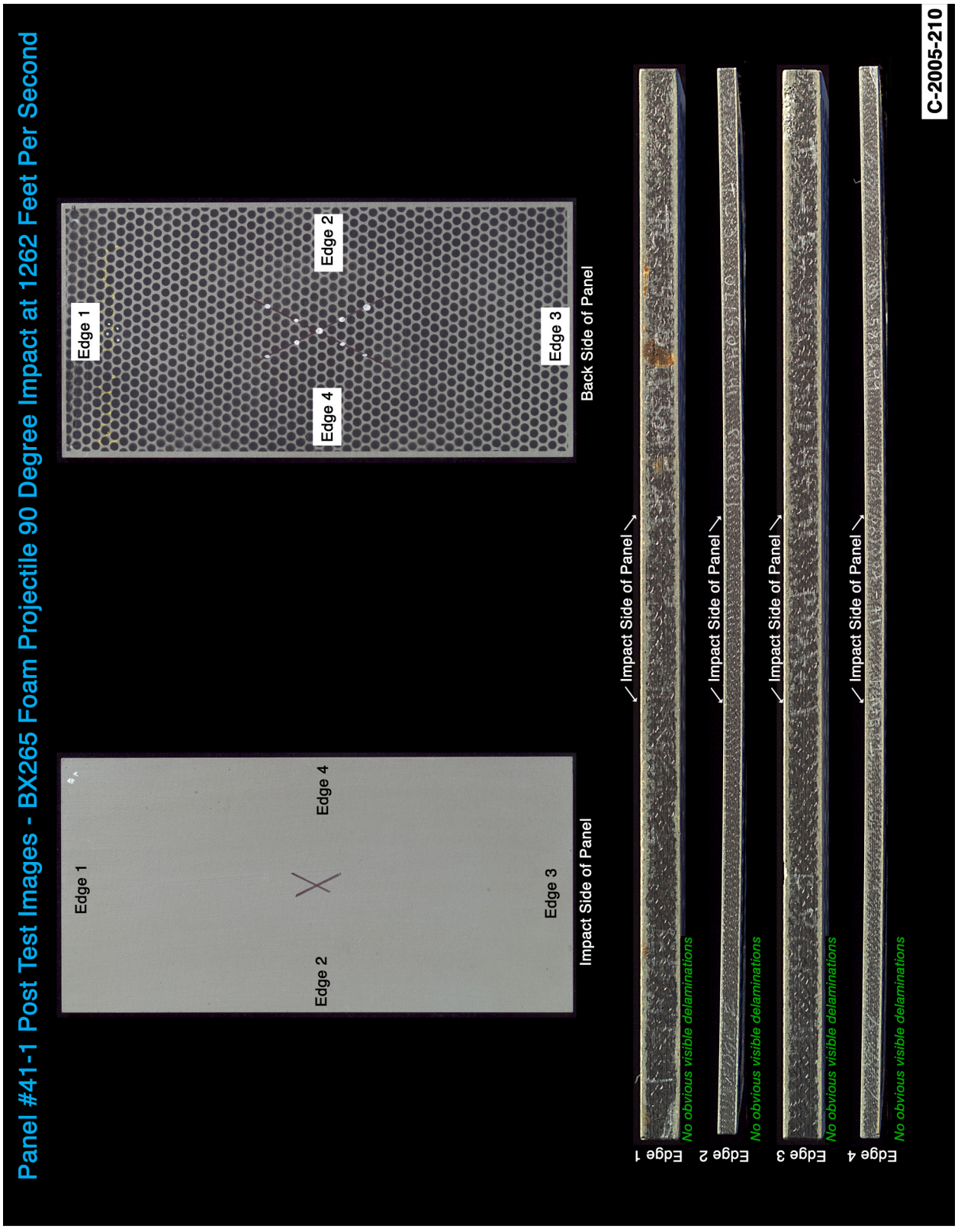

Figure C6–1.—Digital photography of edges and faces of panel 41–1 at 1262 ft/s with a BX–265 foam cylinder (nominally 1.5 in. in diameter by 3 in.) at a 90° impact angle. Test GRCC 161.

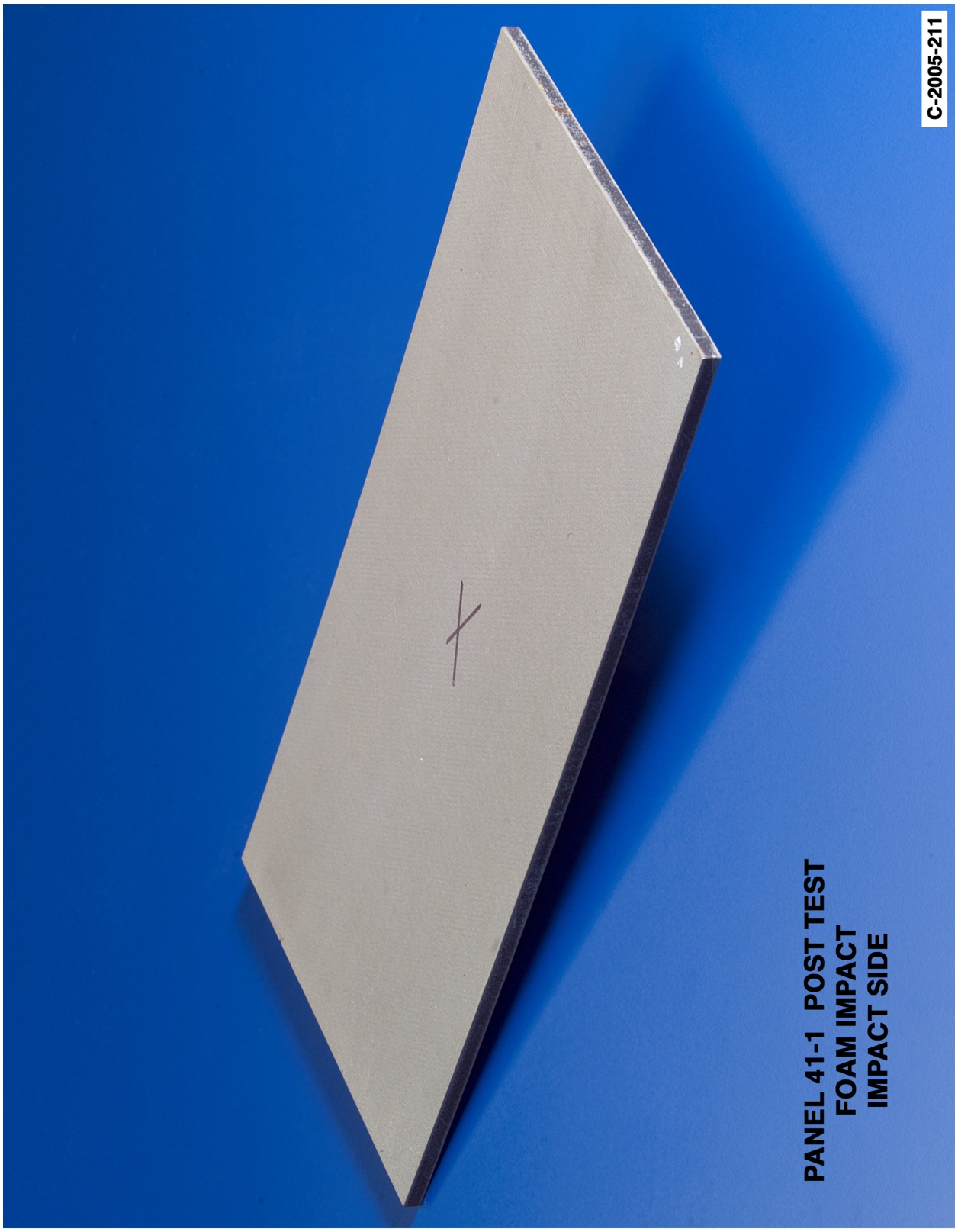

Figure C6–2.—Digital photography front (impact side) face of panel 41–1 at 1262 ft/s with a BX–265 foam cylinder (nominally 1.5 in. in diameter by 3 in.) at a 90° impact angle. Test GRCC 161.

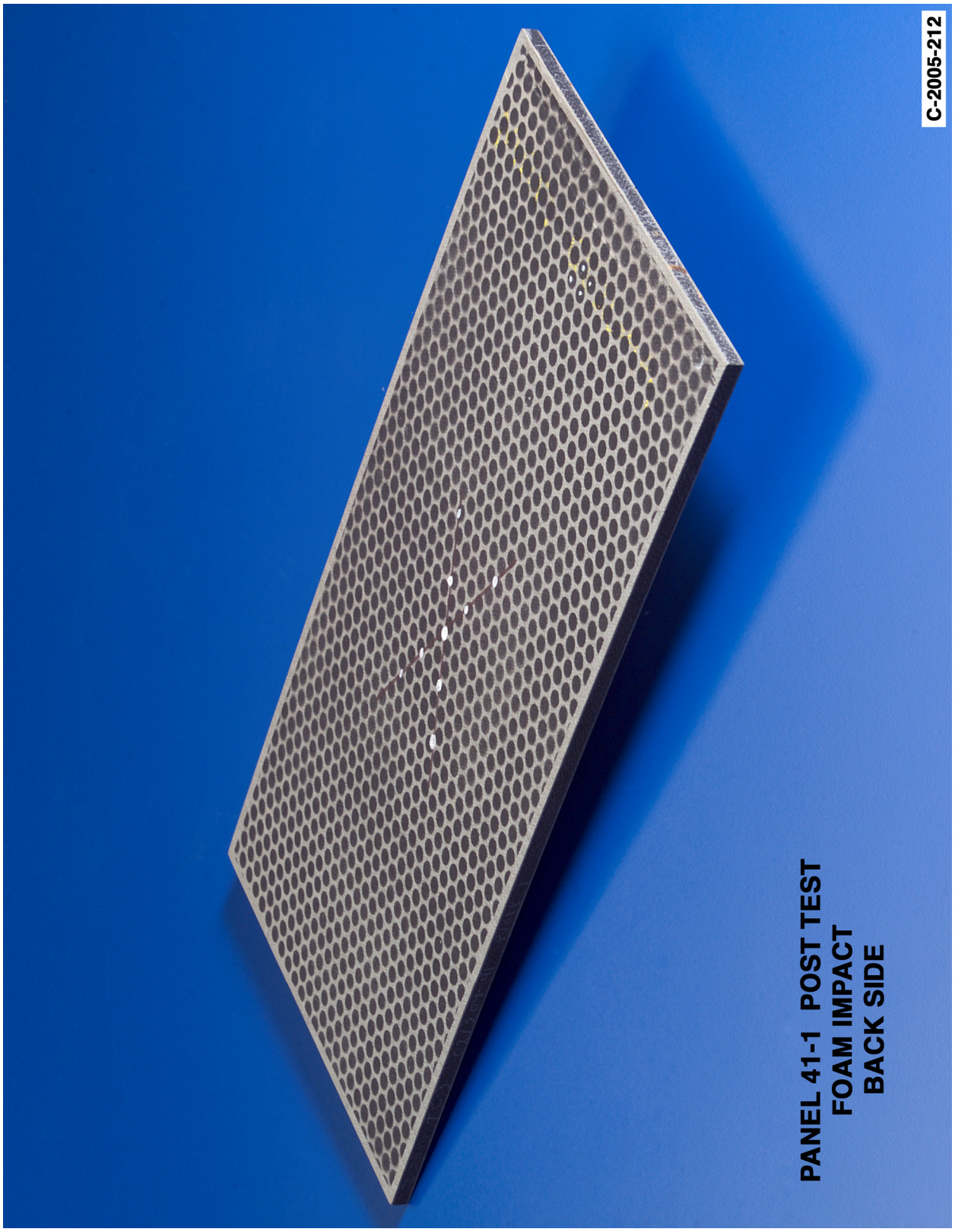

Figure C6–3.—Digital photography of back face of panel 41–1 at 1262 ft/s with a BX–265 foam cylinder (nominally 1.5 in. in diameter by 3 in.) at a 90° impact angle. Test GRCC 161.

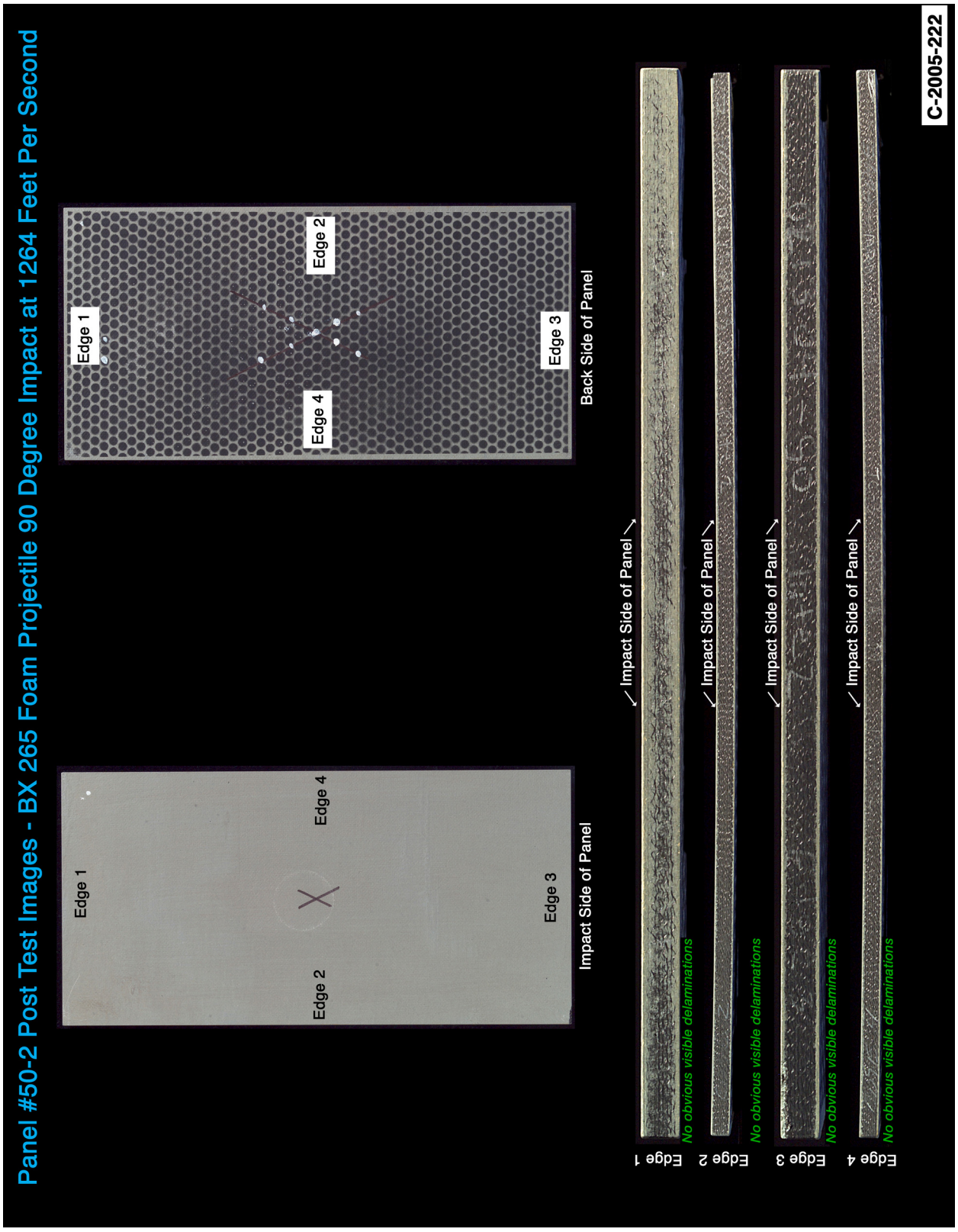

Figure C7–1.—Digital photography of edges and faces of panel 50–2 at 1264 ft/s with a BX–265 foam cylinder (nominally 1.5 in. in diameter by 3 in.) at a 90° impact angle. Test GRCC 168.

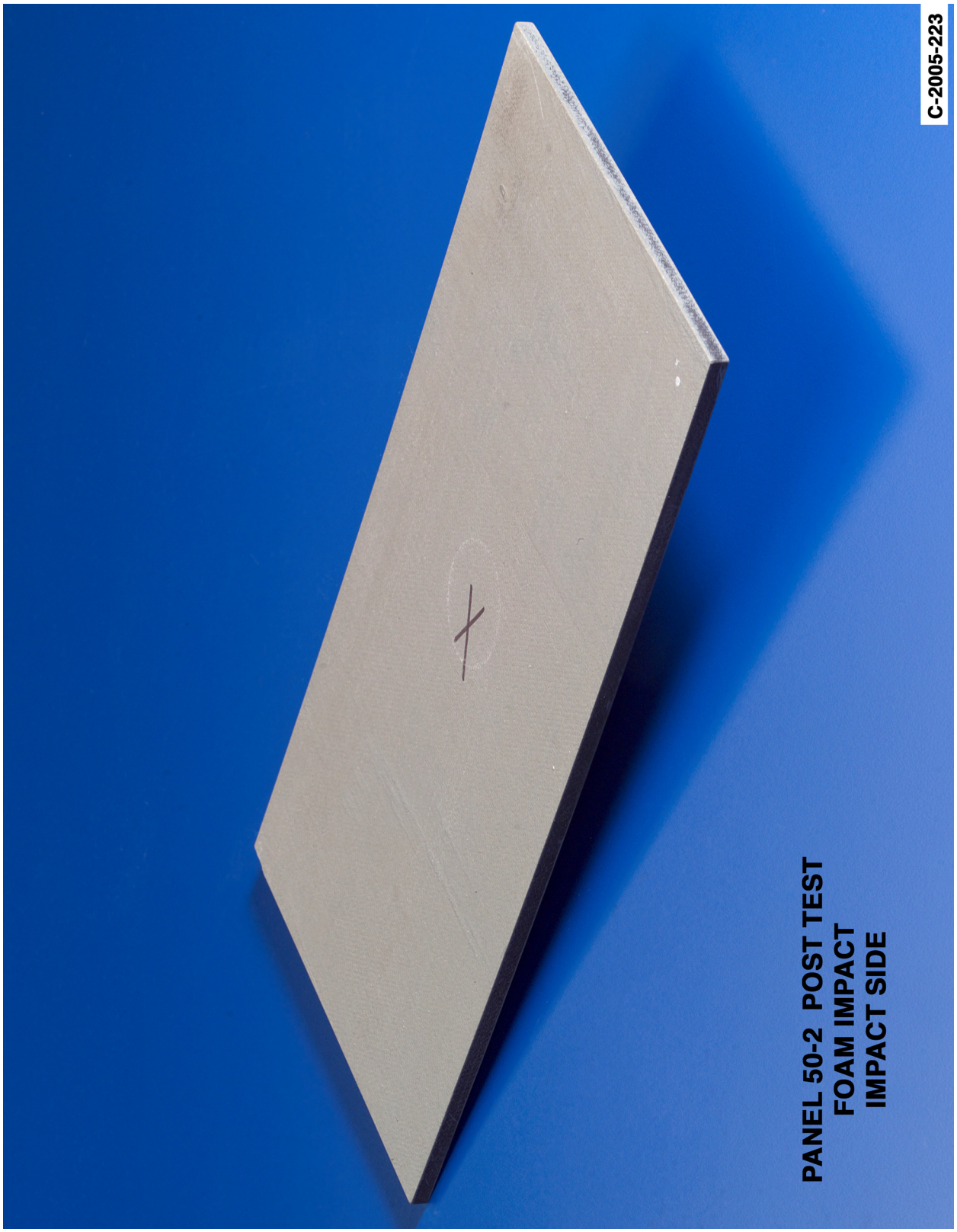

Figure C7–2.—Digital photography front (impact side) face of panel 50–2 at 1264 ft/s with a BX–265 foam cylinder (nominally 1.5 in. in diameter by 3 in.) at a 90° impact angle. Test GRCC 168.

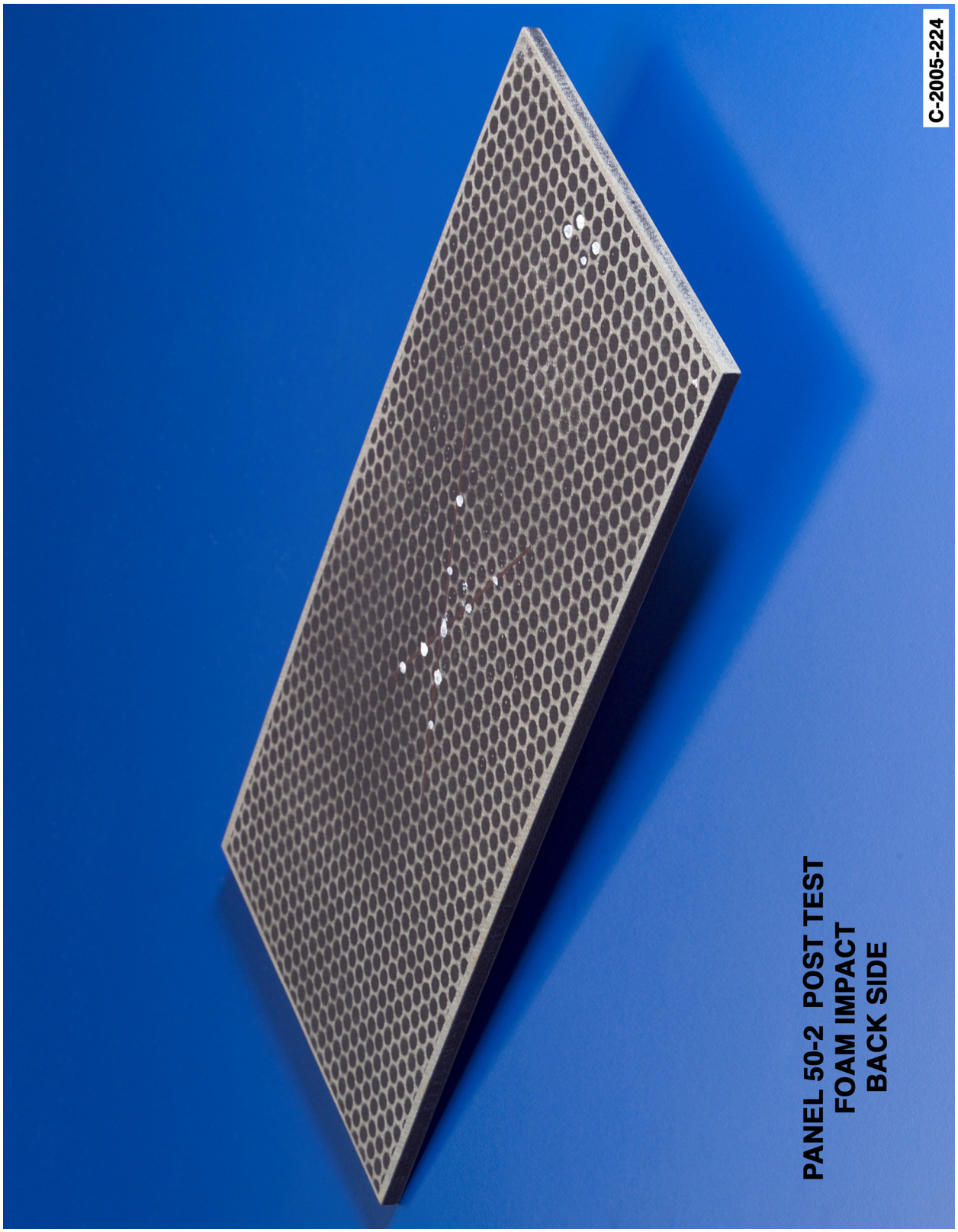

Figure C7–3.—Digital photography of back face of panel 50–2 at 1264 ft/s with a BX–265 foam cylinder (nominally 1.5 in. in diameter by 3 in.) at a 90° impact angle. Test GRCC 168.

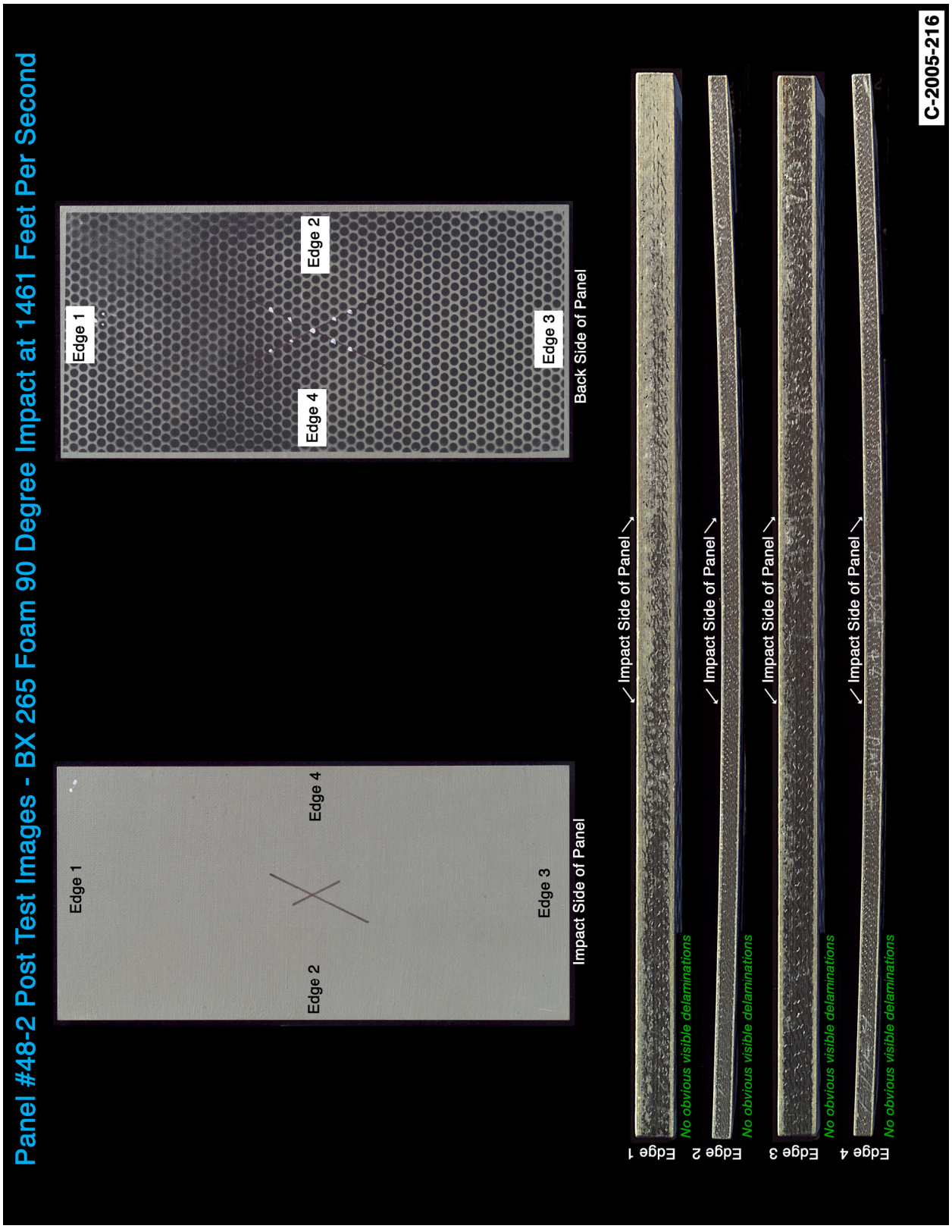

Figure C8–1.—Digital photography of edges and faces of panel 48–2 at 1461 ft/s with a BX–265 foam cylinder (nominally 1.5 in. in diameter by 3 in.) at a 90° impact angle. Test GRCC 165.

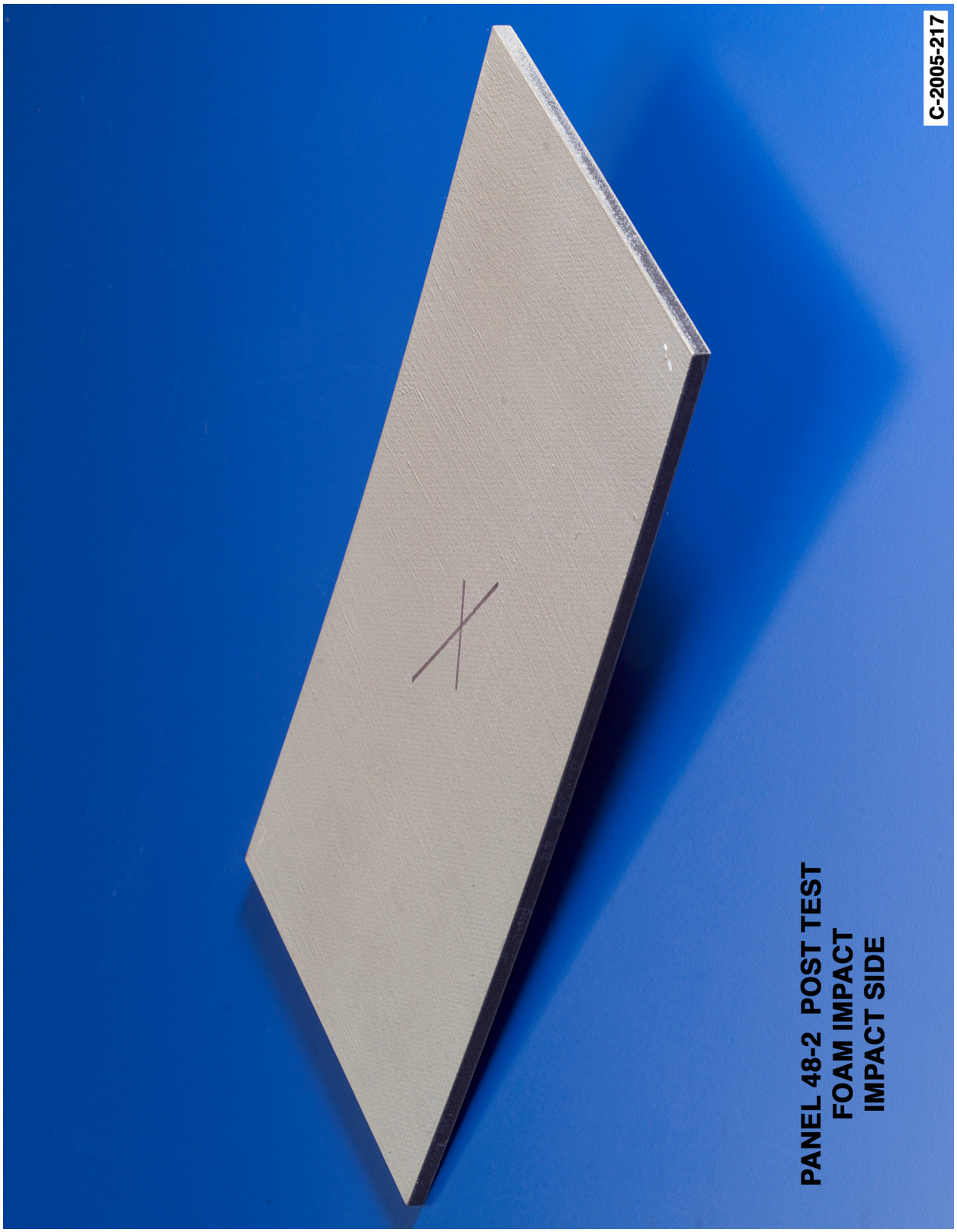

Figure C8–2.—Digital photography front (impact side) face of panel 48–2 at 1461 ft/s with a BX–265 foam cylinder (nominally 1.5 in. in diameter by 3 in.) at a 90° impact angle. Test GRCC 165.

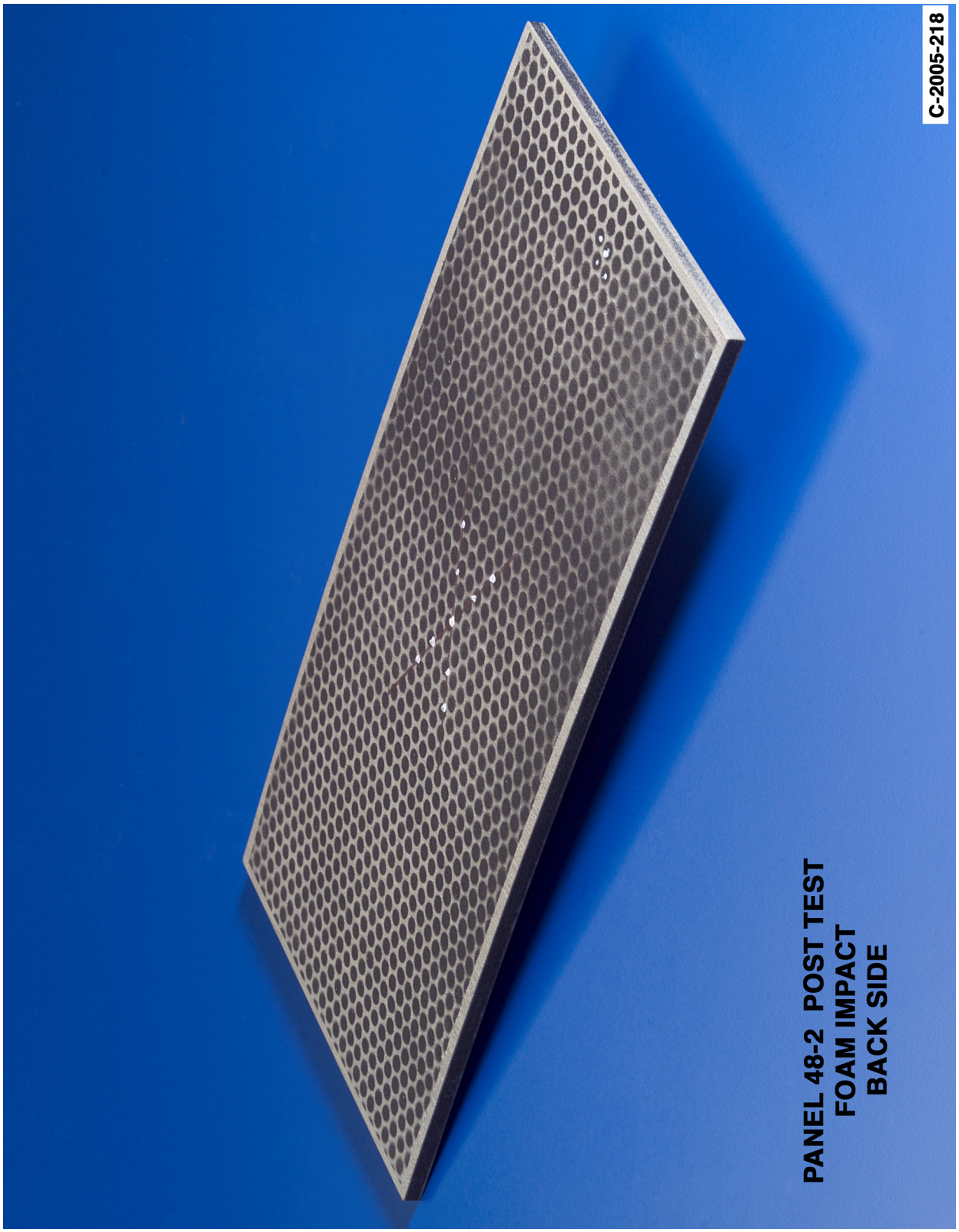

Figure C8–3.—Digital photography of back face of panel 48–2 at 1461 ft/s with a BX–265 foam cylinder (nominally 1.5 in. in diameter by 3 in.) at a 90° impact angle. Test GRCC 165.

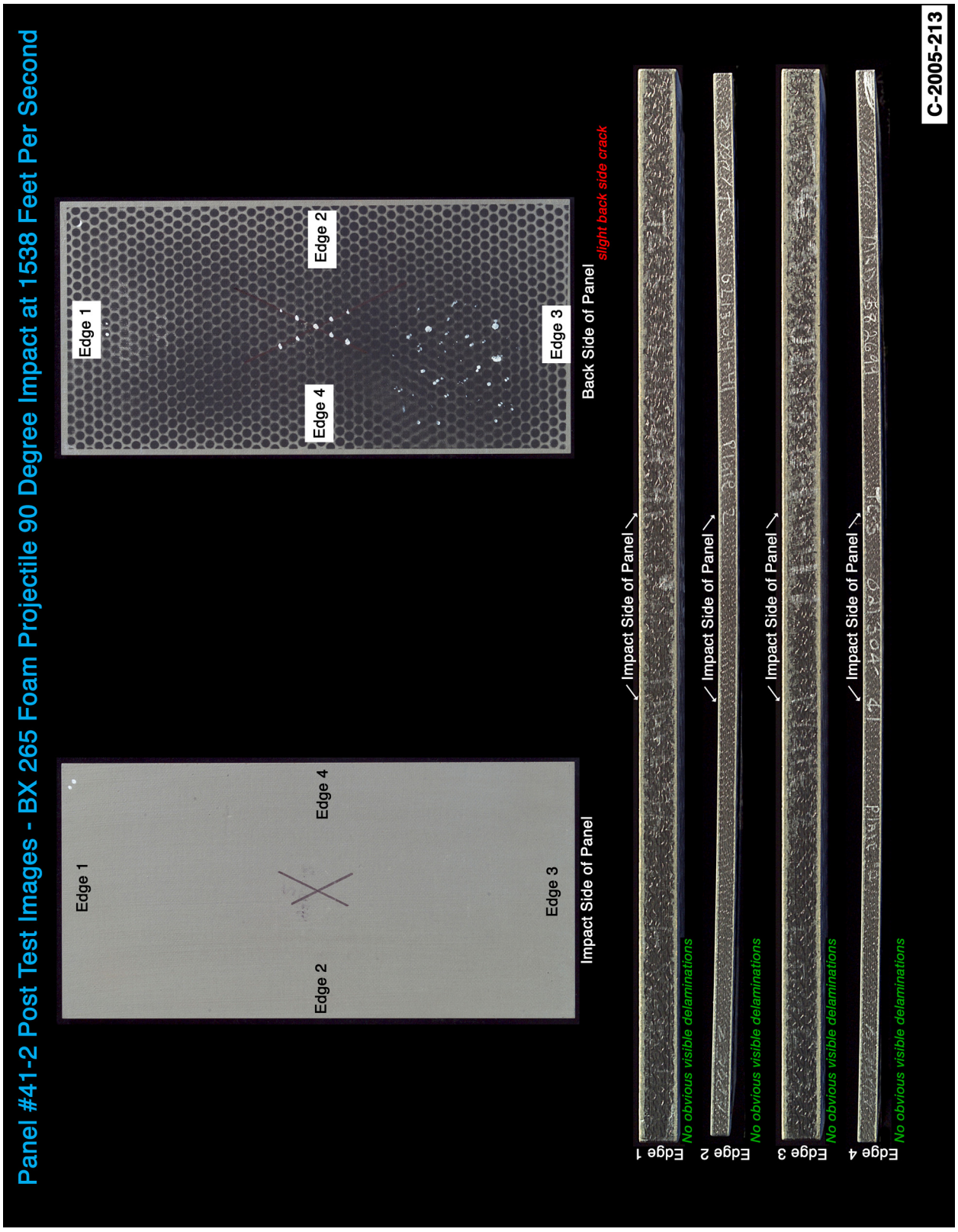

Figure C9–1.—Digital photography of edges and faces of panel 41–2 at 1538 ft/s with a BX–265 foam cylinder (nominally 1.5 in. in diameter by 3 in.) at a 90° impact angle. Test GRCC 163.

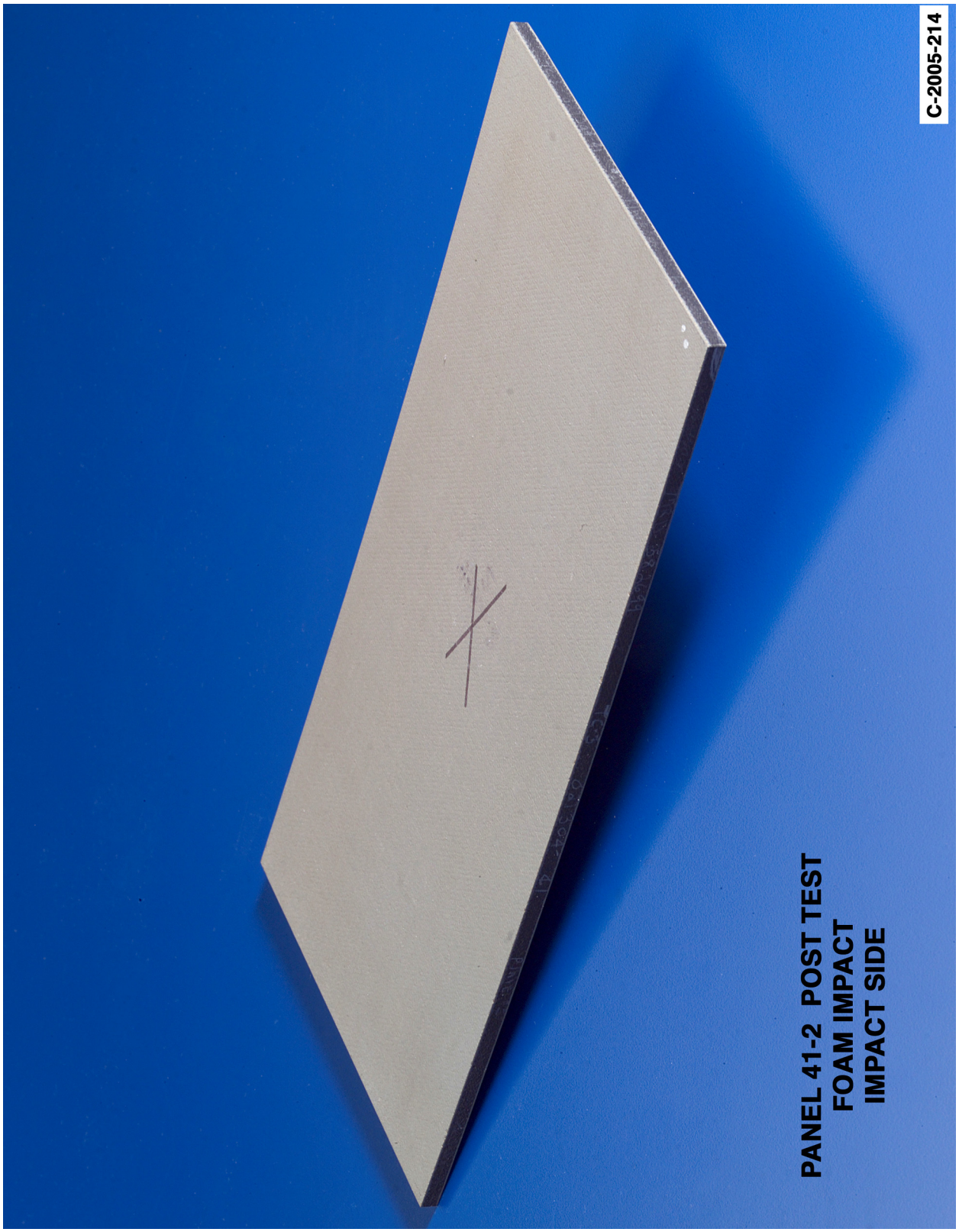

Figure C9–2.—Digital photography front (impact side) face of panel 41–2 at 1538 ft/s with a BX–265 foam cylinder (nominally 1.5 in. in diameter by 3 in.) at a 90° impact angle. Test GRCC 163.

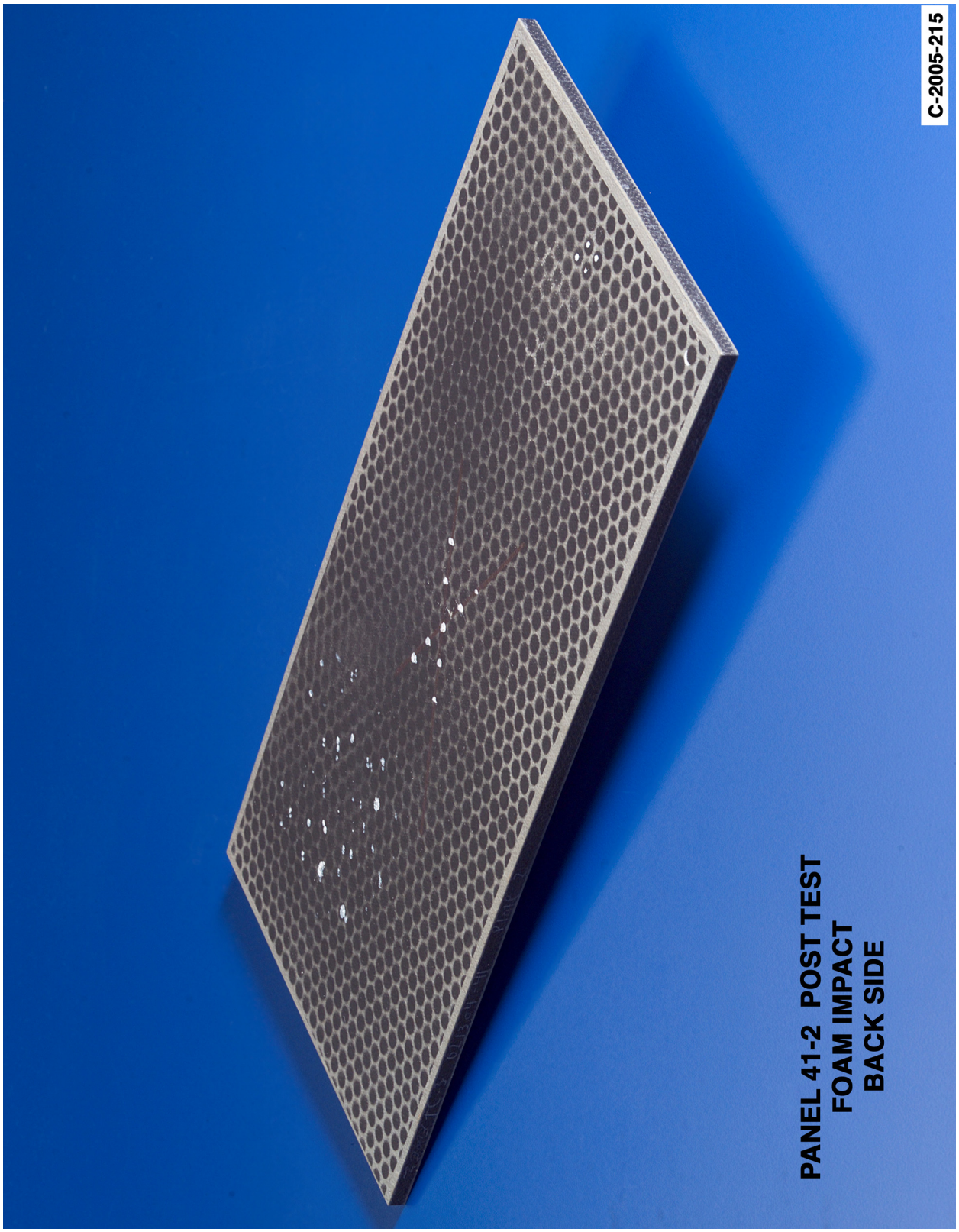

Figure C9–3.—Digital photography of back face of panel 41–2 at 1538 ft/s with a BX–265 foam cylinder (nominally 1.5 in. in diameter by 3 in.) at a 90° impact angle. Test GRCC 163.

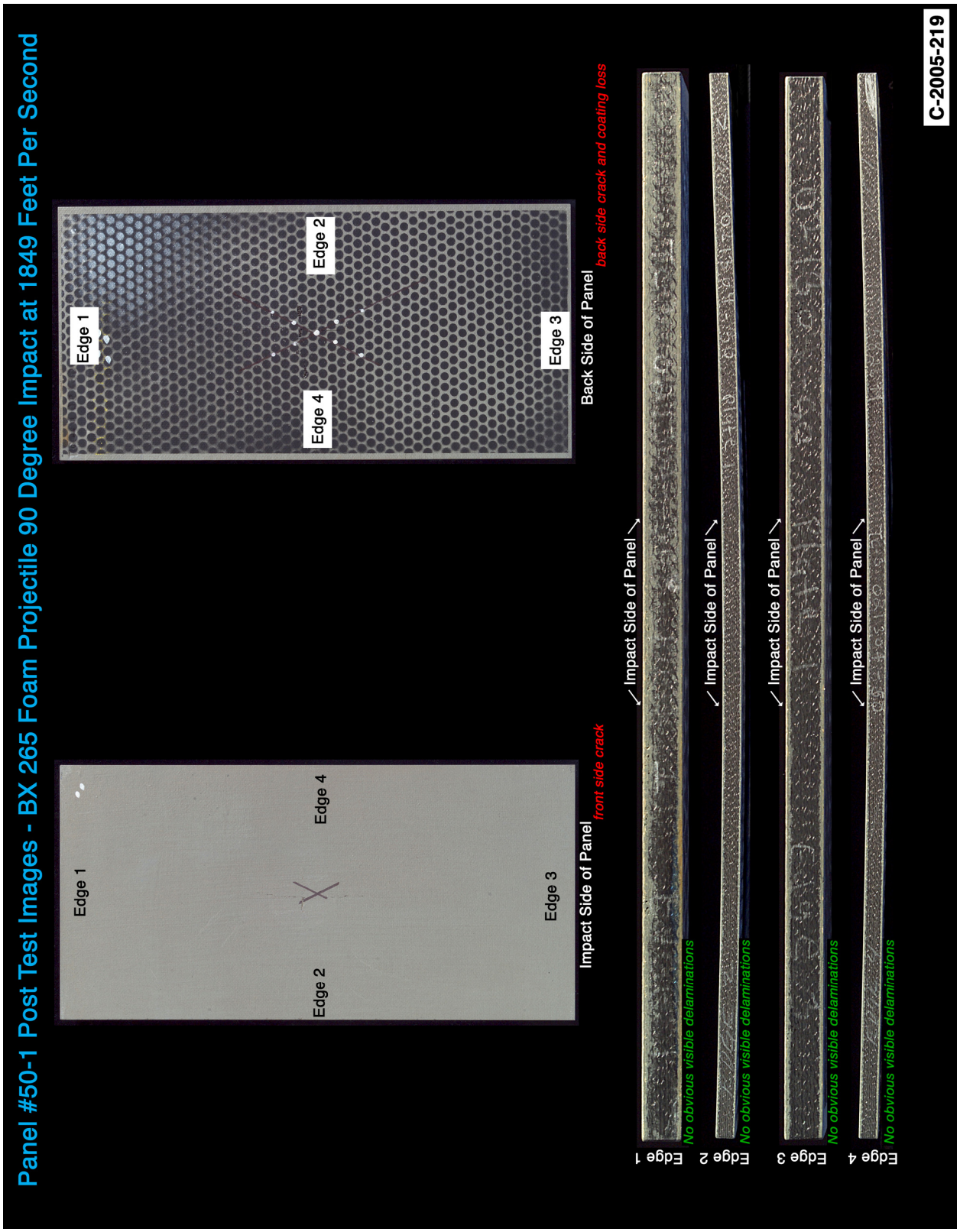

Figure C10–1.—Digital photography of edges and faces of panel 50–1 at 1849 ft/s with a BX–265 foam cylinder (nominally 1.5 in. in diameter by 3 in.) at a 90° impact angle. Test GRCC 167.

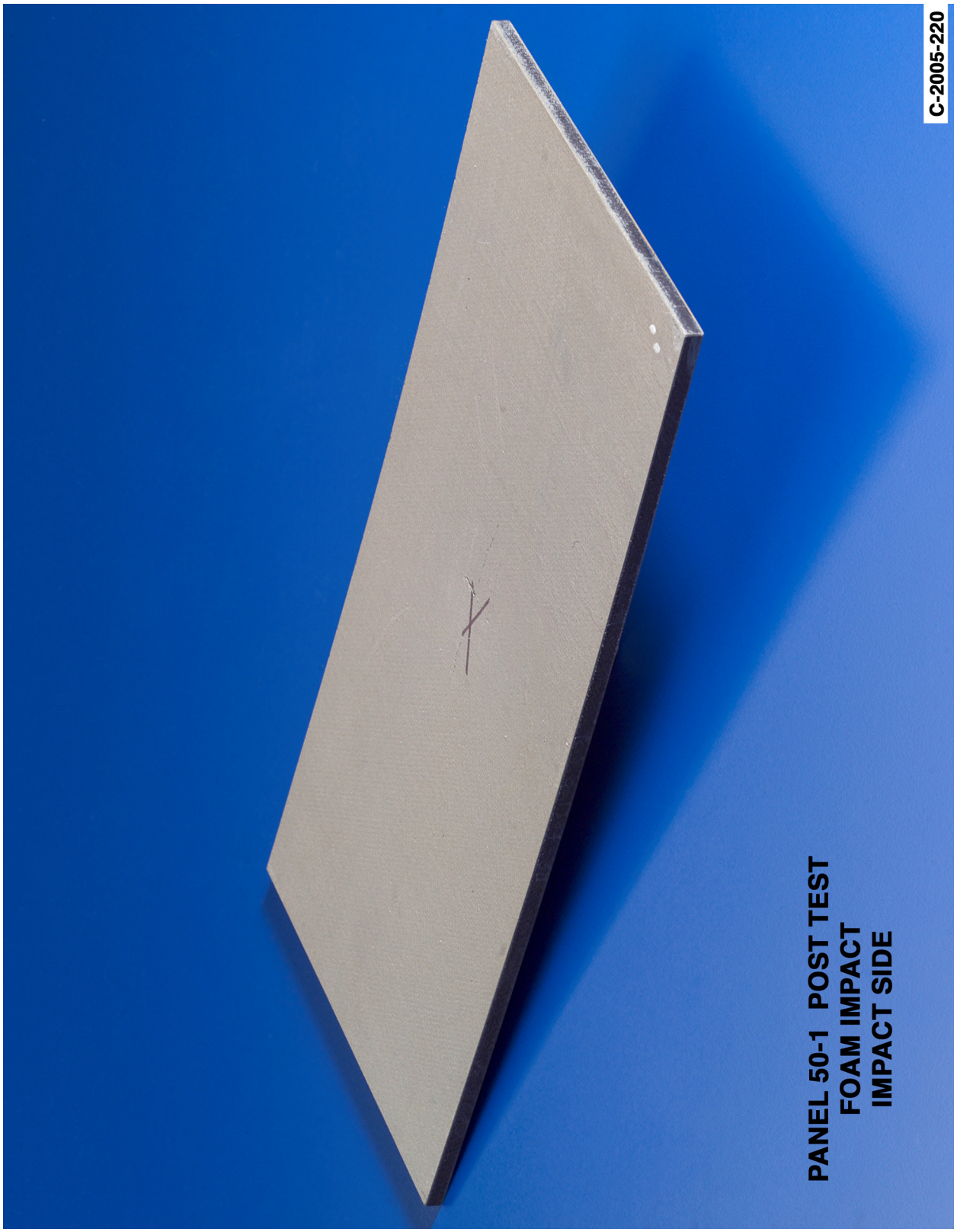

Figure C10–2.—Digital photography front (impact side) face of panel 50–1 at 1849 ft/s with a BX–265 foam cylinder (nominally 1.5 in diam. by 3 in.) at a 90° impact angle. Test GRCC 167.

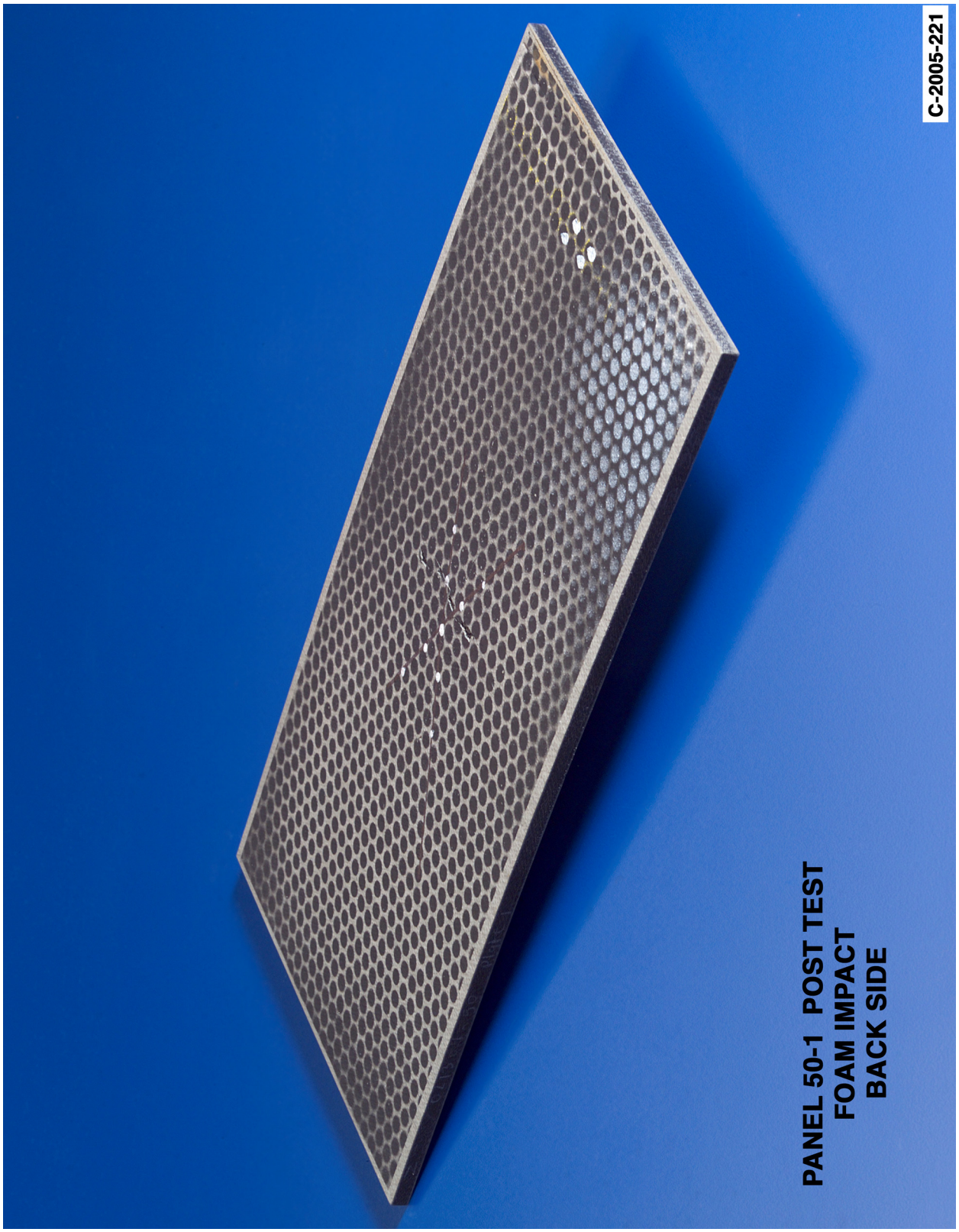

Figure C10–3.—Digital photography of back face of panel 50–1 at 1849 ft/s with a BX–265 foam cylinder (nominally 1.5 in. in diameter by 3 in.) at a 90° impact angle. Test GRCC 167.

Appendix D.—Test Data

BX–265 External Tank Foam Impact Testing at 45° Angle on 6- by 12-in. Reinforced Carbon-Carbon (RCC) Flat Panels

Notable Observations From the Appendix D Test Series

1. The RCC material used in this test series was tested in the as-manufactured condition.
2. Note that in figures D2–1 and D2–2, the sampling rate is 69.44 μs than the other test series taken at 37.17 μs. This is due to the change in the viewing area for this series being photographed at higher resolution to capture the larger rectangular plates (this was not done for the test series detailed in appendix C). Sample rate is directly correlated to capture resolution on the Phantom high-speed digital cameras.
3. The 6- by 12-in. panel tests were only simply supported on two ends. As a consequence, the wave propagation in these panels were dramatically different and less controlled than in the 6- by 6-in. panels resulting in additional modes of vibration in the panels being significant. This behavior can be seen in both the D2–1 and D3–1 figures. In D2–1, this is noted by the irregular deformation contours plot as a function of time. In D3–1 the secondary modes of vibration are seen in the first loading cycle and dampen out in the second cycle.
4. In test GRCC 178, the foam projectile broke into two pieces which were tracked at 1970 and 2000 ft/s respectively at impact on RCC panel 57–1. No visible or NDE damage was detected due to this test.
5. Lot 3, (37–57) in the following test series table refers to Lockheed Set 3A, processing Batch 37–57, made specifically for the Return to Flight Program.

Appendix D Test Series

BX-265 45 Degree Impact Test Parameters on 6" x 12" Reinforced Carbon-Carbon Panels

Test No.	Glenn Test Reference Number	Impact Velocity (ft/sec)	Panel ID Number	Lot Number	Average Panel Thickness (inches)	Visual Damage Observations	Mass of panel before test (grams)	Mass of panel after test (grams)	Projectile Weight (g)	Projectile Length (in)	Projectile Diameter (in)	Test Date	Projectile ID Number
1-45-542-14	GRCC172	1381	54-2	3, (37-57)	0.221	No significant indications	400.55	400.41	2.74	2.99	1.4905	1/26/05	Foam: BX 265, 1930-7-21-8
1-45-551-15	GRCC174	1795	55-1	3, (37-57)	0.223	No significant indications	404.92	404.83	2.82	2.989	1.483	1/27/05	Foam: BX 265, 1930-7-21-2
1-45-552-16	GRCC176	1853	55-2	3, (37-57)	0.220	No significant indications	402.70	402.52	2.84	2.964	1.4925	1/27/05	Foam: BX 265, 1930-7-21-9
1-45-572-18	GRCC180	2230	57-2	3, (37-57)	0.221	Back side coating fracture & loss	405.12	404.99	2.91	2.997	1.485	1/28/05	Foam: BX 265, 1930-6-20-10
1-45-571-17	GRCC178	1970-2000	57-1	3, (37-57)	0.224	No significant indications	406.15	406.08	2.6	2.969	1.487	1/28/05	Foam: BX 265, 1930-7-21-6

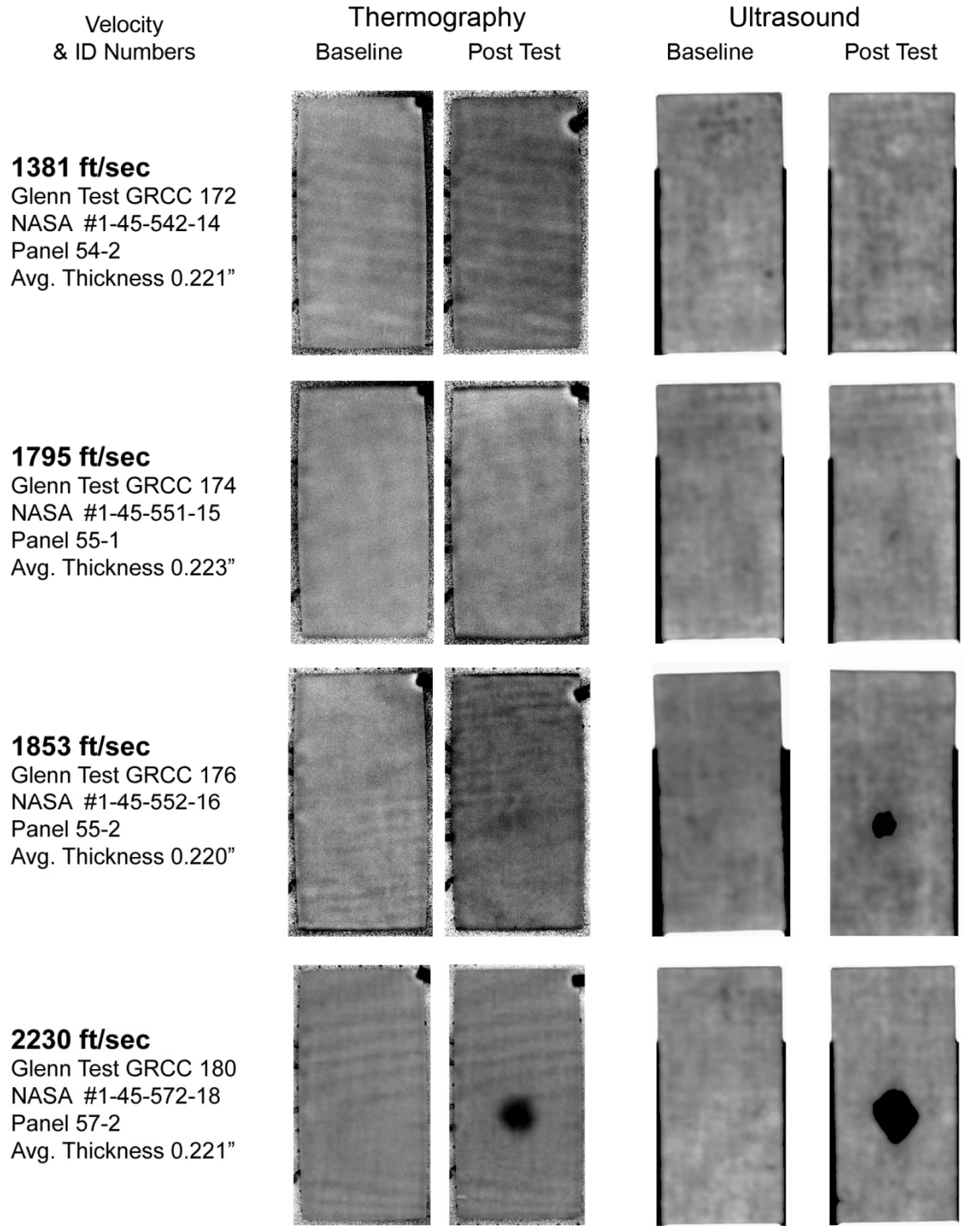

Figure D1–1.—Pulse thermography and ultrasound post impact pretest and posttest images of reinforced carbon-carbon 6- by 12-in. flat panels impacted with BX–265 foam cylinders (nominally 1.5 in. in diameter by 3 in.) at a 45° angle.

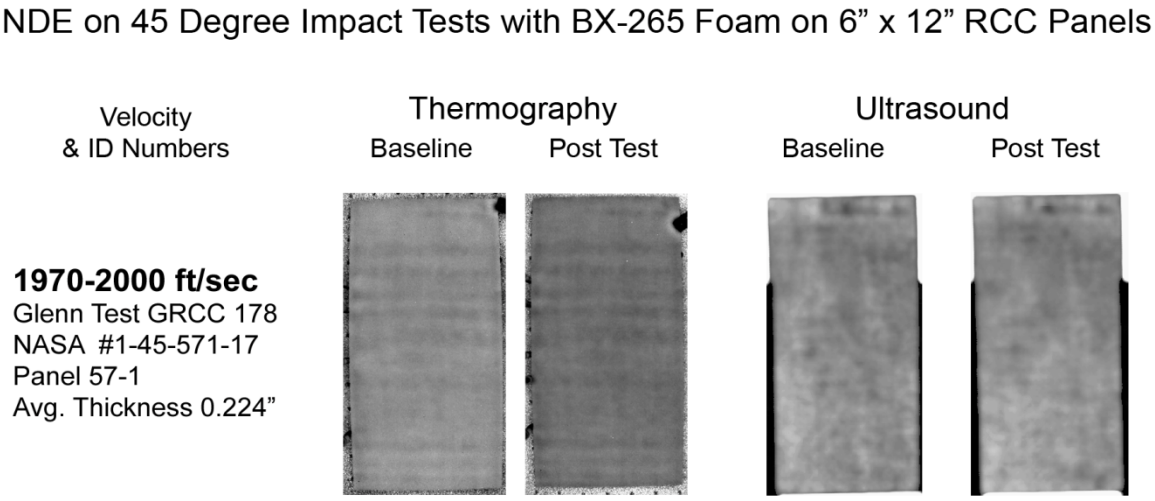

Figure D1–2.—Pulse thermography and ultrasound post impact pretest and posttest images of reinforced carbon-carbon 6- by 12-in. flat panels impacted with BX–265 foam cylinders (nominally 1.5 in. in diameter by 3 in.) at a 45° angle.

Aramis Displacement Contours from 45 Degree Impact Tests with BX-265 on 6” x 12” RCC Panels

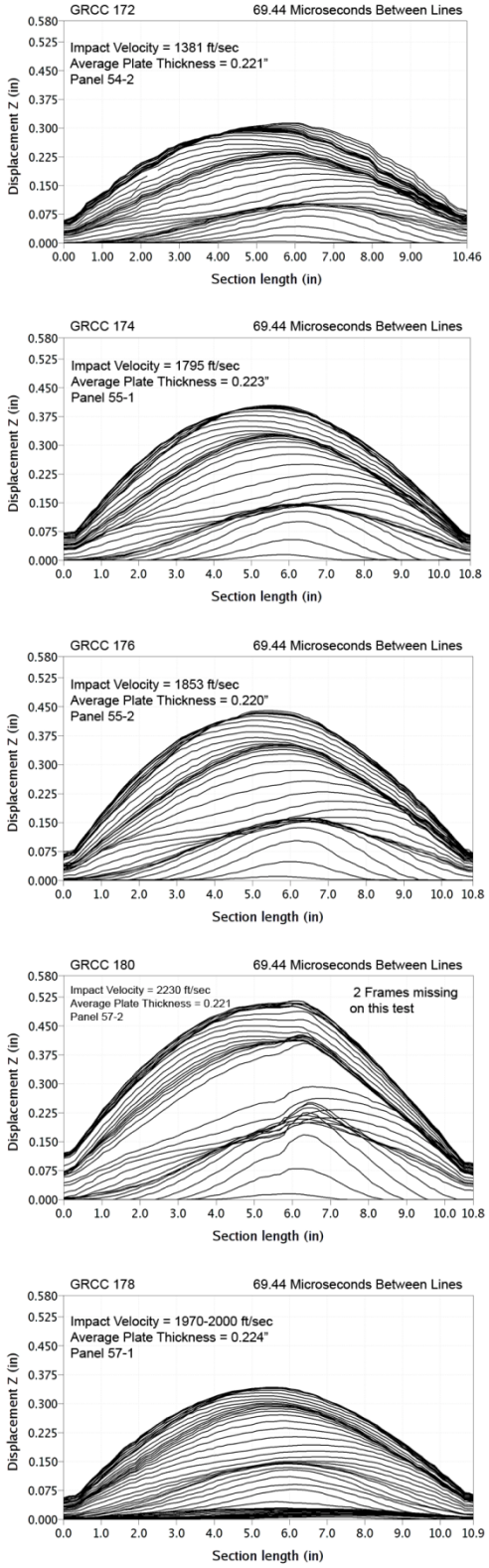

Figure D2–1.—ARAMIS out-of-plane deformation contours across centerline of 6- by 12-in. reinforced carbon-carbon flat panels measured at 69-μs increments undergoing impact with BX–265 foam cylinders (nominally 1.5 in. in diameter by 3 in.) at a 45° angle.

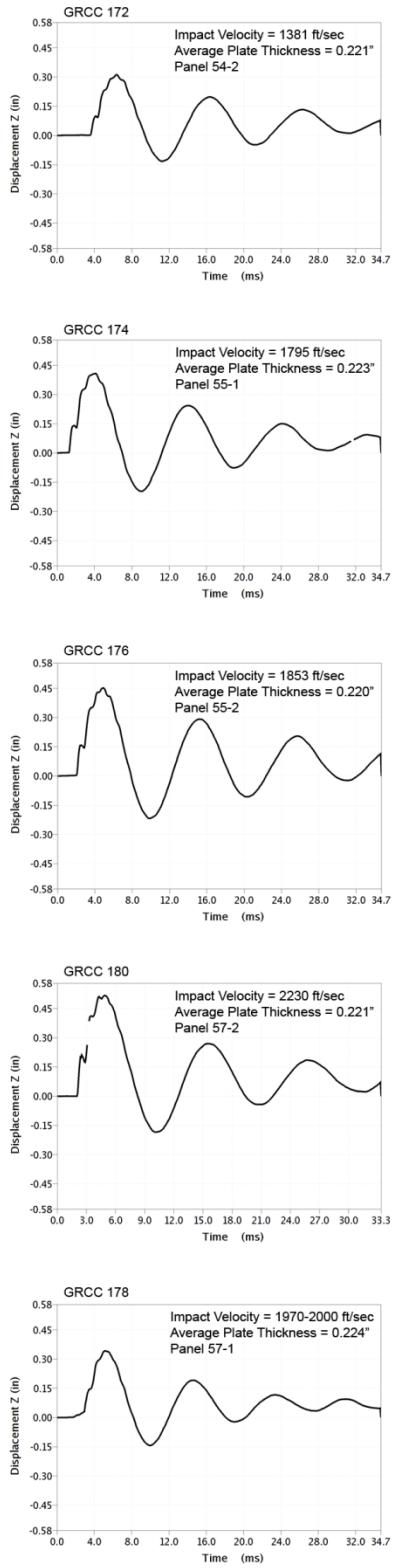

Figure D3–1.—ARAMIS centerpoint out-of-plane deformation vs. time of 6- by 12-in. reinforced carbon-carbon flat panels impacted with BX–265 foam cylinders (nominally 1.5 in. in diameter by 3 in.) at a 45° angle.

Aramis Maximum Displacement Fringe Plots from 45 Degree Impact Tests
with BX-265 Foam on 6” x 12” RCC Panels

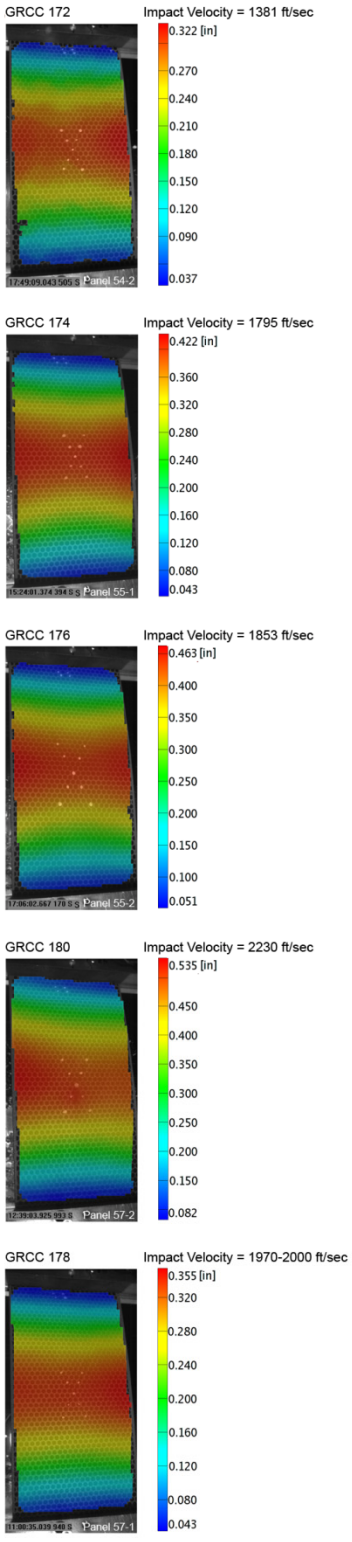

Figure D4–1.—ARAMIS color fringe plots depicting maximum deformation prior to material failure of 6- by 12-in. reinforced carbon-carbon flat panels as they undergo impact with BX–265 foam cylinders (nominally 1.5 in. in diameter by 3 in.) at a 45° angle.

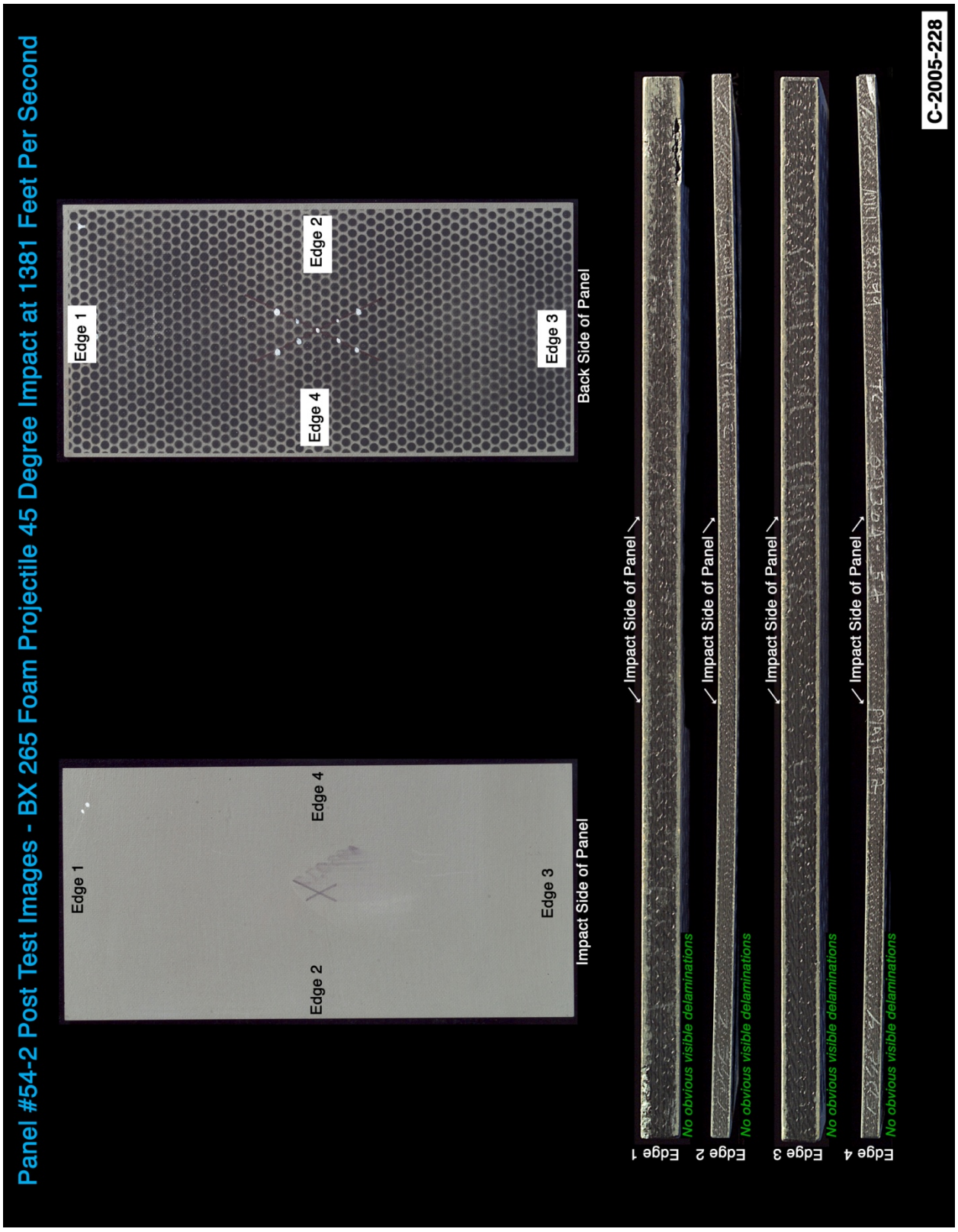

Figure D5–1.—Digital photography of edges and faces of panel 54–2 at 1381 ft/s with a BX–265 foam cylinder (nominally 1.5 in. in diameter by 3 in.) at a 45° impact angle. Test GRCC 172.

Figure D5–2.—Digital photography front (impact side) face of panel 54–2 at 1381 ft/s with a BX–265 foam cylinder (nominally 1.5 in. in diameter by 3 in.) at a 45° impact angle. Test GRCC 172.

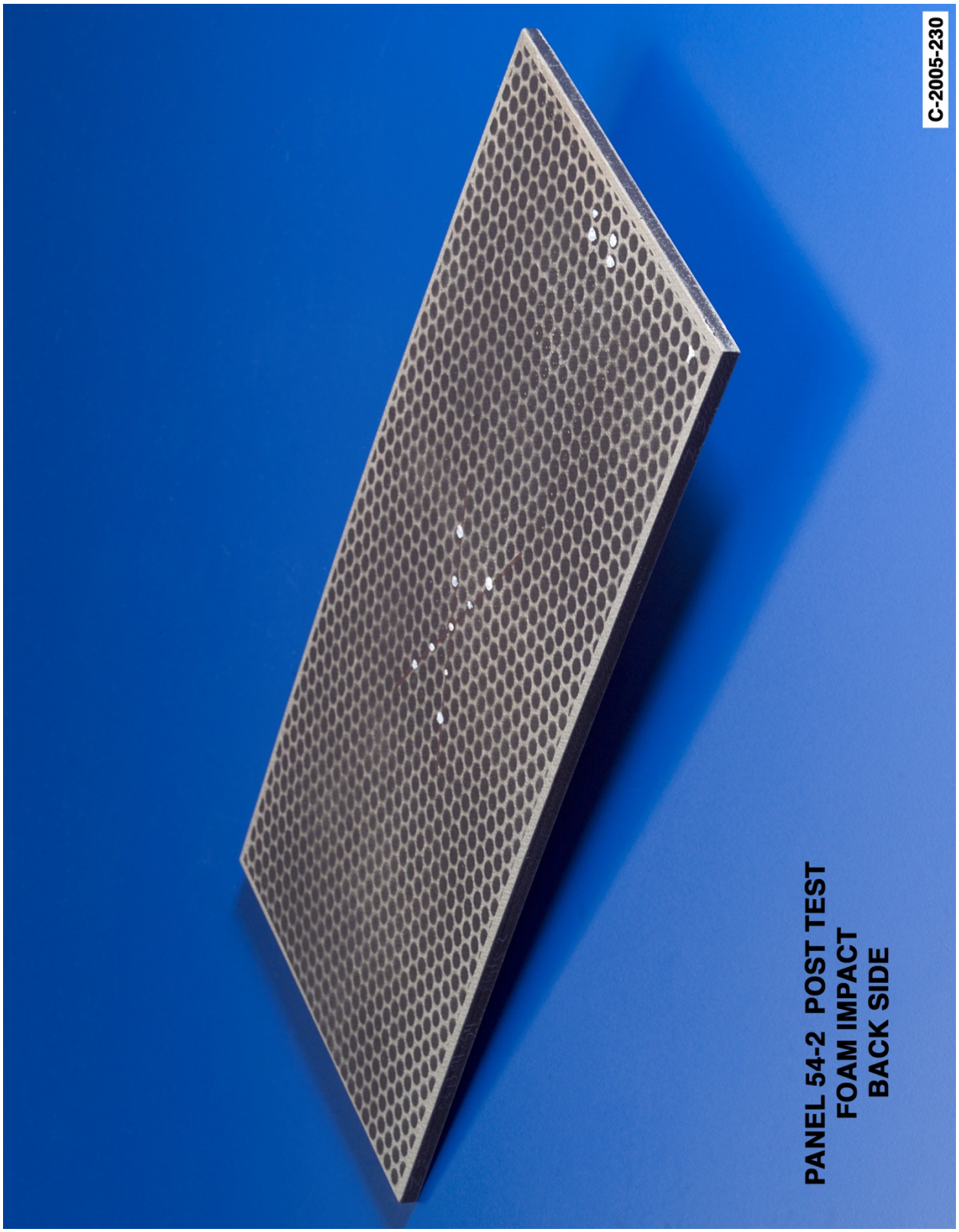

Figure D5–3.—Digital photography of back face of panel 54–2 at 1381 ft/s with a BX–265 foam cylinder (nominally 1.5 in. in diameter by 3 in.) at a 45° impact angle. Test GRCC 172.

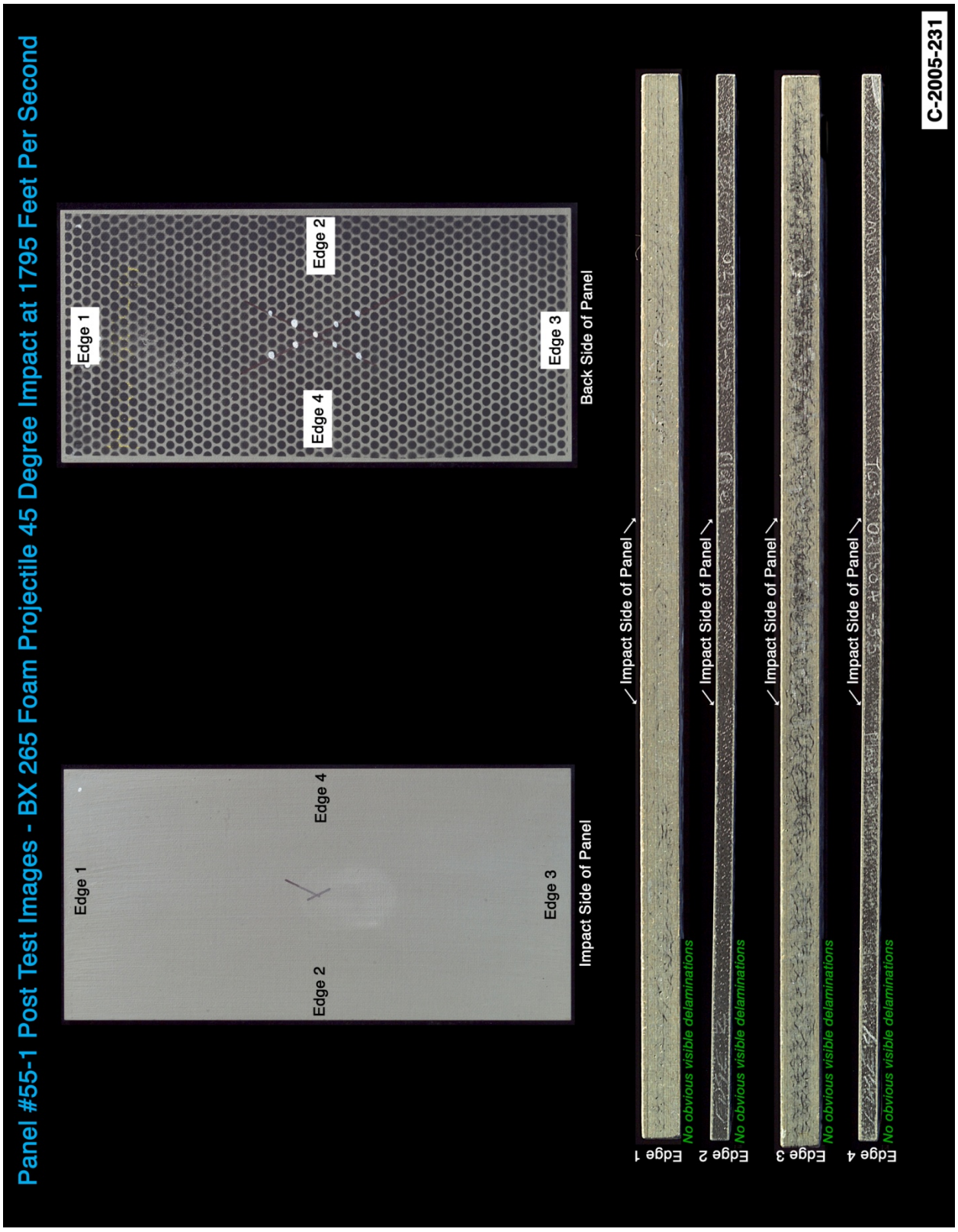

Figure D6–1.—Digital photography of edges and faces of panel 55–1 at 1795 ft/s with a BX–265 foam cylinder (nominally 1.5 in. in diameter by 3 in.) at a 45° impact angle. Test GRCC 174.

Figure D6–2.—Digital photography front (impact side) face of panel 55–1 at 1795 ft/s with a BX–265 foam cylinder (nominally 1.5 in. in diameter by 3 in.) at a 45° impact angle. Test GRCC 174.

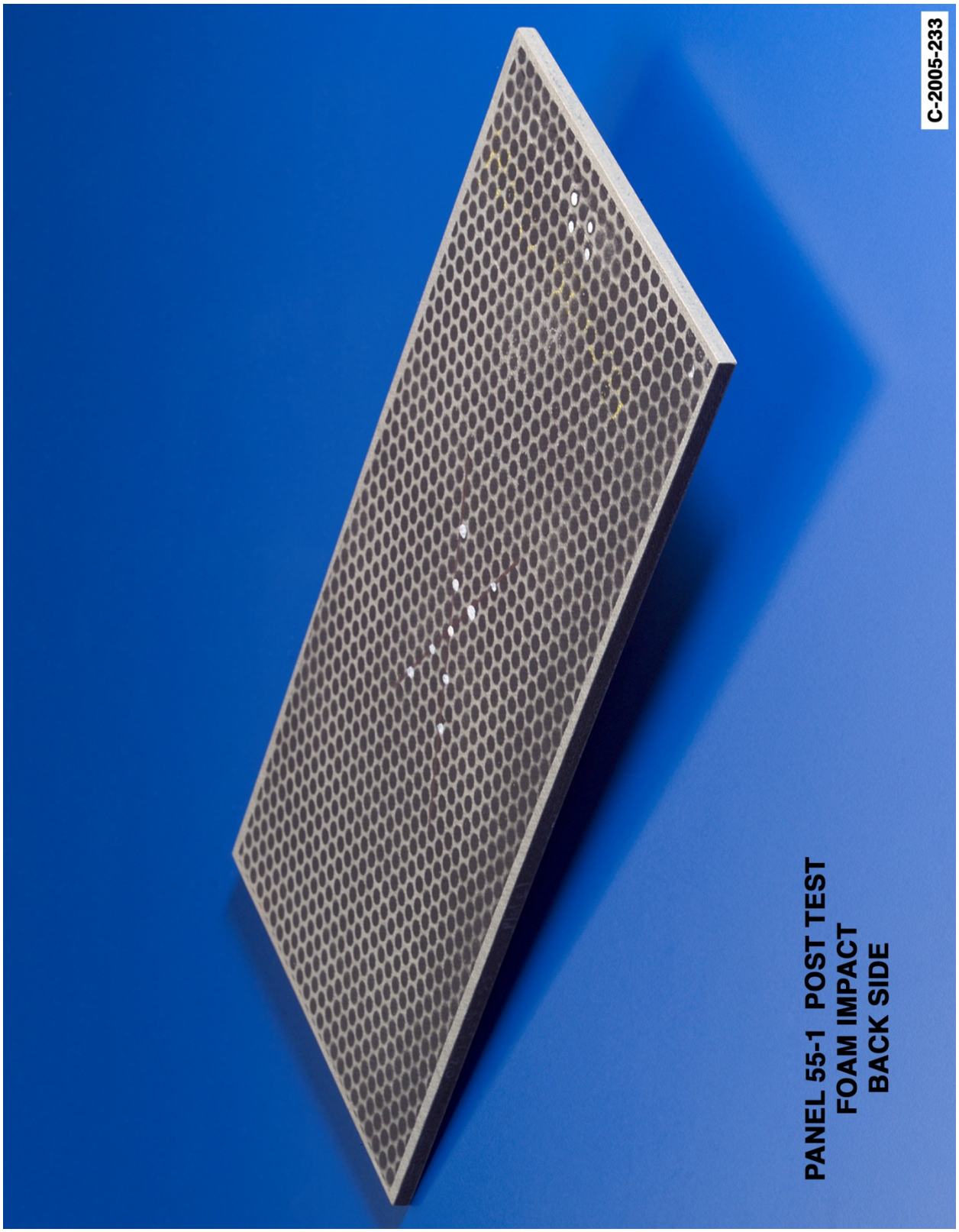

Figure D6–3.—Digital photography of back face of panel 55–1 at 1795 ft/s with a BX–265 foam cylinder (nominally 1.5 in. in diameter by 3 in.) at a 45° impact angle. Test GRCC 174.

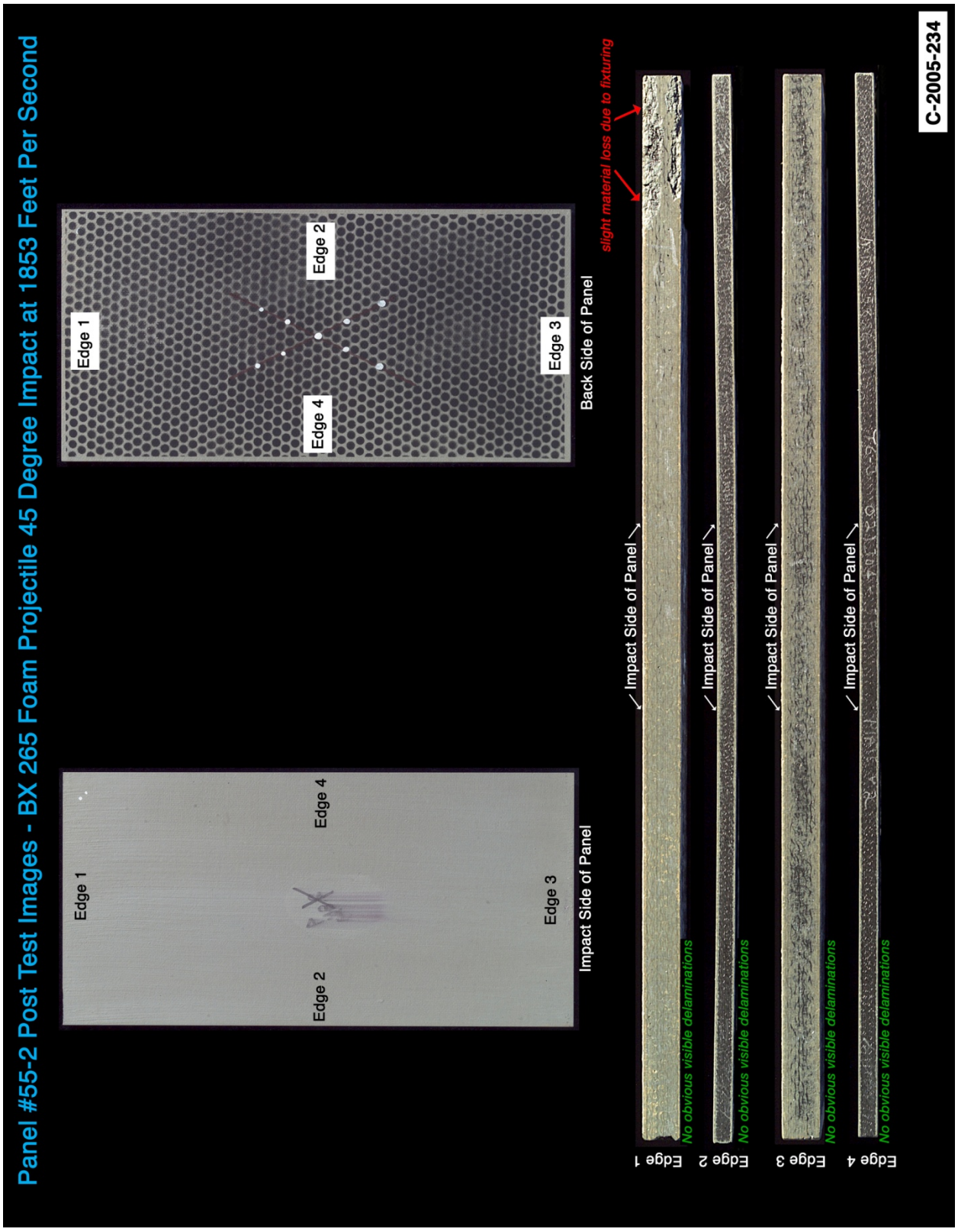

Figure D7–1.—Digital photography of edges and faces of panel 55–2 at 1853 ft/s with a BX–265 foam cylinder (nominally 1.5 in. in diameter by 3 in.) at a 45° impact angle. Test GRCC 176.

Figure D7–2.—Digital photography front (impact side) face of panel 55–2 at 1853 ft/s with a BX–265 foam cylinder (nominally 1.5 in. in diameter by 3 in.) at a 45° impact angle. Test GRCC 176.

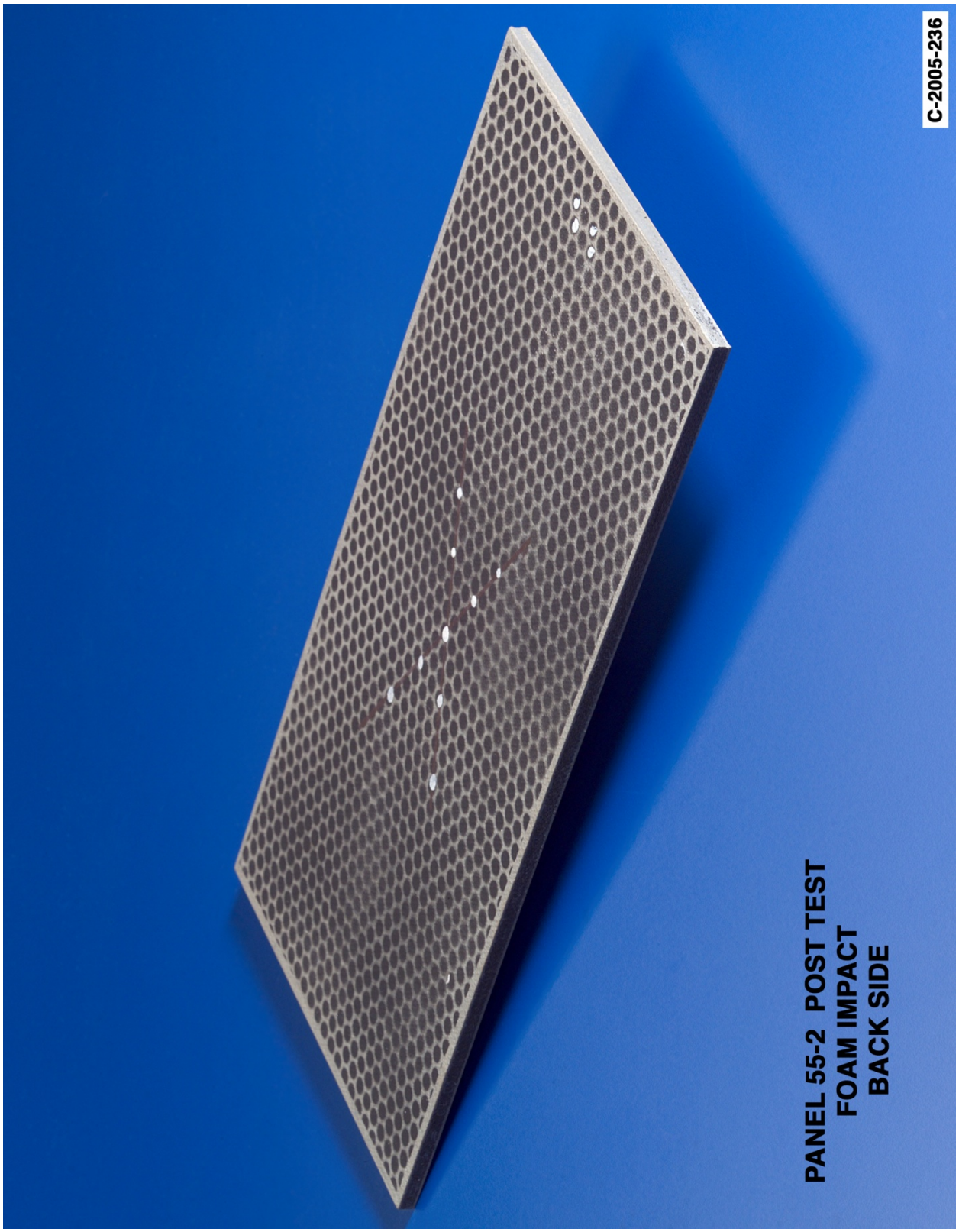

Figure D7–3.—Digital photography of back face of panel 55–2 at 1853 ft/s with a BX–265 foam cylinder (nominally 1.5 in. in diameter by 3 in.) at a 45° impact angle. Test GRCC 176.

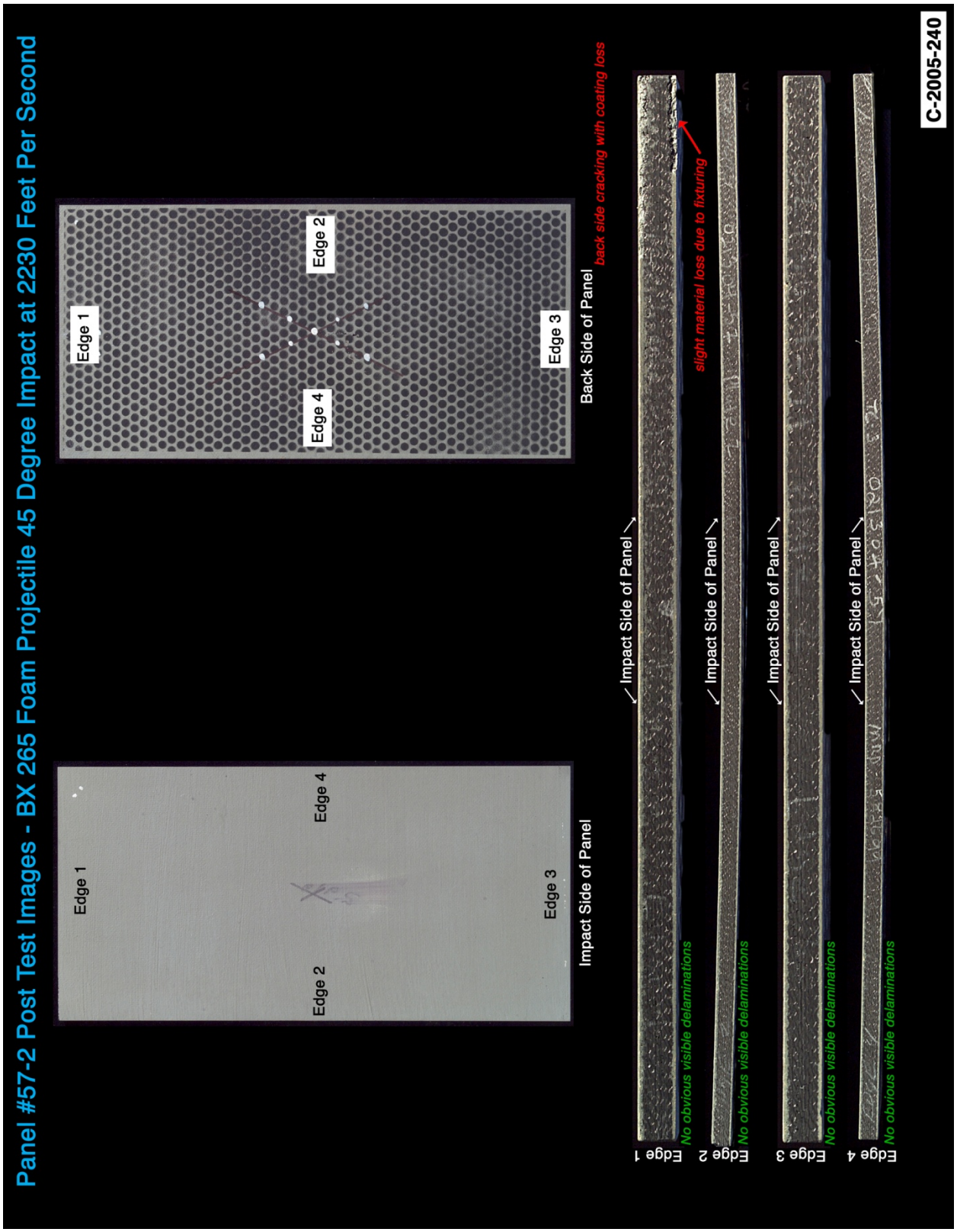

Figure D8–1.—Digital photography of edges and faces of panel 57–2 at 2230 ft/s with a BX–265 foam cylinder (nominally 1.5 in. in diameter by 3 in.) at a 45° impact angle. Test GRCC 180.

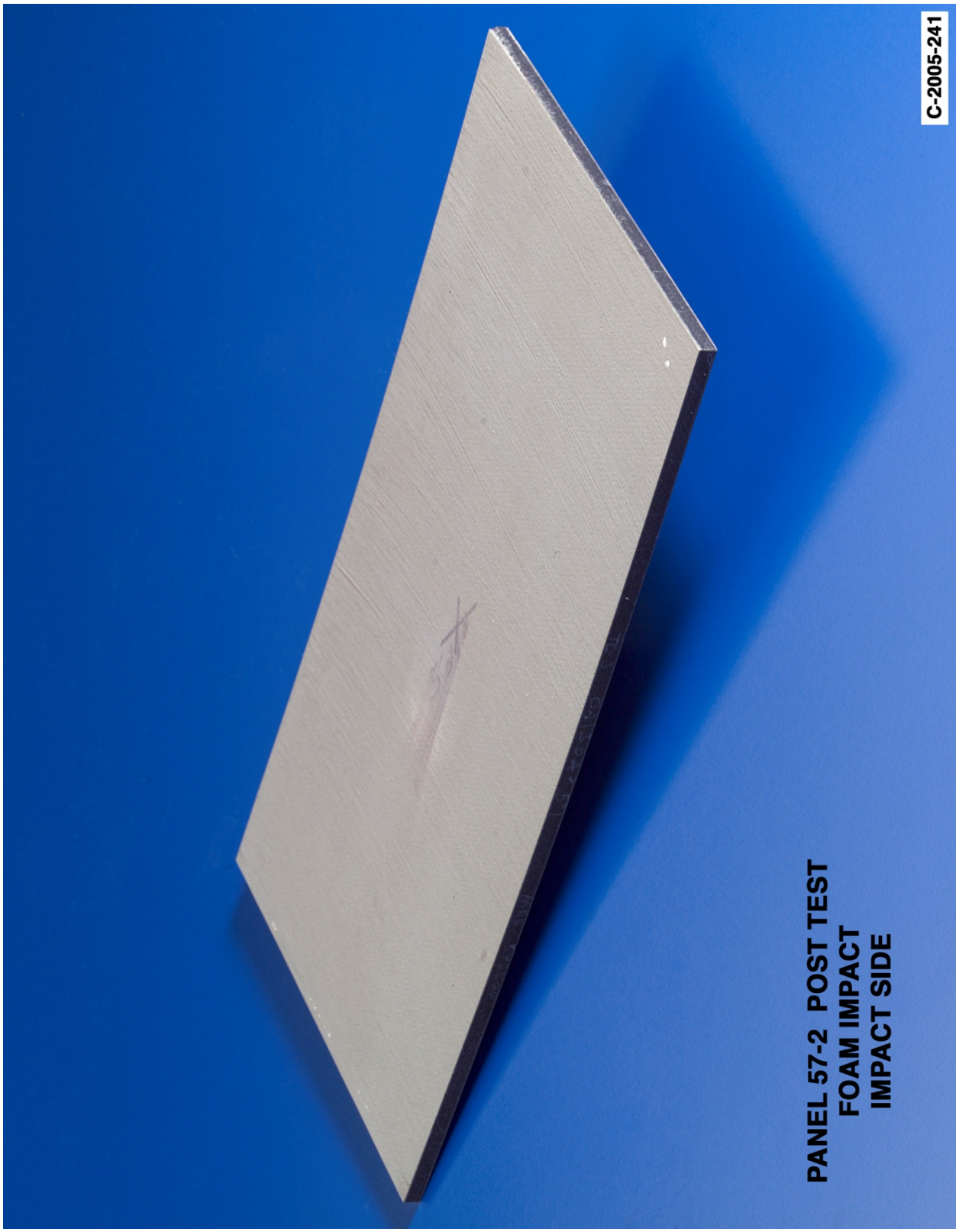

Figure D8–2.—Digital photography front (impact side) face of panel 57–2 at 2230 ft/s with a BX–265 foam cylinder (nominally 1.5 in. in diameter by 3 in.) at a 45° impact angle. Test GRCC 180.

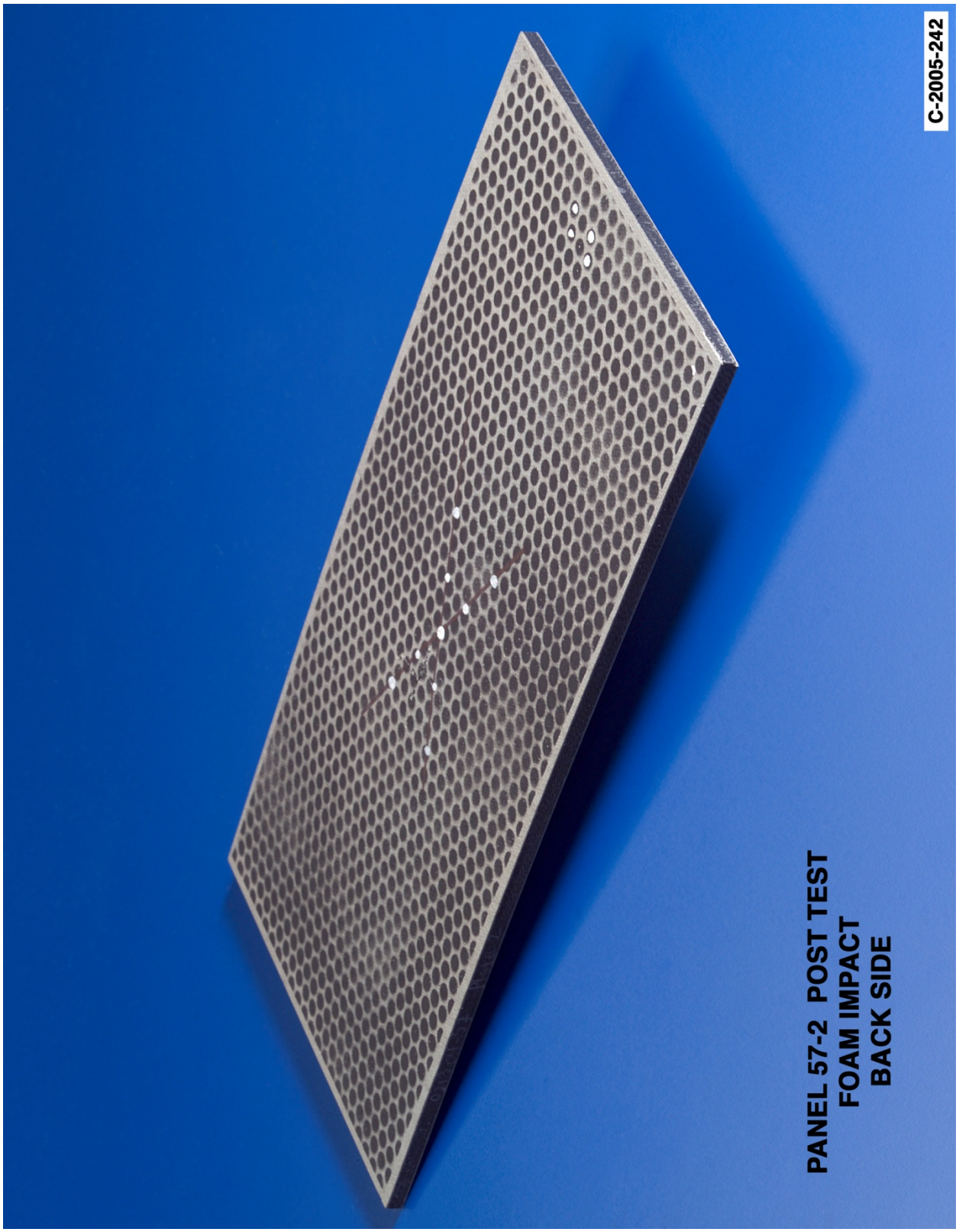

Figure D8–3.—Digital photography of back face of panel 57–2 at 2230 ft/s with a BX–265 foam cylinder (nominally 1.5 in. in diameter by 3 in.) at a 45° impact angle. Test GRCC 180.

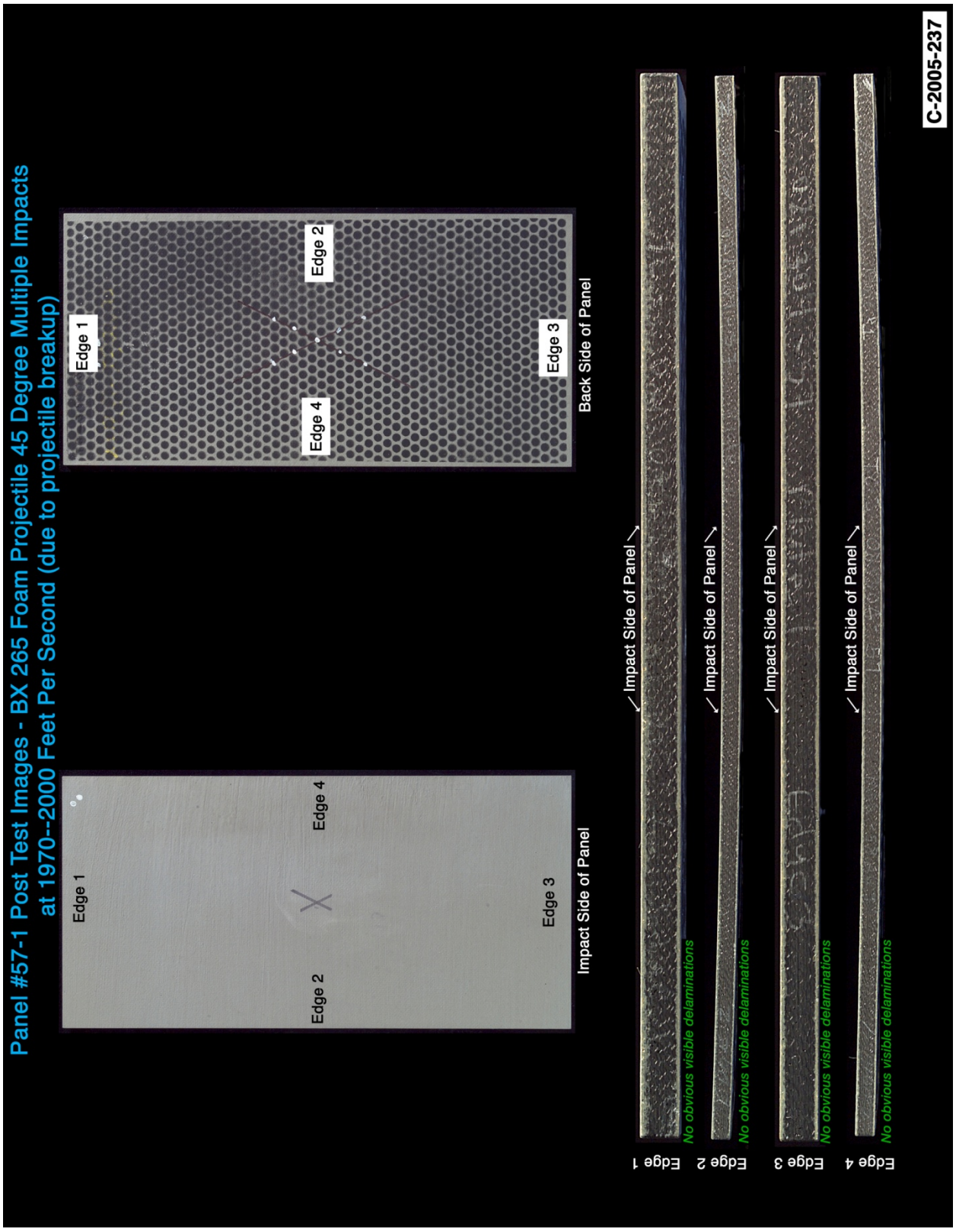

Figure D9–1.—Digital photography of edges and faces of panel 57–1 at 1970 to 2000 ft/s with a BX–265 foam cylinder (nominally 1.5 in. in diameter by 3 in.) at a 45° impact angle. Test GRCC 178.

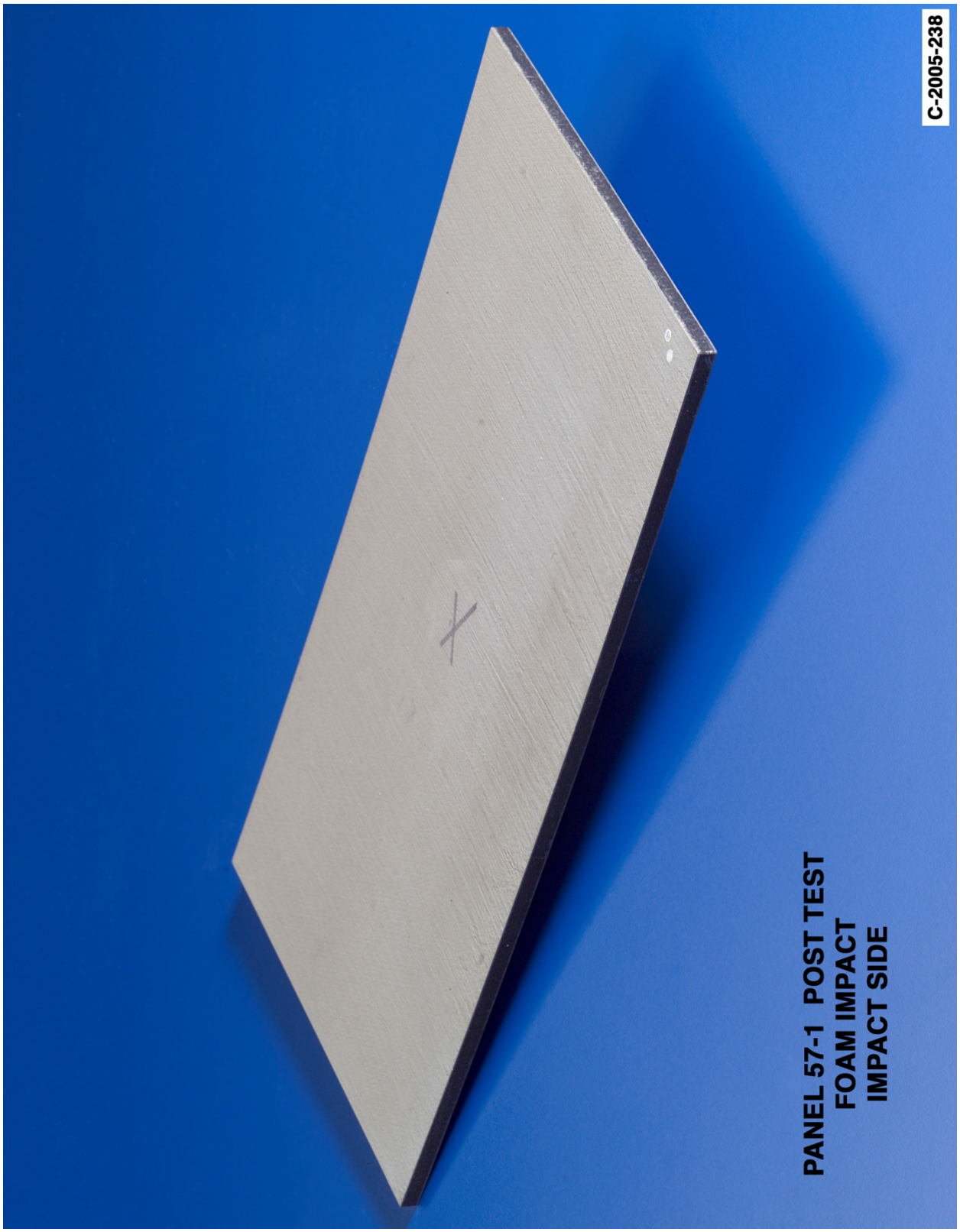

Figure D9–2.—Digital photography front (impact side) face of panel 57–1 at 1970 to 2000 ft/s with a BX–265 foam cylinder (nominally 1.5 in. in diameter by 3 in.) at a 45° impact angle. Test GRCC 178.

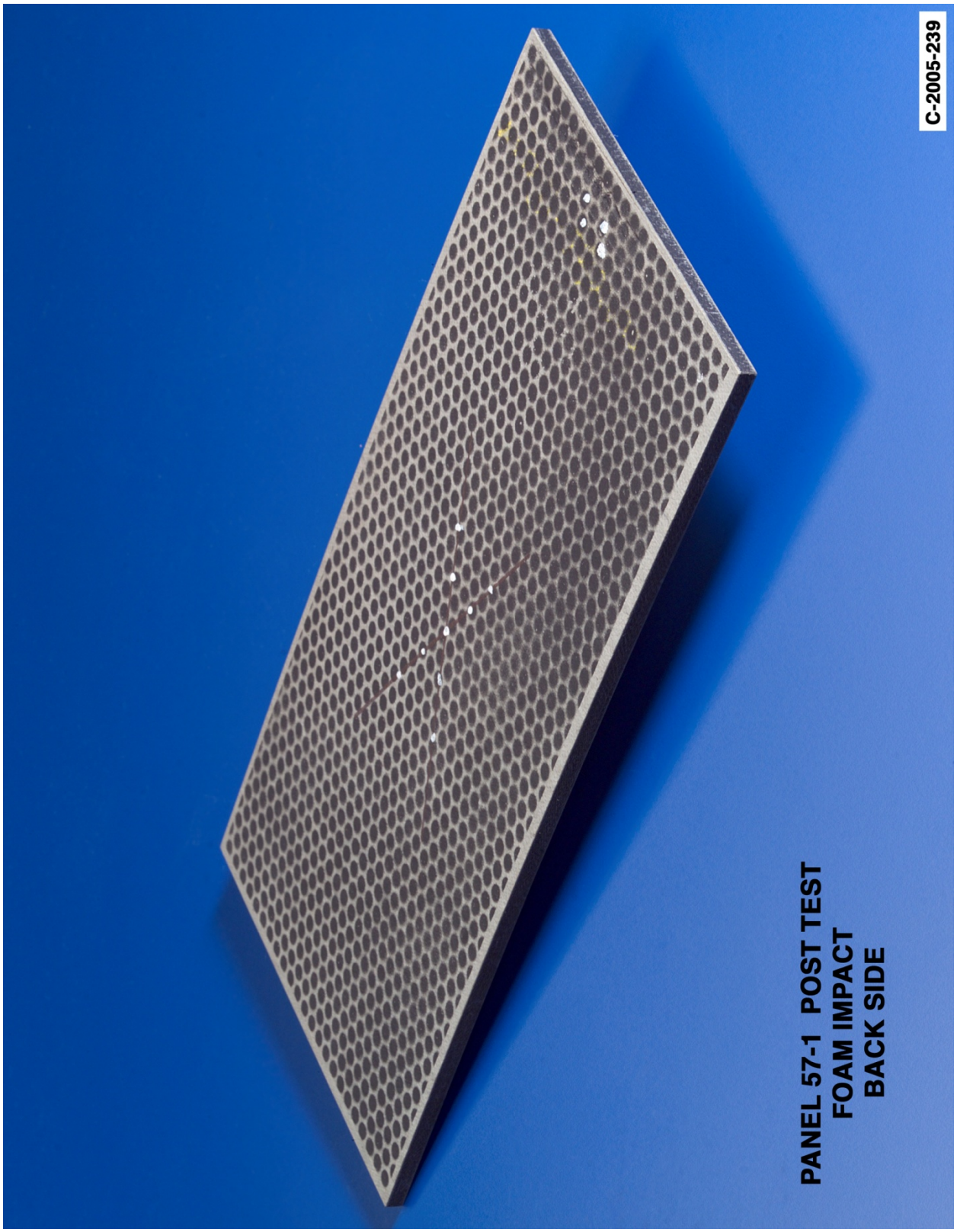

Figure D9–3.—Digital photography of back face of panel 57–1 at 1970 to 2000 ft/s with a BX–265 foam cylinder (nominally 1.5 in. in diameter by 3 in.) at a 45° impact angle. Test GRCC 178.

Appendix E.—Test Data

PDL External Tank Foam Impact Testing at 90° Angle on 6- by 6-in. Reinforced Carbon-Carbon (RCC) Flat Panels

Notable Observations From the Appendix E Test Series

1. The RCC material used in this test series was tested in the as-manufactured condition.
2. Lot 3,(22–36) in the following test series table refers to Lockheed Set 3A, processing Batch 22–36, made specifically for the Return to Flight Program.

Appendix E Test Series

PDL 90 Degree Impact Test Parameters on 6" x 6" Reinforced Carbon-Carbon Panels

Test No.	Glenn Test Reference Number	Impact Velocity (ft/sec)	Panel ID Number	Lot Number	Average Panel Thickness (inches)	Visual Damage Observations	Mass of panel before test (grams)	Mass of panel after test (grams)	Projectile Weight (g)	Projectile Length (in)	Projectile Diameter (in)	Test Date	Projectile ID Number
4-90-231-01	GRCC192	960	23-1	3,(22-36)	0.225	Misfire - no damage per NDE	209.19	no test	2.00	1.676	1.252	4/20/05	PDL 1911 12-18
4-90-263-06	GRCC208	1267	26-3	3,(22-36)	0.220	No significant indications	206.50	206.45	2.01	1.724	1.247	4/27/05	1928 PDL-10W-13
4-90-272-08	GRCC213	1350	27-2	3,(22-36)	0.222	No significant indications	207.97	208.00	2.00	1.774	1.246	4/28/05	1928 PDL-10W-7
4-90-271-07	GRCC211	1392	27-1	3,(22-36)	0.226	No significant indications	209.05	209.04	2.00	1.707	1.248	4/28/05	1928 PDL-10W-4
4-90-262-04	GRCC200	1459	26-2	3,(22-36)	0.219	Small backside coating chips lost	204.39	204.36	1.96	1.742	1.251	4/26/05	1928 PDL-10W-10
4-90-241-02	GRCC195	1541	24-1	3,(22-36)	0.225	Small backside coating chips lost	207.00	206.95	2.02	1.637	1.245	4/20/05	PDL 1911 12-05
4-90-261-03	GRCC198	1718	26-1	3,(22-36)	0.223	Significant backside crack, coating loss	205.50	205.44	2.00	1.742	1.251	4/26/05	1928 PDL-10W-17
4-90-242-05	GRCC203	1825	24-2	3,(22-36)	0.223	Significant front and backside damage	207.58	207.15	2.03	1.722	1.249	4/26/05	1928 PDL-10W-14

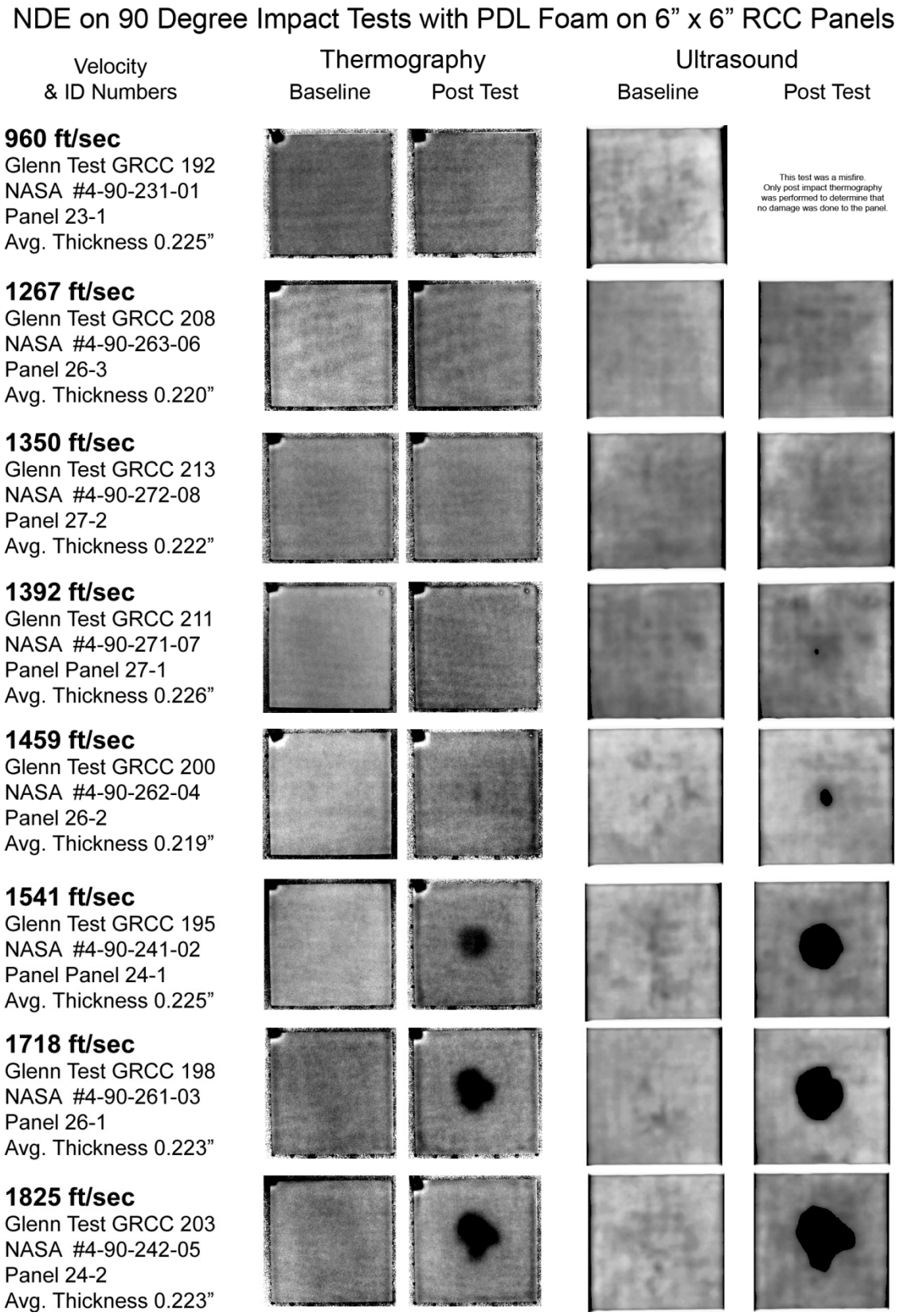

Figure E1–1.—Pulse thermography and ultrasound post impact pretest and posttest images of reinforced carbon-carbon 6- by 6-in. flat panels impacted with PDL foam cylinders (nominally 1.5 in. in diameter by 3 in.) at a 90° angle.

Aramis Displacement Contours from 90 Degree Impact Tests with PDL on 6” x 6” RCC Panels

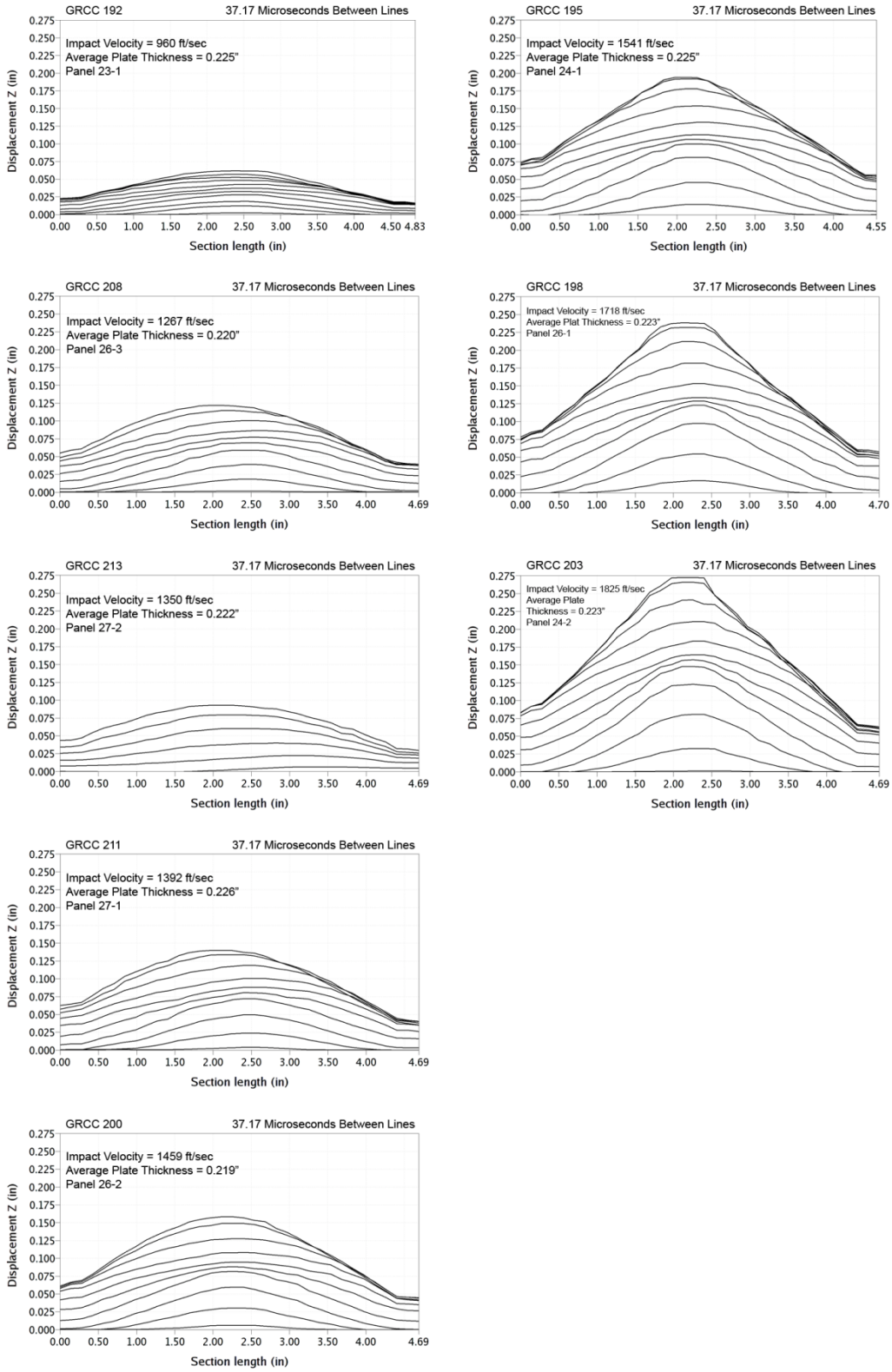

Figure E2–1.—ARAMIS out-of-plane deformation contours across centerline of 6- by 6-in. reinforced carbon-carbon flat panels measured at 37.1-μs increments undergoing impact with PDL foam cylinders (nominally 1.5 in. in diameter by 3 in.) at a 90° angle.

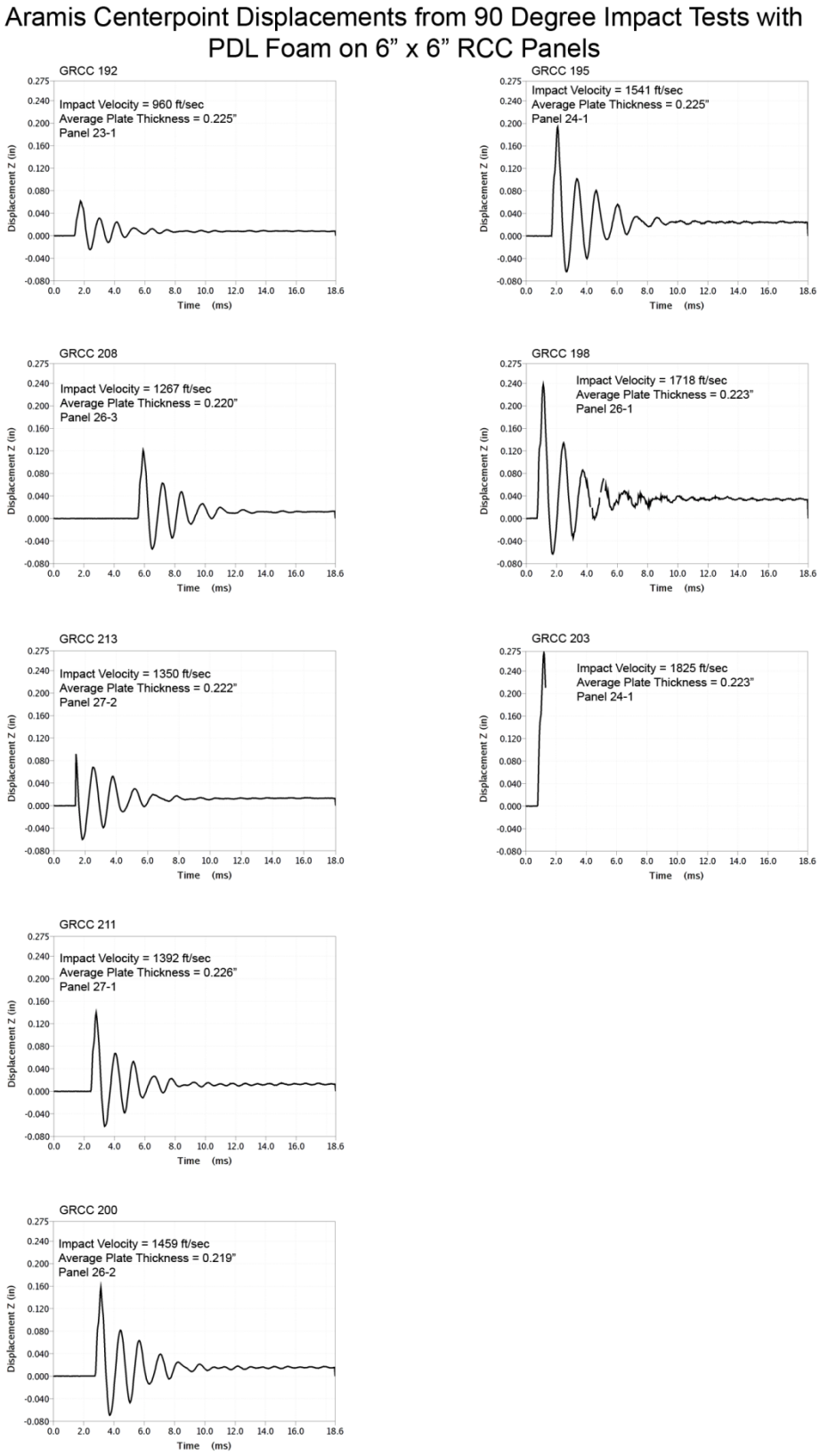

Figure E3–1.—ARAMIS centerpoint out-of-plane deformation vs. time of 6- by 6-in. reinforced carbon-carbon flat panels impacted with PDL foam cylinders (nominally 1.5 in. in diameter by 3 in.) at a 90° angle.

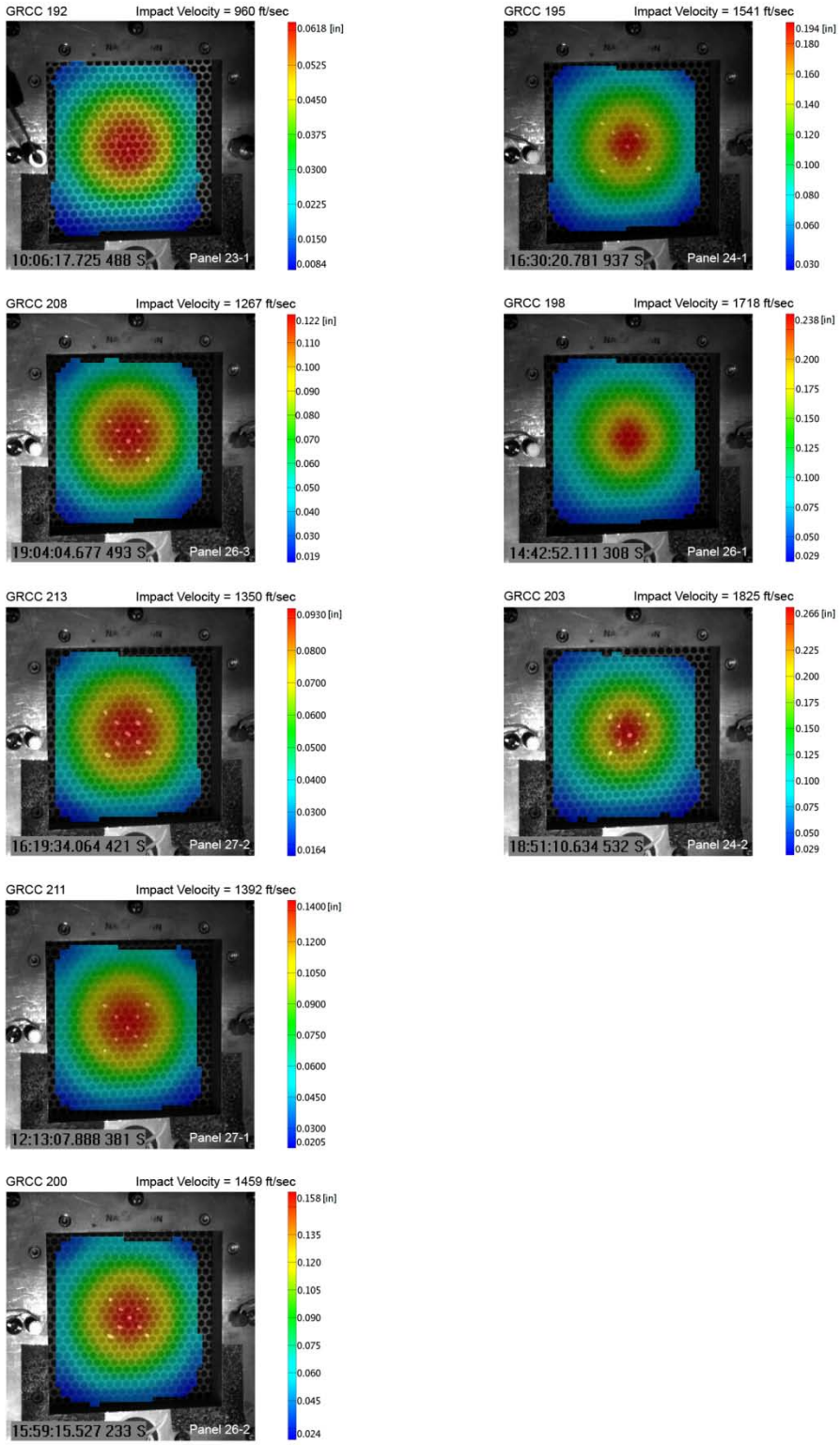

Figure E4-1.—ARAMIS color fringe plots depicting maximum deformation prior to material failure of 6- by 6-in. reinforced carbon-carbon flat panels as they undergo impact with PDL foam cylinders (nominally 1.5 in. in diameter by 3 in.) at a 90° angle.

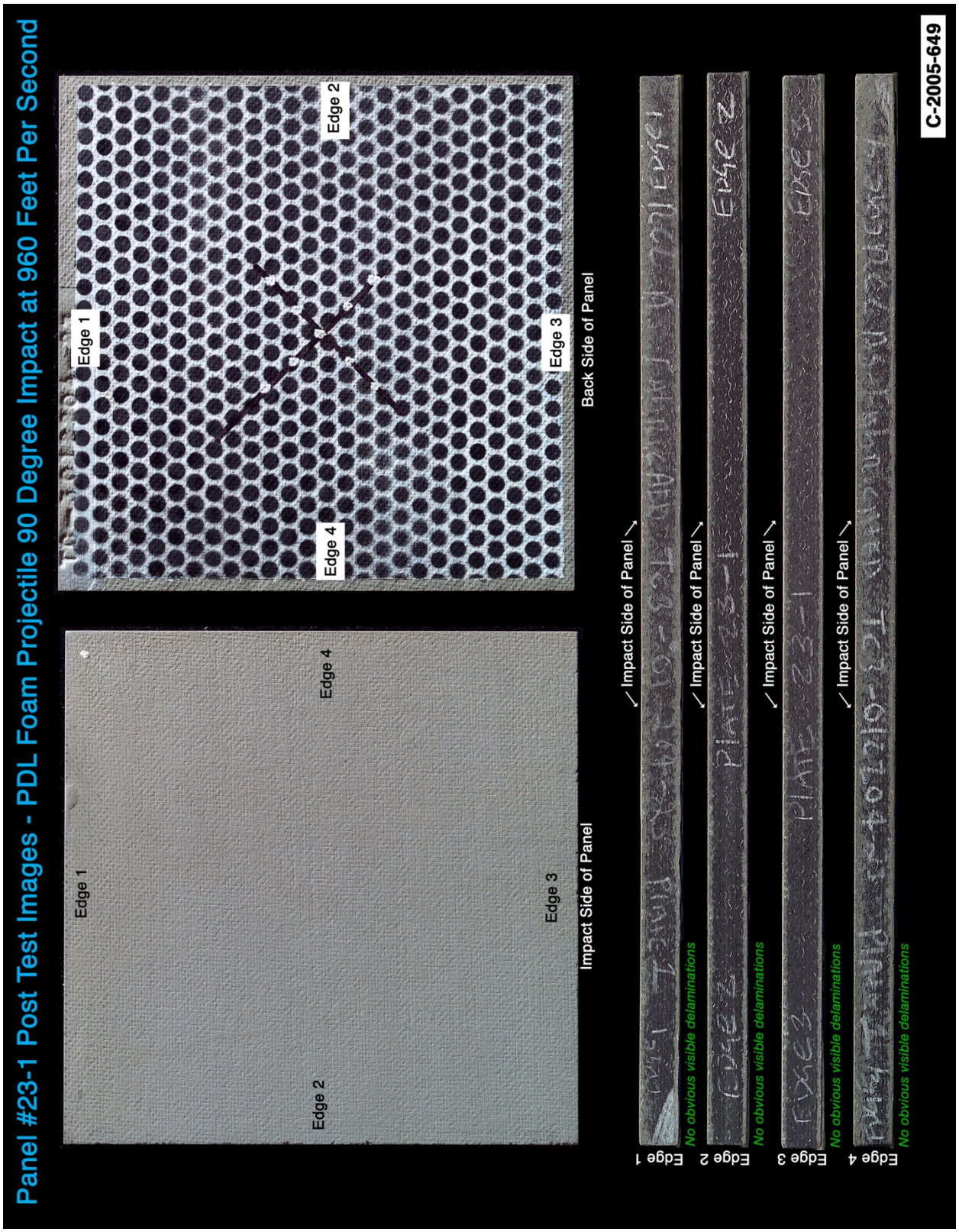

Figure E5–1.—Digital photography of edges and faces of panel 23–1 at 960 ft/s with a PDL foam cylinder (nominally 1.5 in. in diameter by 3 in.) at a 90° impact angle. Test GRCC 192.

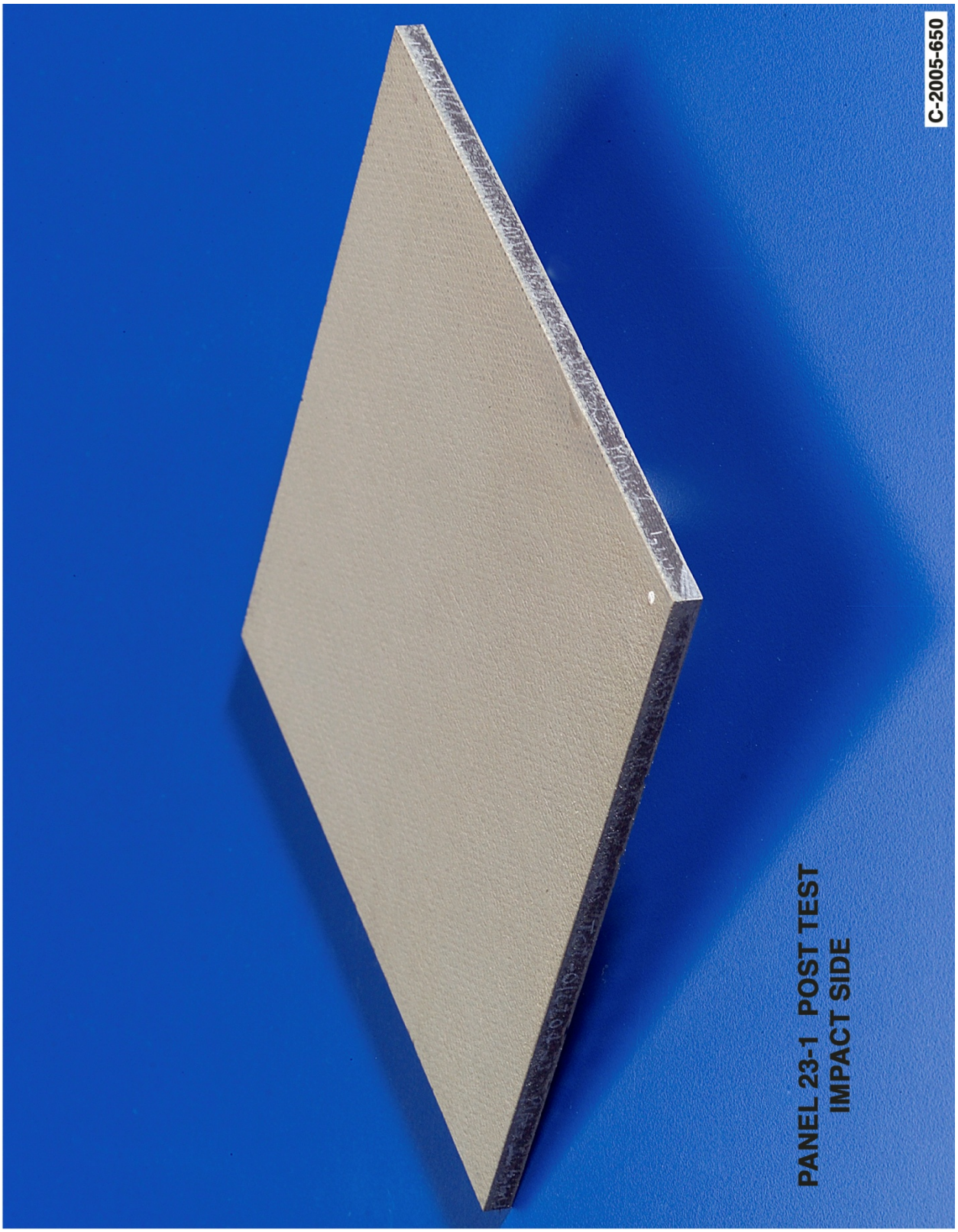

Figure E5–2.—Digital photography front (impact side) face of panel 23–1 at 960 ft/s with a PDL foam cylinder (nominally 1.5 in. in diameter by 3 in.) at a 90° impact angle. Test GRCC 192.

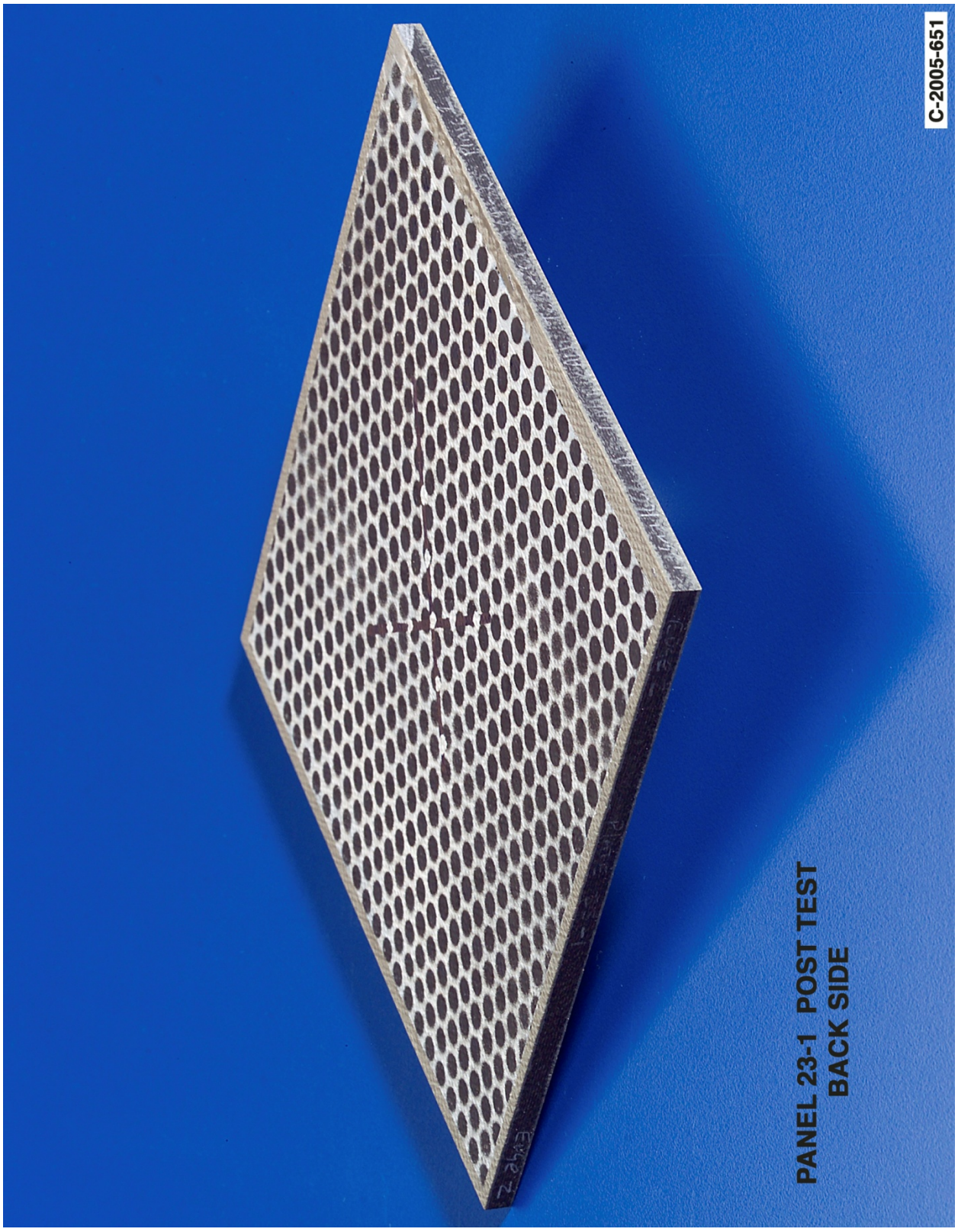

Figure E5–3.—Digital photography of back face of panel 23–1 at 960 ft/s with a PDL foam cylinder (nominally 1.5 in. in diameter by 3 in.) at a 90° impact angle. Test GRCC 192.

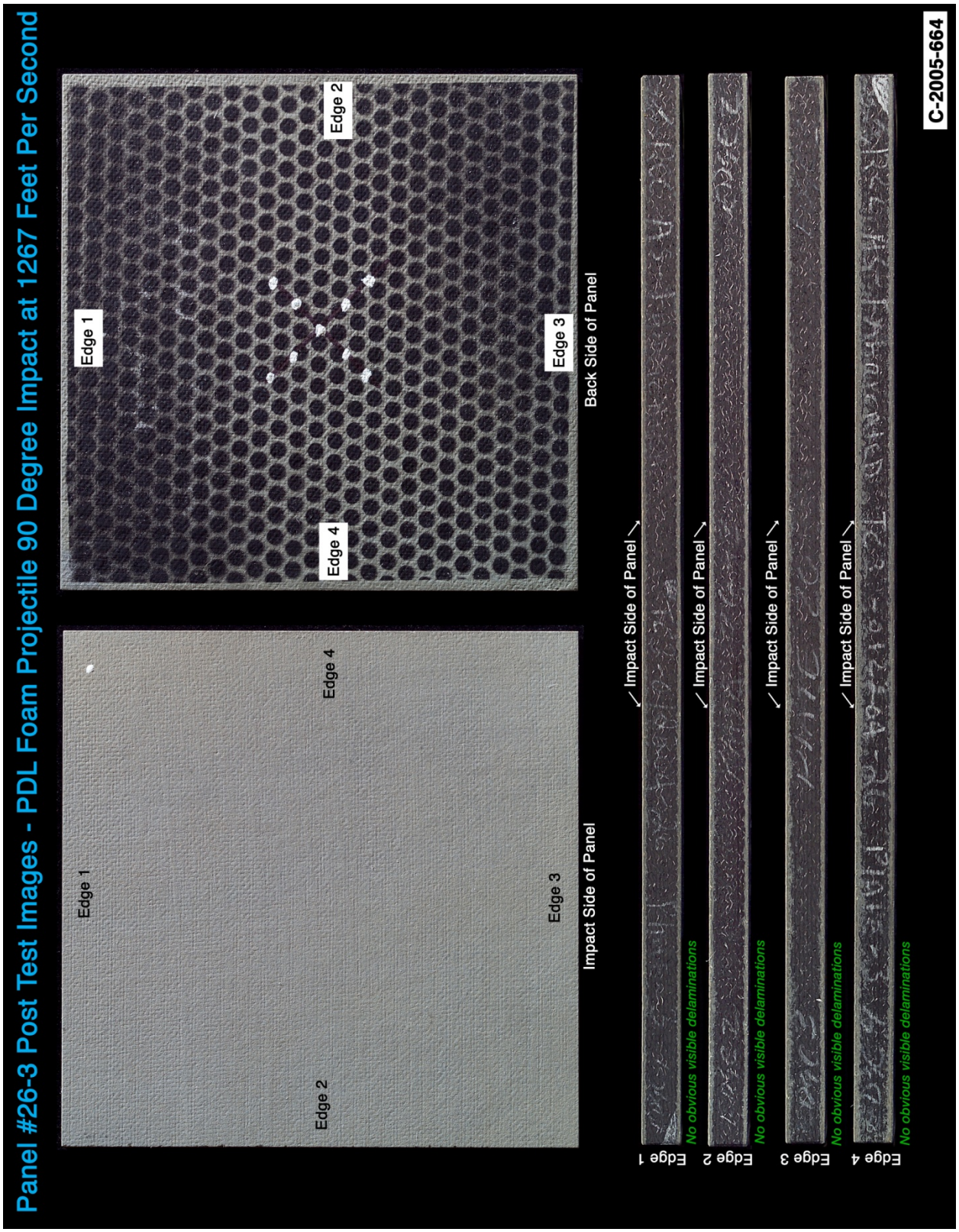

Figure E6–1.—Digital photography of edges and faces of panel 26–3 at 1267 ft/s with a PDL foam cylinder (nominally 1.5 in. in diameter by 3 in.) at a 90° impact angle. Test GRCC 208.

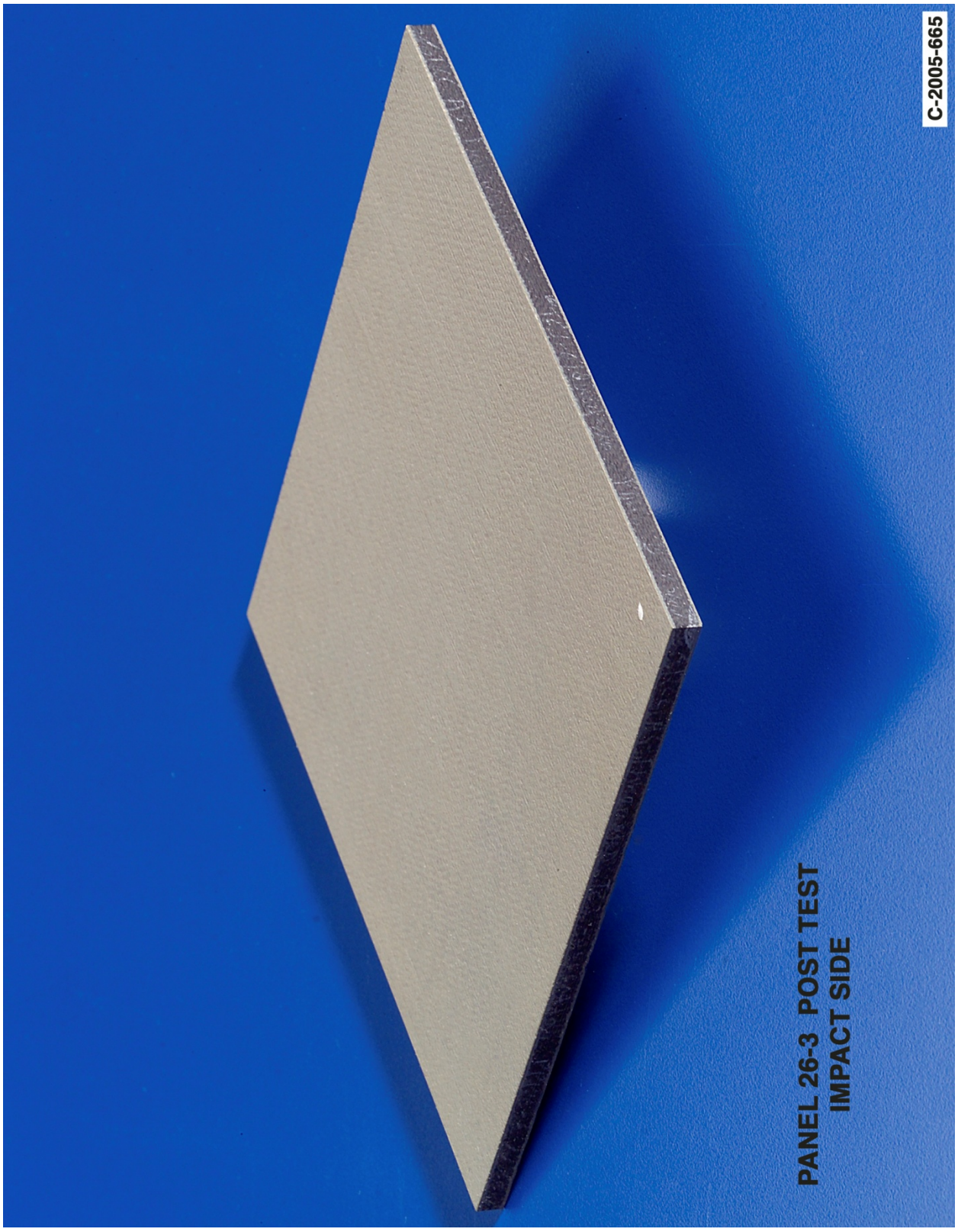

Figure E6–2.—Digital photography front (impact side) face of panel 26–3 at 1267 ft/s with a PDL foam cylinder (nominally 1.5 in. in diameter by 3 in.) at a 90° impact angle. Test GRCC 208.

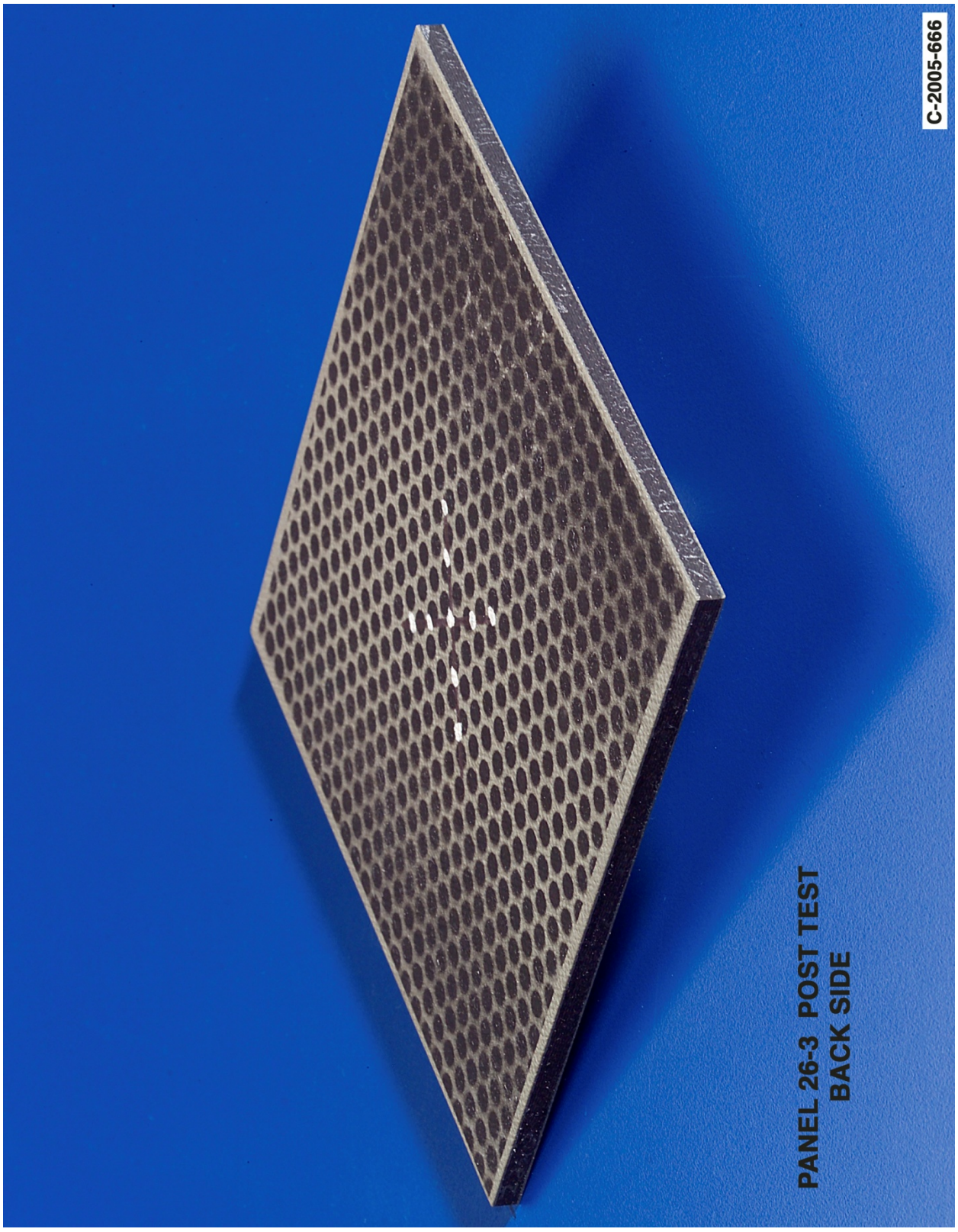

Figure E6–3.—Digital photography of back face of panel 26–3 at 1267 ft/s with a PDL foam cylinder (nominally 1.5 in. in diameter by 3 in.) at a 90° impact angle. Test GRCC 208.

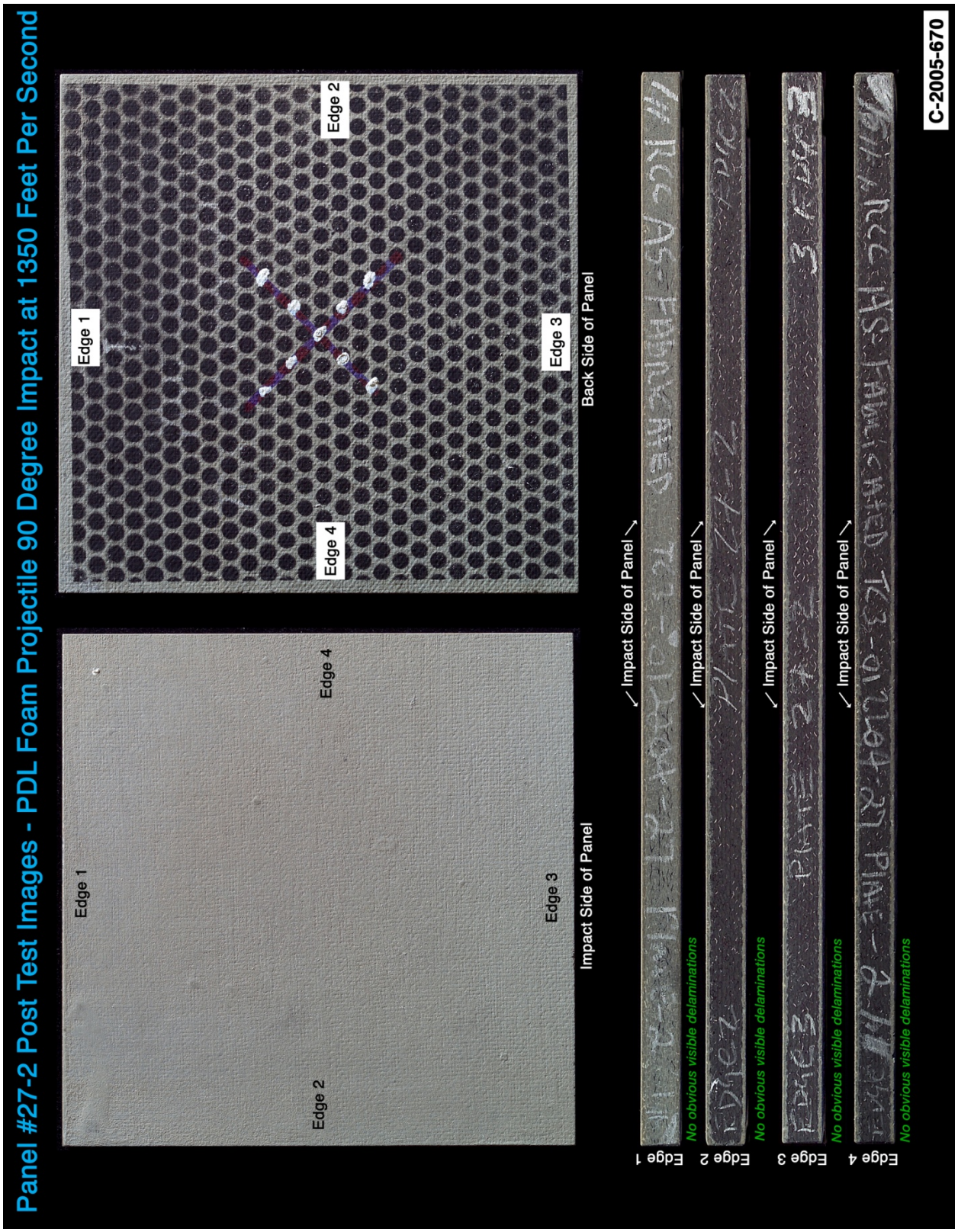

Figure E7–1.—Digital photography of edges and faces of panel 27–2 at 1350 ft/s with a PDL foam cylinder (nominally 1.5 in. in diameter by 3 in.) at a 90° impact angle. Test GRCC 213.

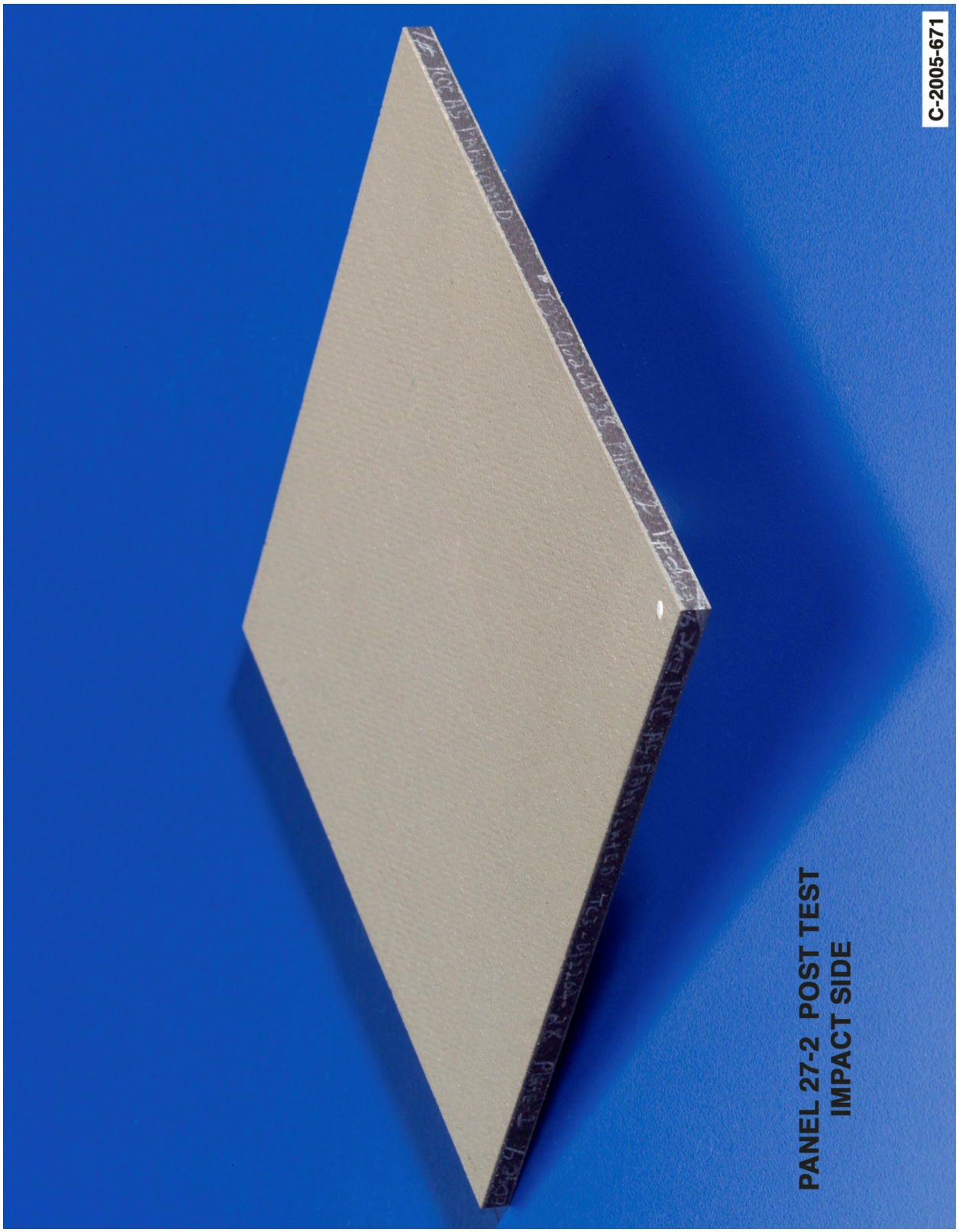

Figure E7–2.—Digital photography front (impact side) face of panel 27–2 at 1350 ft/s with a PDL foam cylinder (nominally 1.5 in. in diameter by 3 in.) at a 90° impact angle. Test GRCC 213.

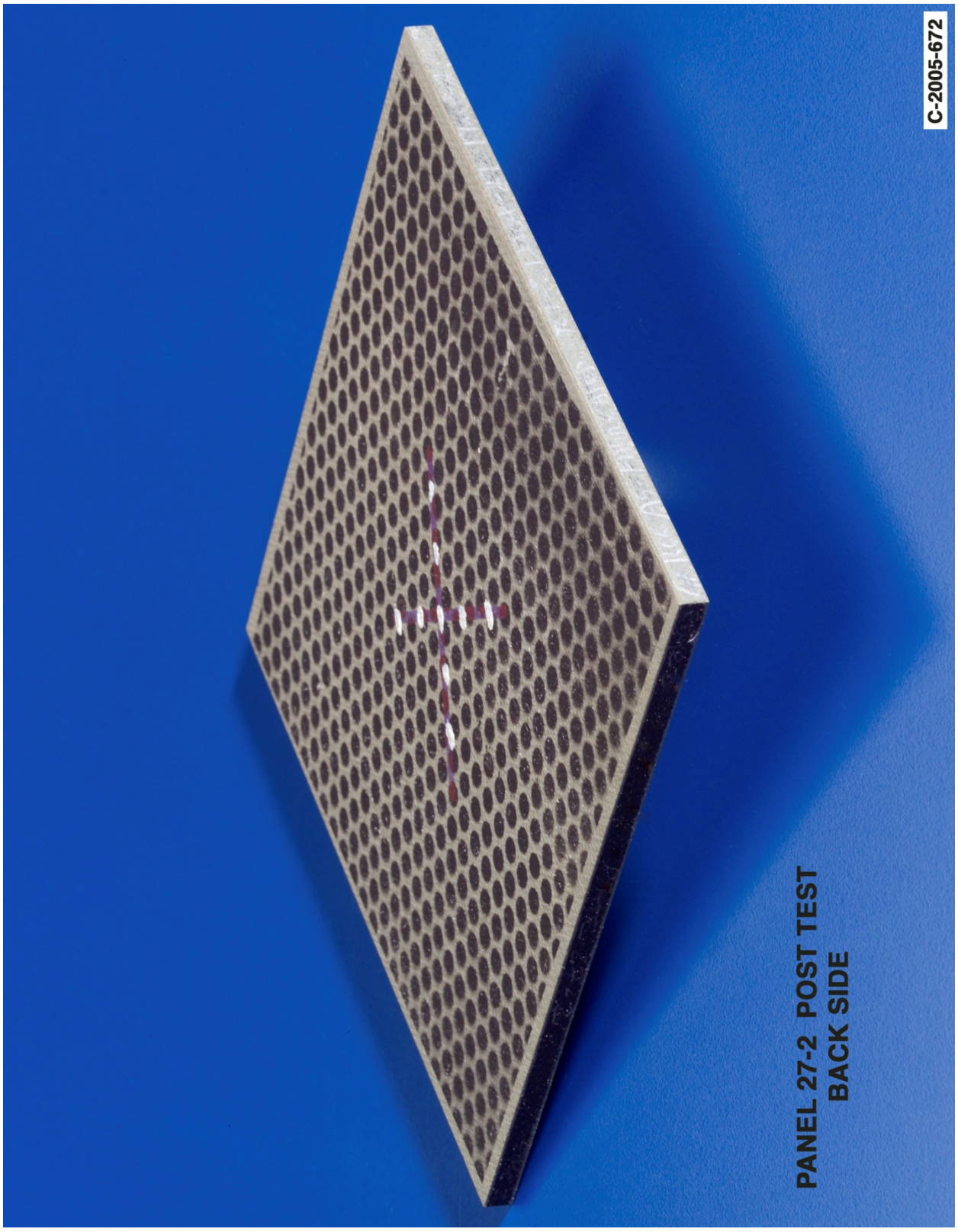

Figure E7–2.—Digital photography front (impact side) face of panel 27–2 at 1350 ft/s with a PDL foam cylinder (nominally 1.5 in. in diameter by 3 in.) at a 90° impact angle. Test GRCC 213.

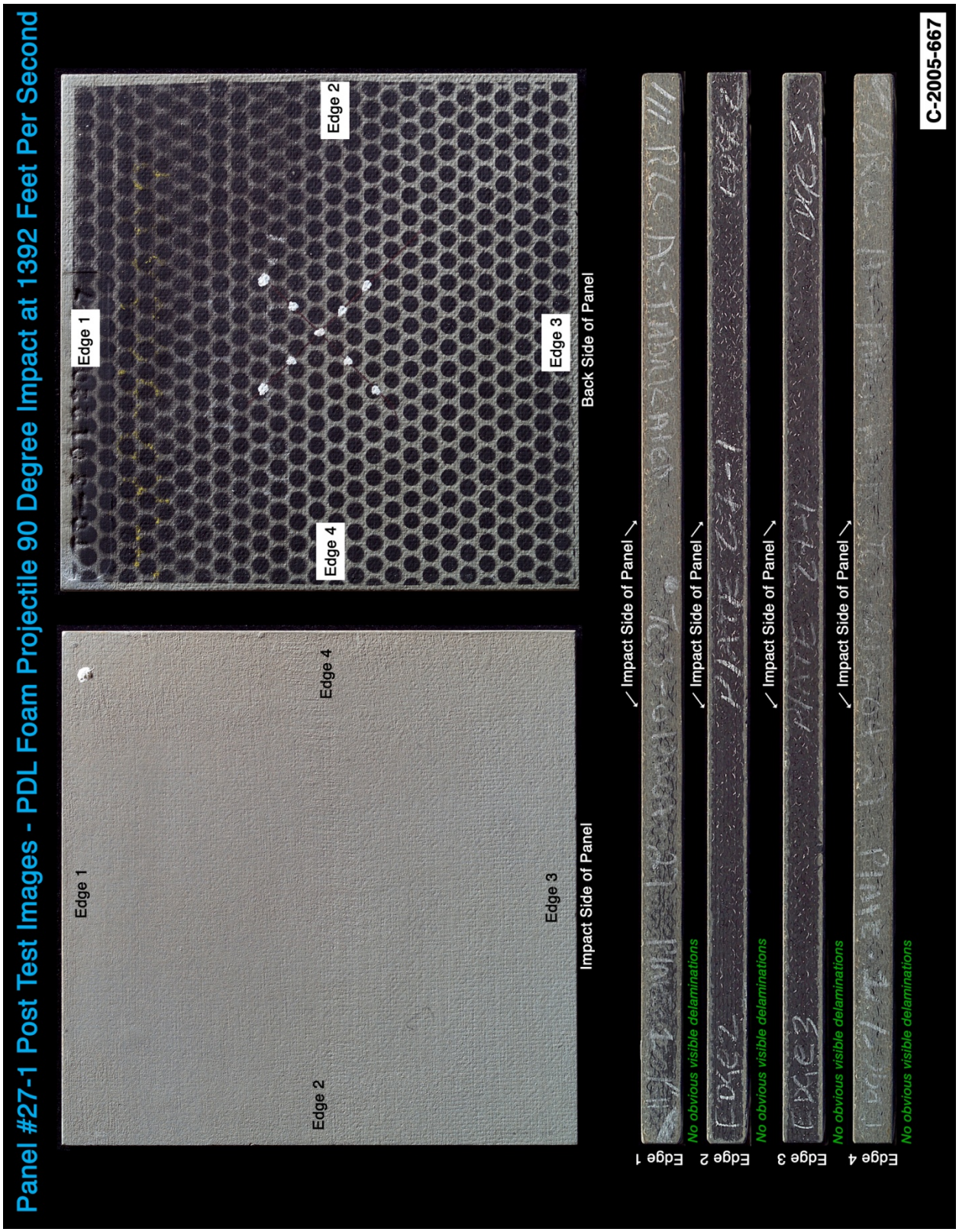

Figure E8–1.—Digital photography of edges and faces of panel 27–1 at 1392 ft/s with a PDL foam cylinder (nominally 1.5 in. in diameter by 3 in.) at a 90° impact angle. Test GRCC 211.

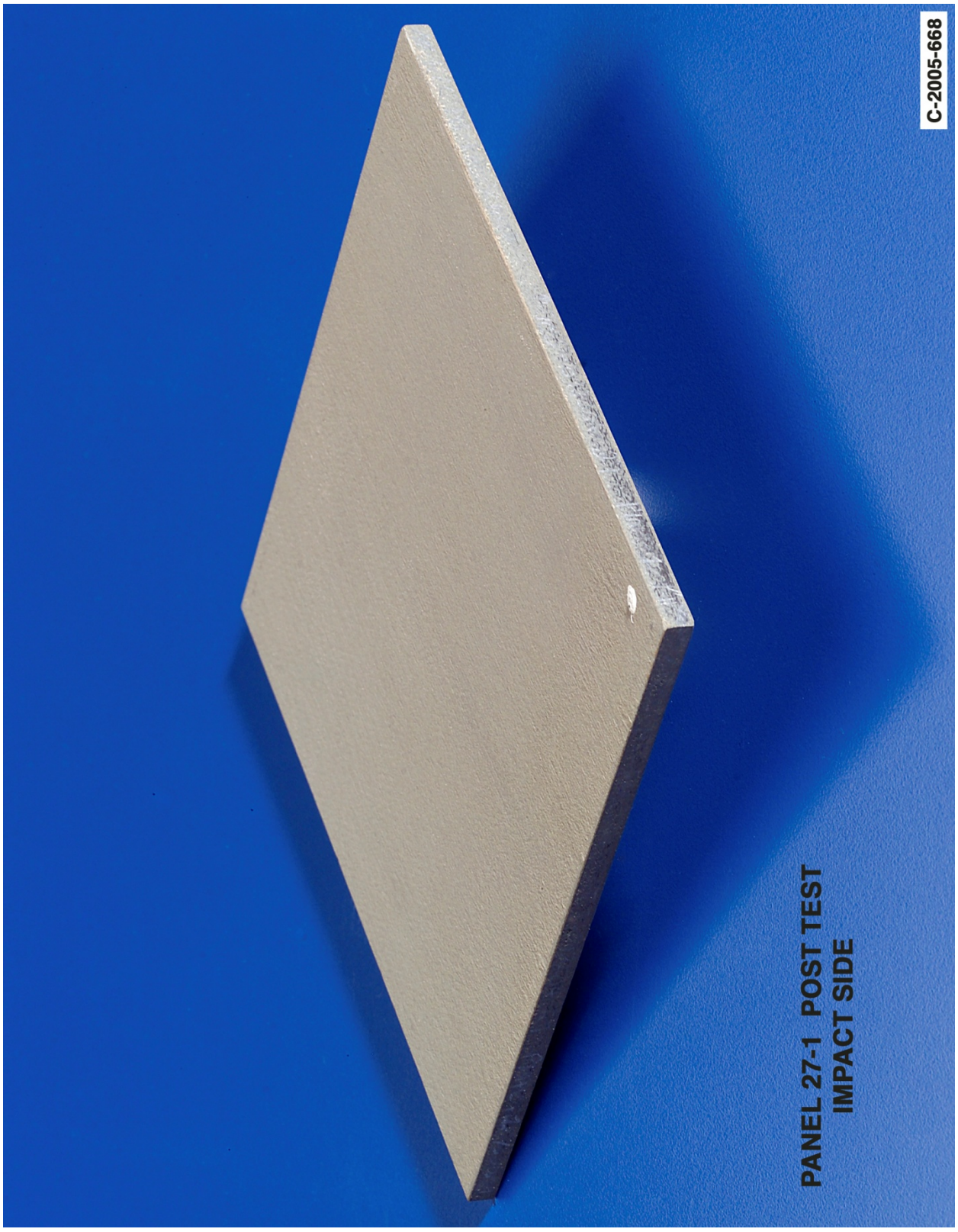

Figure E8–2.—Digital photography front (impact side) face of panel 27–1 at 1392 ft/s with a PDL foam cylinder (nominally 1.5 in. in diameter by 3 in.) at a 90° impact angle. Test GRCC 211.

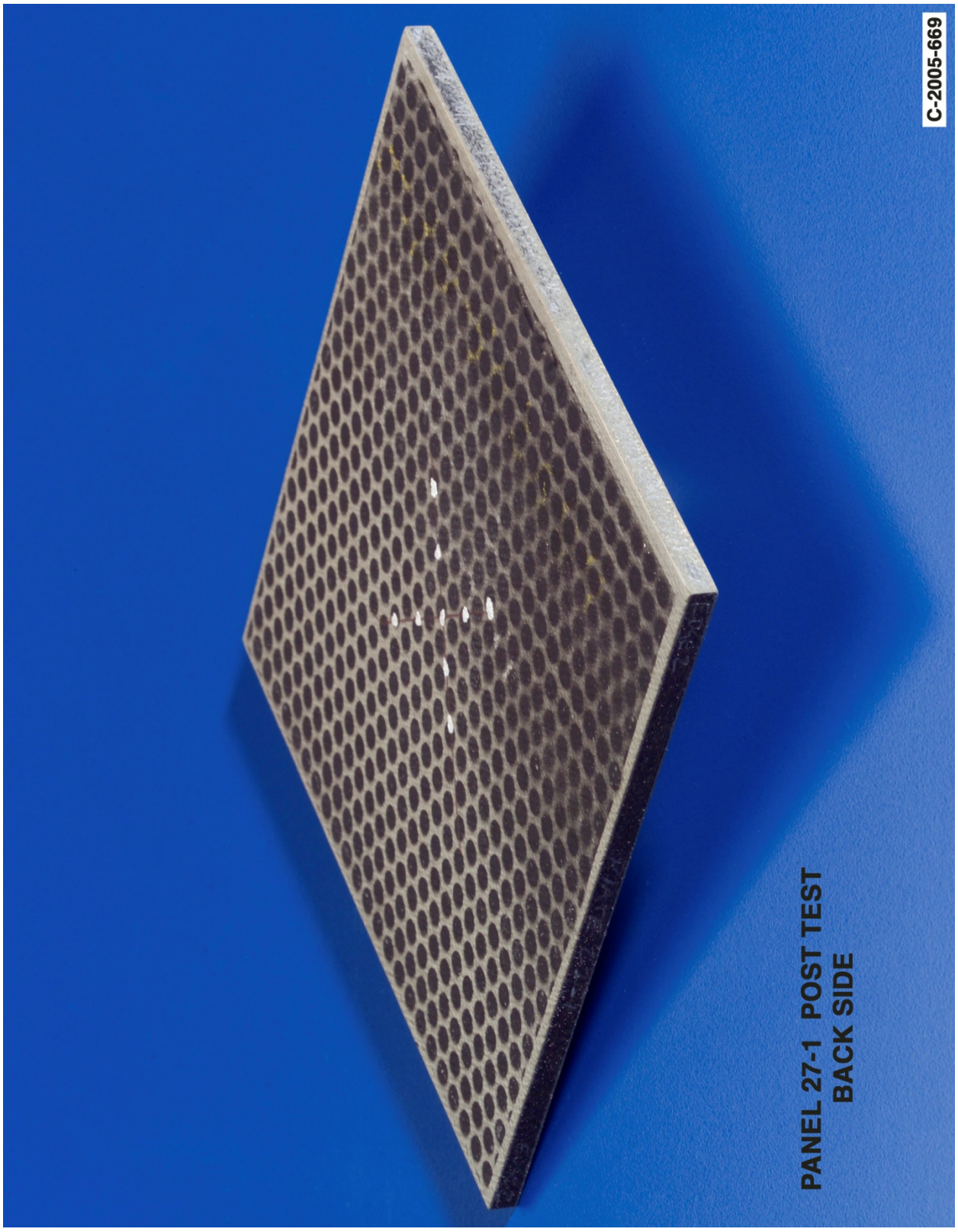

Figure E8–3.—Digital photography of back face of panel 27–1 at 1392 ft/s with a PDL foam cylinder (nominally 1.5 in. in diameter by 3 in.) at a 90° impact angle. Test GRCC 211.

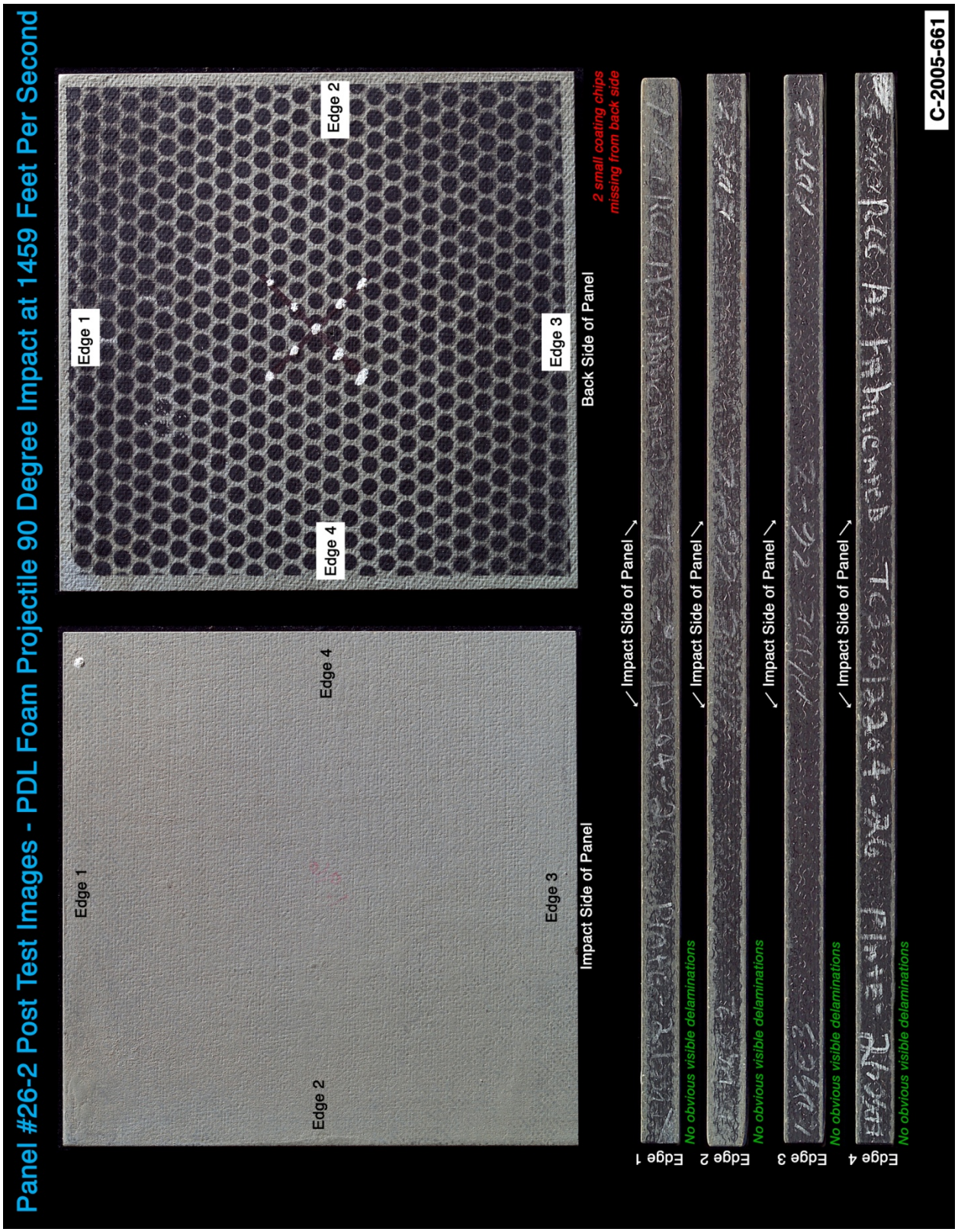

Figure E9–1.—Digital photography of edges and faces of panel 26–2 at 1459 ft/s with a PDL foam cylinder (nominally 1.5 in. in diameter by 3 in.) at a 90° impact angle. Test GRCC 200.

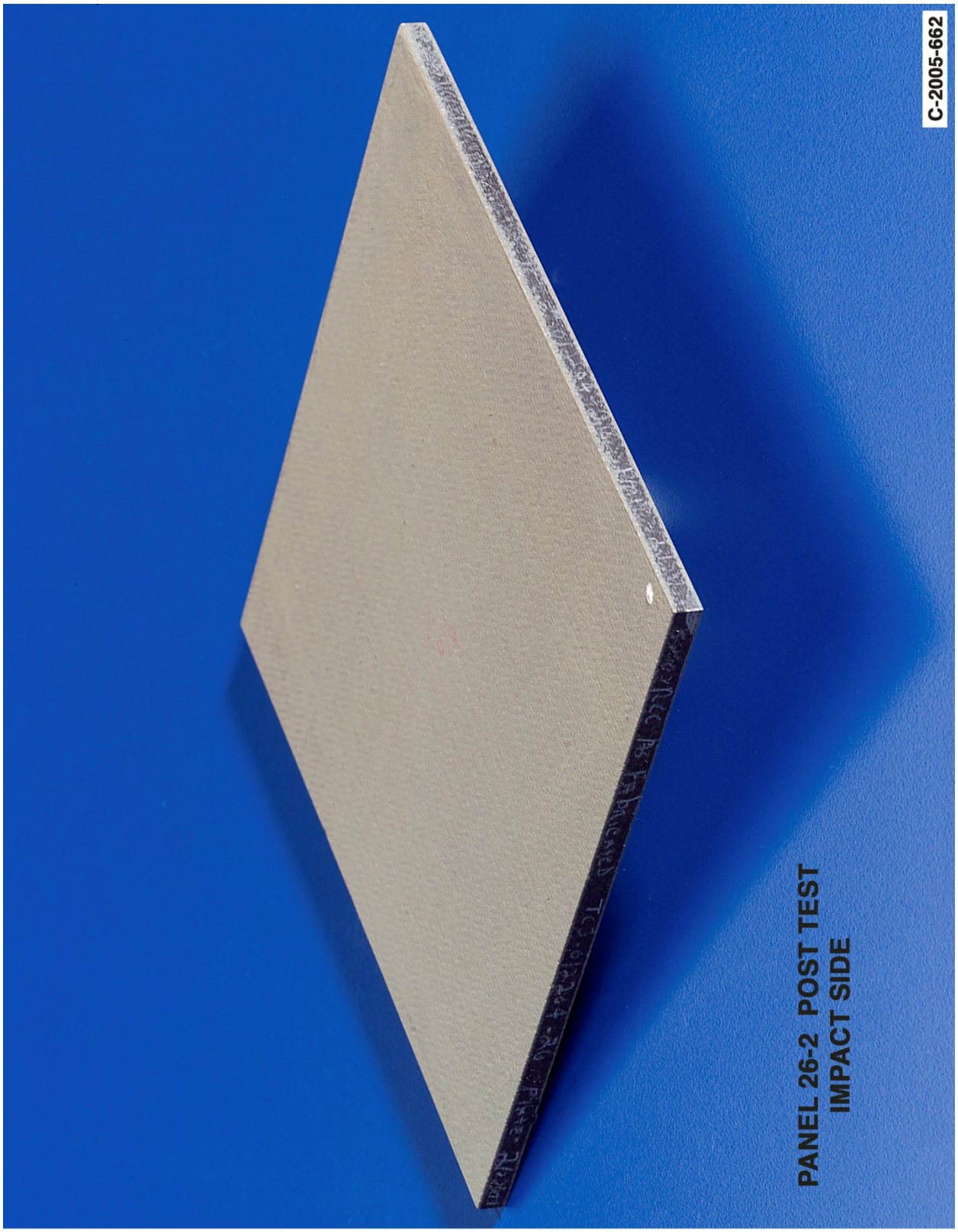

Figure E9–2.—Digital photography front (impact side) face of panel 26–2 at 1459 ft/s with a PDL foam cylinder (nominally 1.5 in. in diameter by 3 in.) at a 90° impact angle. Test GRCC 200.

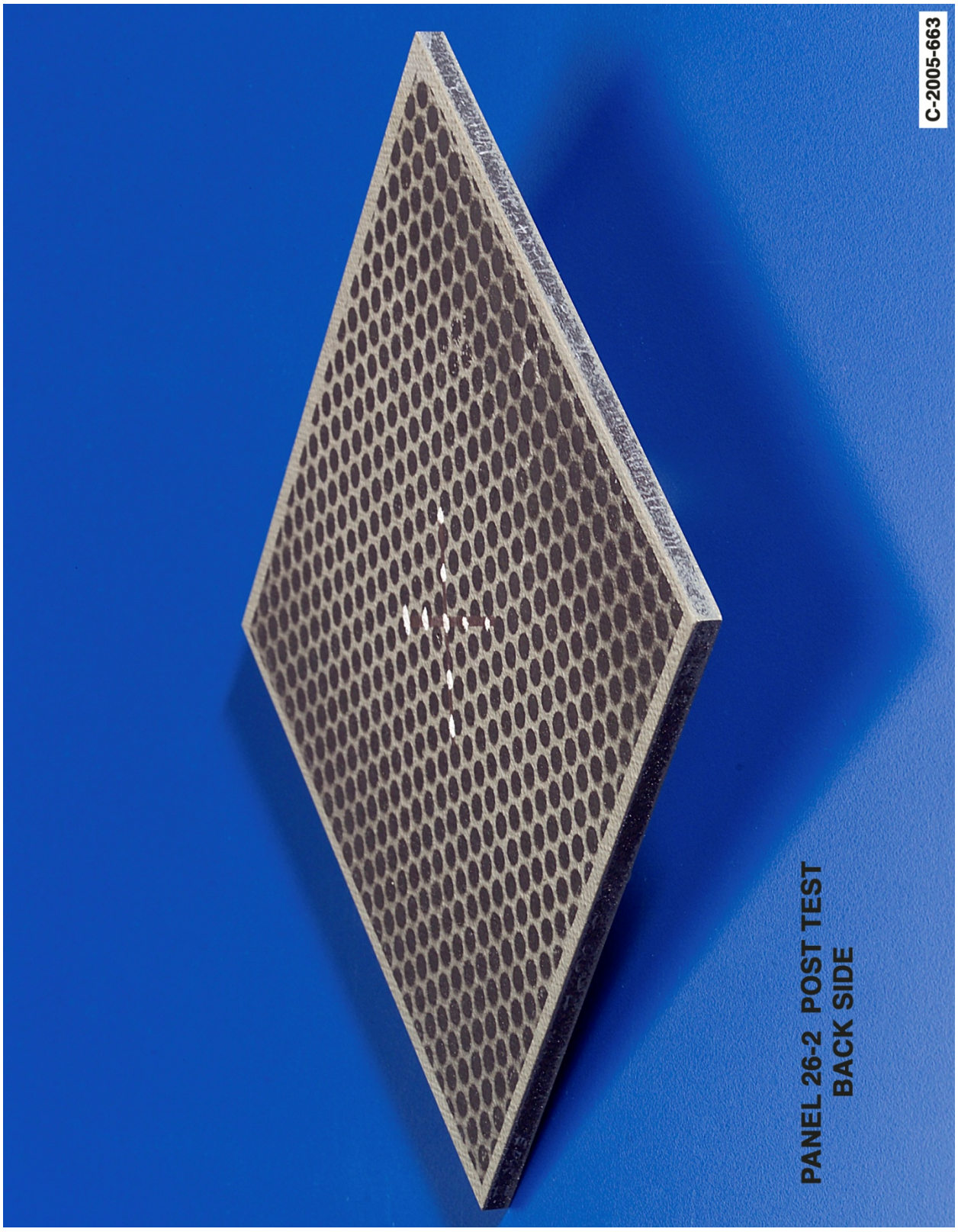

Figure E9–3.—Digital photography of back face of panel 26–2 at 1459 ft/s with a PDL foam cylinder (nominally 1.5 in. in diameter by 3 in.) at a 90° impact angle. Test GRCC 200.

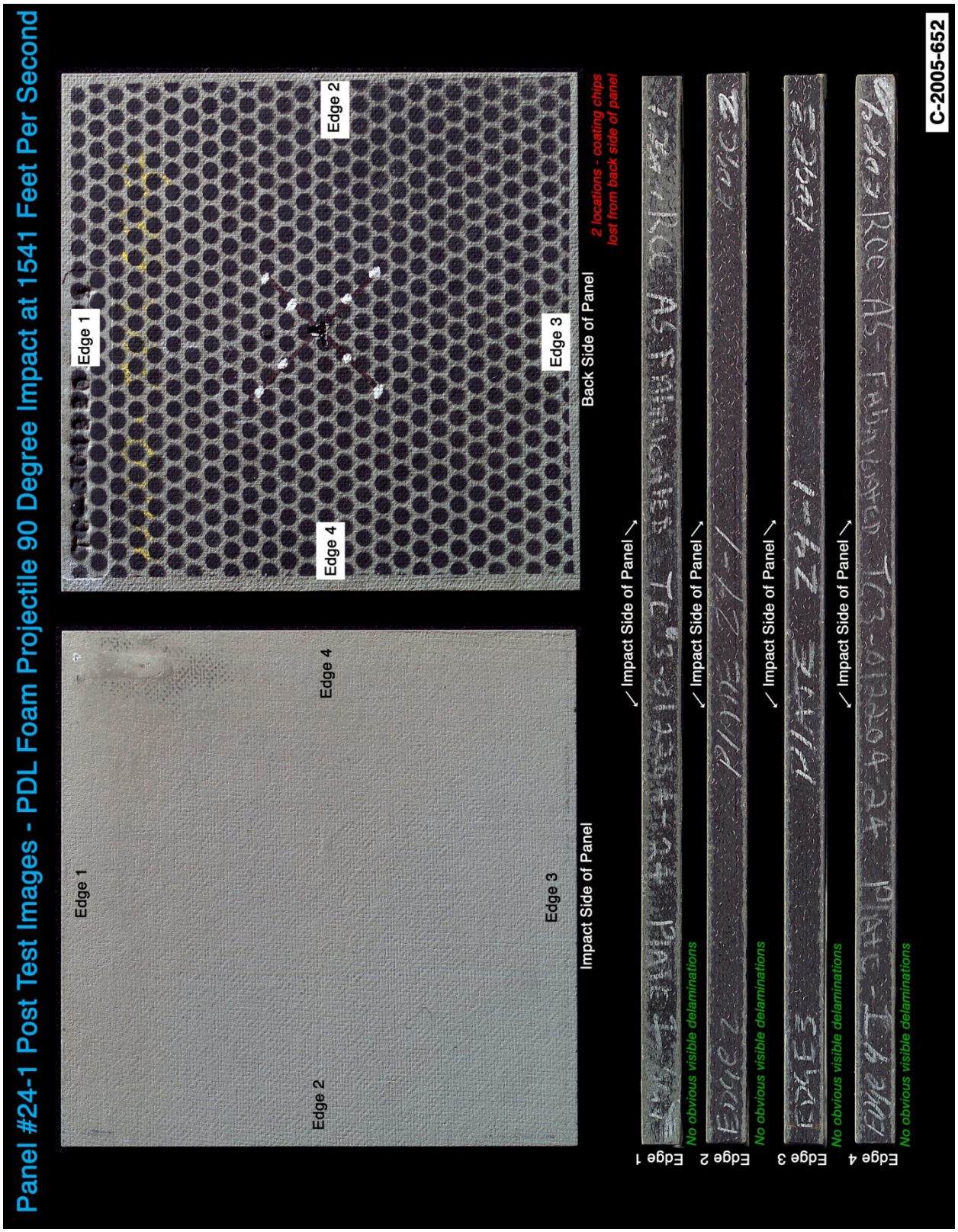

Figure E10–1.—Digital photography of edges and faces of panel 24–1 at 1541 ft/s with a PDL foam cylinder (nominally 1.5 in. in diameter by 3 in.) at a 90° impact angle. Test GRCC 195.

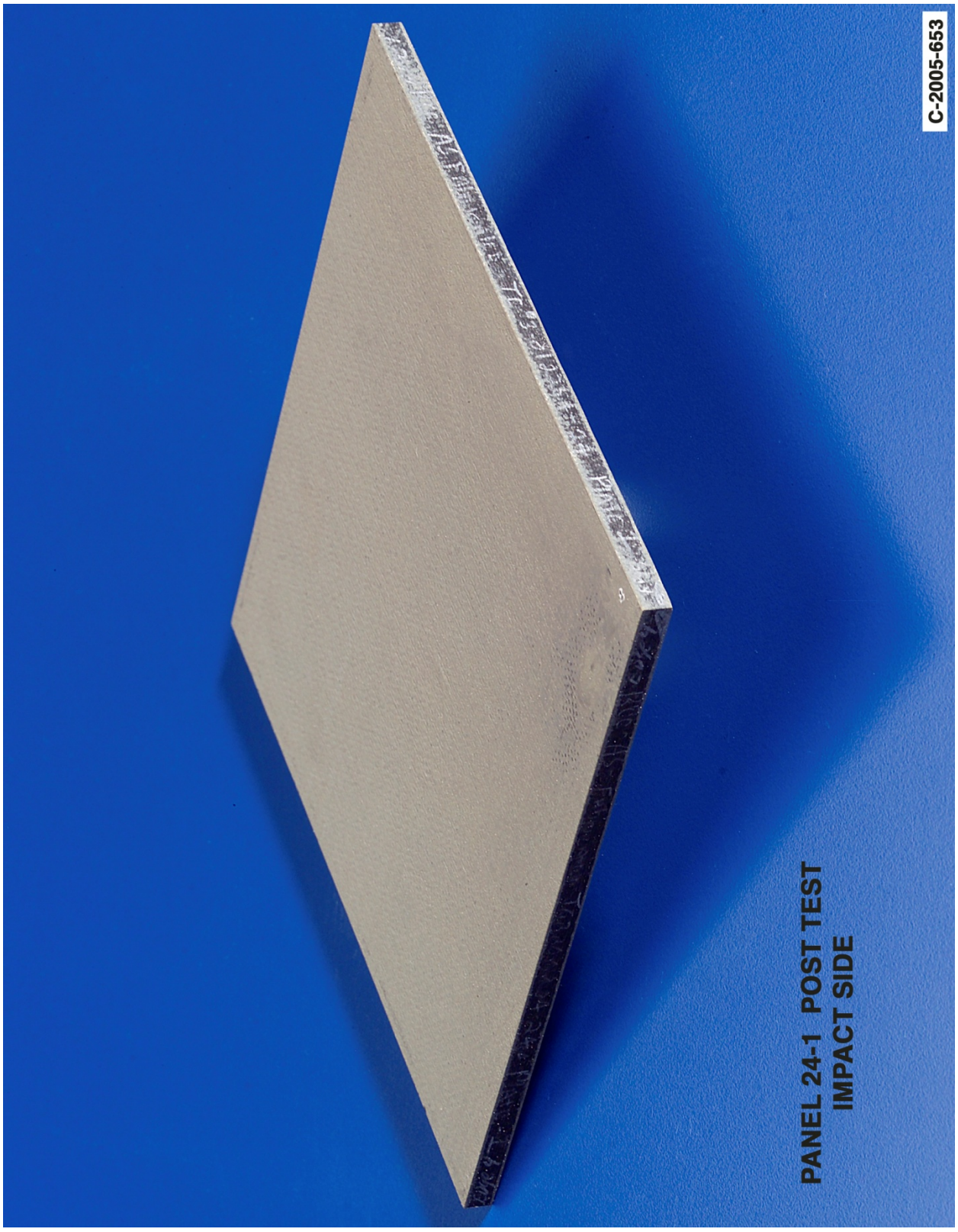

Figure E10–2.—Digital photography front (impact side) face of panel 24–1 at 1541 ft/s with a PDL foam cylinder (nominally 1.5 in. in diameter by 3 in.) at a 90° impact angle. Test GRCC 195.

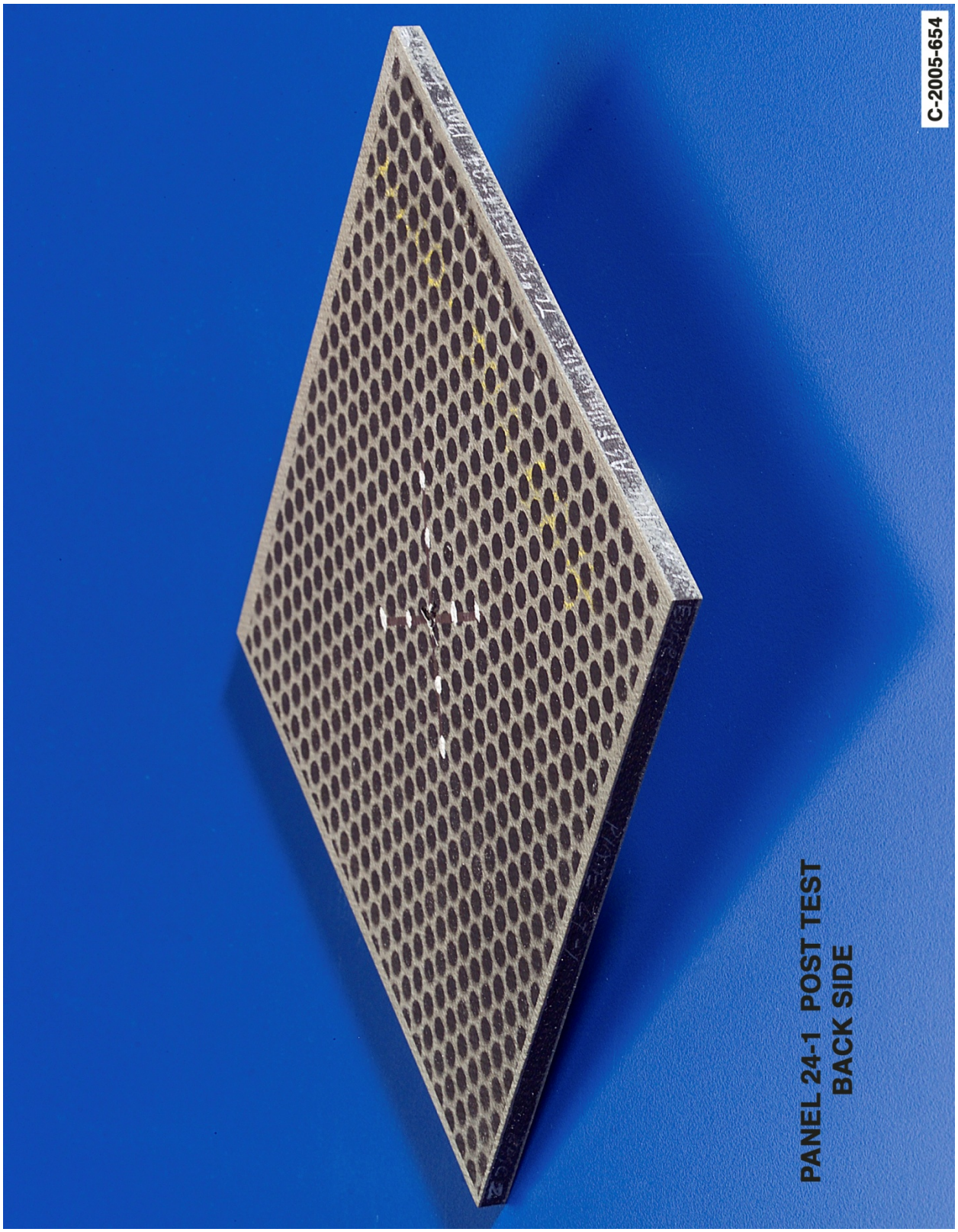

Figure E10–3.—Digital photography of back face of panel 24–1 at 1541 ft/s with a PDL foam cylinder (nominally 1.5 in. in diameter by 3 in.) at a 90° impact angle. Test GRCC 195.

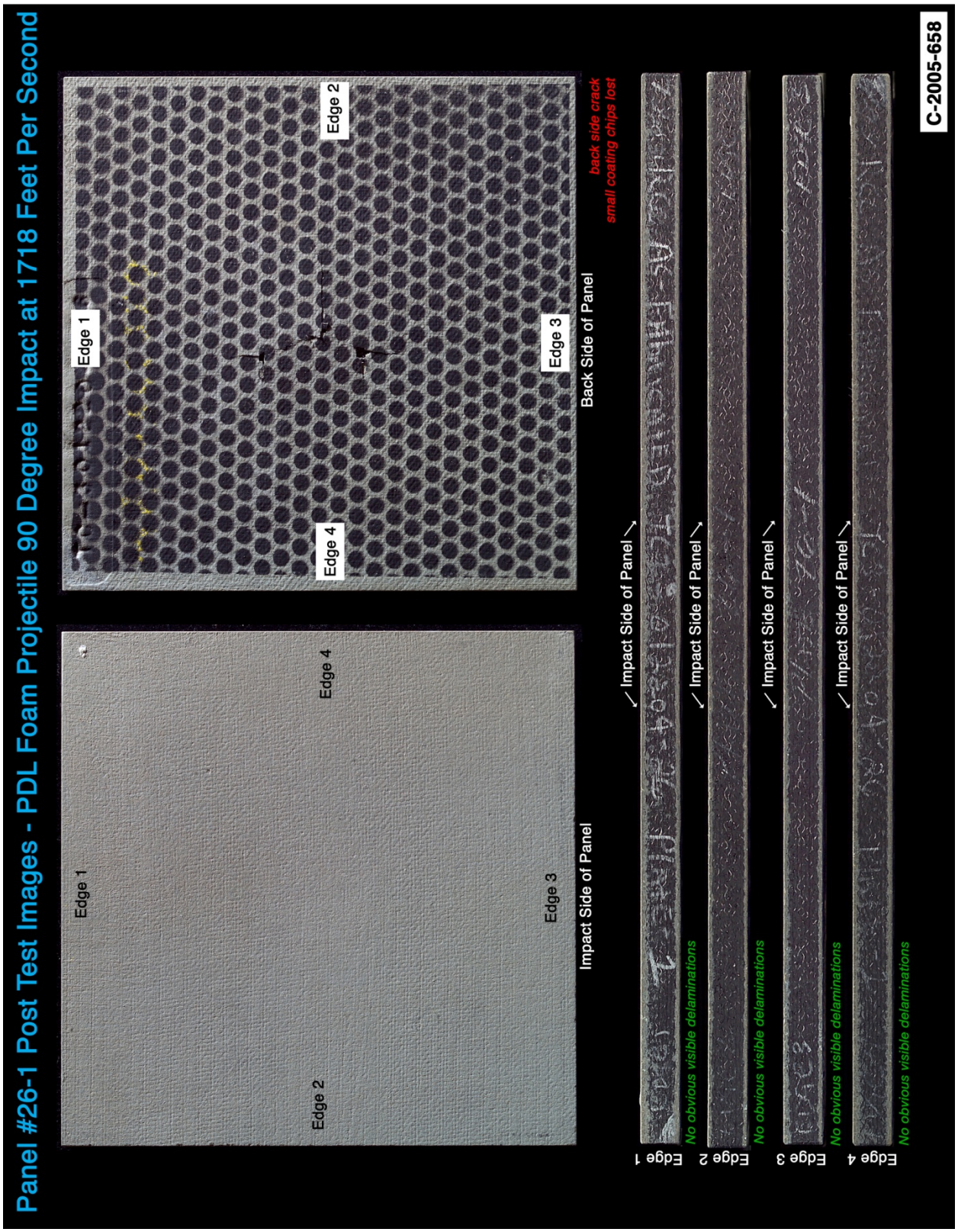

Figure E11–1.—Digital photography of edges and faces of panel 26–1 at 1718 ft/s with a PDL foam cylinder (nominally 1.5 in. in diameter by 3 in.) at a 90° impact angle. Test GRCC 198.

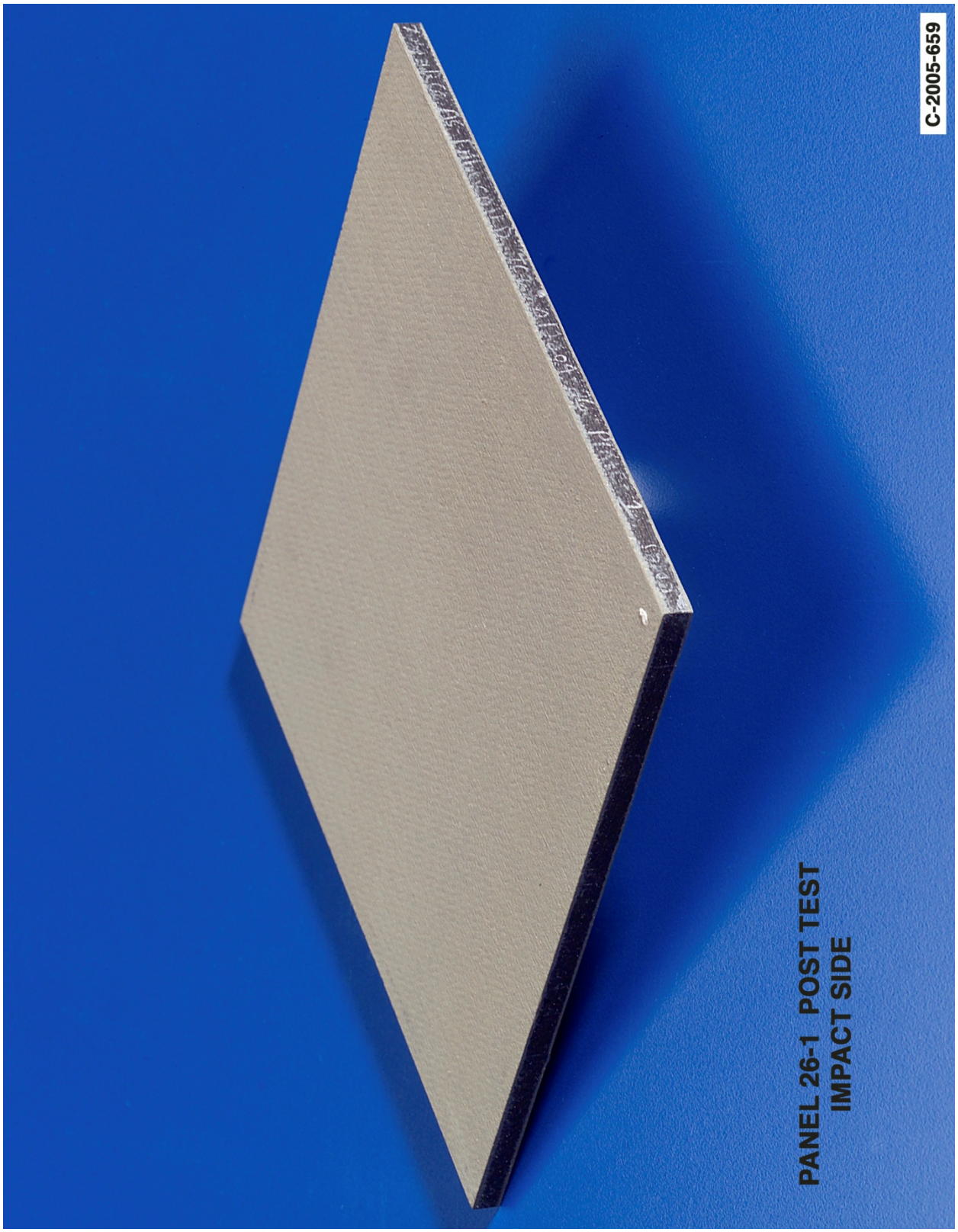

Figure E11–2.—Digital photography front (impact side) face of panel 26–1 at 1718 ft/s with a PDL foam cylinder (nominally 1.5 in. in diameter by 3 in.) at a 90° impact angle. Test GRCC 198.

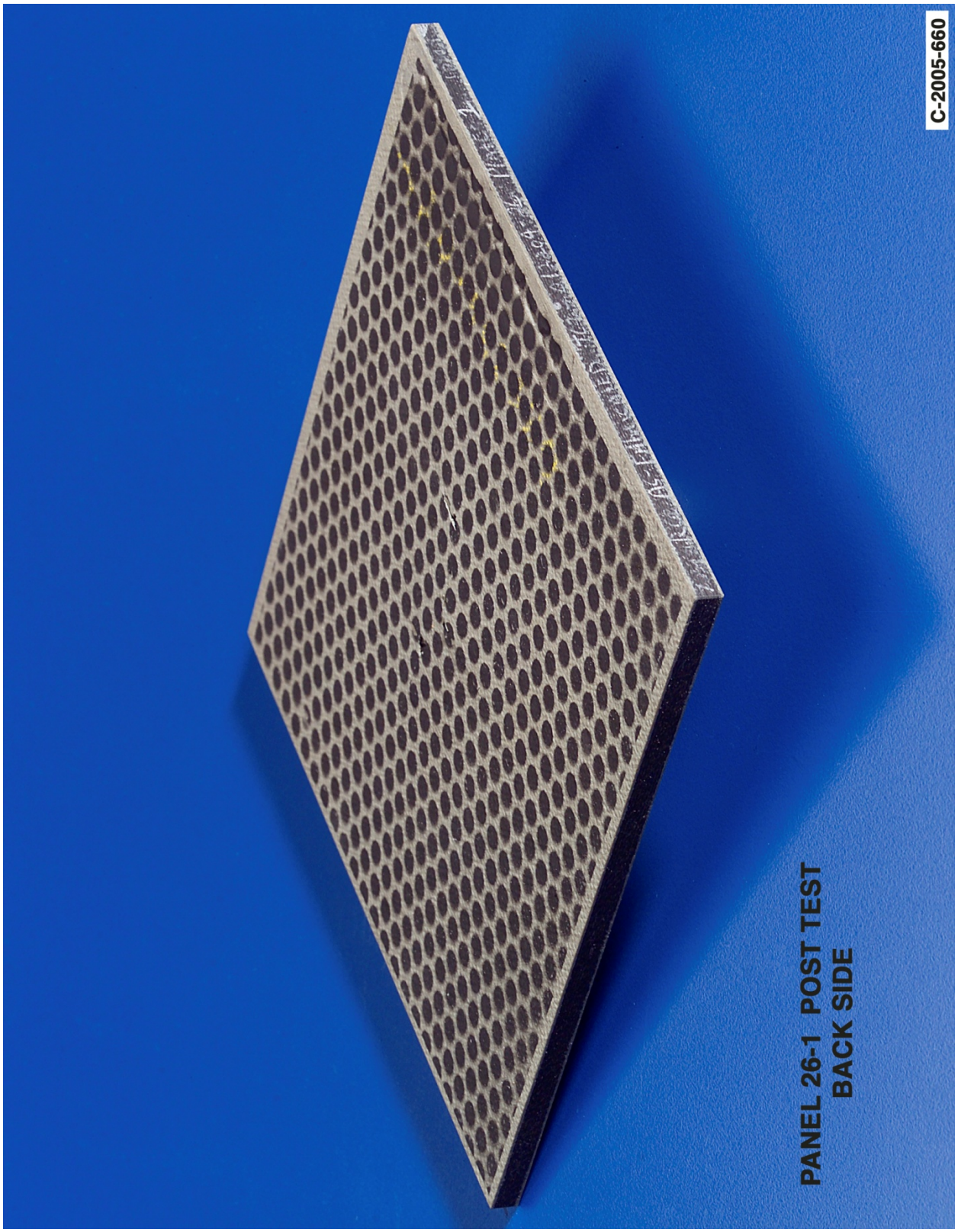

Figure E11–3.—Digital photography of back face of panel 26–1 at 1718 ft/s with a PDL foam cylinder (nominally 1.5 in. in diameter by 3 in.) at a 90° impact angle. Test GRCC 198.

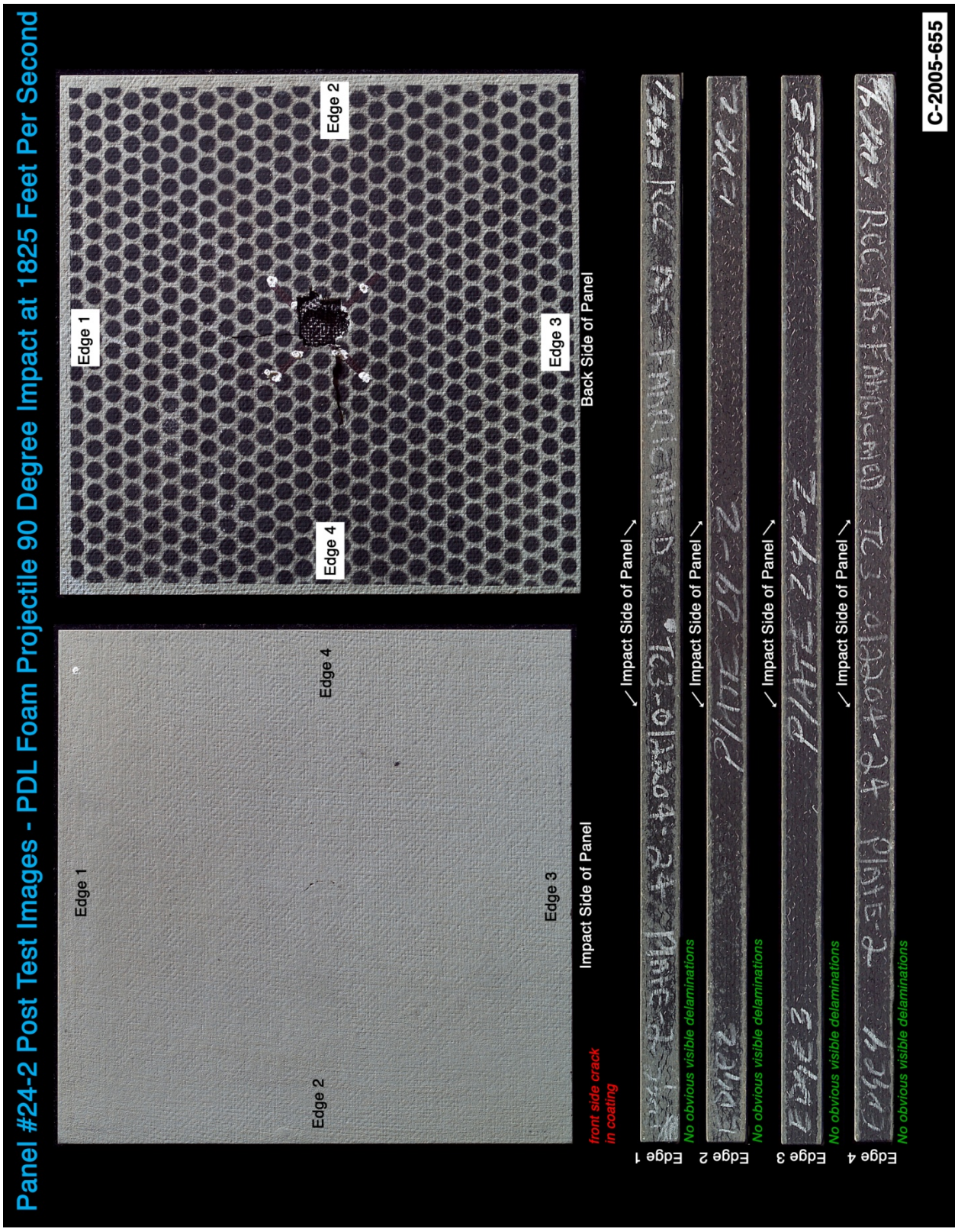

Figure E12–1.—Digital photography of edges and faces of panel 24–2 at 1825 ft/s with a PDL foam cylinder (nominally 1.5 in. in diameter by 3 in.) at a 90° impact angle. Test GRCC 203.

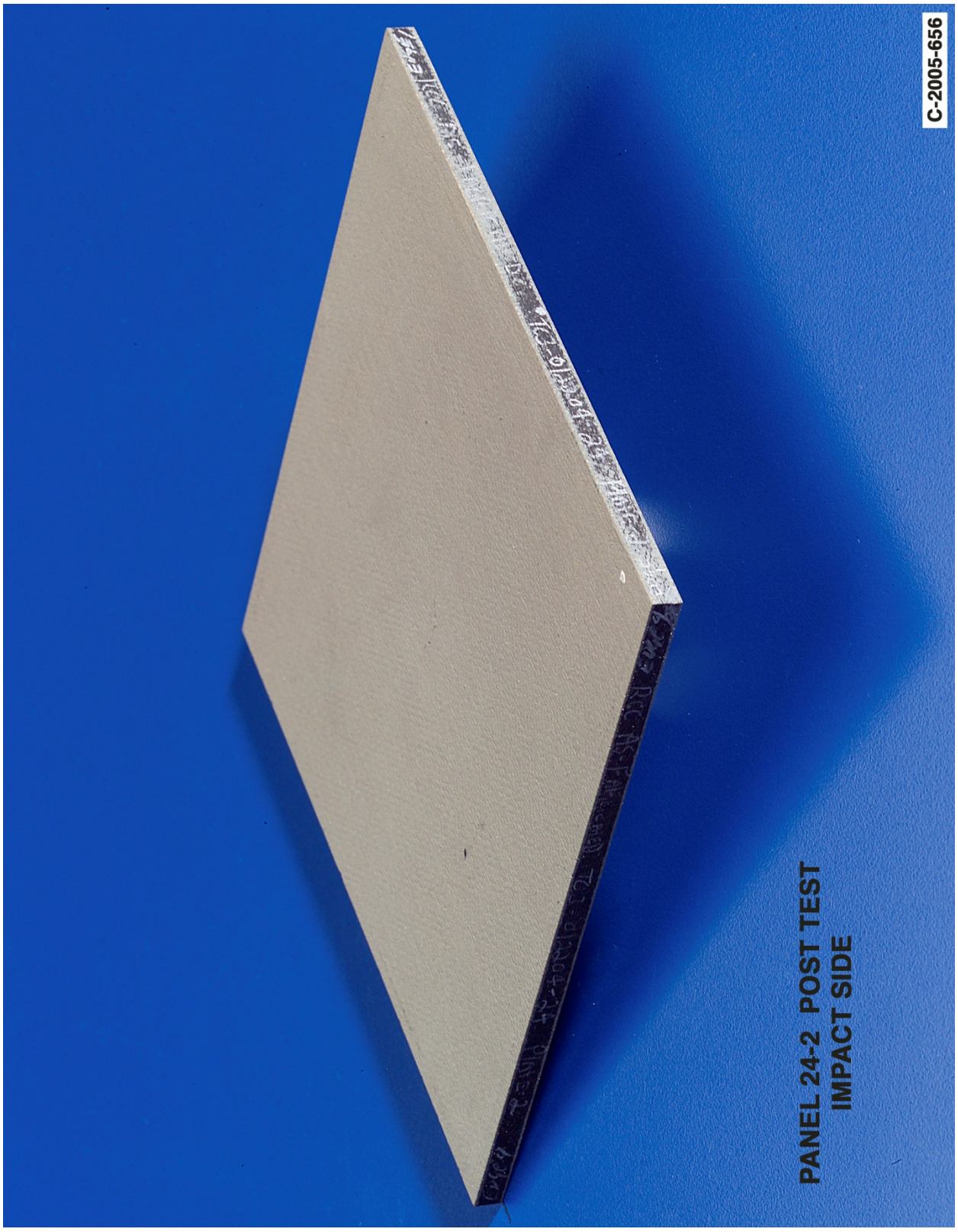

Figure E12–2.—Digital photography front (impact side) face of panel 24–2 at 1825 ft/s with a PDL foam cylinder (nominally 1.5 in. in diameter by 3 in.) at a 90° impact angle. Test GRCC 203.

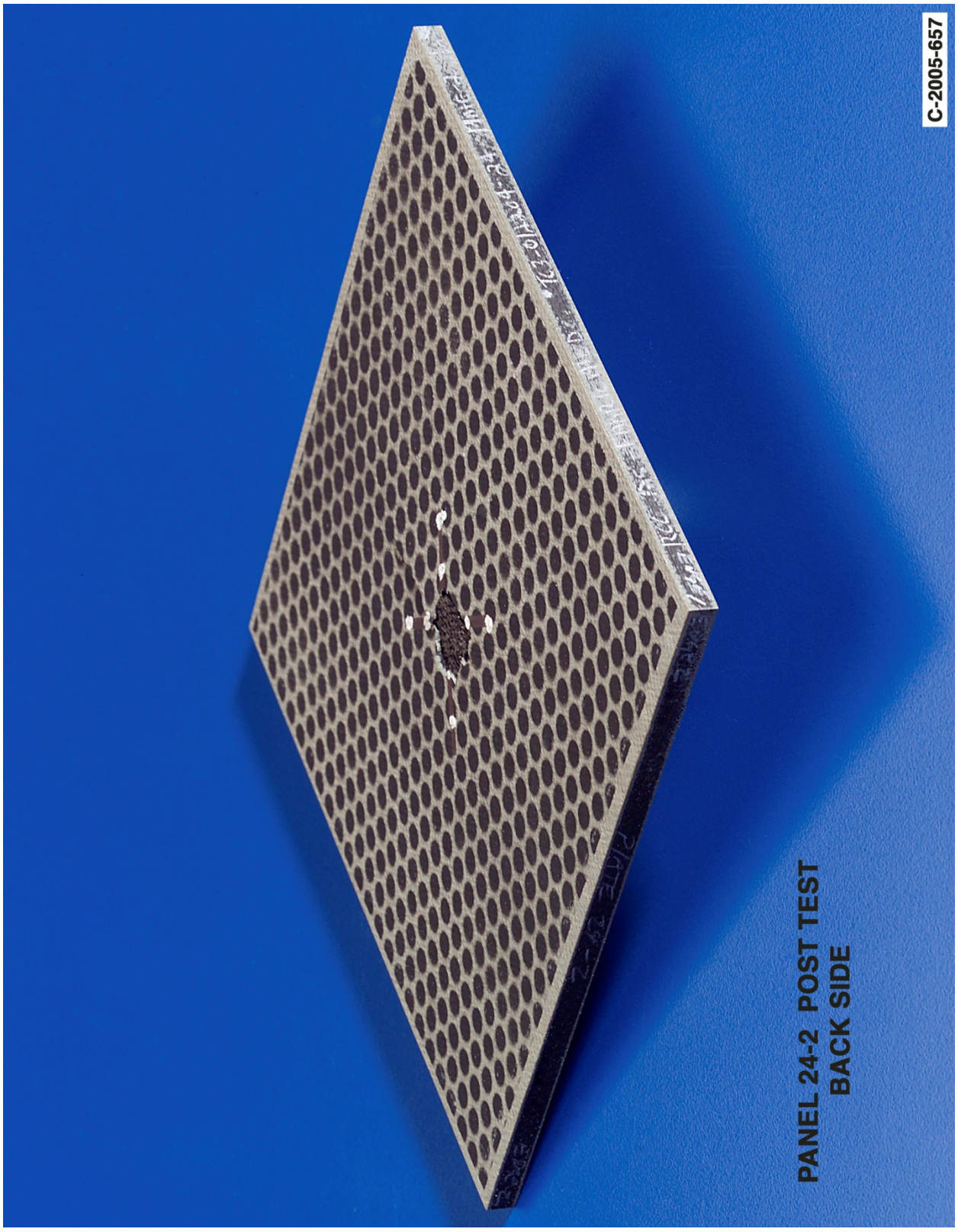

Figure E12–3.—Digital photography of back face of panel 24–2 at 1825 ft/s with a PDL foam cylinder (nominally 1.5 in. in diameter by 3 in.) at a 90° impact angle. Test GRCC 203.

Appendix F.—Test Data

PDL External Tank Foam Impact Testing at 45° Angle on 6- by 6-in. Reinforced Carbon-Carbon (RCC) Flat Panels

Notable Observations From the Appendix F Test Series

1. The RCC material used in this test series was tested in the as-manufactured condition.
2. GRCC 230 ARAMIS data was obscured due to coating and substrate debris throughout the run. This can be seen in the data dropouts on the deformation contours and trace plots for this test.
3. Lot 3, (22–36) in the following test series table refers to Lockheed Set 3A, processing Batch 22–36, made specifically for the Return to Flight Program.

Appendix F Test Series

PDL 45 Degree Impact Test Parameters on 6" x 6" Reinforced Carbon-Carbon Panels

Test No.	Glenn Test Reference Number	Impact Velocity (ft/sec)	Panel ID Number	Lot Number	Average Panel Thickness (inches)	Visual Damage Observations	Mass of panel before test (grams)	Mass of panel after test (grams)	Projectile Weight (g)	Projectile Length (in)	Projectile Diameter (in)	Test Date	Projectile ID Number
4-45-281-01	GCRR217	1122	28-1	3,(22-36)	0.221	No significant indications	206.83	206.79	3.00	1.821	1.496	5/3/05	1829 PDL-P2-13
4-45-282-07	GRCC229	1266	28-2	3,(22-36)	0.221	No significant indications	208.90	208.10	2.99	1.826	1.492	5/5/05	1829 PDL-P2-7
4-45-293-04	GRCC223	1296	29-3	3,(22-36)	0.221	No significant indications	207.01	207.02	3.01	1.831	1.498	5/4/05	1829 PDL-P2-14
4-45-291-02	GRCC220	1495	29-1	3,(22-36)	0.224	No significant indications	205.89	205.88	3.01	1.835	1.498	5/4/05	1829 PDL-P2-17
4-45-292-03	GRCC222	1723	29-2	3,(22-36)	0.223	Backside coating chips lost	204.97	204.96	3.00	1.829	1.502	5/4/05	1829 PDL-P2-19
4-45-361-05	GRCC225	1920	36-1	3,(22-36)	0.220	Significant backside crack, coating loss	205.22	205.17	3.00	1.822	1.495	5/4/05	1829 PDL-P2-16
4-45-363-08	GRCC230	1998	36-3	3,(22-36)	0.220	Significant backside crack, coating loss	206.62	206.46	3.01	1.835	1.498	5/5/05	1829 PDL-P2-22
4-45-362-06	GRCC227	2105	36-2	3,(22-36)	0.221	Significant front and backside damage	205.02	204.79	3.01	1.828	1.495	5/4/05	1829 PDL-P2-18

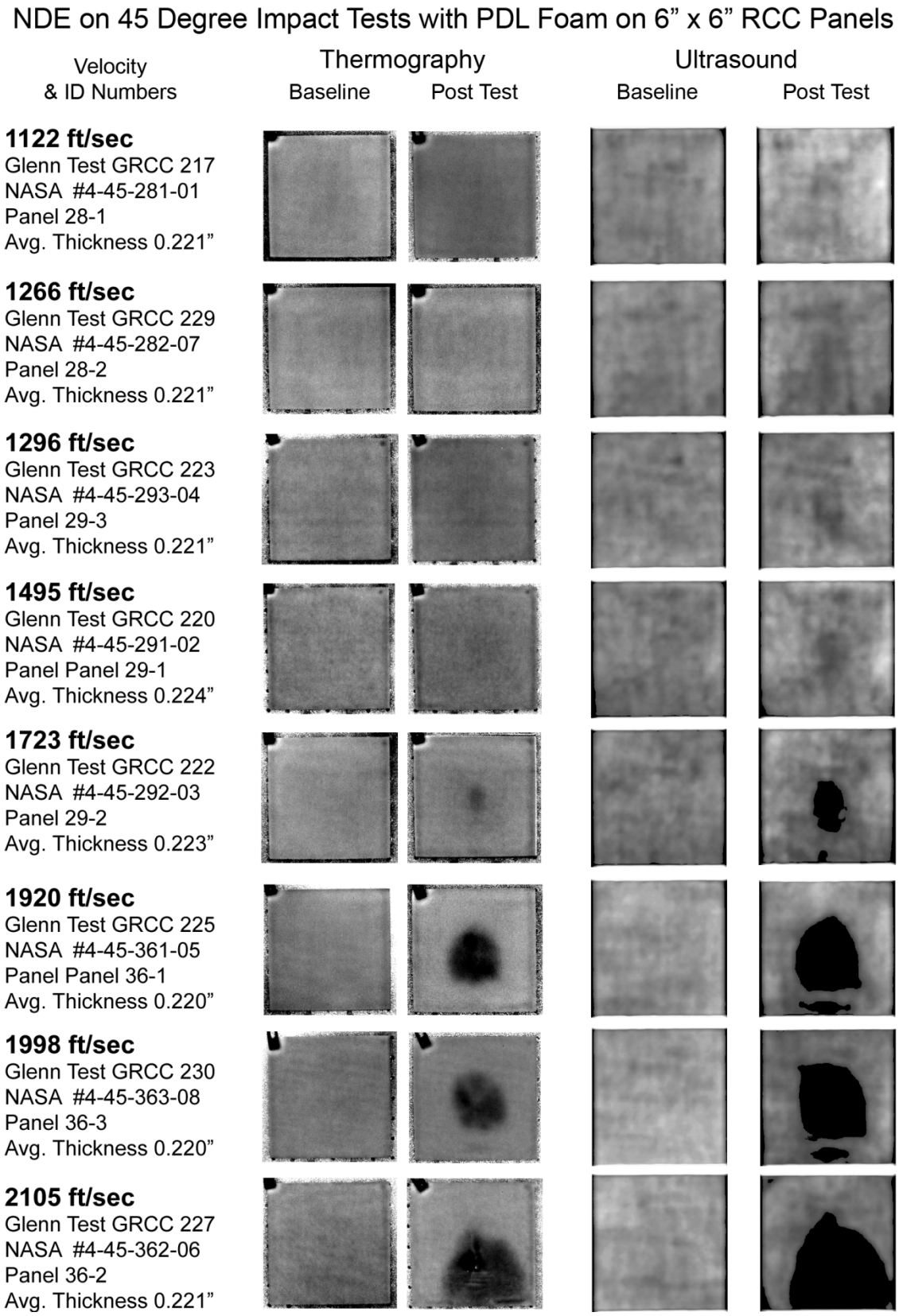

Figure F1–1.—Pulse thermography and ultrasound post impact pretest and posttest images of reinforced carbon-carbon 6- by 6-in. flat panels impacted with PDL foam cylinders (nominally 1.5 in. in diameter by 3 in.) at a 45° angle.

Aramis Displacement Contours from 45 Degree Impact Tests with PDL on 6” x 6” RCC Panels

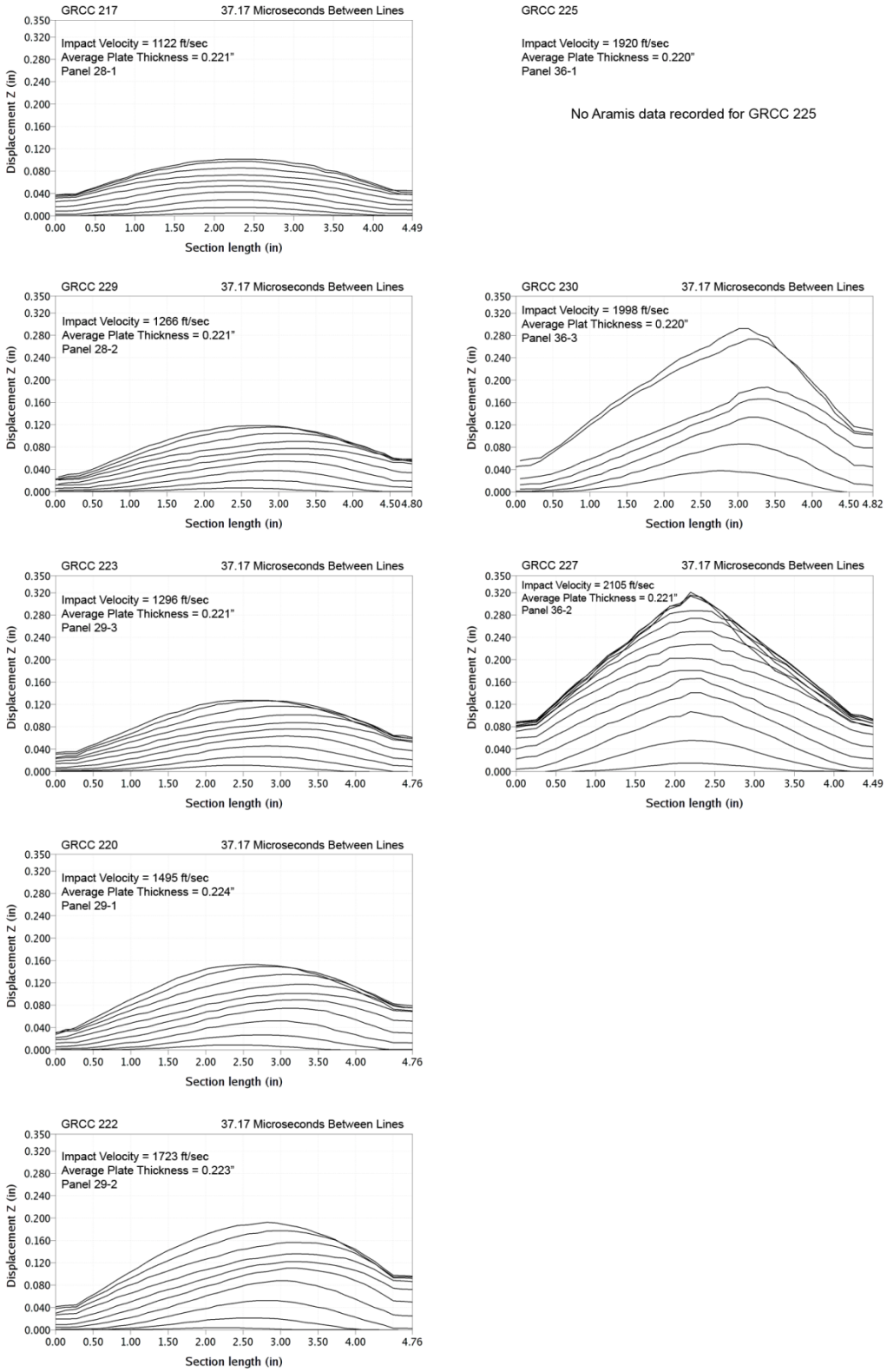

Figure F2–1.—ARAMIS out-of-plane deformation contours across centerline of 6- by 6-in. reinforced carbon-carbon flat panels measured at 37.1-μs increments undergoing impact with PDL foam cylinders (nominally 1.5 in. in diameter by 3 in.) at a 45° angle.

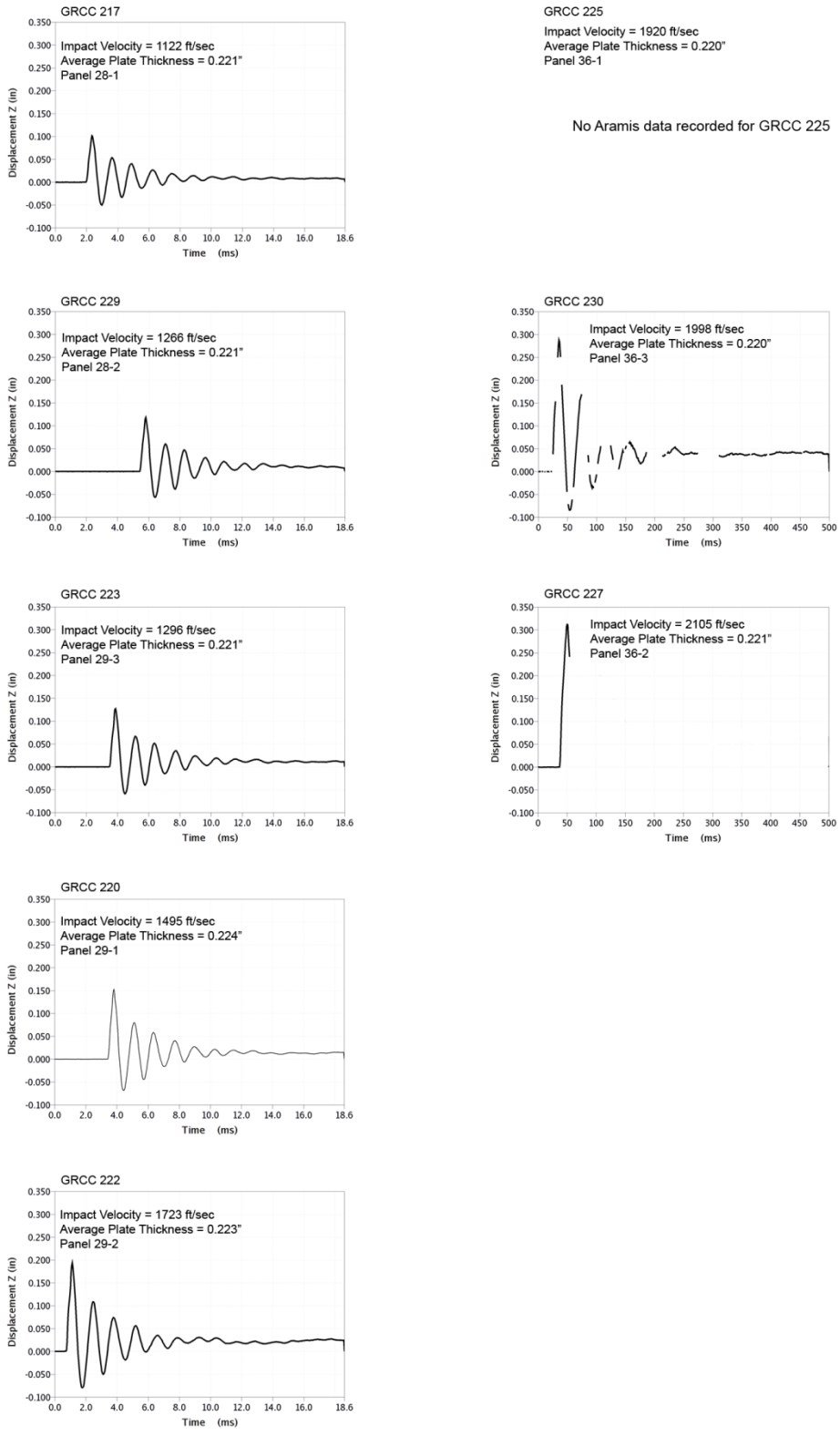

Figure F3–1.—ARAMIS centerpoint out-of-plane deformation vs. time of 6- by 6-in. reinforced carbon-carbon flat panels impacted with PDL foam cylinders (nominally 1.5 in. in diameter by 3 in.) at a 45° angle.

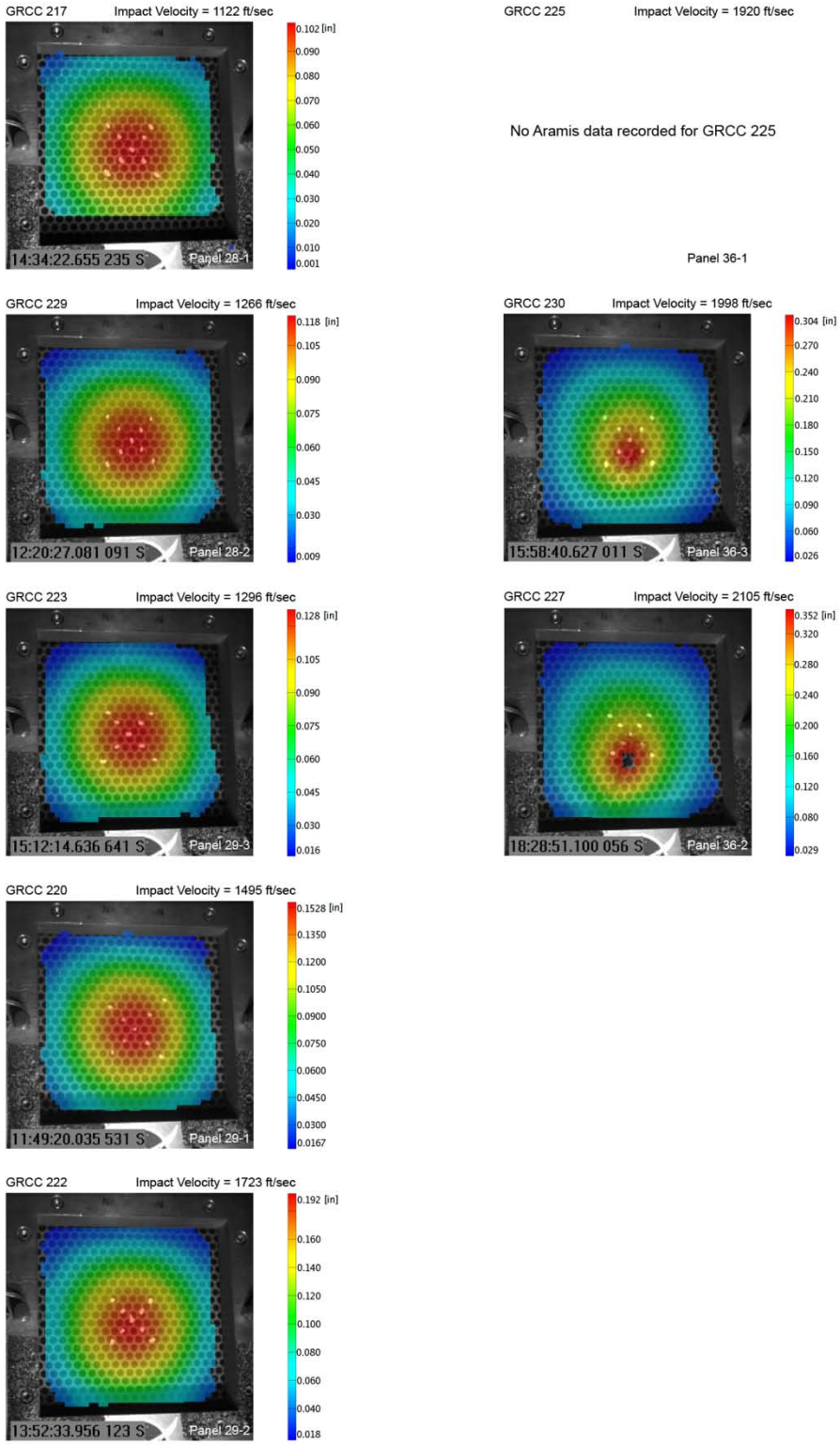

Figure F4–1.—ARAMIS color fringe plots depicting maximum deformation prior to material failure of 6- by 6-in. reinforced carbon-carbon flat panels as they undergo impact with PDL foam cylinders (nominally 1.5 in. in diameter by 3 in.) at a 45° angle.

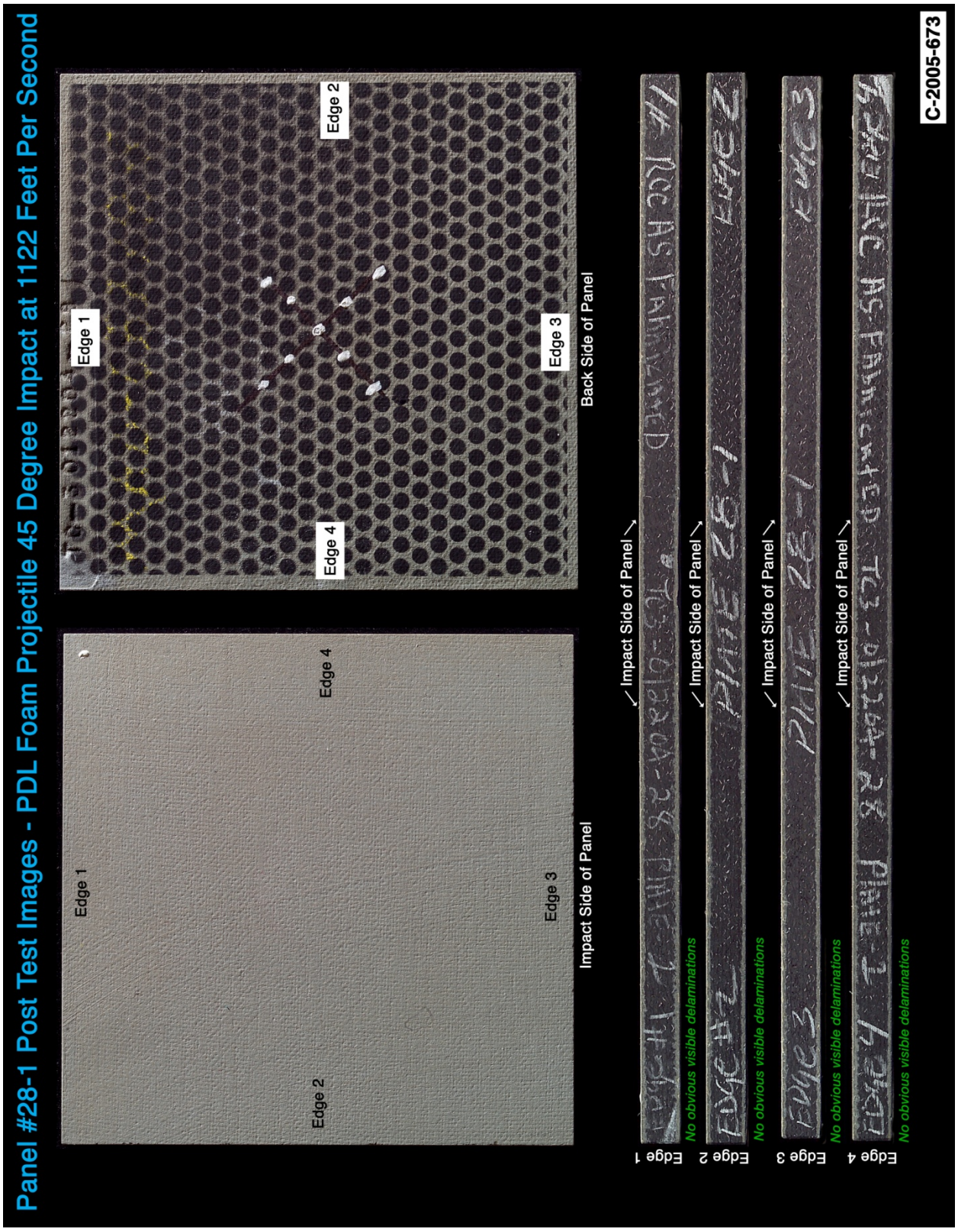

Figure F5–1.—Digital photography of edges and faces of panel 28–1 at 1122 ft/s with a PDL foam cylinder (nominally 1.5 in. in diameter by 3 in.) at a 45° impact angle. Test GRCC 217.

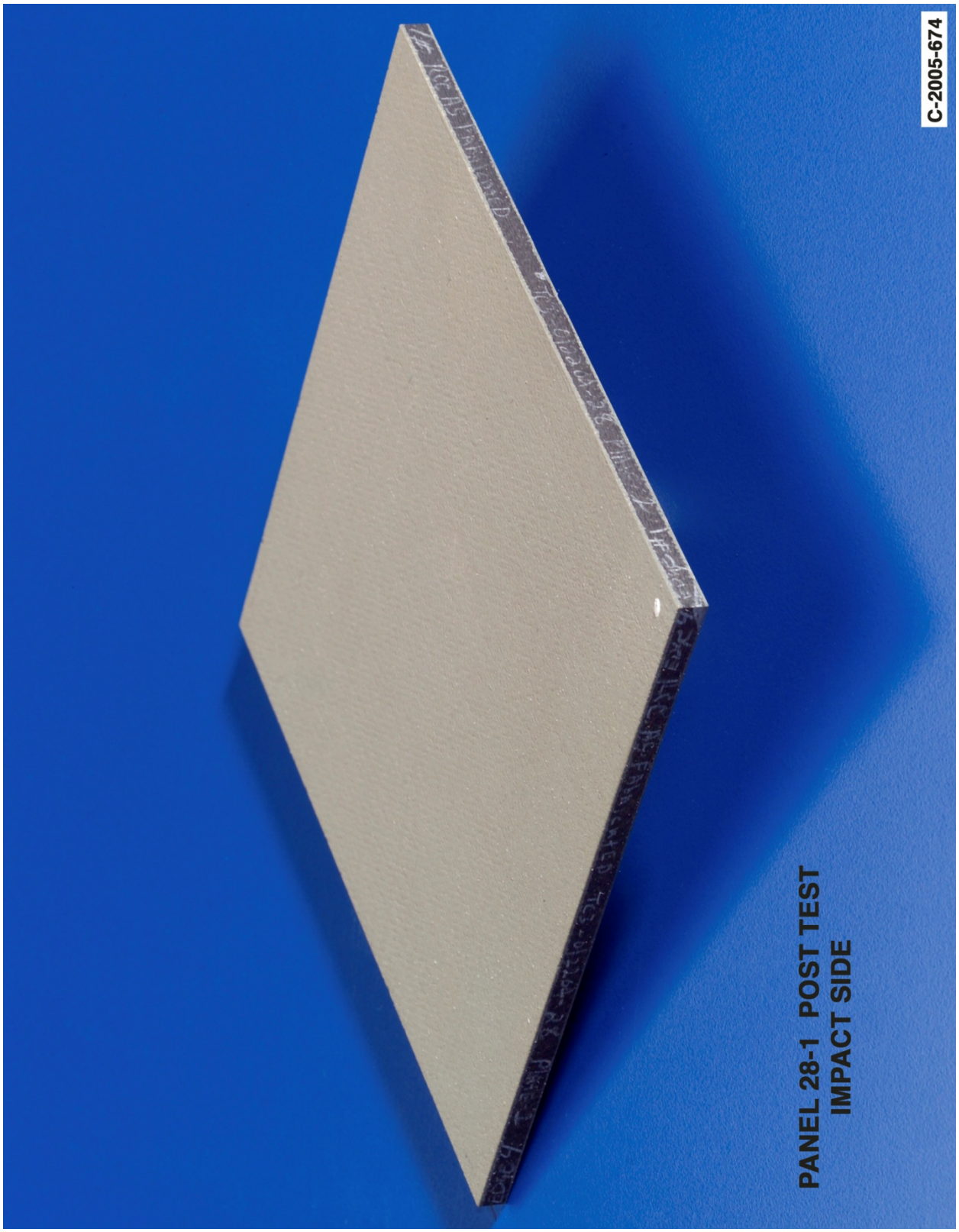

Figure F5–2.—Digital photography front (impact side) face of panel 28–1 at 1122 ft/s with a PDL foam cylinder (nominally 1.5 in. in diameter by 3 in.) at a 45° impact angle. Test GRCC 217.

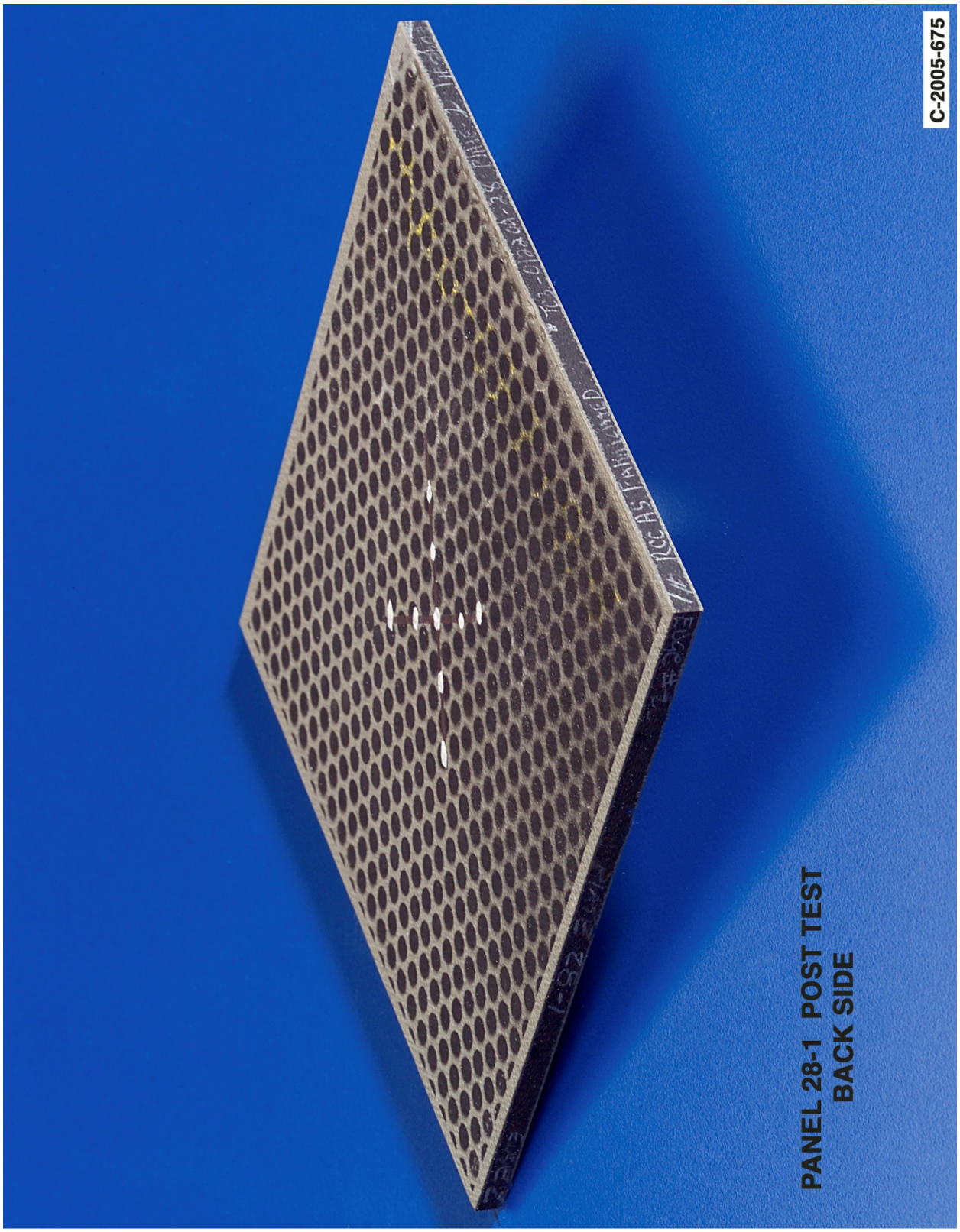

Figure F5–3.—Digital photography of back face of panel 28–1 at 1122 ft/s with a PDL foam cylinder (nominally 1.5 in. in diameter by 3 in.) at a 45° impact angle. Test GRCC 217.

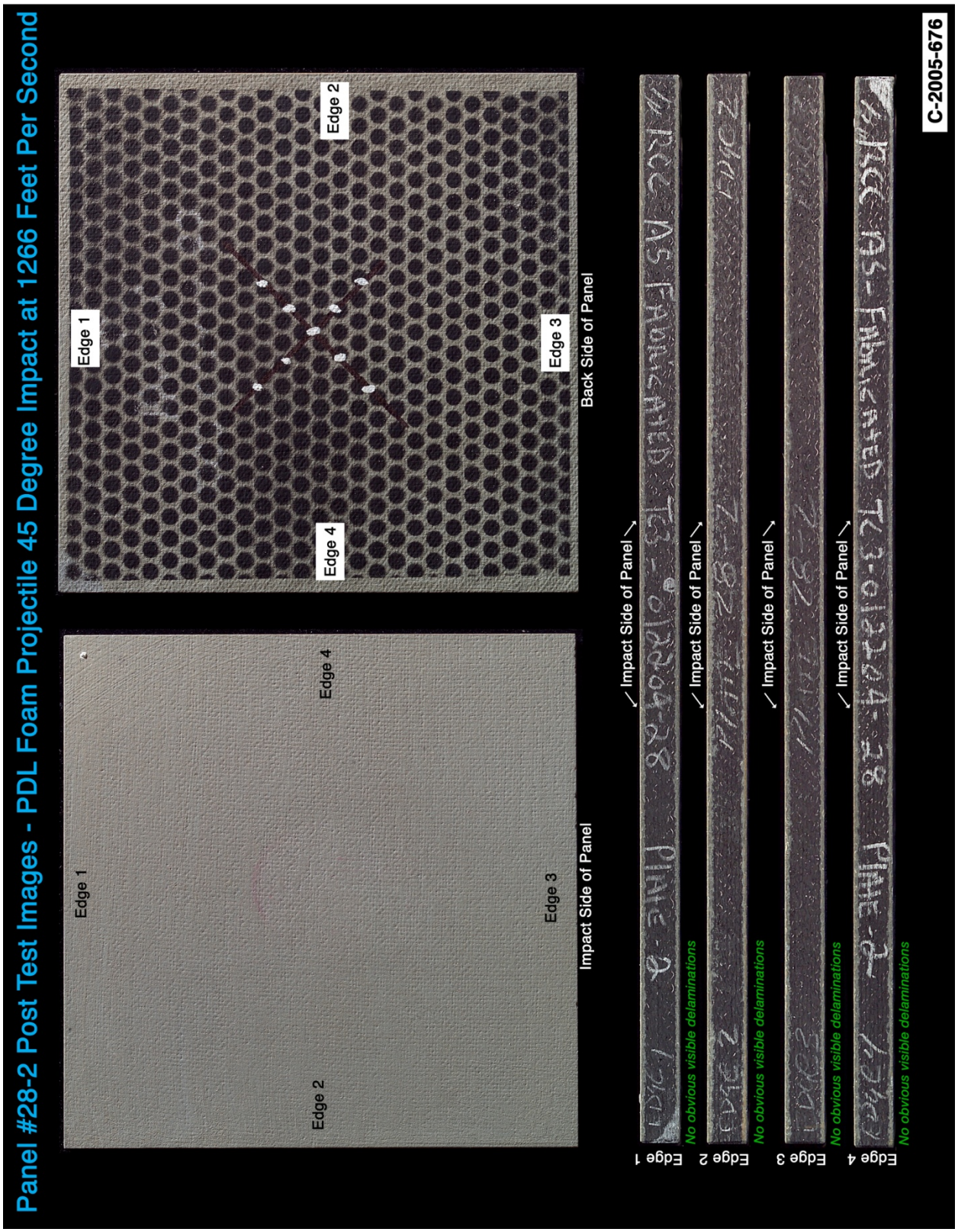

Figure F6–1.—Digital photography of edges and faces of panel 28–2 at 1266 ft/s with a PDL foam cylinder (nominally 1.5 in. in diameter by 3 in.) at a 45° impact angle. Test GRCC 229.

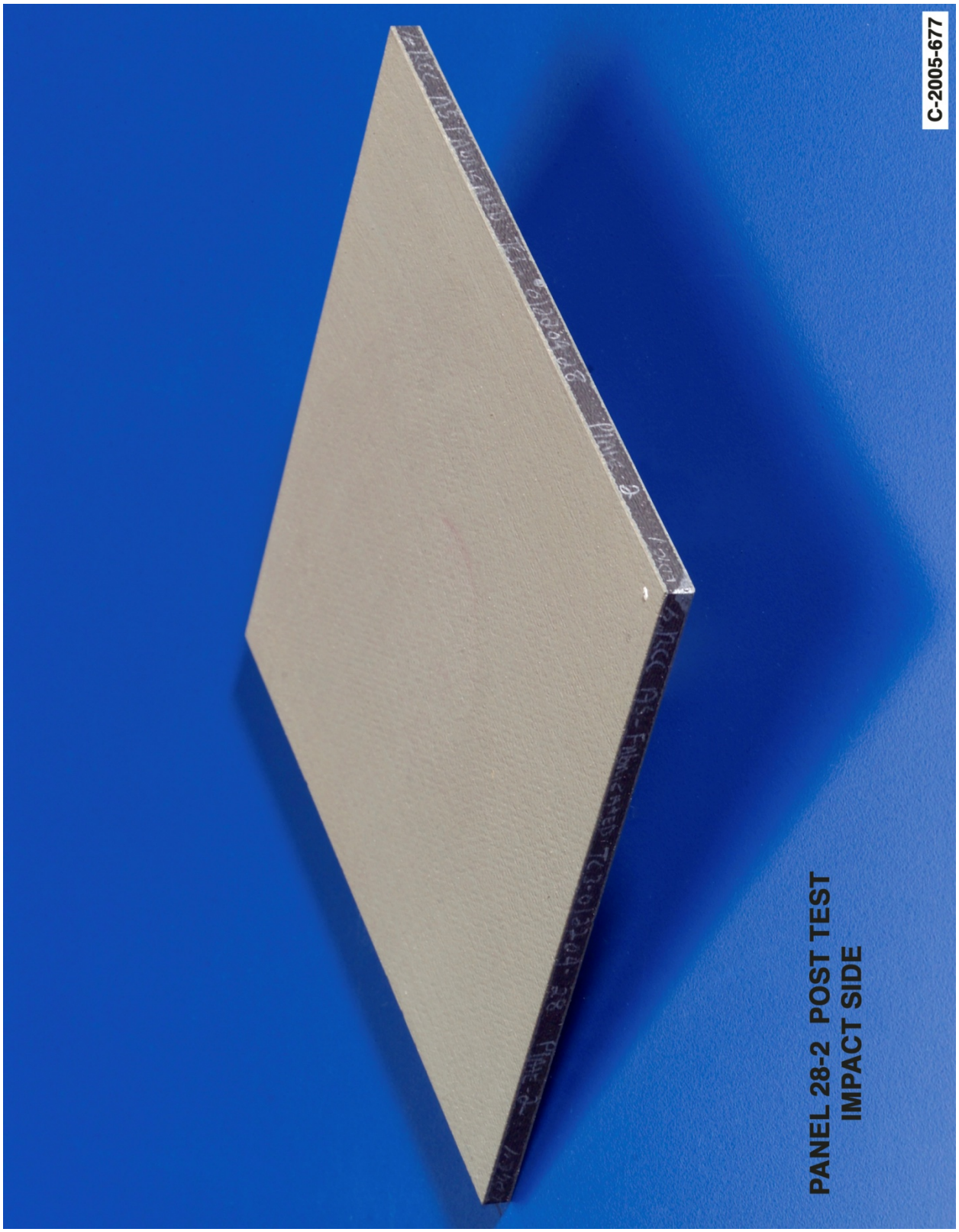

Figure F6–2.—Digital photography front (impact side) face of panel 28–2 at 1266 ft/s with a PDL foam cylinder (nominally 1.5 in. in diameter by 3 in.) at a 45° impact angle. Test GRCC 229.

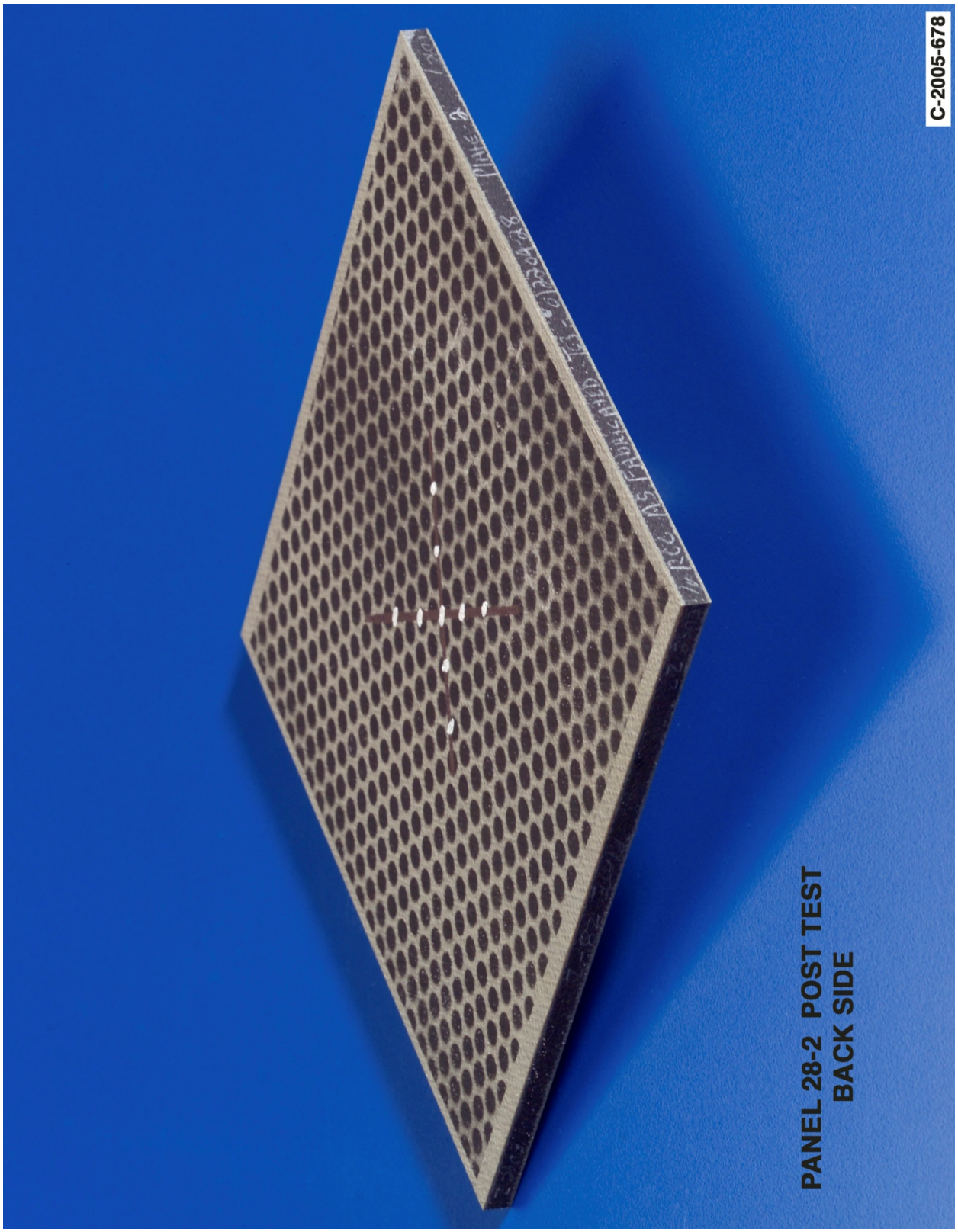

Figure F6–3.—Digital photography of back face of panel 28–2 at 1266 ft/s with a PDL foam cylinder (nominally 1.5 in. in diameter by 3 in.) at a 45° impact angle. Test GRCC 229.

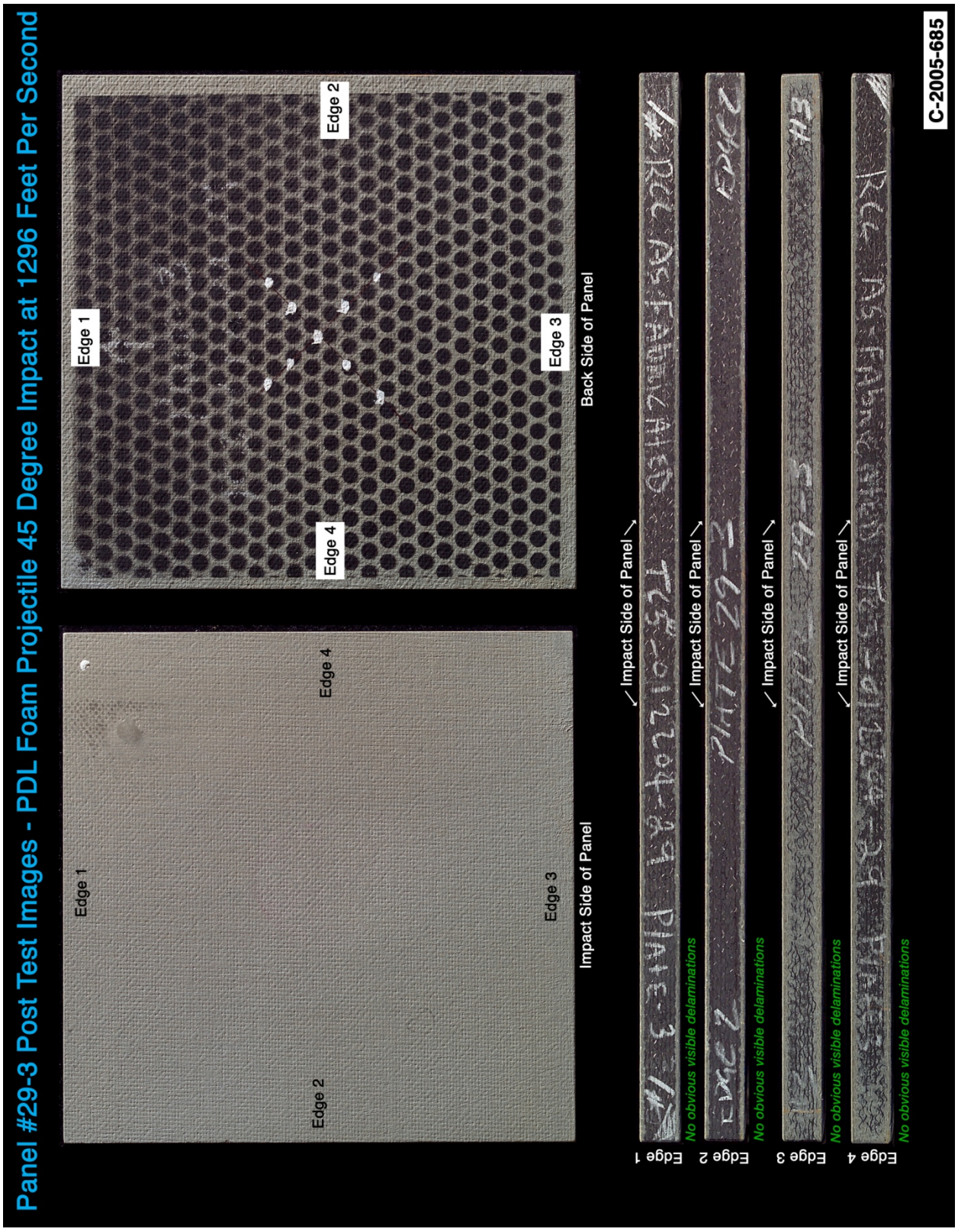

Figure F7–1.—Digital photography of edges and faces of panel 29–3 at 1296 ft/s with a PDL foam cylinder (nominally 1.5 in. in diameter by 3 in.) at a 45° impact angle. Test GRCC 223.

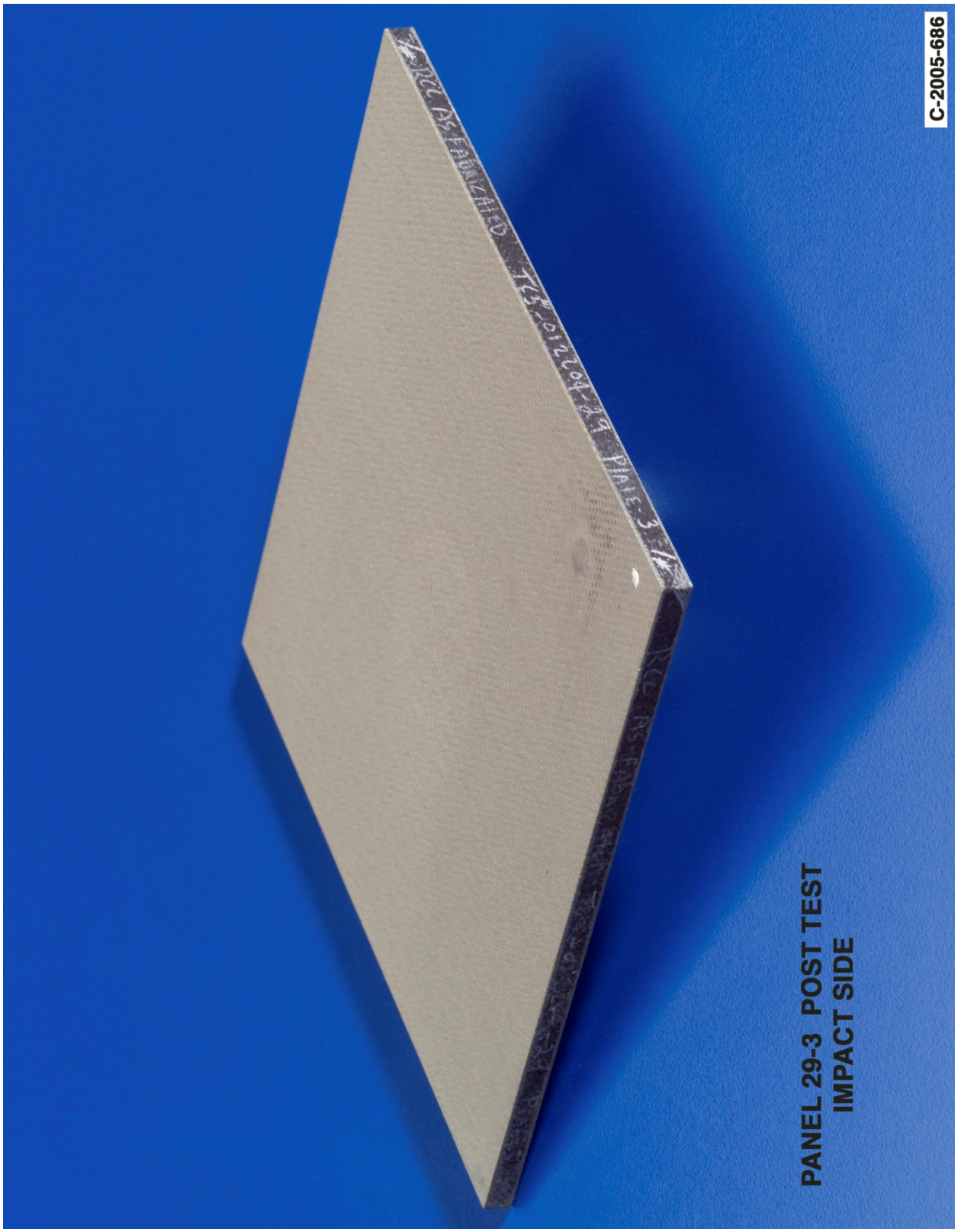

Figure F7–2.—Digital photography front (impact side) face of panel 29–3 at 1296 ft/s with a PDL foam cylinder (nominally 1.5 in. in diameter by 3 in.) at a 45° impact angle. Test GRCC 223.

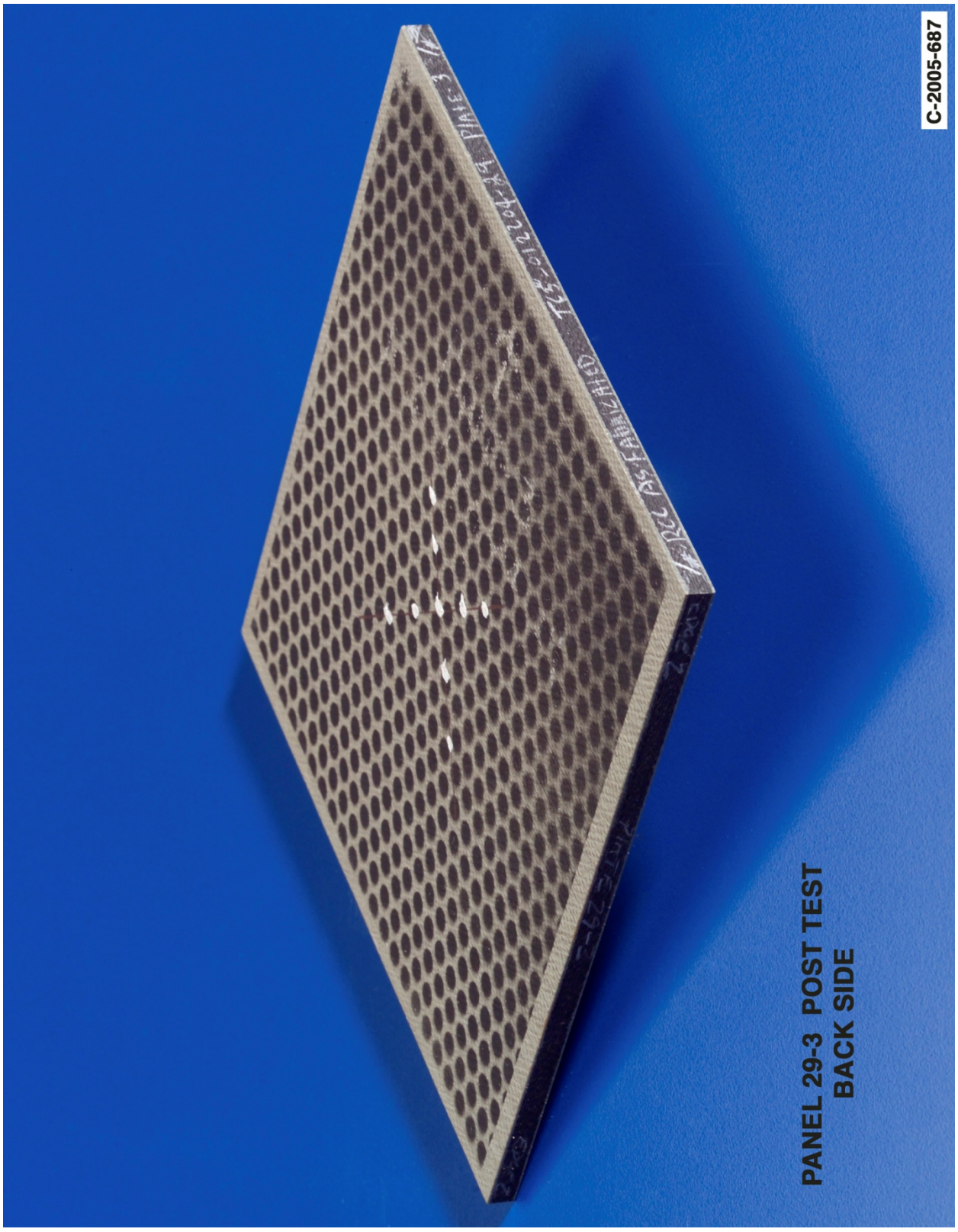

Figure F7–3.—Digital photography of back face of panel 29–3 at 1296 ft/s with a PDL foam cylinder (nominally 1.5 in. in diameter by 3 in.) at a 45° impact angle. Test GRCC 223.

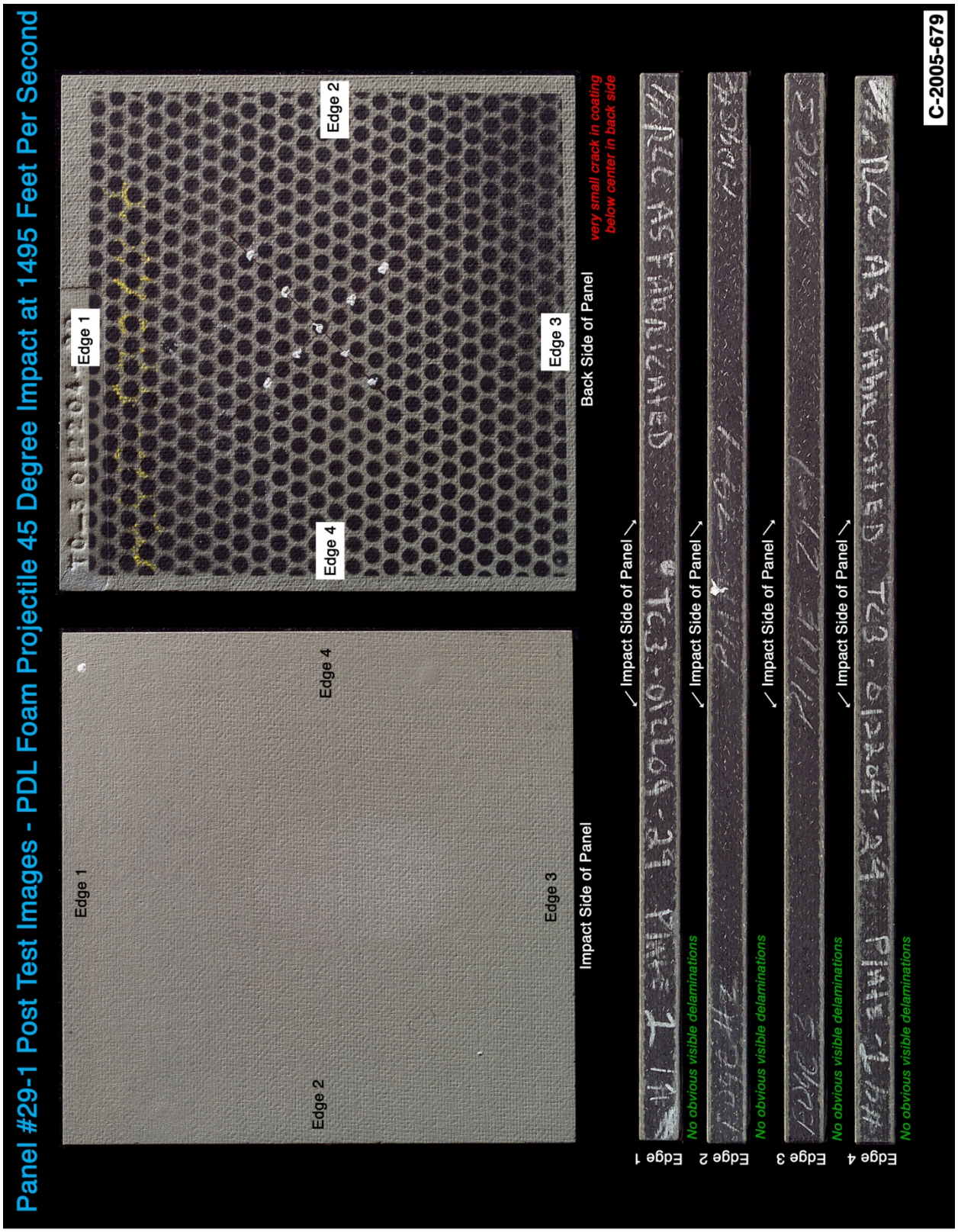

Figure F8–1.—Digital photography of edges and faces of panel 29–1 at 1495 ft/s with a PDL foam cylinder (nominally 1.5 in. in diameter by 3 in.) at a 45° impact angle. Test GRCC 220.

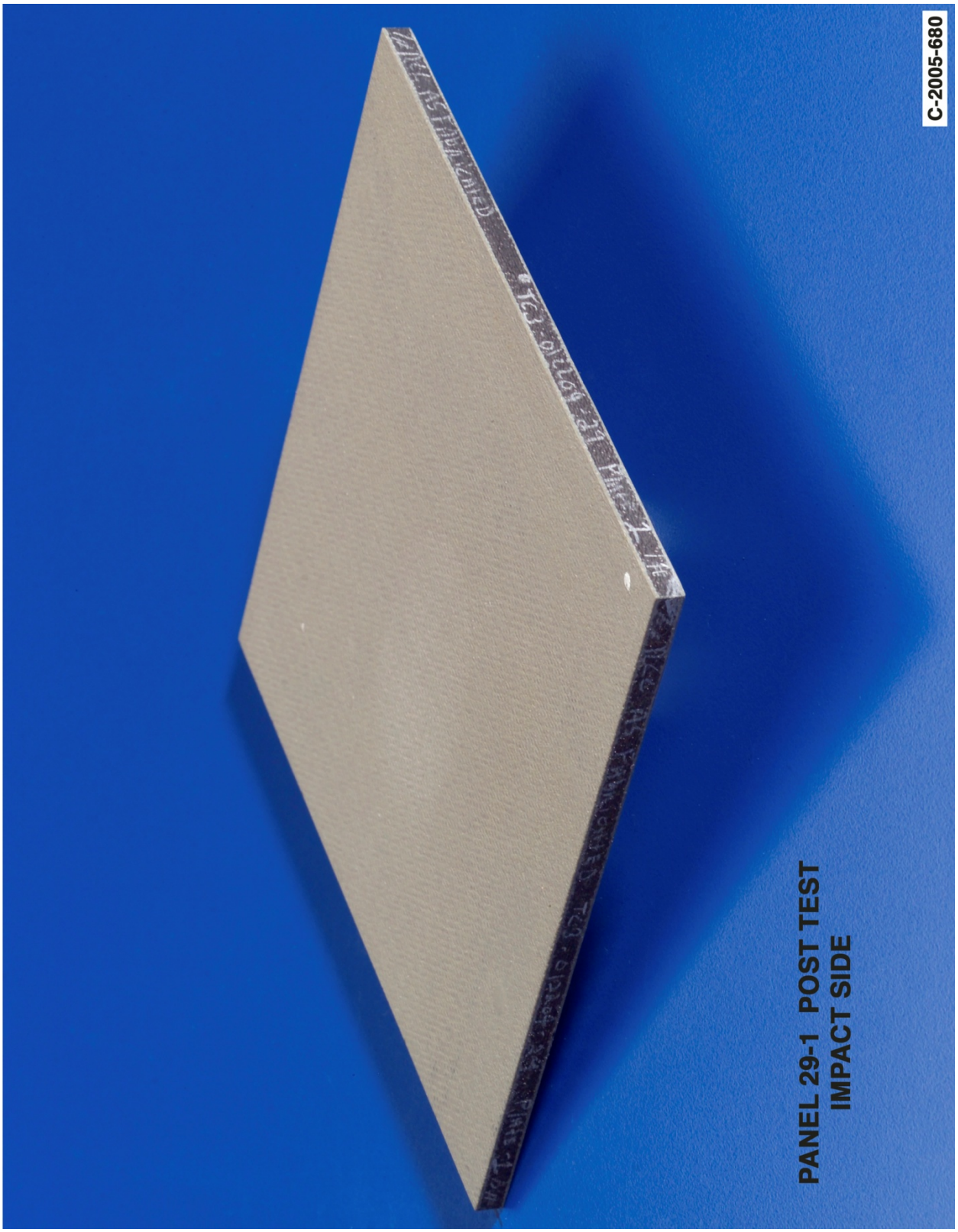

Figure F8–2.—Digital photography front (impact side) face of panel 29–1 at 1495 ft/s with a PDL foam cylinder (nominally 1.5 in. in diameter by 3 in.) at a 45° impact angle. Test GRCC 220.

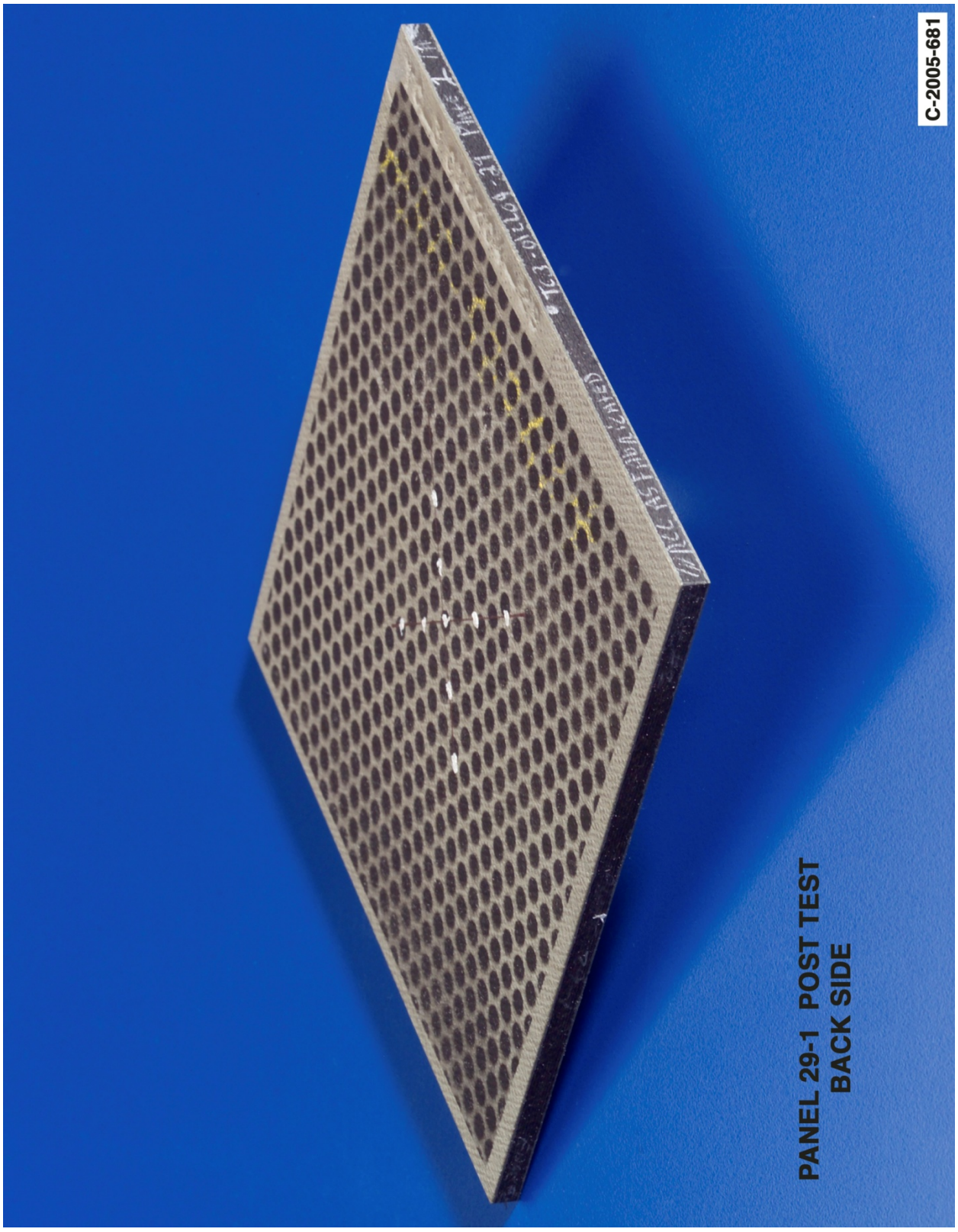

Figure F8–3.—Digital photography of back face of panel 29–1 at 1495 ft/s with a PDL foam cylinder (nominally 1.5 in. in diameter by 3 in.) at a 45° impact angle. Test GRCC 220.

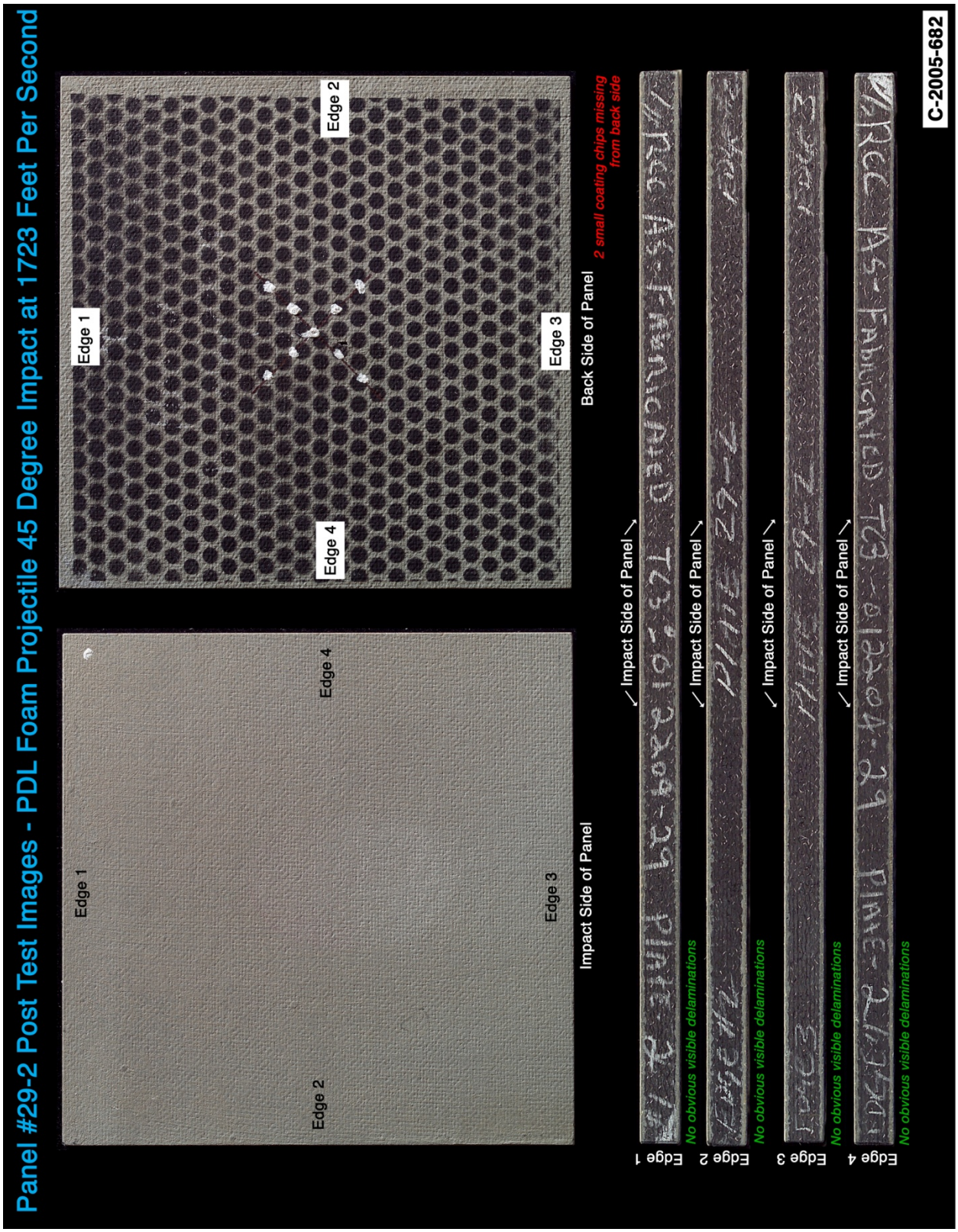

Figure F9–1.—Digital photography of edges and faces of panel 29–2 at 1723 ft/s with a PDL foam cylinder (nominally 1.5 in. in diameter by 3 in.) at a 45° impact angle. Test GRCC 222.

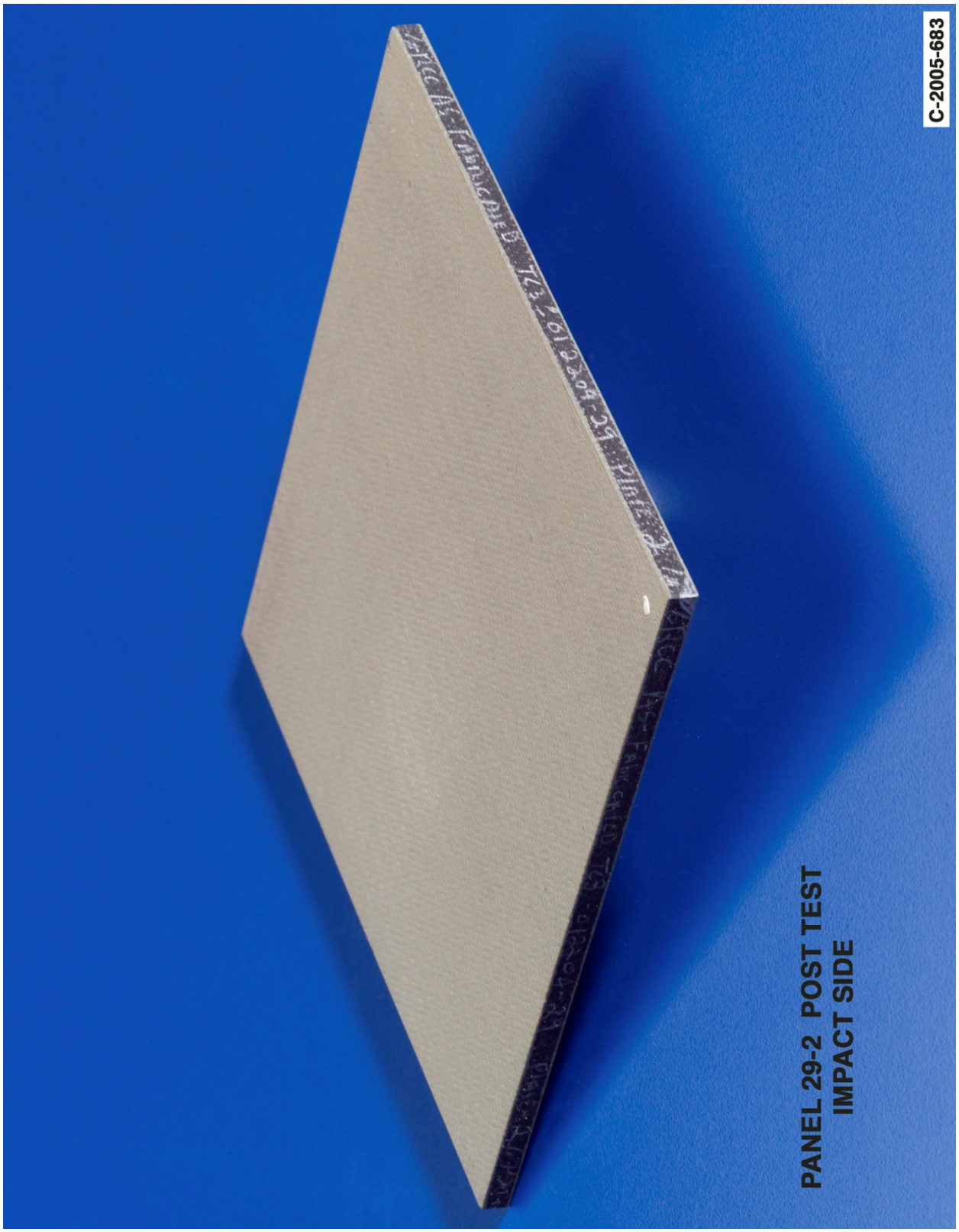

Figure F9–2.—Digital photography front (impact side) face of panel 29–2 at 1723 ft/s with a PDL foam cylinder (nominally 1.5 in. in diameter by 3 in.) at a 45° impact angle. Test GRCC 222.

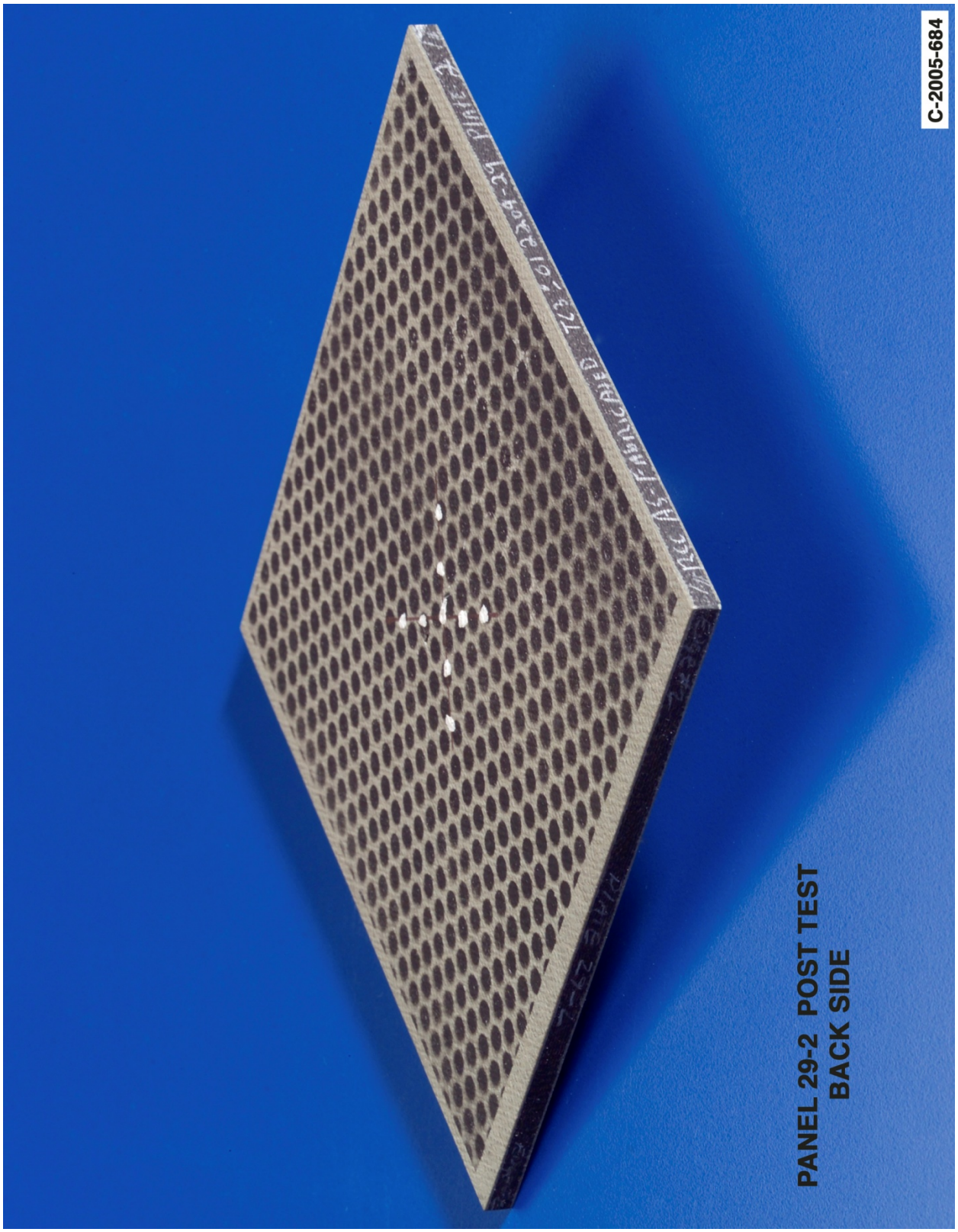

Figure F9–3.—Digital photography of back face of panel 29–2 at 1723 ft/s with a PDL foam cylinder (nominally 1.5 in. in diameter by 3 in.) at a 45° impact angle. Test GRCC 222.

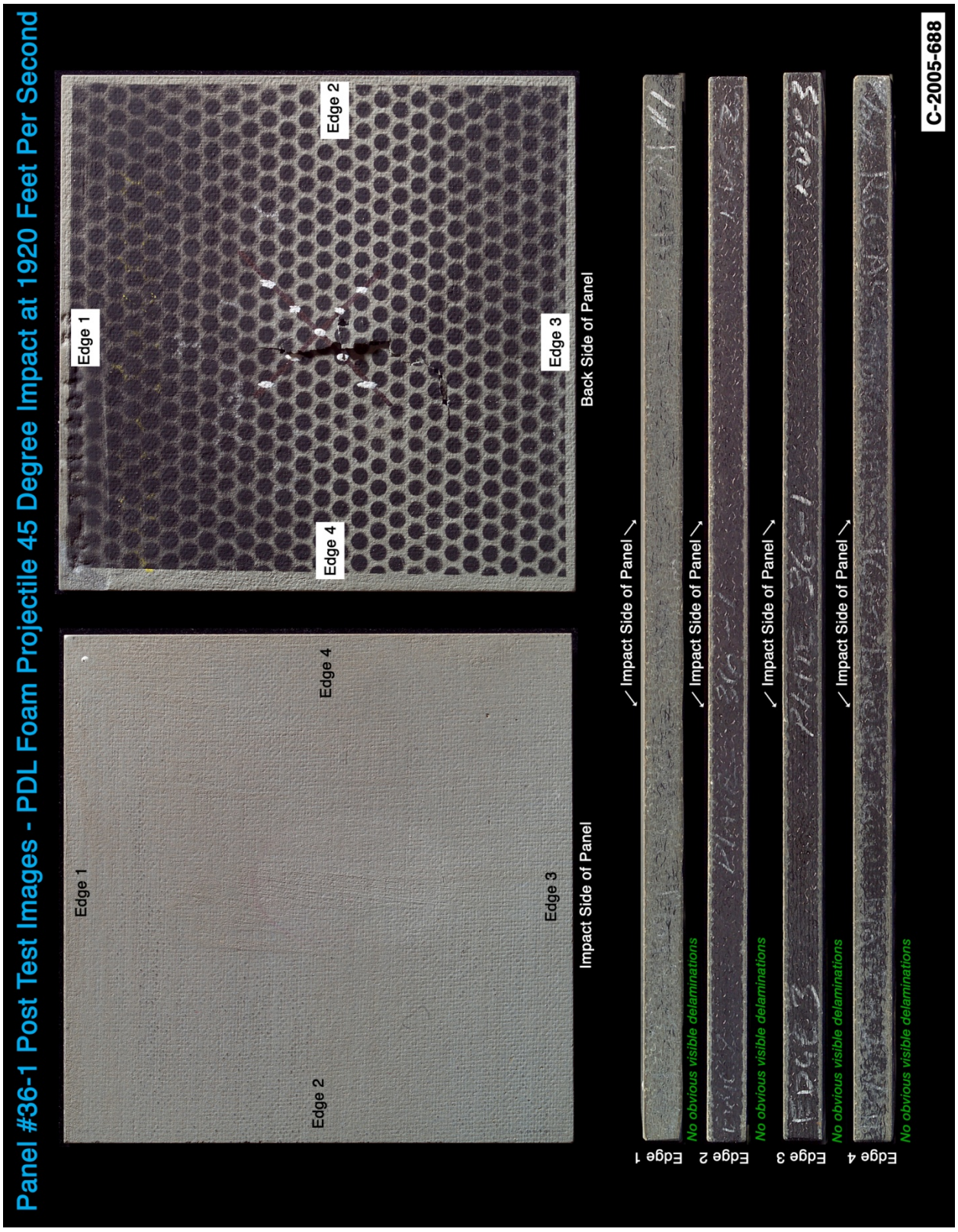

Figure F10–1.—Digital photography of edges and faces of panel 36–1 at 1920 ft/s with a PDL foam cylinder (nominally 1.5 in. in diameter by 3 in.) at a 45° impact angle. Test GRCC 225.

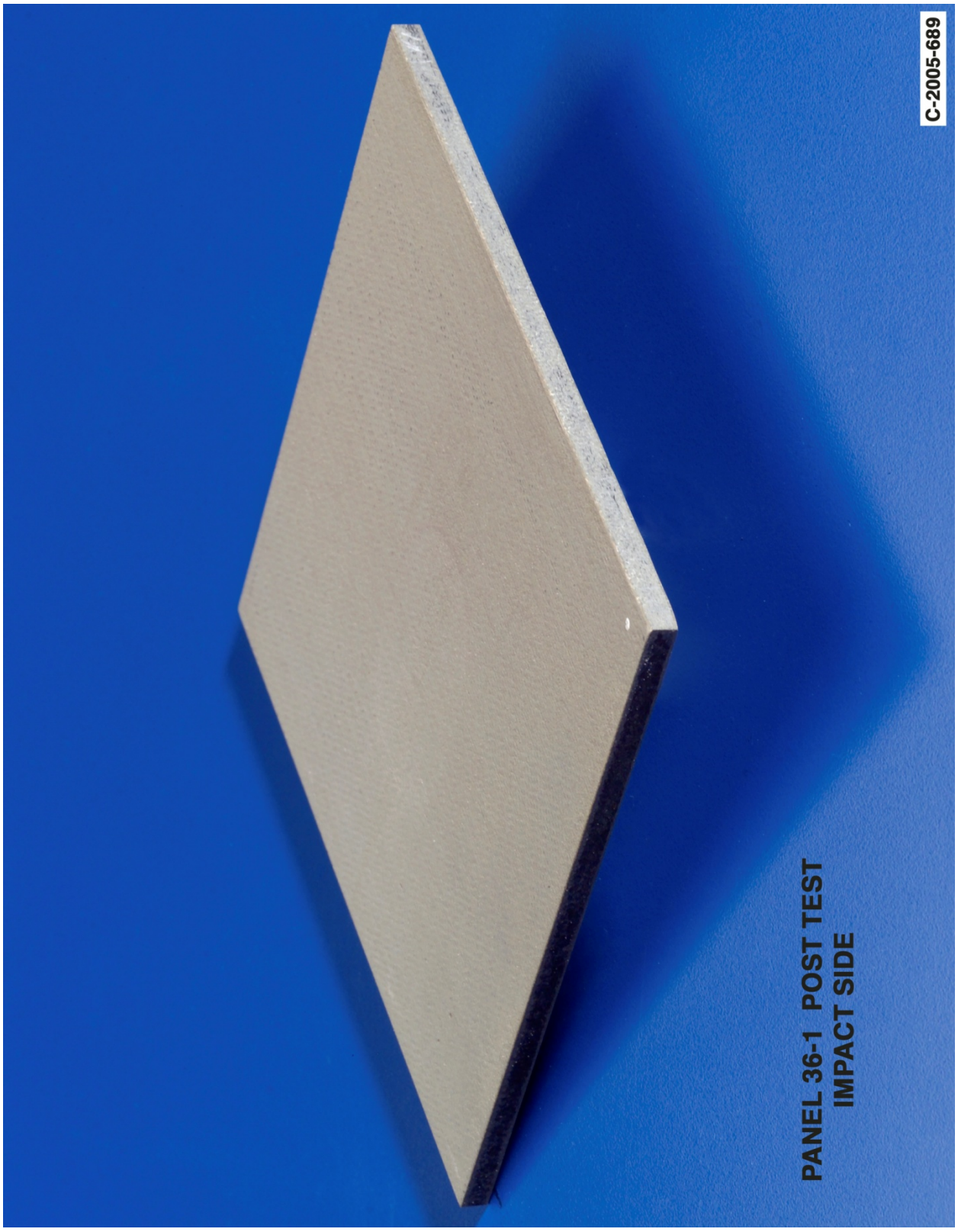

Figure F10–2.—Digital photography front (impact side) face of panel 36–1 at 1920 ft/s with a PDL foam cylinder (nominally 1.5 in. in diameter by 3 in.) at a 45° impact angle. Test GRCC 225.

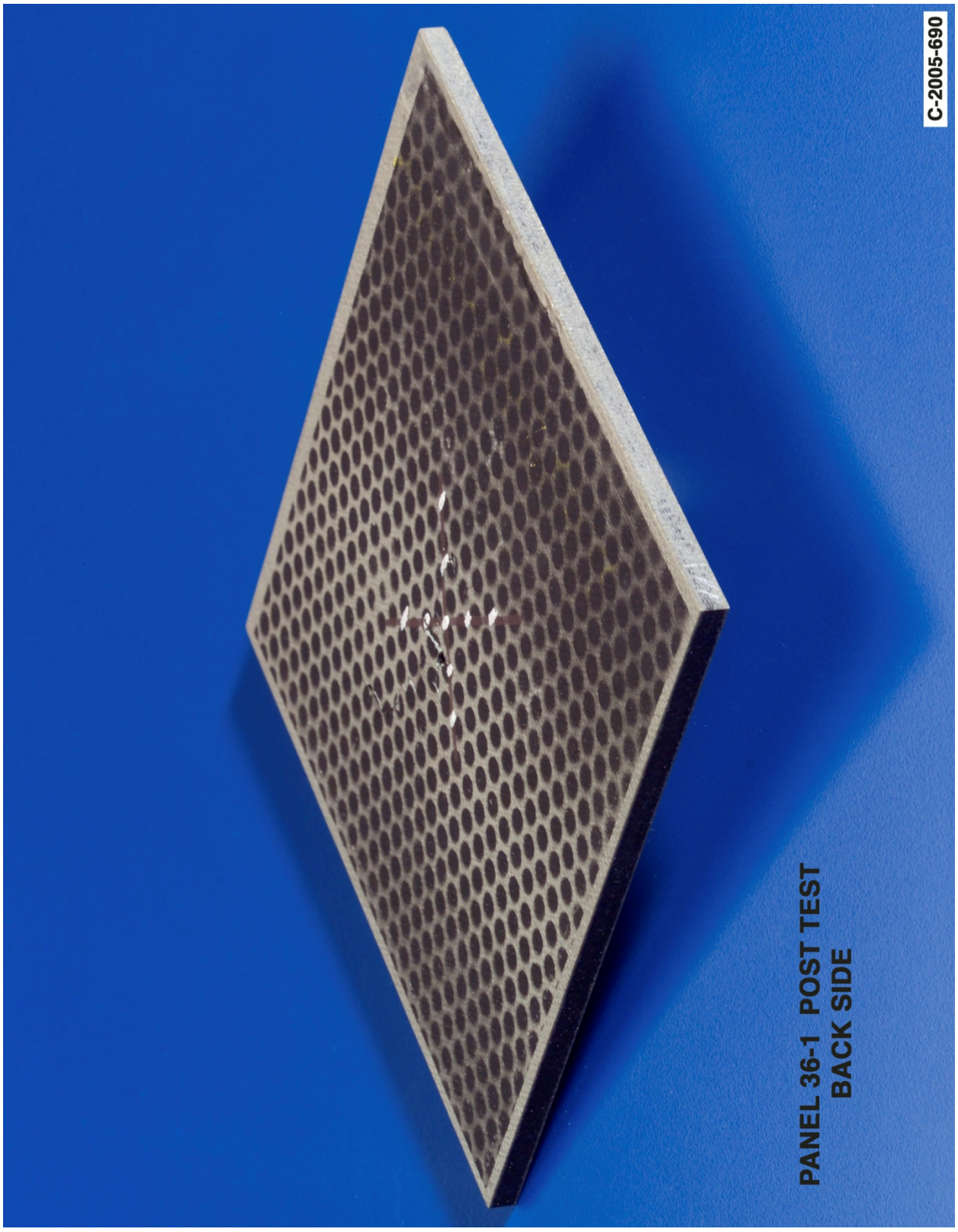

Figure F10–3.—Digital photography of back face of panel 36–1 at 1920 ft/s with a PDL foam cylinder (nominally 1.5 in. in diameter by 3 in.) at a 45° impact angle. Test GRCC 225.

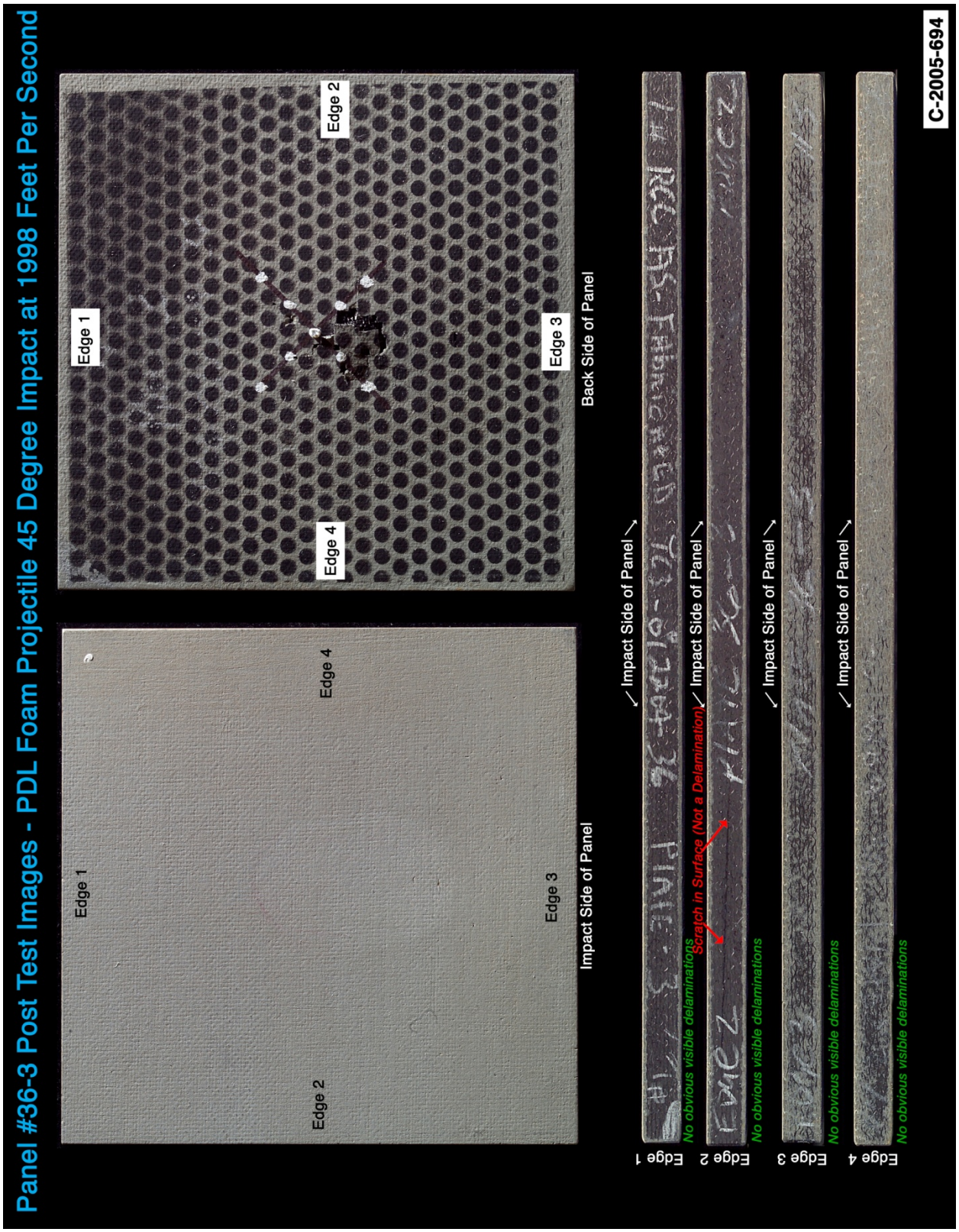

Figure F11–1.—Digital photography of edges and faces of panel 36–3 at 1998 ft/s with a PDL foam cylinder (nominally 1.5 in. in diameter by 3 in.) at a 45° impact angle. Test GRCC 230.

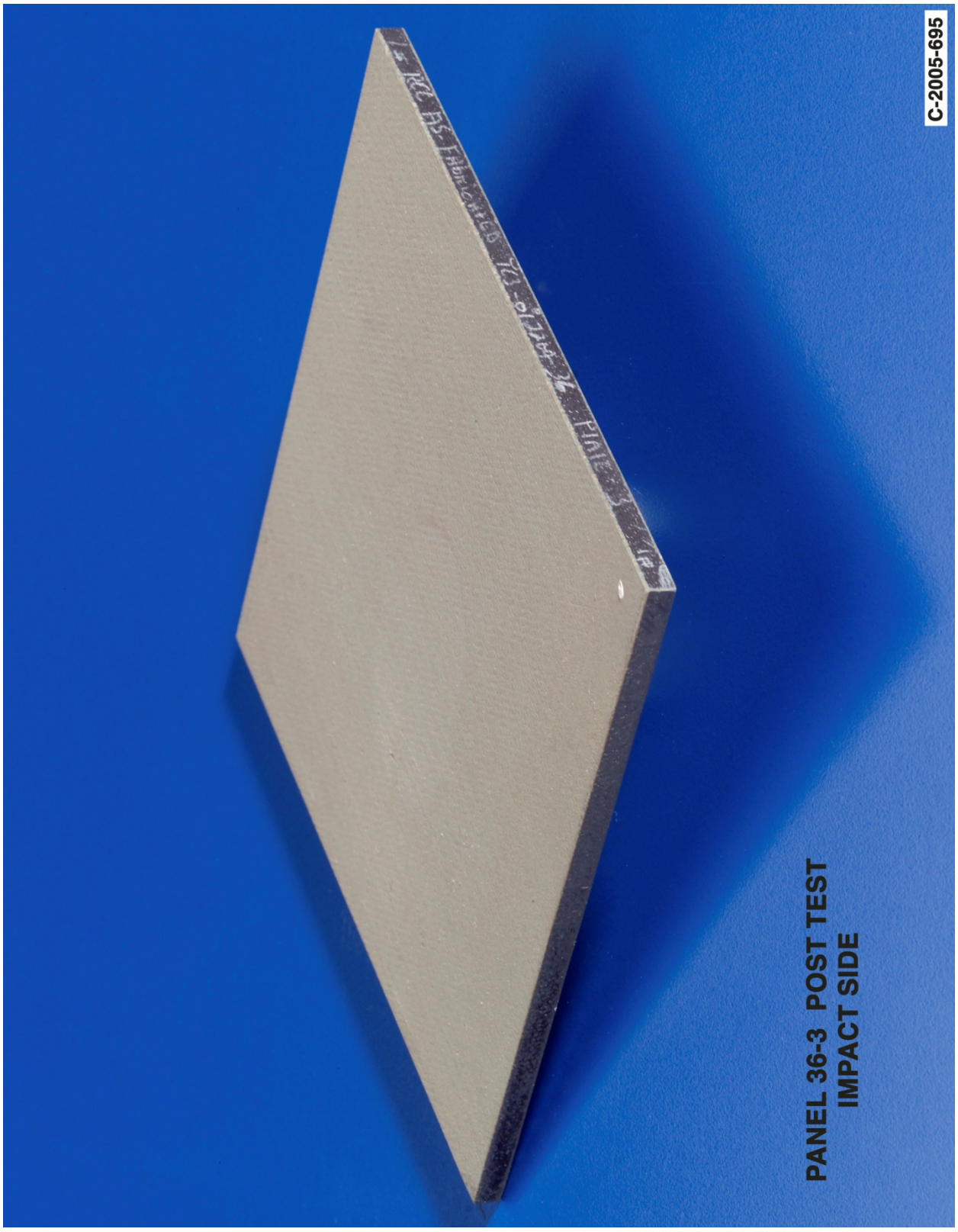

Figure F11–2.—Digital photography front (impact side) face of panel 36–3 at 1998 ft/s with a PDL foam cylinder (nominally 1.5 in. in diameter by 3 in.) at a 45° impact angle. Test GRCC 230.

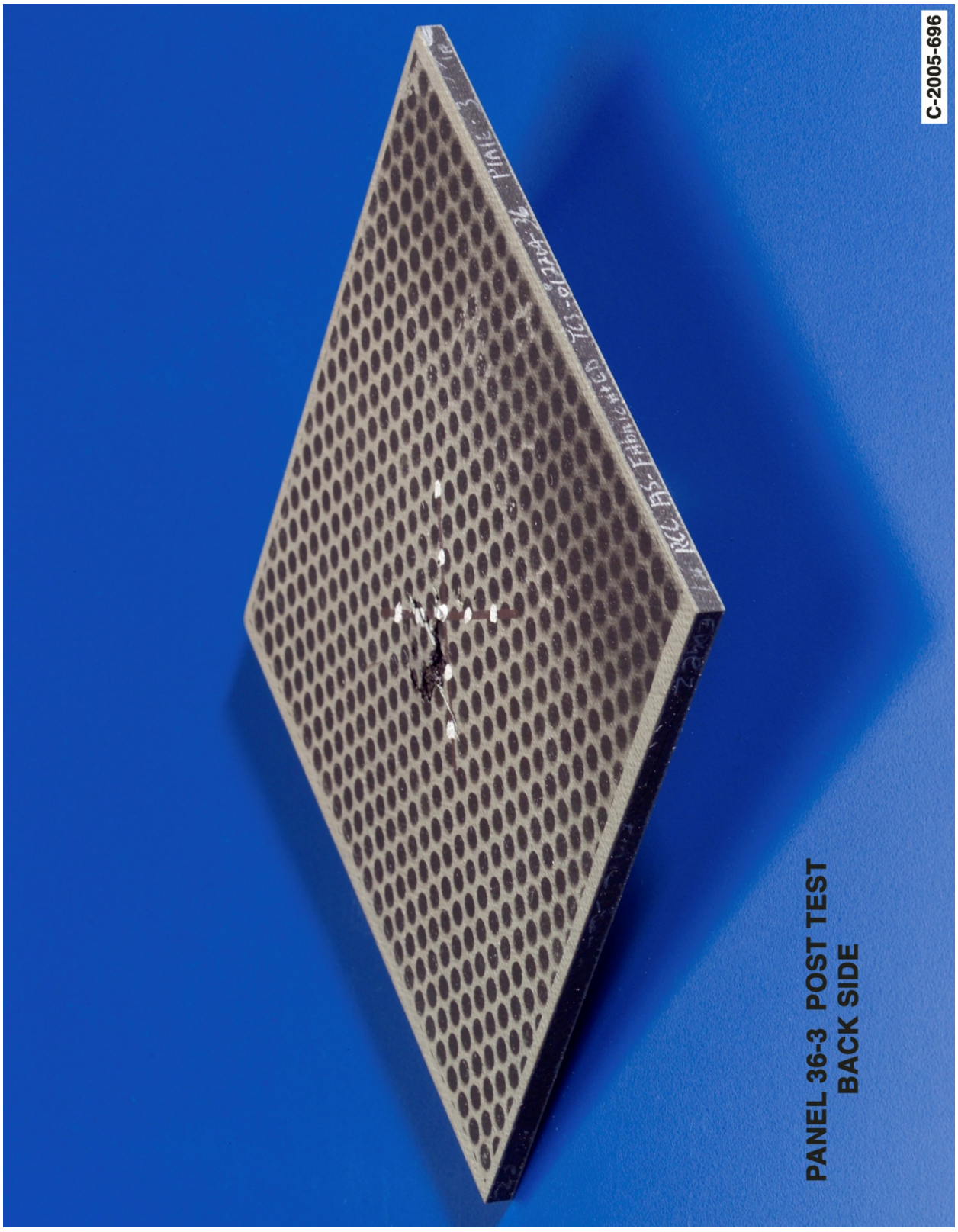

Figure F11–3.—Digital photography of back face of panel 36–3 at 1998 ft/s with a PDL foam cylinder (nominally 1.5 in. in diameter by 3 in.) at a 45° impact angle. Test GRCC 230.

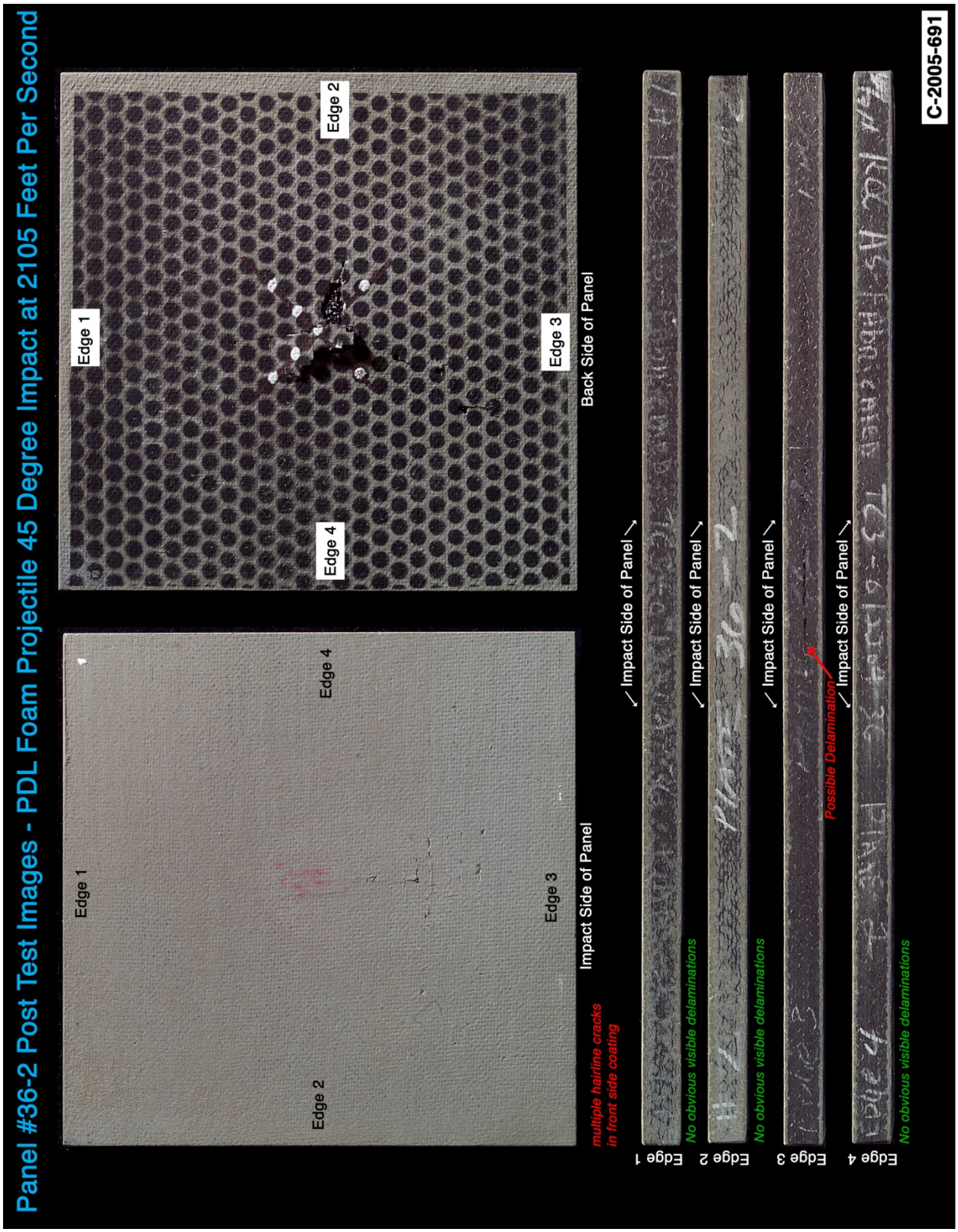

Figure F12–1.—Digital photography of edges and faces of panel 36–2 at 2105 ft/s with a PDL foam cylinder (nominally 1.5 in. in diameter by 3 in.) at a 45° impact angle. Test GRCC 227.

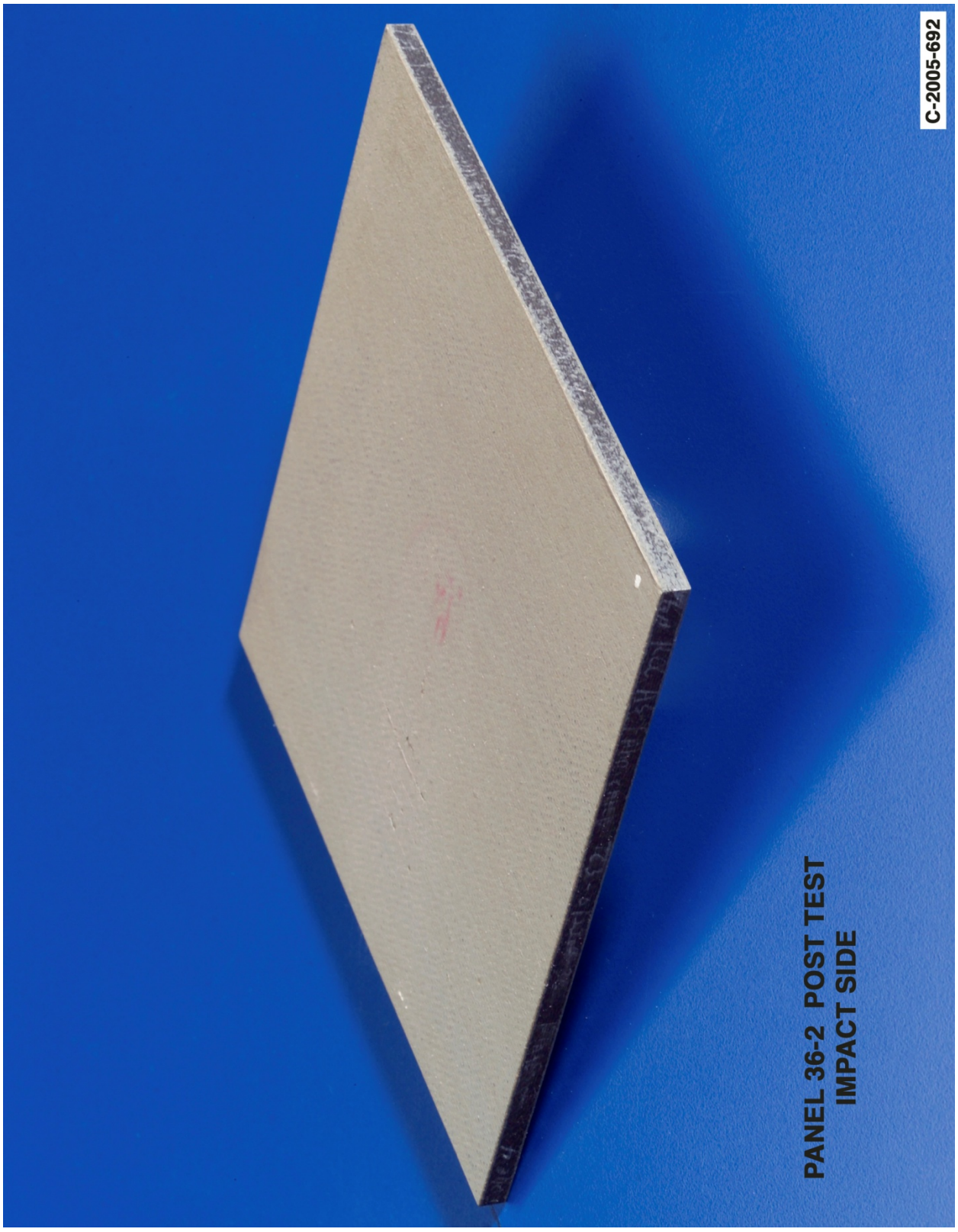

Figure F12–2.—Digital photography front (impact side) face of panel 36–2 at 2105 ft/s with a PDL foam cylinder (nominally 1.5 in. in diameter by 3 in.) at a 45° impact angle. Test GRCC 227.

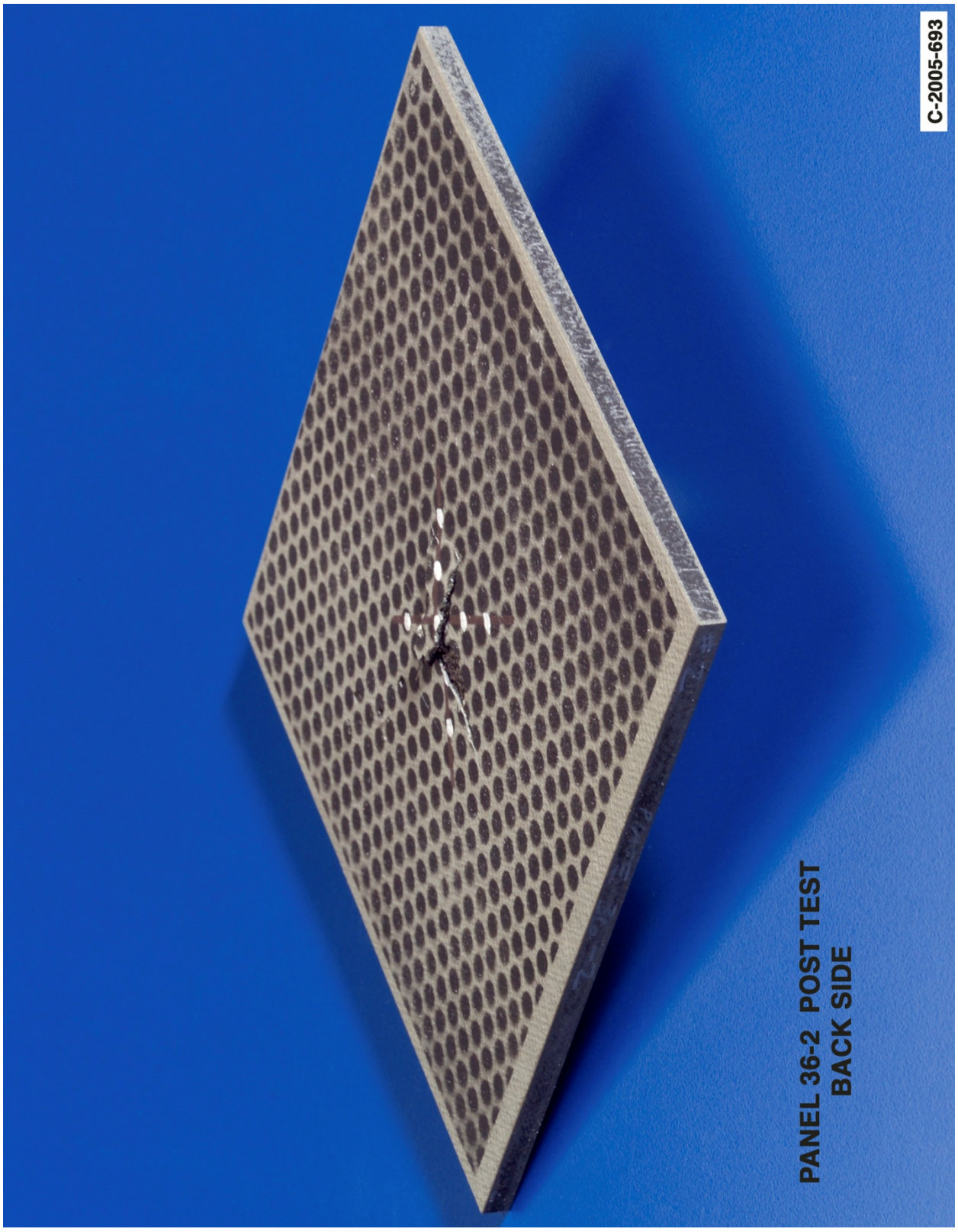

Figure F12–3.—Digital photography of back face of panel 36–2 at 2105 ft/s with a PDL foam cylinder (nominally 1.5 in. in diameter by 3 in.) at a 45° impact angle. Test GRCC 227.

References

1. Gehman, Howard W., et al.: Columbia Accident Investigation Board Report. Vol. 1, NASA–00194, U.S. Government Printing Office, Washington, DC, Aug. 2003.
2. LS–DYNA Keyword User's Manual. Version 970, Livermore Software Technology Corporation, Livermore, CA, 2003.
3. Impact Testing on Reinforced Carbon-Carbon Flat Panels With Ice for the Space Shuttle Return to Flight Program, Final Test Report. NASA/TM—2007-213641, 2007.
4. Orbiter RCC Flat Panel Impact Testing Plan.
5. Vision Research. High Speed Digital Imaging Systems, Vision Research, Inc., Wayne, NJ, 2007. www.visionresearch.com Accessed July 11, 2007.
6. Photron. Precision High-Speed Imaging Systems, Photron USA, Inc., San Diego, CA, 2007. www.photron.com Accessed July 11, 2007.
7. GOM. Optical Measuring Techniques, GOM mbH. Braunschweig, Germany, 2007. www.gom.com Accessed July 11, 2007.
8. Trilion. Optical Quality Systems. Trilion Quality Systems, West Conshohocken, PA, 2007. www.trilion.com. Accessed July 11, 2007.
9. Schmidt, T.; Tyson, J.; and Galanulis, K.: Full-Field Dynamic Displacement and Strain Measurement Using Advanced 3D Image Correlation Photogrammetry: Part I. Exp. Tech., vol. 27, no. 3, 2003, pp. 47–50.
10. Lee, Mikyong, et al.: Application of 3D Measurement System With CCD Camera in Microelectronics. Advanced Packaging, 2003, pp. 33–34.
11. Koenig, J. : Silicon Carbide Coating Thickness Measurements of Various RCC panels and Plates, Final Report to NASA MSFC, George C. Marshall Space Flight Center, Huntsville, AL 35812. Contract No. NAS8-00159, December 2005. SRI–ENG–05–23–10359.14.
12. Koenig, J.: Correlation of RCC Substrate Properties, Final Report to NASA MSFC, George C. Marshall Space Flight Center, Huntsville, AL 35812. Contract No. NAS8-00159, April 2005. SRI–ENG–06–22–10359.14
13. Curry, Donald M.; Wong, Kenneth A.; and Baccus, Ronald K.: Mechanical Property Characterization of Reinforced Carbon-Carbon (RCC) for the Space Shuttle Return to Flight Effort. NASA JSC–63036, 2006.
14. Gilat A.; and Goldberg R.K.: Experimental Study of the High Strain Rate Tensile and Shear Response of Reinforced Carbon Carbon (RCC) Composites. NASA TM–213644 (to be published), 2007.
15. Carney, Kelly, et al.: Material Modeling of Space Shuttle Leading Edge and External Tank Materials for Use in the Columbia Accident Investigation. Proceedings of the 8th International LS–DYNA Users Conference, Dearborn, MI, 2004.
16. Goldberg, Robert K.; and Carney, Kelly S.: Modeling the Nonlinear, Strain Rate Dependent Deformation of Shuttle Leading Edge Materials With Hydrostatic Stress Effects Included. Proceedings of the 8th International LS–DYNA Users Conference, Dearborn, MI, 2004.
17. Lyle, Karen H., et al.: Application of Non-Deterministic Methods to Assess Modeling Uncertainties for Reinforced Carbon-Carbon Debris Impacts. Proceedings of the 8th International LS–DYNA Users Conference, Dearborn, MI, 2004.
18. Fasanella, Edwin L., et al.: Test and Analysis Correlation of Form Impact Onto Space Shuttle Wing Leading Edge RCC Panel 8. Proceedings of the 8th International LS–DYNA Users Conference, Dearborn, MI, 2004.
19. Gabrys, Jonathan, et al.: The Use of LS–DYNA in the Columbia Accident Investigation and Return to Flight Activities. Proceedings of the 8th International LS–DYNA Users Conference, Dearborn, MI, 2004.

20. Fasanella, Edwin L.; Boitnott, Richard L.; and Kellas, Sotiris: Dynamic Crush Characterization of Ice. NASA/TM—2006-214278, 2006.
21. Fasanella, Edwin L., et al.: Test and Analysis Correlation of Foam Impact Onto Space Shuttle Wing Leading Edge RCC Panel 8. NASA/TM—2005-213774 (ARL–TR–3490), 2005.
22. Pereira, J. Michael, et al.: Forces Generated by High Velocity Impact of Ice on a Rigid Structure. NASA/TM—2006-214263, 2006.
23. Pereira, J. Michael; Melis, Matthew E., and Revilock, Duane M.: A Summary of the Space Shuttle Columbia Tragedy and the Use of Digital High Speed Photography in the Accident Investigation and NASA's Return-to-Flight Effort. Proceedings of the SPIE 26th International Congress on High-Speed Photography and Photonics, vol. 5580, Alexandria, VA, 2004.
24. Goldberg, Robert K.; Baccus, Ronald K.; and Carney, Kelly S.: Analysis of the Nonlinear Deformation Response of Shuttle Leading Edge Materials Including Coating Effects. NASA/TM—2005-213842, 2005.
25. Fasanella, Edwin L., et al.: Dynamic Impact Tolerance of Shuttle RCC Leading Edge Panels Using LS–DYNA; Final Report. AIAA Paper 2005–3631, 2005.
26. Schulson, Erland M.; Iliescu, Daniel; and Fortt, Andrew: Characterization of Ice for Return-to-Flight of the Space Shuttle. Part 1—Hard Ice. NASA/CR—2005-213643/PART1, 2005.
27. Schulson, Erland M.; and Iliescu, Daniel: Characterization of Ice for Return-to-Flight of the Space Shuttle. Part 2—Soft Ice. NASA/CR—2005-213643/PART2, 2005.
28. Shazly, Mostafa; Prakash, Vikas; and Lerch, Bradley A.: High-Strain-Rate Compression Testing of Ice. NASA/TM—2006-213966, 2006.
29. Carney, Kelly S., et al.: A Phenomenological High Strain Rate Model With Failure for Ice. Int. J. Solids Struct., vol. 43, no. 25–26, 2006, pp. 7820–7839.

REPORT DOCUMENTATION PAGE		Form Approved OMB No. 0704-0188

1. REPORT DATE *(DD-MM-YYYY)*	2. REPORT TYPE	3. DATES COVERED *(From - To)*
01-12-2009	Technical Memorandum	

4. TITLE AND SUBTITLE
Impact Testing on Reinforced Carbon-Carbon Flat Panels With BX-265 and PDL-1034 External Tank Foam for the Space Shuttle Return to Flight Program

5a. CONTRACT NUMBER

5b. GRANT NUMBER

5c. PROGRAM ELEMENT NUMBER

6. AUTHOR(S)
Melis, Matthew, E.; Revilock, Duane, M.; Pereira, Michael, J.; Lyle, Karen, H.

5d. PROJECT NUMBER

5e. TASK NUMBER

5f. WORK UNIT NUMBER
WBS 377816.06.03.02.04

7. PERFORMING ORGANIZATION NAME(S) AND ADDRESS(ES)
National Aeronautics and Space Administration
John H. Glenn Research Center at Lewis Field
Cleveland, Ohio 44135-3191

8. PERFORMING ORGANIZATION REPORT NUMBER
E-15130

9. SPONSORING/MONITORING AGENCY NAME(S) AND ADDRESS(ES)
National Aeronautics and Space Administration
Washington, DC 20546-0001

10. SPONSORING/MONITOR'S ACRONYM(S)
NASA

11. SPONSORING/MONITORING REPORT NUMBER
NASA/TM-2009-213642-REV1

12. DISTRIBUTION/AVAILABILITY STATEMENT
Unclassified-Unlimited
Subject Categories: 24, 15, and 27
Available electronically at http://gltrs.grc.nasa.gov
This publication is available from the NASA Center for AeroSpace Information, 443-757-5802

13. SUPPLEMENTARY NOTES

14. ABSTRACT
Following the tragedy of the Orbiter Columbia (STS-107) on February 1, 2003, a major effort commenced to develop a better understanding of debris impacts and their effect on the space shuttle subsystems. An initiative to develop and validate physics-based computer models to predict damage from such impacts was a fundamental component of this effort. To develop the models it was necessary to physically characterize reinforced carbon-carbon (RCC) along with ice and foam debris materials, which could shed on ascent and impact the orbiter RCC leading edges. The validated models enabled the launch system community to use the impact analysis software LS-DYNA (Livermore Software Technology Corp.) to predict damage by potential and actual impact events on the orbiter leading edge and nose cap thermal protection systems. Validation of the material models was done through a three-level approach: Level 1-fundamental tests to obtain independent static and dynamic constitutive model properties of materials of interest, Level 2-subcomponent impact tests to provide highly controlled impact test data for the correlation and validation of the models, and Level 3-full-scale orbiter leading-edge impact tests to establish the final level of confidence for the analysis methodology. This report discusses the Level 2 test program conducted in the NASA Glenn Research Center (GRC) Ballistic Impact Laboratory with external tank foam impact tests on flat RCC panels, and presents the data observed. The Level 2 testing consisted of 54 impact tests in the NASA GRC Ballistic Impact Laboratory on 6- by 6-in. and 6- by 12-in. flat plates of RCC and evaluated two types of debris projectiles: BX-265 and PDL-1034 external tank foam. These impact tests helped determine the level of damage generated in the RCC flat plates by each projectile and validated the use of the foam and RCC models for use in LS-DYNA.

15. SUBJECT TERMS
Space shuttle; Debris; Impact; Reinforced Carbon Carbon; BX-265; PDL-1043; External tank; Foam; Thermal protection system

16. SECURITY CLASSIFICATION OF:			17. LIMITATION OF ABSTRACT	18. NUMBER OF PAGES	19a. NAME OF RESPONSIBLE PERSON
a. REPORT	b. ABSTRACT	c. THIS PAGE			STI Help Desk (email:help@sti.nasa.gov)
U	U	U	UU	215	19b. TELEPHONE NUMBER *(include area code)* 443-757-5802